Models for efficient control and fair sharing of assets in energy communities

Sonam Norbu

Supervisor: Dr. Valentin Robu

Co-supervisor: Prof. David Flynn

Institute of Sensors, Signals and Systems
School of Engineering and Physical Sciences
Heriot-Watt University

This dissertation is submitted for the degree of
Doctor of Philosophy

August 2023

Abstract

In recent times, energy communities have gained significant interest. These communities empower citizen prosumers by leveraging their own renewable energy generation and storage assets to manage their energy requirements and engage in the broader energy market. Such communities offer a promising solution for sustainable energy systems, promoting renewable integration and active user involvement. Within energy communities, members can engage in energy trading and invest in shared assets like production units, energy storage, and network infrastructure. However, efficiently controlling these assets in real-time and equitably distributing energy outputs among diverse members with varying needs remains a vital challenge. Addressing this concern is of both research and practical importance. It is essential to consider technical constraints like local low-voltage network characteristics and power ratings during this process.

To tackle these challenges, this thesis presents a model that examines the techno-economic benefits of community-owned versus individually-owned energy assets, accounting for physical asset degradation and network constraints. Employing cooperative game theory principles, the thesis proposes a redistribution model for community benefits based on the marginal contribution of each household. This redistribution mechanism utilizes the concept of marginal value from coalitional game theory and distributed AI (specifically the multi-agent system). Study results demonstrate that the proposed marginal cost redistribution mechanism is fairer and more computationally manageable than existing state-of-the-art methods, thus providing a scalable approach for economic sharing of joint assets in community energy systems.

However, integration of centrally shared community-owned energy assets may face limitations due to network/grid constraints. To address this issue, the thesis proposes a novel framework for a local peer-to-community (P2C) market mechanism as an alternative solution to investing in community-owned assets. The dynamics of the P2C market mechanism are studied for three different types of P2C sellers with non-uniform pricing schemes and tested across various community settings (comprising a mix of prosumers and consumers) and different rates of renewable energy adoption. All proposed models are validated and applied to a real case study from a large-scale smart energy demonstration project in the UK, using a substantial dataset of real renewable generation and demand. This practical case study provides confidence in the robustness of the experimental comparison results presented in the thesis.

Acknowledgements

First and foremost, I would like to express my heartfelt gratitude to my PhD supervisor, Dr. Valentin Robu, for his invaluable guidance and unwavering support throughout this thesis. His expert insights, thoughtful considerations, and prompt responses to my queries played a pivotal role in completing this research swiftly. Additionally, I extend my thanks to my co-supervisor, Prof. David Flynn, for his genuine encouragement, in-depth analysis, and continuous support, which enabled me to successfully complete this thesis and associated publications.

Second, I would like to thank my PhD thesis examiners Prof. Hongjian Sun and Dr. Wolf-Gerrit Fruh for their invaluable expertise, constructive feedback, and unwavering academic support. Their guidance and visionary insights have significantly improved the content of this thesis and shaped my research trajectory.

I am deeply thankful for the support of the UK Engineering and Physical Sciences Council (EPSRC) Doctoral Training Programme (DTP) grant (EP/R513040/1), which enabled my PhD research study at Heriot-Watt University, Edinburgh campus. Additionally, I acknowledge the support of Innovate UK Responsive Flexibility (ReFlex) project [ref:104780], which aligned with my research work and allowed me to collaborate frequently with Dr. Benoit Couraud, the project leader. I express my special appreciation to Dr. Benoit Couraud for his expert supervision, guidance, and unwavering support throughout my PhD journey. His invaluable insights and expertise were crucial in achieving successful research outcomes, including publications in journals and sharing the project's results with stakeholders.

I am grateful to my colleagues and friends in the Smart Systems Group. Especially to Dr. Merlinda Andoni for sharing the resources. Her excellent achievements in her PhD works was a great source of inspiration for my PhD research works.

My special thanks to former colleagues of the Electrical Engineering Department, and friends at College of Science and Technology, Royal University of Bhutan for their warm moral support. I am also immensely grateful to The Bhutan Society of the UK, especially Dee Cano, the student liaison officer, for her unwavering encouragement and continuous correspondence. Her dedication to keeping the Bhutanese community in the UK connected at all times has been invaluable to me throughout my PhD journey.

Finally, a special word of thanks to my parents, sisters and relatives back at Bhutan for all their blessings. Last but not the least, I would like to express my genuine thanks to my wife Yangdon and son Jigme Yonten Norbu for their unconditional love and support, and all the worthy sacrifices, while trying to fulfil my dreams.

Inclusion of Published Works Form

Declaration

This thesis contains one or more multi-author published works. I hereby declare that the contributions of each author to these publications is as follows:

Citation details	**S. Norbu**, B. Couraud, V. Robu, M. Andoni, and D. Flynn, "*Modeling Economic Sharing of Joint Assets in Community Energy Projects Under LV Network Constraints,"* IEEE access, vol. 9, pp. 112019–112042, 2021, doi:https://doi.org/10.1109/ACCESS.2021.3103480
Sonam Norbu	Review of relevant research, model and algorithm development, analysis of results, writing up of publication, general management of paper submission
All other authors	Supervision on work, Feedback/comments on publication, Proofreading

Citation details	**S. Norbu**, B. Couraud, V. Robu, M. Andoni, and D. Flynn, "*Modelling the redistribution of benefits from joint investments in community energy projects*," Applied energy, vol. 287, p. 116575, 2021, doi:https://doi.org/10.1016/j.apenergy.2021.116575
Sonam Norbu	Review of relevant research, model and algorithm development, analysis of results, writing up of publication, general management of paper submission
All other authors	Supervision on work, Feedback/comments on publication, Proofreading

Table of contents

List of tables

List of figures

Nomenclature

Subscripts and Sets

i for agents (households)

c for community

N set of the number of agents (households)

T set of the number of time periods

K set of of indices of the cheapest to most expensive ranked P2C sellers

L set of of indices of the smallest to largest demand ranked P2C buyers

Parameters

η^c battery charging efficiency

η^d battery discharging efficiency

SoC^{initial} initial battery SoC [%]

SoC^{max} maximum battery SoC [%]

SoC^{min} minimum battery SoC [%]

DoD battery depth of discharge [%]

$p^{\text{bat,max}}$ maximum power that battery can charge/discharge [kW]

$V^{\text{slack bus}}$ voltage of the slack/reference bus [V]

$P^{\text{curtailed}}$ curtailed power i.e curtailment of export from renewable generator (solar PV/wind turbine), or curtailment of export/import from/to battery [kW]

$\tau^s(t)$ selling price (export tariff) at t [pence/kWh]

$\tau^b(t)$ buying price (import tariff) at t [pence/kWh]

$\tau^{\text{LowPrice}}(t)$ low selling price of P2C seller at t [pence/kWh]

$\tau^{\text{MediumPrice}}(t)$ medium selling price of P2C seller at t [pence/kWh]

$\tau^{\text{HighPrice}}(t)$ high selling price of P2C seller at t [pence/kWh]

$c_i^A(T)$ annualized cost of the asset for agent i, where $T = 1$ year [£/kWh for battery, and £/kW for solar PV/wind turbine]

$c_C^A(T)$ annualized cost of the asset for community C, where $T = 1$ year [£/kWh for battery, and £/kW for solar PV/wind turbine]

Variables

t time period

Δt duration of the time period t

$SoC(t)$ battery state of charge at t [%]

$\text{DF}^{\text{regular}}$ depreciation factor due to regular cycle

$\text{DF}^{\text{irregular}}$ depreciation factor due to irregular cycle

$V^{\text{bus}}(t)$ bus voltage at t [V]

$P^{\text{bus}}(t)$ bus power at t [kW]

$g_i^{\text{wind/solar}}(t)$ power from the renewable generator of agent i at t [kW]

$g_C^{\text{wind/solar}}(t)$ power from the renewable generator of community C at t [kW]

$p_i^{\text{grid}}(t)$ power from the utility grid of agent i at t [kW]

$p_C^{\text{grid}}(t)$ power from the utility grid of community C at t [kW]

$p_i^{\text{bat}}(t)$ power of the battery for agent i at t [kW], charging(-ve) and discharging(+ve)

$p_C^{\text{bat}}(t)$ power of the battery for community C at t [kW], charging(-ve) and discharging(+ve)

$P_i^{\text{excess}}(t)$ excess power generated by the agent i at t [kW]

$P_i^{\text{deficit}}(t)$ deficit power required by the agent i at t [kW]

$P_C^{\text{excess}}(t)$ excess power generated by the community i at t [kW]

$P_C^{\text{deficit}}(t)$ deficit power required by the community i at t [kW]

$d_i(t)$ power consumed by the agent i at t [kW]

$d_C(t)$ power consumed by the community C at t [kW]

$e_i^s(t)$ energy exported by agent i at t [kWh]

$e_C^s(t)$ energy exported by community C at t [kWh]

$e_i^b(t)$ energy imported by agent i at t [kWh]

$e_C^b(t)$ energy imported by community C at t [kWh]

$P^{\text{P2C}}(t)$ power avialble for local P2C market at t [kW]

$P^{\text{Grid Import}}(t)$ power imported from utility grid at t [kW]

$P^{\text{Grid Export}}(t)$ power exported to utility grid at t [kW]

$b_i(T)$ annual bill for agent i, where $T = 1$ year [£]

$b_i^0(T)$ baseline annual bill for agent i without any assets, where $T = 1$ year [£]

$b_i^*(T)$ new annual bill for agent i after redistribution of savings, where $T = 1$ year [£]

$b_i^{*(\neg)}(T)$ new annual bill for agent i after redistribution of savings without network constraints, where $T = 1$ year [£]

$b_i^{*(\text{NC})}(T)$ new annual bill for agent i after redistribution of savings with network constraints, where $T = 1$ year [£]

$b_C(T)$ annual bill for community C, where $T = 1$ year [£]

$b_C^{\text{NC}}(T)$ annual bill for community C with network constraints, where $T = 1$ year [£]

$b_C^{\neg}(T)$ annual bill for community C without network constraints, where $T = 1$ year [£]

$\Pi_C(T)$ saving of the community C after 1 year ($T = 1$ year) [£]

$\Theta_i(T)$ marginal contribution of an agent i [£]

$\Gamma_i(T)$ benefits redistributed to agent i after period T [£]

$\tau^{\text{P2C}}_{\text{clearing price}}(t)$ clearing price of the multi-unit auction P2C market mechansim at every operational time period t

Abbreviations

ANM Active Network Management

BESS Battery Energy Storage System

CES Community Energy Storage

DERs Distributed Energy Resources

DF Depreciation Factor

DNOs Distribution Network Operators

DoD Depth of Discharge

DR Demand Response

DSM Demand Side Management

DSOs Distribution System Operator

EMS Energy Management System

EoL End of Life

FITs Feed-in Tariffs

HEMS Home Energy Management System

HES Household Energy Storage

ICT Information and Communication Technology

LACE Levelized Avoided Cost of Electricity

LCOE Levelized Cost of Electricity

LEMs Local Energy Markets

LV Low Voltage

MAS Multi-Agent System

MIDAS UK Met Office Integrated Data Archive System

P2C Peer-to-Community

P2P Peer-to-Peer

ReFLEX Responsive Flexibility

RES Renewable Energy Sources

RUL Remaining Useful Life

SCR Self Consumption Rate

SLES Smart Local Energy System

SoC State of Charge

SRR Self Sufficiency Rate

ToU Time of Use

TSOs Transmission System Operators

List of publications

2 first-author and 7 co-author of scientific publications in peer-reviewed journals, 3 articles published in peer-reviewed conference proceedings, 2 white papers on Energy Communities and Smart Local Energy System.

Original scientific peer-reviewed journal articles

1. B. Couraud, M. Andoni, V. Robu, **S. Norbu**, S. Chen, and D. Flynn, "Responsive FLEXibility: A smart local energy system," *Renewable and Sustainable Energy Reviews*, Volume 182, August 2023, 113343, ISSN 1364-0321, doi:https://doi.org/10.1016/j.rser.2023.113343

2. P. de Bekker, S. Cremers, **S. Norbu**, D. Flynn, and V. Robu, "Improving the Efficiency of Renewable Energy Assets by Optimizing the Matching of Supply and Demand Using a Smart Battery Scheduling Algorithm," *Energies*, vol. 16, no. 5, p. 2425, Mar. 2023, doi: 10.3390/en16052425.

3. S. Cremers, V. Robu, P. Zhang, M. Andoni, **S. Norbu**, and D. Flynn, "Efficient methods for approximating the Shapley value for asset sharing in energy communities," *Applied energy*, vol. 331, p. 120328, 2023, doi: 10.1016/j.apenergy.2022.120328.

4. D. Kirli, B. Couraud, V. Robu, M. Salgado-Bravo, **S. Norbu**, M. Andoni, I. Antonopoulos, M. Negrete-Pincetic, D. Flynn, and A. Kiprakis, "Smart contracts in energy systems: A systematic review of fundamental approaches and implementations," *Renewable & sustainable energy reviews*, vol. 158, p. 112013, 2022, doi:10.1016/j.rser.2021.112013.

5. B. Couraud, V. Robu, D. Flynn, M. Andoni, **S. Norbu**, and H. Quinard, "Real-Time Control of Distributed Batteries With Blockchain-Enabled Market Export Commitments," *IEEE transactions on sustainable energy*, vol. 13, no. 1, pp. 579–591, 2022, doi: 10.1109/TSTE.2021.3121444.

6. **S. Norbu**, B. Couraud, V. Robu, M. Andoni, and D. Flynn, "Modeling Economic Sharing of Joint Assets in Community Energy Projects Under LV Network Constraints," *IEEE access*, vol. 9, pp. 112019–112042, 2021, doi: 10.1109/ACCESS.2021.3103480.

7. **S. Norbu**, B. Couraud, V. Robu, M. Andoni, and D. Flynn, "Modelling the redistribution of benefits from joint investments in community energy projects," *Applied energy*, vol. 287, p. 116575, 2021, doi: 10.1016/j.apenergy.2021.116575.

8. M. Andoni, V. Robu, B. Couraud, W.-G. Fruh, **S. Norbu**, and D. Flynn, "Analysis of Strategic Renewable Energy, Grid and Storage Capacity Investments via Stackelberg-Cournot Modelling," *IEEE access*, vol. 9, pp. 37752–37771, 2021, doi: 10.1109/ACCESS.2021.3062981.

9. I. Antonopoulos, V. Robu, B. Couraud, D. Kirli, **S. Norbu**, A. Kiprakis, D. Flynn, S. Elizondo-Gonzalez, and S. Wattam, "Artificial intelligence and machine learning approaches to energy demand-side response: A systematic review," *Renewable & sustainable energy reviews*, vol. 130, p. 109899, 2020, doi: 10.1016/j.rser.2020.109899.

Articles in peer-reviewed conference proceedings

1. S. Cremers, V. Robu, D. Hofman, T. Naber, K. Zheng, and **S. Norbu**, "Efficient methods for approximating the Shapley value for asset sharing in energy communities," 2022. *In Proceedings of the Thirteenth ACM International Conference on Future Energy Systems (e-Energy '22)*. Association for Computing Machinery, New York, NY, USA, 320–324. https://doi.org/10.1145/3538637.3538861

2. B. Couraud, **S. Norbu**, M. Andoni, V. Robu, H. Gharavi and D. Flynn, "Optimal Residential Battery Scheduling with Asset Lifespan Consideration," 2020, *IEEE PES Innovative Smart Grid Technologies Europe (ISGT-Europe)*, The Hague, Netherlands, 2020, pp. 630-634, doi: 10.1109/ISGT-Europe47291.2020.9248889.

3. B. Couraud, P. Kumar, V. Robu, D. Jenkins, **S. Norbu**, D. Flynn, A.R. Abhyankar, "Assessment of Decentralized Reactive Power Control Strategies for Low Voltage PV Inverters," 2019, *8th International Conference on Power Systems (ICPS)*, Jaipur, India, 2019, pp. 1-6, doi: 10.1109/ICPS48983.2019.9067367.

Publications directed at societies of expertise

1. M. Andoni, **S. Norbu**, B. Couraud, D. Flynn, S. Chen, V. Robu, (2022). Decentralized Energy White Paper: Adaptive Local Energy Communities. University Of Glasgow. https://doi.org/10.36399/gla.pubs.278207

2. M. Andoni, **S. Norbu**, B. Couraud, D. Flynn, S. Chen, V. Robu, (2022). Democratising Energy: Placing citizens and communities at the heart of the energy revolution. University Of Glasgow. https://doi.org/10.36399/gla.pubs.278206

.

Chapter 1

Introduction

The decarbonization initiatives to achieve net-zero targets and the development of renewable and low carbon technologies are changing the electricity systems in UK and worldwide. A radical transformation towards more distributed, resilient, decarbonised and equitable energy systems has started at a global scale [1]. Access to affordable renewable energy resources (RES) represents a key element of an inclusive energy transition, represented as one of the core UN sustainable development goals [2]. Enhancing the use of locally-generated renewable energy is envisioned to reduce the energy system contribution to climate change [3], achieve net-zero [4], and speed up the transition to a low carbon economy [1]. This has led to an exponential growth in the deployment of RES. The increasing number of distributed energy resources (DERs) connected to low-voltage (LV) distribution networks is shifting the development of energy systems towards a more decentralized structure, enabling a significant shift in market power form large producers to individual prosumers (consumers with their own local renewable generation capacity and storage) [5].

A number of regions, such as the European Union [6] and the United Kingdom [7] are providing supportive regulations to encourage communities of prosumers to shift away from the dependence on centralized energy generation, and towards more decentralized and local energy generation and storage systems. A recent trend, emerging in both rural communities and smart city neighbourhoods, is for groups of household prosumers to form local energy communities that invest together in jointly owned renewable generation and storage systems, sharing the benefits from these assets. Examples include the Responsive Flexibility project on the Orkney Islands [8], the Brooklyn Microgrid project in the US [9], the Grid Friend project in Amsterdam North [10], and the many energy communities emerging in developing countries, such as Auroville [11] in India. Looking forward, such energy communities are expected to play a key role in building a more decentralised, decarbonised, and democratised energy system in which consumers use more locally-generated renewable energy, and take control of their energy supply.

The main research work presented in this thesis is relevant to the research fields of community energy systems, techno-economic data analysis and game theory. The research in this study is focused on the complex issue of how to achieve smart (optimal)

control of shared energy assets (including renewable generation and storage) in energy communities. This thesis provides a model that first studies the comparison of techno-economic benefits obtained when households/agents investment in their own distributed individually-owned energy assets versus investment in a larger jointly-owned community energy assets, considering the physical assets degradation and network/grid constraints. Based on the case study presented in this thesis,the benefits of a jointly-owned or pooled energy assets approach are evident. Next, the methodology in this thesis provides a several practically applicable and computationally efficient mechanism to redistribute the benefits obtained from these jointly-owned assets between homes in a fair way. The proposed redistribution mechanism makes use of the key concept of marginal value – borrowed from coalitional game theory and distributed AI (specifically, the multi-agent system), looking at what each member contributes to (and costs) the local community.

Mechanisms for real-time control of energy community assets from an economic and technical perspective is provided through the methodologies described in this thesis. Compared to existing work on energy communities, the research in this study investigates in greater detail the complex interdependencies within the system, such as using real state-of-the art battery control which incorporates the power flow (physical network/grid constraints), and physical degradation of the asset into the community energy optimization models. Moreover, the research in this study includes a full model of power flows in a LV distribution network describing an energy community, and, to the best of our understanding, work in this thesis represents one of the initial endeavours to explicitly model the effect of network constraints and curtailment imposed by the system operator to maintain LV network operational compliance. This is coupled to both the algorithm for the smart control of the battery and generation source, but also extends to the redistribution algorithm. This represents a significant and novel contribution to the current state of the art.

The final part of this thesis focuses on providing a framework for a local peer-to-community (P2C) market mechanisms. A crucial aspect of a community energy models and projects is that they often involve sharing of some joint resources and assets. One approach consists in creating a community energy coalition in the case of jointly-owned community energy assets. Another approach is to facilitate local P2C or peer-to-peer (P2P) trading in the case of individually-owned energy assets. The study is focussed mainly in exploring the suitable characteristics that makes the community with P2C local market mechanism profitable as compared to the previous setting of the community with jointly-owned community assets and individually-owned assets without P2C market mechanisms.

Furthermore, the proposed methods are all implemented and validated based on real commercially-available, dynamic tariffs from the UK market, as well as a whole year of high-granularity demand and renewable generation data. More specifically, the context of the research in this thesis is based on the Responsive Flexibility (ReFLEX) smart energy demonstrator project that aims to develop a large-scale demonstrator for community energy integration in Orkney, Scotland, UK [8]. This study is the largest whole system demonstrator project in the UK. Results and methodology are fully detailed to allow replication by other researchers. Given the topic of the thesis, it is intended to have

significant appeal to both the scientific communities, but also to decision makers in government, energy charities and industry, who have interests in an inclusive energy transition, particularly in implementing community energy schemes. First, it has a clear appeal to a number of scientific audiences and sub-audiences working in the energy space. To give some examples: for researchers working in battery monitoring for renewable energy integration, the community energy model provides a very attractive application area, and the work in this thesis is the first of a kind to integrate a network/grid constraints and battery depreciation model in community energy modelling. Moreover, for researchers interested in cooperative game theory application in energy (which is a growing research area), the model provided in this thesis is one of the first to use such concepts in a community energy setting. Specifically, the research in this thesis proposes a redistribution model for benefits in a community based on marginal value, a key concept in cooperative game theory.

The following sections of this Chapter 1 introduce the background area of topic, along with the aims, objectives and main contributions of the research work presented in this thesis.

1.1 Motivation and research question

Given the emergency our societies face against climate change, nations around the world have mandated net-zero emissions targets. The decarbonisation agenda includes a fundamental shift in generation and supply by moving away from centrally produced carbon-based fossil fuels towards local low-carbon and renewable DERs [4]. The increasing number of DERs is shifting the market power from large centralised utility companies to decentralised individual prosumers. These individual households/agents may also form communities and collaborate to optimise their resources or invest in renewable projects. Prosumers not only consume energy, but also produce energy from own assets (such as, wind turbine, solar PVs, EVs, and batteries) and inject it back to the grid. On top of consumer empowerment, which is expected to play a greater role in future energy systems, the energy transition is also enabled by the integration of ICT and data technologies to energy systems, which are providing new opportunities for more efficient operation of energy systems [12]. For transmission system operators (TSOs) and distribution system operators (DSOs), this increasing trend and local place-based energy transitions means that generation and demand are more closely located, which could enable more local resilience to failures in the power system if local flexibility such as storage is adequately incentivized.

However, the increase in penetration of distributed generation results in new challenges for the operation of distribution networks. A key challenge with RES generators is that they are intermittent, small-sized and distributed across the distribution network. They are gradually transforming networks into active and two-way energy flow networks, crucially challenging the way they are traditionally designed and managed. For instance, power flows become reversed and the distribution network is no longer a passive circuit supplying loads but becomes an active system with power flows and voltages determined by the local embedded generation output as well as the loads [13]. Voltage out-of-bounds excursions

(i.e. temporary fluctuations of voltage outside safe accepted limits, often determined by regulation) are an example of the new challenges for the DSOs face when managing the network in real-time.

In addition to the challenges faced by DSOs, the increasing electricity retail prices and decreasing feed-in tariff rates have reduced the incentives for household and business consumers to invest in distributed renewable energy sources. While feed-in-tariffs support has led to fast embedded renewable adoption, they are also a very expensive, and hence financially unsustainable support mechanism in the long-term. As a consequence, in many developed countries worldwide (such as the UK or the EU), guaranteed FITs for renewable electricity generated by small DERs are being phased out as a support mechanism, i.e. they are gradually reduced or are well below retail tariffs available from large operators [14]. For instance, in the UK, FITs are no longer available to producers of any size since 31^{st} March 2019 [15]. Still, the energy transition that has started in many countries requires households to keep investing in renewable energy generation. This is increasingly leading to a need for establishing a consumer-centric business models (incentives) with substantial innovation in the way the local networks are managed and balanced. This has led to the emergence of smart local energy system (SLES) and transactive energy models such as energy communities and local energy markets (LEMs) where household and business prosumers aim to maximize behind-the-meter self-consumption from local renewable generation to make DERs more profitable [16]. Proliferation of prosumers and DERs are leading to a radical transformation of the centralised energy system into becoming more decentralised, volatile and harder to manage. Consumer-centred transactive energy models such as energy communities and LEMs are emerging as promising methods to coordinate generation, storage, and demand-side flexibility in a local area. In this context, how local energy systems are designed and shared, are open research questions that require novel modelling paradigms that place end-users in the centre of the decision-making for the energy system.

Smart local energy systems consist in energy systems that connects different energy assets, infrastructures, and demand of energy services in a local area, and provide value locally in an intelligent way [17]. SLES provides multi-vector (i.e encompassing electricity, heat & transport) energy system that utilizes digitalization as key enabler for achieving distributed generation and flexibility from low-carbon energy sources. SLES may be connected to the national energy system and aim to deliver a clean, fair and reliable energy sources to local consumers. These systems adapt the local context and leverage innovative technologies, such as Big Data Analysis, machine learning, IoT or blockchain technologies that favour the local economy and social development by promoting local initiatives, such as local production, energy management and energy exchanges [18]. An energy community is made up of a number of individual prosumers connected to a low-voltage distribution network, usually behind the same primary sub-station. Prosumer assets (i.e. renewable generation capacity and storage) can be either distributed at individual households or centrally installed and thus shared within the community. LEMs provide a way for local prosumers to sell electricity to other members of the community, through

specific local market mechanisms such as P2C or P2P energy trading markets [19]. Designs of LEMs solutions and citizen-led energy communities differ widely in the literature and are topics of intensive research. Generally, potential benefits of LEMs and SLES provide opportunities for revenue generation or cost reduction for end-users and local communities and enable market access to small-scale generation and storage, which may untap the value of demand-side flexibility and improve wider network and system management, but depend on the market design.

A key research area in this context is the development of appropriate community schemes and control strategies for optimal scheduling of end-user production and consumption. Therefore, there is an increasing interest from academics and industry in community energy models for the optimization of self-consumption [20] in community microgrids. Recently, several community energy projects have emerged in the UK, the EU and worldwide. For instance, In the UK, Community Energy Scotland (a key local organization supporting the development community energy projects) lists more than 300 community energy projects on their website [21]. Similar rising trends in smart energy community initiatives can be seen across the United States (such as the Brooklyn Microgrid project [9]), and across Europe (refer [22] for an overview). An area of focus for policy makers is empowering communities with the development of innovative and integrated local energy systems and networks as identified in the Scottish Energy Strategy [23]. In a similar fashion, the UK government has committed to an extensive program to support SLES initiatives and projects in order to reduce, purchase, manage and generate energy by identifying clean growth as one of the four grand challenges in the UK's Industrial Strategy [24]. These policy initiatives show that governments have an instrumental interest in SLES and seek to facilitate consumer-led, transformational and sustainable energy transitions. Furthermore, the number of deployed and planned SLES demonstrator projects has increased rapidly in the UK and worldwide. ReFLEX (Responsive Flexibility) [8] based in Orkey island Scotland is one such initiative representing the largest SLES demonstration and 'living lab' projects in UK. Another such active SLES demonstrator project is Energy Superhub Oxford (ESO) [25] project that reduces the stress on the grid locally by integrating smart EV charging, hybrid battery energy storage, low carbon heating and smart energy management technologies. Similarly, Project Leo (local Energy Oxfordshire) [26] is another active project that uses local flexibility to manage grid constraints and provide routes to market and investment models supporting local renewable and distributed power generation. These SLES demonstrator projects bring together the academia and relevant industries to explore the innovation in local technology, markets and communities. This clearly shows that the SLES scheme is an active area of research not only from academia but also a strong drive from industry.

The main aim of such energy community microgrids is to increase the financial benefits and the local consumption. In turn, this enables the community to use more locally generated renewable generation, and shifts the market power from large utility companies to individual prosumers. From the grid manager point of view, local energy communities are also an incentive to increase local self-consumption, which will reduce the technical

impacts of low carbon technologies on the grid, such as voltage violations. As a result, energy communities are identified as a promising technical, social and economical solution to the energy transition providing both incentives and technical solutions to the adoption of low carbon technologies. Recently, this aspect of the local energy communities has led regulatory bodies to implement frameworks that incentivise the deployment of such energy communities [27]. For instance, in France, citizens living in an area determined by a diameter of approximately 2km are allowed to gather into local energy communities for a total power that does not exceed 3MW [28].

A crucial aspect of transactive energy models and community energy projects is that they often involve sharing of some joint resources and assets. One approach is to facilitate local energy market mechanisms in the case of individually-owned assets, in which prosumers invest in their own energy assets (such as solar PV panels, wind turbine, and or battery storage) and buy and sell energy with their neighbours directly, based on their individually-owned assets. In this scenario, each prosumer is metered separately and pays the value of its *net metered* electricity demand (demand after using its generation and storage capacity). Local energy markets, allow energy communities with individually-owned assets to trade electricity to other members of the community, through a specific market mechanism [29]. Market mechanisms can either implement a full P2P market, which ensures that a community member "*A*" is trading electricity to another community member "*B*", with solutions such as in automated negotiations schemes [19], or can implement a P2C scheme, in which case electricity from a specific community member is traded to the community, without knowing exactly who will benefit from this electricity, such as what is achieved through double auction market clearing mechanisms [30].

Another approach consists in creating a community energy coalition in the case of jointly-owned community energy assets, where an aggregator or community energy operator is responsible for managing and distributing the benefits from shared assets to members of the community. Here, the whole community is *"behind the meter"*, i.e. pays for the net demand of the entire community over the billing period. A successful examples of such transactive energy models include the "Ecovillage" of Findhorn in Scotland, UK [31], Grid Friend project in Amsterdam North [10], and the many energy communities emerging in developing countries, such as Auroville in India [11]. While energy communities are a promising concept, a key challenge is how these assets can be efficiently controlled in real time, how the useful lifetime of the asset can be modelled and enhanced using AI, and how the energy outputs from these jointly-owned community assets should be shared fairly among community members, given that not all members have the same size, energy needs or demand profiles.

The physical network (the LV distribution grid) is an essential entity that allows the exchange of energy in the settings of the energy communities. However, an important aspect that has often been neglected in existing research on energy community models is the relevance of the distribution grid's technical limits. Installation of renewable generator (solar PV/wind turbine) or batteries in the grid changes power flows, and might create congestions, voltage excursions, or line over-heating. In such cases, the grid operator

might consider the need for an Active Network Management (ANM) to remotely control the injection of distributed renewable generator and storage assets. Therefore, due to this congestion/voltage excursion, assets might be prevented from exporting/consuming to/from the grid, reducing the benefits from their owners. For instance, when the grid is constrained with voltage excursions, then the exports form PV/wind turbine and exports/imports from/to battery can be curtailed as it is currently the case in Orkney Islands [32], UK. Therefore, such curtailment events need to be accounted for in the energy community setting by including power flow (physical network/grid constraints) in the techno-economic analysis. For example, in most of the prior literature, the studied models of energy communities do not consider the impact of physical network constraints in the assessment of the techno-economic benefits of community-owned energy assets compared to individually-owned energy assets.

Another challenge is that management of energy community assets consisting of renewable generation and storage (integrated renewable energy systems) require careful consideration of assets' cost, sizing and operation, such as to maximize their Remaining Useful Lifetime (RUL), and hence return on investment. Technically, for instance, the depth to which a battery is discharged, the discharge current and the chemistry used has a direct effect on its remaining useful lifetime. This translates into a considerable impact on the total cost of operation and maintenance of the battery, especially as energy storage is one of the most expensive components of an integrated renewable energy system. Moreover, the frequent charging and discharging operations leads to cyclic ageing and incurs an extra cost as it accelerates the depreciation of the battery. Along with the fact that batteries' lifetime is comparatively shorter than that of renewable generators, this highlights the importance of using an appropriate battery control mechanism to extend the system's useful life. In most of the literature reviewed, studies show that the community battery storage system offers higher benefits as compared to individual household distributed batteries [33, 16, 34–36]. However, most of existing studies, to our knowledge, do not consider the battery degradation cost when determining the optimal battery capacity. The battery lifetime depends on the charge/discharge cycles, which in turn are shaped by the control scheme. Thus, there is a need to accurately estimate the depreciation of the battery from the operating profiles and therefore assess the operational cost and overall economic value of an integrated renewable renewable energy system.

Furthermore, although higher benefits can be achieved by investing in community assets, how to redistribute these benefits among the individual households in the community still remains a key open question, of both research and practical interest. Current energy communities usually employ algorithms based on proportionality of consumption to redistribute the benefits from the community-owned generator assets. However, such methods are not fair (they provide an inherent advantage to large consumers), and not applicable in the case of energy storage assets, where the proportionality of the asset usage does not apply. Hence, there is a need to design an efficient and fair redistribution mechanisms that applies to both community-owned renewable generator and storage assets, while incorporating the asset's degradation, and the physical network and operational

constraints. Specifically, the prosumers share the outputs of jointly-owned energy assets, as well as the energy bill for the aggregate residual demand, i.e. the part of the demand not covered by the local generation and storage assets. Therefore, the community aggregator is not only responsible for the control and distribution of energy in the community but also for allocating any revenues from exporting energy and the bills of the residual demand. Clearly, one of the key challenges in this setting is the redistribution of such costs and benefits to the prosumers in a *fair* way.

Cooperative (or coalitional) game theory has long studied such redistribution problems in a wide variety of systems. Game theory provides an insightful analytical and conceptual framework along with mathematical tools to study and analyse the complex interaction among independent rational players (in the case of this thesis, the households/agents) [37]. In the context of decentralized energy systems, coalitional game theory has been identified as a promising solution for designing incentive mechanisms for community energy trading and sharing. In a cooperative/coalitional game, players form coalitions to maximise a common objective for mutual benefit. Then, the benefit is distributed equally or fairly among themselves using incentive-based solution concepts, such as the Shapley value [38]. Recently, the Shapley value has begun receiving substantial attention in the energy applications – with a rapid increase in the number of papers using Shapley value in energy systems (detail review presented in Chapter 2). However, a major challenge faced by community energy schemes utilising coalition game theory is the issue of scalability [39, 40]. Specifically, when determining the Shapley values in a coalition, the computation becomes highly complex and time-consuming, as the number of players increases in the coalition, making an exact computation intractable beyond a small number of agents. Moreover, most of the existing redistribution frameworks are developed without considering network constraints, in which case the computation becomes more challenging. Thus, there is still a need to develop a redistribution mechanism that is fair, but also provide tractable computational performance that scales well with the increasing number of members in the energy community coalition, while considering operational network constraints.

This thesis explores the expanding range of opportunities that arise when citizens join forces to form an energy community. The main objective is to optimize the generation, consumption and storage of energy within such communities. Several modelling tools, solutions and frameworks for SLES and energy communities are provided in this context. Specifically, a techno-economic modelling tools that enables real-time controls and fair sharing of renewable energy resources subjected to physical assets degradation and network constraints. Findings of this study are related to a number of strands including community energy system research and cooperative game-theoretic applications for energy systems, but also to the area of electrical engineering and physical asset health monitoring of batteries. Finally, as part of the contributions of this thesis, the proposed methods are implemented in realistic community case studies, both in terms of demand, generation, tariffs and battery data used, and in terms of size (up to 200 households), granularity and duration (half-hourly data over a whole year). More specifically, the context of the research in this thesis is based on the Responsive Flexibility (ReFLEX) smart energy demonstrator

project that aims to develop a large-scale demonstrator for community energy integration in Orkney, Scotland, UK [8]. This provides a highly realistic case study to provide confidence in the robustness of all the experimental comparison results presented in this thesis.

Relevant literature to this vein of work is discussed in great detail in Chapter 2. Next, the research aims and objectives are presented along with a summary of the main contributions of the work undertaken for the completion of this thesis.

1.2 Research objectives and contributions

The previous section introduced the broader topic area, major challenges and problem statement of the research work presented in this thesis. In this section, the reader can find a detail discussion on the specific research objectives and the novelty of the research work undertaken in the context of this thesis.

The main objective of this thesis is *to explore new optimization, smart control strategies and fair sharing of renewable resources in energy communities using the tools from distributed AI (specifically multi-agent systems) and cooperative game theory, incorporating the physical assets, network/grid and operational constraints.* The specific goals contributing towards the main broader objectives can be summarised in to the following:

- The thesis aims to provide an in-depth review of **state of the art research and practice in the field of smart local energy system (SLES) and transactive energy models focused on energy communities and local energy markets (LEMs) such as P2C or P2P energy trading schemes.** The review aims to presents the significance of the identified research topic and how it fits to the broader context of the thematic research area of resilient local or community energy systems.

- Primarily, this thesis aims to address the three major research problems identified to align the focus to thematic research area of local resilient community energy system. First, the **Optimization Problem:** the need for AI techniques and smart real-time control strategies for optimal scheduling of local generation and consumption, battery charging/discharging control, selection of pricing schemes, agent strategies and demand response.

- Second, the **Impact Problem:** the need to assess the various impact of the proposed new solutions to the existing electrical grid/network utilization, power quality, network constraints and the overall distribution system planning and operation. Specifically, the need to include the network/grid constraints in the development of new solutions for SLES system and transactive energy models.

- Third, the **Incentive Design Problem:** the need to explore the potential of game theoretic models and tools from distributed AI (specifically the multi-agent systems) to design appropriate incentive mechanisms and consumer-centred business models that are tailored to local communities and end-user needs.

- Finally, the thesis aims **to demonstrate the application of the developed theoretical models in real-world community settings**. To achieve this, the proposed methods will be implemented and validated using a real case study from the UK-based smart local energy demonstration projects using real commercially available, dynamic tariffs from the UK market, as well as a whole year of high-granularity demand and renewable generation data.

With these objectives in mind, this thesis developed several models and outputs, the findings of which can be related to fields of smart local energy systems, energy economics, distributed AI (specifically, the multi-agent systems), cooperative game-theoretic applications for energy systems, but also to the area of electrical engineering and physical asset health monitoring of batteries. The main contributions and outputs of the work are summarised in the following summary statements:

- First, this thesis provided a principled model of community investment and sharing of energy assets, such as renewable generation and battery storage. More specifically, research is focused on the techno-economic comparison between two configurations of energy communities connected to a low-voltage distribution network. Initially, the study considers a configuration with individually-owned distributed energy assets, such as solar PV and residential batteries. Then, a second configuration in which distributed energy assets are jointly-owned by the community, and installed in a single location. The proposed two configurations of energy communities are compared by studying the economic impacts of installing various energy assets on the grid for both fixed and dynamic time of use (ToU) tariffs.

- Secondly, this thesis provided the modelling of single prosumer and energy community control algorithm for maximization of the self-consumption behind the meter by incorporating the latest heuristics of battery state of health into such control algorithm, both at individual prosumer and community level. A battery degradation model is integrated with renewable energy optimization by considering the battery depth of discharge in each control cycle. To achieve this, the control scheme employs a battery state of health degradation model based on the battery depth of discharge in each control cycle. The proposed control algorithm takes into consideration the battery's depreciation cost, which is determined by the accurate enumeration of battery cycles, including partial cycling i.e. battery cycles that do not start or end at 100% of SoC.

- Then, the control algorithm is extended to incorporate the effects of network/grid constraints and curtailment imposed by the system operator to maintain the LV network operational compliance. In practice, the addition of solar PV or batteries in the LV grid changes power flows, and might create congestions or voltage excursions (i.e temporary fluctuations of voltage outside safe accepted limits). Therefore, due to this congestion/voltage excursion, assets might be prevented from exporting/consuming to/from the grid, reducing the benefits from their owners. Most of the current

state-of-the-art community energy models do not or rarely consider physical LV network constraints in their modelling. To our knowledge, the model in this thesis is the first that considers such curtailment events in the energy community setting by including the power flow (network/grid constraints) in techno-economic analysis of investment in distributed individually-owned energy assets versus jointly-owned community assets.

- Next, inspired by coalitional game theory methods, this thesis provided a novel algorithm to fairly redistribute among community members the benefits obtained from jointly-owned community energy assets, which is shown to have desirable redistribution and computational benefits, compared to existing methods for sharing output of community owned energy assets. This thesis have explored a number of benefit redistribution schemes (four in total, based on different parameters). Some are intuitive and based on current practice, but we also proposed one based on the marginal contribution, a key coalitional game-theoretic principle, an established methodology for designing redistribution schemes in a number of practical domains. Results from the study shows that the proposed marginal cost redistribution mechanism achieves better performance than the others and it is also computationally tractable. These are assessed in different scenarios and on a number of criteria, ranging from costs and financial benefits to each prosumer, and correlation with intermittent renewable output. The computation of savings from the proposed redistribution schemes for various prosumer sizes has been conducted. The assessment includes evaluating fairness and examining the impact of different redistribution schemes on the potential uptake of renewable in energy communities. Furthermore, this thesis has proposed an approximated marginal cost redistribution method to address the computational challenge while considering the network/grid constraints. The results showed that the individual agents' yearly bills obtained after redistribution by approximated marginal cost redistribution method are similar to results obtained by redistribution mechanism without approximation, with the correlation coefficient of 99.99% for both the fixed and dynamic tariffs. Hence, while considering the network constraints, approximated marginal cost redistribution method can be used to redistribute the benefits from community owned assets, as it is much more computationally tractable particularly while considering the large realistically-sized community settings. This represents a significant contribution to the state-of-the-art.

- Next, this thesis proposed a novel framework for peer-to-community (P2C) local market mechanism to share and trade energy in the case with individually-owned energy assets. A multi-unit auction market clearing mechanism is proposed. There are indeed auctions every half-hourly of the operation, but there is one multi-unit auction where the price (pence) per unit (kWh) is averaged for each unit. Within the proposed P2C market mechanism, an assumption is made that each consumer is obligated to meet their energy demands, drawing from either the grid or the local P2C market. To ensure fairness in cost sharing, the approach adopted involves averaging

over the multiple price units in that market.To incentivize households to participate in local energy trading, such as P2C or P2P local markets, a proposed approach ensures the fair distribution of the total energy available for the P2C local market among the buyers and sellers. Furthermore, this thesis explored several settings of the community to understand the suitable characteristics of the community that makes the community with P2C local markets profitable as compared to centrally shared community projects.

- Finally, the proposed energy community model is implemented and validated using a real case study from large-scale ReFLEX (Responsive Flexibility) smart energy demonstrator project based on the islands of Orkney, Scotland, UK [8], one of the UK's largest smart local energy demonstrator project. To our best knowledge, this thesis models the control of energy community assets from an economic and technical perspective with an unprecedented level of detail. This includes for example, incorporating real state-of-the-art battery control and degradation functions, using real commercially-available, dynamic tariffs from the UK market, as well as a whole year of high-granularity demand and renewable generation data. Additionally, the results of the thesis have been shared with industrial stakeholders involved in implementing real community energy schemes. They expressed considerable interest in the findings and found the information to be valuable and informative for their ongoing projects. Although, while the experiments and validation are based on the UK project, the proposed community energy methods are general in scope, and can apply to any country where such community energy schemes are undertaken. The concept of energy communities is equally important - arguably even more so - in developing countries, where energy users in such communities often have limited or no access to electricity from a central power grid, and hence rely on the community energy project for their power needs. The following section presents the outline of the thesis report.

1.3 Thesis organization

Chapter 1 has so far presented an introduction and the research motivation of the topic of this thesis. It highlights the energy landscape of current and future energy systems, where prosumers with distributed energy resources play a key role in deregulation of energy markets. Specifically, Chapter 1 introduces the transactive energy models and elaborates on the need for real-time control strategies and fair redistribution mechanisms incorporating the network/grid and operational constraints, two key topics that form the core research of this thesis. Research aims and objectives are presented in detail along with a summary of the novelty and main contributions of this research work.

Chapter 2 of this thesis presents relevant literature reviews on the topics of SLES, modelling of local energy communities and prosumer, sharing mechanisms in energy communities, and modelling of physical network constraints. The significance of the

identified research topic and how it fits to the broader context of the thematic research area of resilient local or community energy systems is explored through an extensive literature survey presented in this Chapter 2.

In Chapter 3, a single prosumer model along with the battery control algorithm, and deprecation model is described. Chapter 3 focuses mainly on the integration of battery degradation model and renewable energy optimization. Finally, this chapter also describes a detail techno-economic study of behind-the-meter batteries for a single prosumer, and discusses future scenarios in which batteries would become more profitable. The model inputs, tariff structures, unitary cost of energy assets and the battery depreciation aspects described in this Chapter 3 is applied to the community setting described in the following Chapter 4, 5, and 6. Furthermore, the battery control algorithm described in this Chapter 3 is applied to each 200 individual agents as well as the aggregated community described in Chapter 4 and 6. The same battery control algorithm is modified in Chapter 5 by incorporating the voltage control mechanism to include the network constraints.

Chapter 4 presents a principled model of community investment and sharing of energy assets for both fixed and dynamic tariffs. This includes a comprehensive data-driven techno-economic analysis to quantify savings of community-owned versus individually-owned energy assets. Then, a mechanism design for fair redistribution of benefits from community-owned assets to individual households is provided. Chapter 4 explores a variety of benefit redistribution schemes (four in total), each based on different parameters. Some are intuitive and based on current practice, but this thesis also proposed one based on the marginal contribution, a key coalitional game-theoretic principle. The results demonstrate that this novel approach outperforms the other methods while remaining computationally tractable. Furthermore, the optimal capacity for both individual assets and jointly-owned community assets obtained in this Chapter 4 is applied to the community setting described in following Chapter 5.

In Chapter 5, the energy community model is extended by incorporating the physical network/grid and operational constraints. Chapter 5 studies the effect of network constraints and curtailment events in the energy community setting by including the power flow (network/grid constraints) in techno-economic analysis of investment in distributed individually-owned energy assets versus jointly-owned community assets. Furthermore, Chapter 5 discusses the savings of the proposed benefit redistribution schemes for different sizes of prosumers, and asses the effect of physical network/grid and operational constraints on computational tractability of different redistribution schemes.

Chapter 6 studies the added value of facilitating local peer-to-community (P2C) market mechanism for the energy community with distributed individually-owned energy assets. This Chapter 6 of the thesis presents local P2C market based on centrally operated mechanism, in which a community aggregator determines each trade's characteristics (price and quantity) by running the multi-unit auction. The dynamics of the P2C market mechanism is studied for three different type of P2C sellers (non-uniform pricing scheme) and tested for three different types of community settings (mix of prosumers and consumers) under different rates of renewable energy adoption.

Finally, the thesis is concluded in Chapter 7, where key findings of the thesis work are summarised. Directions on future work are also outlined in this final chapter of the thesis.

Additional materials and information on the methodology and data used in this thesis are shown in the Appendix A.

Chapter 2

Background and related work

Chapter 2 discusses prior research works that are most related to the scope of the thesis, as found in the literature survey. Specifically, Chapter 2 presents the state of the art research and practice in the field of smart local energy system (SLES) focused on energy communities and local energy markets (LEMs) such as Peer-to-Peer (P2P) energy trading schemes. An extensive review of state-of-the-art research that models prosumers and energy communities with renewable generation and storage assets is presented, as this is the base of the work proposed in this thesis. Furthermore, this chapter highlights the key current research gaps such as need for a fair and computationally tractable redistribution schemes for energy communities, need for the integration of physical assets degradation and network constraints in community optimization models, and need for robust P2P market dynamics that exhibit acceptable characteristics such as fair market clearing mechanisms.

2.1 State of the art in smart local energy system (SLES)

Net-zero targets and development of low carbon technologies are changing electricity systems. Proliferation of prosumers (i.e. consumers with micro generation and/or storage) and distributed energy resources (DERs) are leading to a radical transformation of the centralised energy system into becoming more decentralised, volatile and harder to manage. Smart Local Energy Systems (SLES) consist in energy systems that connects different energy assets, infrastructures, and demand of energy services in a local area, and provide value locally in an intelligent way [17]. The SLES concept models multi-vector (i.e encompassing electricity, heat & transport) energy system, that utilizes digitalization as key enabler for achieving distributed generation and flexibility from low-carbon energy sources. SLES may be connected to the national energy system and aim to deliver a clean, fair and reliable energy sources to local consumers. These systems adapt the local context and leverage innovative technologies, such as big data analysis, machine learning, IoT or blockchain technologies that favour the local economy and social development by promoting local initiatives, such as local production, energy management and energy exchanges [18].

SLES such as local energy communities and LEMs are emerging as promising new methods to coordinate generation, storage, and demand-side flexibility in a local area [41]. In energy communities, end-users may trade energy with each other or invest in shared-ownership assets, such as production units, energy storage, or shared network infrastructure [42]. LEMs provide a way for local prosumers to sell electricity to other members of the community, through specific local market mechanisms such as P2P energy trading markets [19]. Designs of LEMs solutions and citizen-led energy communities differ widely in the literature and are topics of intensive research.

Local or community energy models consist of a group of households that are able to generate, store and trade energy with each other. This has led to decentralised energy systems with significant shift in the market power from large utility companies to individual prosumers [43]. This local place-based energy transition means that the generation and consumption are more closely located, which could enable more local resiliency to failures in the power system. Hence, there has been a growing effort in the U.K and the world at large to enhance the local energy resiliency, particularly at the community level [4]. An area of focus for policy makers is empowering communities with the development of innovative and integrated local energy systems and networks as identified in the Scottish Energy Strategy [23]. In a similar fashion, the UK government has committed to an extensive program to support SLES initiatives and projects in order to reduce, purchase, manage and generate energy by identifying clean growth as one of the four grand challenges in the UK's Industrial Strategy [24]. Similar rising trends in smart energy community initiatives can be seen across the United States (such as the Brooklyn Microgrid project [9]), and across Europe (see [22] for an overview). These policy initiatives show that governments have an instrumental interest in SLES and seek to facilitate consumer-led, transformational and sustainable energy transitions. Therefore, there is an increasing interest from academics and industry in the development of appropriate SLES schemes.

SLES schemes are a fast-growing area of research that have gained increased attention in the literature. For instance, the relevant literature identified using the Scopus search engine shows that the number of scientific publications on the subject has seen an increasing order of magnitude (around 10 times), between 2012 and 2021, as shown in Figure 2.1. The Scopus search engine is the largest abstract and citation database of peer-reviewed literature. The queries used in the search engine are: "Local AND Energy System", "Energy AND Communities", "Local AND Energy Market". All the results obtained from Scopus' queries have been carefully reviewed and filtered to include the papers related to SLES only, not just part of the wider energy domain.

Power, transport and heat are the three main energy vectors that are expected to be fully decarbonized to achieve a realistic and sustainable net-zero energy system [45]. This low-carbon energy transition calls for a significant adoption of DERs and electricity-based loads such as electric vehicles (EVs) and heat pumps. The connection of these intermittent DERs and electricity-based loads to physical network (low-voltage grid) changes the power and increases the local voltage out-of-bounds excursion, line over-heating and congestion at the distribution grid level. To lower these impacts, distribution system

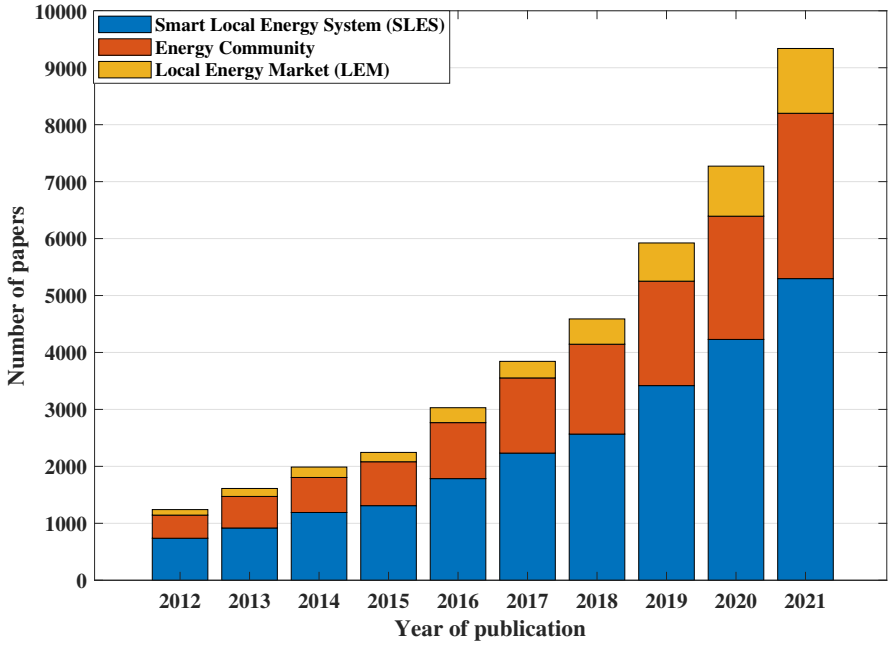

Figure 2.1: Evolution of scientific publications related to smart local energy system (SLES) based on the Scopus search engine [44].

operators (DSOs) can enforce curtailment of local renewable generation at times of out-of-bounds deviations, otherwise DSOs must resolve with expensive and lengthy traditional solution of grid reinforcement. SLES such as local flexibility markets are identified as a promising low-cost solutions to address these grid issues as an alternative option to expensive grid reinforcement and unnecessary curtailment [46]. Furthermore, in addition to achieving the desired decarbonization and providing the grid services, SLES provides resilience and reliability by enabling distributed assets to supply local consumers in case of disconnection with the main grid. This requires SLES to include a diversity of energy production assets and to have the ability to manage these local assets to ensure robust operation in islanded mode [47].

The empowerment of local communities to actively manage their own energy system is at the heart of SLES, that also seek to develop local employment opportunities, local redistribution of wealth and local energy services in line with community values. Recently, the SLES scheme has gained increased attention from social perceptive focussed on social-technical transition of the energy system. For instance, Ford *et al.* [18] have explored the socio-technical transition and its impacts of SLES as compared to the already adopted centralised energy system. Their study shows that the most important challenges in the transition to digitalization and decentralization are non-technical, including the fact that the local actors (local authorities and stakeholders) participation may face strong resistance of change from dominant incumbents, and they stress that the social barrier can be more challenging than the technical barrier in the successful implementation of SLES. A recent study by Walker *et al.* [48] focused on placed-based narratives, specifically to explore and understand the term 'local' in the context of SLES. The study highlights that the 'local' is

project specific defined by placed-based and geo-spatial boundaries. It recommends that a well-defined collective place-based approach is crucial in understanding of how SLES can leverage both 'smart' and 'local' elements, within a system boundary, to deliver additional value and co-benefits to that locality.

Rae *et al*. [49] have conducted a detailed review of the key technical barriers that have been identified during the planning and operating phases of the SLES schemes in UK. Technical barriers correspond to characteristics of engineering systems or services that are critical for successful SLES deployment, but have been highlighted as difficult to achieve. Multi-vector integration, grid connection, energy storage systems, smart technology and adoption of EVs were the key barriers identified in the review. According to their study, diversity, uncertainty and integration are the three fundamental technical challenges faced in achieving the successful implementation and adoption of new technologies in those key identified areas. Similarly, Knox *et al*. [50] have reviewed the various antecedents of energy justice in SLES and the role of smart technology can play in mitigating these (in) justices. They have identified various frameworks for social impacts of SLES, and one of the highlights closely related to our work is the importance of fairness and equability of realised benefits. Equal and balanced redistribution of costs and benefits among the community members is identified as one of the hearts of the energy justice in SLES. Vendantham *et al*. [51] have provided an overview of the information and communication technology (ICT) infrastructures associated with SLES. Likewise, Vigurs *et al*. [52] have reviewed various privacy concerns in sharing data in SLES. These studies highlights the need for more investment in ICT infrastructures and data management system for the successful implementation of the SLES. It recommends the development of appropriate data storage solutions to enable data access to relevant stakeholders, and favouring open access to data and scripts.

Morstyn *et al*. [53] have provided an energy management software tool to support SLES, the Open Platform for Energy Networks (OPEN) which is an open-source Python based platform for testing SLES management applications. This clearly shows that the SLES scheme is an active area of research not only from academia but also a strong drive from industry. Recently, the number of deployed and planned SLES demonstrator projects has increased rapidly in the UK and worldwide. ReFLEX (Responsive Flexibility) [8] based in Orkey island Scotland is one such initiative representing the largest SLES demonstration and 'living lab' projects in UK. Recently, Benoit *et al*. [54] provides a detail frameworks and comprehensive list of smart local energy systems key performance indicators (KPI), and lessons learnt from ReFLEX. The key lessons learned from the ReFLEX project are:

- **Integration challenges:** Renewable energy projects often face challenges related to integrating different energy sources, such as wind, solar, and energy storage, into the existing grid infrastructure. Lessons learned from previous projects include the importance of planning for grid stability, grid management, and the need for flexible and scalable solutions.

- **Community engagement:** Engaging with local communities and stakeholders is crucial for the success of renewable energy projects. Lessons learned emphasize the importance of early and ongoing engagement to address concerns, build trust, and ensure community acceptance.

- **Regulatory and policy frameworks:** The regulatory and policy environment plays a significant role in facilitating or hindering renewable energy projects. Lessons learned highlight the importance of stable and supportive regulatory frameworks, clear permitting processes, and consistent policies to encourage investment and innovation.

Another such active SLES demonstrator project is Energy Superhub Oxford (ESO) [25] project that reduces the stress on the grid locally by integrating smart EV charging, hybrid battery energy storage, low carbon heating and smart energy management technologies. The following are key findings that have emerged from the project:

- **Holistic approach:** ESO highlights the importance of taking a holistic approach to energy systems planning and implementation. By integrating various technologies and sectors such as renewable energy, battery storage, electric vehicles, and heat pumps, ESO aims to optimize energy generation, distribution, and usage. The project emphasizes the need to consider multiple facets of the energy system simultaneously to maximize efficiency and carbon reduction.

- **Scalability and replicability:** ESO serves as a testbed for scalable and replicable energy solutions. The project's focus on deploying modular systems allows for easier replication in different locations. Lessons learned from ESO can potentially be applied to similar urban environments or other communities seeking to decarbonize their energy systems. The project's design, technology selection, and operational practices can be fine-tuned and adjusted for different settings, promoting wider adoption of low-carbon energy solutions.

- **Grid flexibility and resilience:** ESO recognizes the importance of grid flexibility and resilience when integrating high levels of intermittent renewable energy sources. The project aims to explore the role of battery storage systems in managing energy supply-demand imbalances and providing grid stability. ESO's experience can provide insights into grid management strategies, demand response mechanisms, and storage optimization, enabling a smoother integration of renewable energy into existing grids.

- **Data and analytics:** ESO emphasizes the value of data collection, analysis, and modeling to optimize energy system performance. By gathering real-time data from various energy assets, ESO can analyze system behaviour, identify patterns, and develop predictive models. These data-driven insights can be used to optimize energy dispatch, storage utilization, and demand-side management, leading to improved energy efficiency and cost savings.

- **Stakeholder engagement:** ESO recognizes the importance of engaging stakeholders throughout the project lifecycle. Collaboration between researchers, industry partners, policymakers, and the local community is crucial for successful implementation and acceptance of new energy technologies. The project highlights the need for effective communication, awareness campaigns, and involvement of end-users in shaping the future energy landscape.

Similarly, Project Leo (local Energy Oxfordshire) [26] is another active project that uses local flexibility to manage grid constraints and provide routes to market and investment models supporting local renewable and distributed power generation. The following lessons represent key takeaways from the project:

- **Local energy marketplaces:** Project Leo has developed a local energy marketplace that allows residents and businesses to trade energy directly with each other. This lesson highlights the potential of localized energy markets in enabling peer-to-peer energy transactions, fostering community engagement, and promoting the use of renewable energy sources.
- **Energy flexibility and demand response:** The project has implemented energy flexibility and demand response mechanisms to optimize energy consumption based on supply and demand conditions. This approach helps balance the grid, reduce peak demand, and increase the integration of renewable energy sources.
- **Virtual power plants:** Project Leo has demonstrated the concept of virtual power plants, where multiple decentralized energy resources are aggregated and coordinated to operate as a unified entity. This lesson showcases the potential of virtual power plants in enhancing grid stability, optimizing energy dispatch, and maximizing the value of distributed energy resources.
- **Local energy tariffs:** The project has explored the development of innovative local energy tariffs that incentivize energy efficiency, renewable energy generation, and demand response behaviours. This highlights the importance of designing pricing structures that align with local energy goals and encourage sustainable energy practices.
- **Data sharing and analytics:** Project Leo has emphasized the importance of data sharing and analytics to enable informed decision-making and optimize energy systems. Lessons can be learned about the value of collecting and analyzing energy consumption data, integrating various data sources, and utilizing advanced analytics techniques to gain insights and improve energy management.
- **Collaboration and partnerships:** Project Leo has engaged in collaborations with various stakeholders, including local authorities, technology providers, and energy companies. This lesson underscores the significance of forming partnerships and collaborations to leverage diverse expertise, resources, and funding to drive successful local energy initiatives.

These SLES demonstrator projects bring together experts from academia and stakeholders from relevant industries and local authorities, to explore the innovation in local technology, markets and communities.

Relevant modelling techniques for community energy models includes multi-agent system (MAS), market frameworks, distributed artificial intelligence (AI) and optimization. Further, modelling should be able to include the technologies (such as blockchains) that empower end users to take control of their own energy. Optimization and integration of such technology with data generated from communication infrastructure is essential for developing appropriate algorithms and mechanisms for more efficient operation of SLES and the power system as a whole. A recent trend, emerging in both rural communities and smart city neighbourhoods, is for groups of household prosumers to form local energy communities. Looking forward, such energy communities formed by citizen prosumers are envisioned to be the future of SLES. The state-of-the art in modelling of the energy communities and prosumers is described in the next section 2.2 .

2.2 Modelling of local energy communities and prosumers

An energy community is made up of a number of prosumers, who are defined to be consumers but also producers of locally generated renewable energy [5]. Prosumer assets (renewable generation capacity and storage) can be either distributed at individual households or centralized and thus shared within the community. A key research area in this context is the development of appropriate community schemes and control strategies for optimal scheduling of end-user production and consumption. Therefore, there is an increasing interest from academics and industry in community energy models [20].

2.2.1 Prosumer models

A prosumer is an owner of various DERs, and is able to generate electricity as well as consume electricity [5]. Recently, the decrease in the cost of solar panels, wind generation and battery storage has enabled individual households and consumers to generate their own electricity. This has lead to a decentralised energy system with significant shift in the market power from large utility companies to individual prosumers (i.e. consumers with micro generation and/or storage) [55].

Figure 2.2 shows the basic prosumer model, such models typically involves distributed renewable electricity generation-usually wind or solar PV, battery energy storage system and flexible/non-flexible demand normally installed behind the meter. Generally, prosumers aim to maximize behind-the-meter self-consumption from local renewable generation to make DERs more profitable. In such settings, prosumers import electricity from the grid when their assets cannot cover their own consumption, whereas they can export electricity to the grid when they have production surplus. A key objectives of the home batteries is the reduction of prosumer electricity bills while home energy management systems (HEMS) are mainly used for the control of the power flows. The recent trend and innovation related

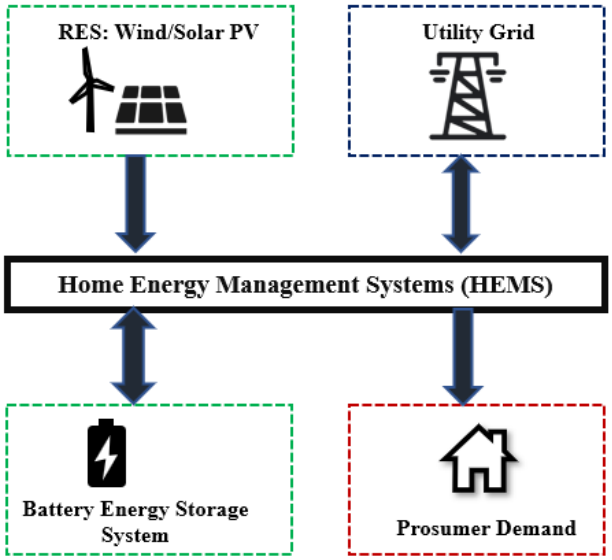

Figure 2.2: Prosumer model.

to the prosumer model is mostly focussed on developing real-time optimization and battery control algorithm embedded with HEMS to maximise self-consumption. For these reasons, the literature survey focuses on the state-of-the-art in HEMS, with special attention to battery storage system degradation aspects. First, the review of the state-of-the-art in HEMS is presented.

Home energy management systems (HEMS) and prosumer optimization for maximization of behind-the-meter self-consumption

In existing literature, self-consumption from renewable generators is mostly achieved at individual household level through home energy management systems (HEMS) [56–58]. In most HEMS systems reviewed, matching of generation and demand profiles is performed through the integration of battery energy storage systems (BESS) with demand side management (DSM) strategies and flexible tariffs. Thus, BESS has become an indispensable asset in HEMS for maximization of self-consumption, which is mostly defined in terms of reduction of the energy bill. In the work of Golmohamadi *et al.* [59] battery is integrated with HEMS to minimize the bill by reducing the energy consumption of thermostatically controllable appliances. Mehrjerdi *et al.* [60] proposed a unified HEMS that coordinates a hybrid system of renewable generators (solar and wind), BESS, demand response and flexible demand, including electrical and hydrogen vehicles. It recommends that BESS should be optimally sized in order to maximize self-consumption. Hemmati & Saboori [61] presented a HEMS with optimal BESS scheduling for optimal utilization of solar PV generation, while also taking into account the uncertainty associated with solar irradiation. In the work of Castillo-Cagigal *et al.* [62], the BESS is integrated with DSM to maximize the self-consumption from solar PV generation. Various optimization techniques are applied by HEMS to reduce energy bills. An extensive review on various

optimization techniques employed in HEMS is presented by Qayyum *et al*. [57] and, Beaudin & Zareipour [63].

End-users such as consumers and prosumers are considered to be an integral part of the smart grid due to the fact that they are able to change their consumption patterns and behaviour based on the information and (dis)incentives they may obtain [64]. Demand Side Management (DSM) especially Demand Response (DR) is an effective mechanism for energy management in residential, commercial and industrial buildings. In DR programs, consumer shift their electric usage by responding to the pricing signal or to the incentives being provided [65]. HEMS is normally a demand response tool that shifts and curtails demand to a house according to electricity price signals and incentives provided [63]. Scheduling of the home appliances in accordance to various DR signals is the major area of research addressed in prior literature [56]. The detailed list of common appliances considered in HEMS is presented by Beaudin & Zareipour [63]. Individual appliances possess unique characteristics, thus many works [63, 58, 64, 65] in literature have attempted to simplify modelling complexity by creating a response classes for all the appliances based on the flexibility it provides in the DR program.

In HEMS, home loads are commonly scheduled based on the DR signals, normally based on the incentive provided on reducing the load during peak hours and minimizing the electricity cost by operating devices during low hours tariff. Shareef *et al*. [58] and Beaudin & Zareipour [63] have presented various appliance scheduling techniques. As shown in Figure 2.3, the optimal scheduling of appliance to DR signals is achieved through rule-based, AI and optimization techniques. In HEMS, various objective functions are

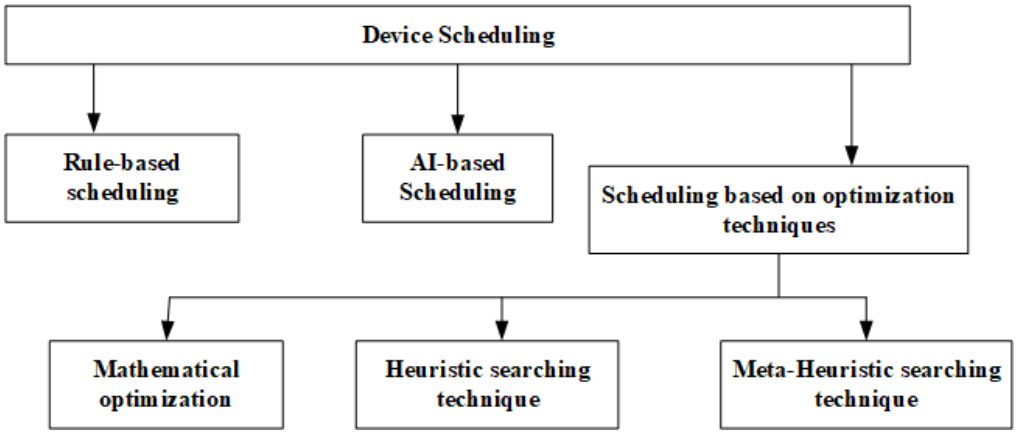

Figure 2.3: HEMS appliance scheduling techniques [58, 63].

used along with the DR programs and scheduling techniques [59]. The most common objective functions used in literature are:

- **Cost**: Minimization of energy cost.
- **Well-being**: Maximization of consumer comfort and satisfaction.
- **Load profiling**: Minimization of peak to average ratio (PAR), reducing the peak demand for the utility, reducing the grid dependence for the consumer, load shifting and valley filling.

- **Emissions**: Reduction of greenhouse gas emissions associated with consumption of electricity.

The pricing scheme is one of the most important signals of DR program. In HEMS, end-users are motivated to shift their electricity usage in response to price signals. The various pricing mechanism adopted in HEMS as reported in the literature includes; Time-of-use (ToU) tariff [60, 66, 67], Stepwise power tariff (SPT) [67–69], Real time pricing (RTP) [70, 59, 71], Incremental block rates (IBR) [72–74], and Critical peak pricing (CPP) [75–77]. ToU price tariff is the most widely adopted pricing scheme. An extensive review on the various optimization techniques employed in HEMS is presented by Qayyum *et al*. [57] and Beaudin & Zareipour [63]. However, by addressing a single objective, the HEMS may fail to find the optimal strategy. For this reason, many studies [60, 66, 67, 59, 74] consider multi-objective optimization to schedule household consumption.

To align with the identified aim and objectives of the research, the literature survey on HEMS is specifically focussed on how renewable energy sources (wind and solar) and BESS has been integrated into HEMS. In HEMS the grid is used as a permanent power supply, renewable energy sources (wind and solar) and BESS as intermittent source. In addition to appliance scheduling based on DR signals, most algorithms are based on the comparison of power from renewable energy sources, the state of charge (SoC) of battery and the availability of the grid power supply and price tariff to the load consumption [56]. BESS is normally used for storing energy during off-peak and low-cost hours, and discharge energy during on-peak and high cost hours [60, 66, 67, 70, 59, 68, 61]. In most of the HEMS schemes the BESS is charged from the renewable energy sources and not from the grid, then surplus energy from renewable energy sources is stored in the BESS and then the rest is sold to grid [61, 60, 67, 70]. The selling price to grid is normally fixed lower than the grid buying price [60, 67, 59, 70]. However, BESS is also designed to store electricity from the commercial grid when the price is low and also from the microgrid in high electricity generation hours [78]. Uncertainty associated with RES are normally modelled using probability distribution function (PDF) [61] and stochastic programming [60, 59].

A few literature sources, Wu *et al*.[79], Liu *et al*. [69] and Erdinc *et al*. [70], have included the network constraints by considering the maximum power that can be sold or injected to the grid as one of the constraints in objective function. Of these three, only Wu *et al*. [69] have considered the voltage constraints-increase in the voltage level caused by power injected into grid. Otherwise, network constraints are not addressed in most of the HEMS schemes. Interaction of the microgrid central controller with the HEMS is presented in work by Liu *et al*. [69]. The microgrid central controller coordinates scheduling of distributed energy resources and energy storage systems at the microgrid level. Most of the research works on HEMS reported in the literature have not considered the exact useful life of batteries in the HEMS models. Battery degradation or useful life is assumed based on the warranty provided by the manufacturers, such as Hemmati [68] has assumed BESS life time of eight years and five years in the work of Lokeshgupta & Sivasubramani [66].

As highlighted through various HEMS schemes, adoption of battery storage assets enables prosumer to maximise the self-consumption and decrease the electricity bills.

However, battery have power and energy limits, and the cost of the battery storage system is high compared to renewable generators. Moreover, the SoC of the battery need to be constantly monitored as their useful lifetime are mostly correlated with charge cycles at different depth of discharge (DoD). Along with the fact that batteries' lifetime is comparatively shorter than that of renewable generators, the frequent charging and discharging operations leads to cyclic ageing and incurs an extra cost as it accelerates the depreciation of the battery. Therefore, there has been a growing effort in developing an appropriate battery control mechanisms and sizing strategies, so that the remaining useful lifetime (RUL), performance and size of the battery storage system can be optimized to meet both economical and technical service requirements. The recent trends and the state-of-the-art battery modelling is discussed in the following subsection.

2.2.2 Modelling of battery energy storage system

i **Battery model:**

For a given BESS, the prediction of battery useful life is important for deciding the system cost and performance analysis. In modelling of batteries in hybrid power system, the most common characteristics to be considered are:

(a) **Performance or charge model:** Focuses on modelling the state of charge of the battery, which is the single most important quantity in system assessments.

(b) **Voltage model:** Used to model the terminal voltage so that it can be used in more detailed modelling of the battery management system and the more detailed calculation of the losses in the battery.

(c) **Lifetime model:** Used for assessing the impact of a particular operating scheme on the expected lifetime of the battery.

Lifetime models are studied in detail to specifically align with the identified aim and objectives of the thesis. In integrating the battery storage system into smart grid, important factors to be considered are cost, lifetime, power delivery, environmental impact and safety [80]. Most common method of calculating the battery lifetime are:

(a) **Calendar life:** This refers to the number of years the battery is expected to last till the battery reaches End of Life (EoL). It is independent of how much the battery is charged and discharged. However, calendar life is dependent on the state of charge of the battery and the temperature. EoL is normally defined as a state of the battery when the maximum capacity of the battery reduces to 80% of its rated initial capacity. Battery degradation under calendar life is refereed as *static degradation* [81].

(b) **Ah-throughput counting & calendar life:** Method assumes that there is a fixed amount of energy that can be cycled through a battery before it requires replacement, regardless of the depth of the individual cycles or any other parameters specific to the way the energy is drawn in or out of the battery. In

most cases the estimated throughput is derived from the depth of discharge versus cycles to failure curve provided by the manufacturer. It simply counts the amount of charge through the battery.

(c) **Cycle counting & calendar life :** The service life of the batteries usually degrades when subjected to repeated charge/discharge cycles. Battery life not only depend on total number of cycles, but also to the DoD of the cycles. This method specifically involves estimation of battery life based on the number of cycles versus DoD data sheet provided by manufacturers. Cycle life is expressed in terms of the number of charging/discharging cycles that the battery can undertake before it has to be replaced. Battery degradation due to cyclic operation is referred as *dynamic degradation* [81].

Calendar life due to self degradation of the battery corresponds to the normal corrosion process, which is independent of its cycling behaviour, and thus normally regarded as constant [82]. For instance, if the battery shelf life is 10 years, it means that the daily degradation is at least 1/365/10 = 0.0274% no matter whether that battery is in operation or not. However, battery degradation due to cyclic operation is not constant, and the battery lifetime depends on the charge/discharge cycles, which in turn is shaped by the control scheme. Technically, for instance, the depth to which the battery is discharged, the discharge current and the chemistry used has direct effect on its remaining useful lifetime. This translate into a considerable impact of the total cost of the operation and maintenance of the battery, especially as BESS is one of the most expensive component of a integrated energy system consisting of renewable generation and storage. The current state-of-the art and methods employed in an estimation of the useful life of the battery is discussed in the following subsection.

ii **Battery degradation model:**

Cycle life due to cycle degradation corresponds to number of charge/discharge cycles a battery can undergo based on certain DoD as specified by the manufacturers. Typically, the number of cycles versus DoD is specified in the data sheet as shown in Figure 2.4. For instance, if the total number of permitted battery cycles is 2000 with 80% DoD, it means every cycle from 100% state of charge (SoC) to 20% SoC consumes 1/2000 = 0.05% of the total life. Specifically, cycle ageing is the life lost each time the battery cycles between charging and discharging. Figure 2.4 shows that, as the DoD of the charging/discharging cycle increases, the expected cycle-life of the battery decreases. This means, a battery that is exposed to shallow charging/discharging cycles is expected to have a longer cycle-life than a battery that is exposed to deeper discharges [83]. It is important to note that the number of cycles versus DoD curve provided by manufacturers is obtained at specific temperature and C-rate.

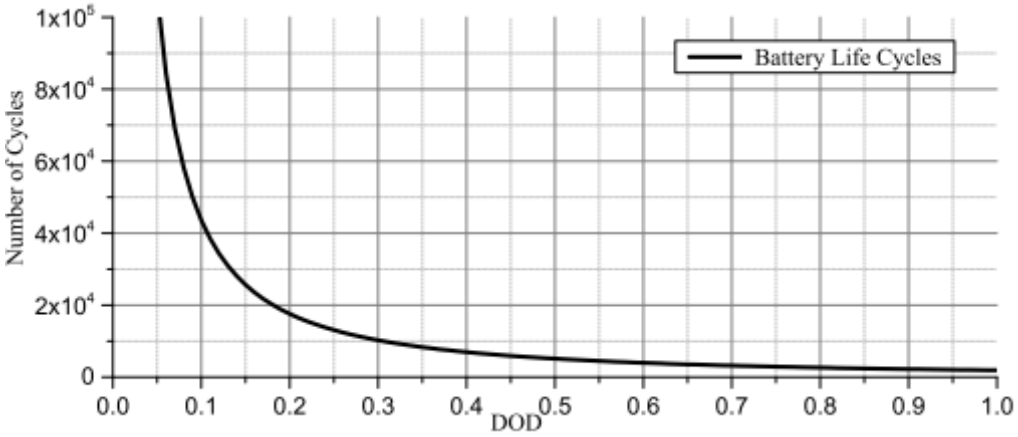

Figure 2.4: Relationship between number of life cycles and DoD of Ni-Cd battery [84].

A cycle is defined to have been completed when the battery depth of discharge has returned to a starting point before discharge and recharge began. Cycles consist of:

- **Full cycles:** Cycle consisting of one equal discharging and charging event. For example, 100%-to-20%-back to-100% SoC or 0%-to-80%-back to-0% SoC.
- **Half cycles:** Cycle consisting of one charging or discharging event. For example, 100%-to-20% SoC or 0%-to-80% SoC.

Further, depending on the starting and ending SoC, battery cycles are categorized as *regular and irregular cycles* [85, 86] or in some literature as *complete and incomplete cycles* [87].

- **Regular/complete cycles:** In this cycling process the starting SoC is 100%, then it is discharged to certain SoC corresponding to specific DoD and recharged back to 100% SoC. For example, 100% SoC-to-50% SoC-back to 100% SoC which corresponds to 50% DoD cycle.
- **Irregular/incomplete cycles:** In this case, the starting SoC is not necessarily 100% SoC, cycles starts at any arbitrary SoC value. For example, 80% SoC-to-30% SoC which also corresponds to 50% DoD cycle.

In both the cases, DoD may be same but the battery degradation is sensitive to starting SoC as most of the number of cycles versus DoD as specified in the data-sheet by manufacturers are based on regular cycles [87, 85, 88, 83]. Although, the cycle-life data-sheet is based on regular cycles, in real life the battery can hardly run regular cycles from 100% SoC to a specific DoD [85]. Thus, a vital aspect in integrating battery storage in power system is to build a battery degradation model to reflect irregular cycle impacts [85, 87, 86, 82, 84]. In order to develop a specific empirical cycle life models, the relationship between battery cycle life and DoD are formulated using different curve fitting techniques as adopted in existing literature:

- Fourth-order polynomial function [89].

- Least square quadratic function [90].
- Exponential function [91, 92, 86, 81, 93].
- Power function [94–96].
- Piecewise linear function [83].
- Numerical curve fitting-extrapolation [97].

The choice of such a model for the battery cycle life curve should not be underestimated as it has an important impact on the estimation of the remaining life of the considered battery after irregular cycles. In almost all the literature surveyed, regardless of the various specific cycle life models a **rainflow counting algorithm** is adopted to calculate the full and half cycles. Then, rainflow counting algorithm is further modified to account for the regular and irregular cycles. The cycle counting method used is known as "rainflow" counting. It was initially proposed by Socie & Downing [98] for material fatigue estimates. The complete rainflow counting algorithm is implemented by Nieslony in MATLAB [99]. The input to this rainflow algorithm is the SoC profile and the following results are the output:

(a) Cycle Amplitude.

(b) Cycle mean value.

(c) Cycle number (0.5 for half cycle and 1 for full cycle).

(d) Cycle begin time.

(e) Cycle end time.

This basic algorithm is further modified in most of the literature to account for the irregular cycles. In almost all the literature the battery lifetime is estimated by comparing the number of cycles at specific DoD determined from simulation to the permitted cycles specified by manufacturer. The cycles are defined as:

(a) Regular and irregular cycles ($\mathrm{ncycles}_{\mathrm{DoD}}^{\mathrm{regular/irregular}}$)

(b) Maximum permitted cycles as per manufacturer ($\mathrm{Ncycles}_{\mathrm{DoD}}^{\mathrm{Max}}$)

For instance, in the work of Ke *et al*. [87] battery life (L) based on regular cycles is calculated as:

$$\mathrm{L}_{\mathrm{DoD}}^{\mathrm{regular}} = \frac{\mathrm{ncycles}_{\mathrm{StartDoD}}^{\mathrm{regular}}}{\mathrm{Ncycles}_{\mathrm{EndDoD}}^{\mathrm{Max}}} \tag{2.1}$$

For, irregular cycles the depreciation factor is calculated as:

$$\mathrm{L}_{\mathrm{DoD}}^{\mathrm{irregular}} = \mathrm{ncycles}_{\mathrm{StartDoD}}^{\mathrm{irregular}} \times [\frac{1}{\mathrm{Ncycles}_{\mathrm{StartDoD}}^{\mathrm{Max}}} - \frac{1}{\mathrm{Ncycles}_{\mathrm{EndDoD}}^{\mathrm{Max}}}] \tag{2.2}$$

Finally;

$$\mathrm{L}_{\mathrm{Total}}^{\mathrm{Equivalent}} = \sum_{\mathrm{DoD}=0\%}^{\mathrm{DoD}=100\%} \mathrm{L}_{\mathrm{DoD}}^{\mathrm{regular}} + \mathrm{L}_{\mathrm{DoD}}^{\mathrm{Irregular}} \tag{2.3}$$

Battery life is estimated based on the Eq. (2.3) as:

$$L = \begin{cases} 0, \text{New battery with rated capacity} \\ 1, \text{Dead battery with zero capcity} \end{cases} \tag{2.4}$$

When $L = 1$, the battery is supposed to be dead with zero capacity, which requires to be replaced by new battery. The proposed method is further analysed based on the empirical values provided in the paper. The maximum permitted number of cycles at specific DoD used in their paper was:

- $\text{Ncycles}^{\text{Max}}_{10\%\text{DoD}} = 5000$
- $\text{Ncycles}^{\text{Max}}_{20\%\text{DoD}} = 1000$
- $\text{Ncycles}^{\text{Max}}_{30\%\text{DoD}} = 500$

Here, if StartDoD $= 10\%$, EndDoD $= 20\%$ and number of cycles counted at this starting DoD is one (ncycles $= 1$). As the starting DoD is not 0% (100% SoC) the cycle is a irregular cycle, as per Eq. (2.2) the battery life ($L^{\text{irregular}}_{10\%\text{DoD}}$) computed is -0.0008, that means battery is permitted to have large number of cycles before L is equal to 1, which is not true in real applications. This shows that at 10% irregular cycle battery will have a very long life. While, in a regular cycle which starts at 0% (100% SoC) for the same 10% DoD the life of a battery ($L_{10\%\text{DoD}^{\text{regular}}}$) determined from Eq. (2.1) is only 0.0002. On careful analysis, a huge difference in the life time estimated between the irregular cycles and the regular cycles was observed. In response to this draw back in the proposed methodology, a much more conservative approach in estimating the battery life due to irregular cycles is proposed in this thesis. Detail explanation is given in section 3.4.2 of chapter 3.

Useful battery lifetime depends on the frequency of charging/discharging and DoD. Most existing and emerging battery degradation models are focused in developing a methodology for estimating the useful life of a battery due to cyclic degradation. Ke *et al*. [87] have proposed an equivalent charge cycle estimation method to evaluate the effect of providing the energy balancing service on battery life. Yan *et al*. [81] incorporated dynamic battery life degradation in cost accounting model of energy storage system used for providing grid frequency regulation in the ancillary services market. Similarly, Ju *et al*. [84] proposed a hybrid energy storage system incorporating the degradation cost of battery and supercapacitor based on DoD and lifetime, while Xu *et al*. [86] developed a semi-empirical battery degradation model that assesses battery-cell life loss from operating profiles. In the work of Wang *et al*. [85], battery degradation and wind-battery optimization models are integrated and used for operation and bidding in real-time electricity markets. Recently, Terlouw *et al*. [100] have proposed a multi-objective optimization framework for energy arbitrage using community energy storage incorporating battery degradation in the optimization problem. However, developing a detailed battery degradation model

for determining the optimal battery capacity using real data, is still an open question. Furthermore, the need to include battery degradation models in the real time decision process of an Energy Management System (EMS) has not been discussed until now.

2.2.3 Community energy schemes

Energy communities formed by prosumers are increasingly becoming a promising solution to delivering sustainable energy systems that promote renewable integration and active participation of end-users. Local energy communities are expected to provide a new source of revenues for DERs owners, that could support the deployment of distributed low carbon energy assets, as direct financial incentives such as feed-in tariffs are being reduced [14] and even removed [15] in many countries. The aim of such energy community microgrids is to increase the financial benefits and meet the local demand with locally generated electricity. In turn, this enables the community to use more locally generated renewable generation, and shifts the market power from large utility companies to individual prosumers. From the grid manager point of view, local energy communities are also an incentive to increase local self-consumption, which will reduce the technical impacts of low carbon technologies on the grid, such as voltage violations. As a result, energy communities are identified as a promising technical, social and economical solution to the energy transition providing both incentives and technical solutions to the adoption of low carbon technologies. Recently, this aspect of the local energy communities has led regulatory bodies to implement frameworks that incentivise the deployment of such energy communities [27]. For instance, in France, citizens living in an area determined by a diameter of approximately 2km are allowed to gather into local energy communities for a total power that does not exceed 3MW [28].

Recently, Gjorgievski *et al*. [101] have reviewed the state-of-art literature on social arrangements, technical designs and the impact of energy communities. They have identified various gaps in the literature, and one of the highlights closely related to the work in this thesis is the need to design a more realistic pay-off distribution among the community members for stable coalition of the energy community. Similarly, Seyfang *et al*. [102] have conducted a detailed UK-wide survey on energy community projects, and concluded that energy communities are diverse and rapidly growing. Recently, the modeling of energy community has gained increased attention from a social perspective focused on niche areas of: socio-technical energy system [103], social innovations and dynamics [104], socio-technical energy transitions [105], social entrepreneurship [106], grassroots innovation [107], multi-sectoral approaches [108], social acceptance and participation [109], social investments [110] and social factors in AI research [111]. Huang *et al*. [112] have reviewed various simulation tools and models available for community energy system planning, design and optimization. Similarly, Mendes *et al*. [113] have surveyed numerous energy optimization and simulation tools for integrated community energy systems planning and analysis. Using a smart energy and AI perspective, other works have modeled a number of related concepts, such as Virtual Power Plant (VPP) optimisation [114–116], demand-side response aggregation [117, 118, 55, 119–122], renewable energy curtailment

in remote communities[123, 124], battery storage monitoring and optimisation [125–128], and P2P energy trading and blockchains [129–132].

Battery energy storage systems, along with renewable generators (solar PV, wind turbine) are the most common assets considered in the existing energy community models. In energy communities, individual households can invest in their own energy assets (renewable generation capacity and storage), or can jointly invest in larger community-owned energy assets and can then share energy and associated financial benefits within the community. Hence, techno-economic assessment between energy communities with individually-owned prosumer assets and models with community-owned assets have recently gained increased attention in the literature [33, 16, 34–36]. Most of the studies focus on comparing the battery storage adoption at the individual household scale with storage adoption at the community scale. For instance, Dong *et al*. [33] have compared community energy storage (CES) to household energy storage (HES). Their results indicate that both HES and CES can improve the community self-consumption rate (SCR) and self-sufficiency rate (SRR). HES is found more suitable for households with lower demand profiles, while households with higher demand profiles benefit more from CES. The same authors' extended their study by comparing the performance of HES and CES with demand side management (DSM) under ToU pricing scheme [16]. CES is found to be more effective at improving self-consumption for consumers and shaving peak demand for network operators. Similarly, Van Der Stelt *et al*. [34] have evaluated the techno-economic analysis of HES and CES for residential prosumers. The economic value of both HES and CES was assessed by considering the cost of energy imported from the grid. The results showed that both HES and CES can reduce the annual energy costs by 22 to 30%, and improve the use of on site PV generation by 23 to 29% compared to a baseline households without storage system. The economic feasibility of both HES and CES is found to be largely determined by the investment cost of the storage capacity per kWh. Similar comparison of storage adoption at the individual household level to storage adoption at the community level is studied by Barbour *et al*. [35]. Their results show that the community battery is better in terms of economic revenues compared to individual household batteries, as it requires less storage capacity overall and increases the self-consumption rate. Likewise, Walker & Kwon [36] have compared the economic and operational performance of individual and community shared storage. Their results also showed that the shared CES can achieve the maximum cost savings and significantly improve the utilization of energy storage.

Recently, Koirala *et al*. [133] have provided an overview of the state of the art in CES. Similarly, an overview of the economic potential and current research on CES was outlined by Sardi & Mithulananthan [134] and Strickland *et al*. [135]. The review states that CES have a huge potential to reduce import from the utility grid and thus maximize the self-consumption of the community. Hence, the advantages of CES over HES is well identified in the literature [33, 16, 34–36, 136–141]. However, most of the existing studies on comparison of individually-owned assets versus centrally located community-owned assets, while considering both the renewable generation and battery, have not included the battery degradation cost in their techno-economic analysis. Moreover, although community

assets are found to provide more benefits compared to individually-owned assets, still, the question of how to allocate financial gains from shared community-owned assets to the members of the community is not addressed in most of the existing frameworks.

Furthermore, several approaches have been proposed recently to integrate the network constraints such as electric cables thermal limits and voltage excursions in the market structures and trading strategies of the energy communities [13, 142–148]. However, most of the existing studies on the techno-economic analysis of individually-owned versus community-owned assets have not considered the network constraints. Installation of renewable generator (solar PV/wind turbine) or batteries in the grid changes power flows, and might create congestions, voltage excursions, or line over-heating. In such cases, the grid operator might consider the need for an Active Network Management (ANM) to remotely control the injection of distributed renewable generator and storage assets. Therefore, due to this congestion/voltage excursion, assets might be prevented from exporting/consuming to/from the grid, reducing the benefits from their owners. For instance, when the grid is constrained with voltage excursions, then the exports form PV/wind turbine and exports/imports from/to battery can be curtailed as it is currently the case in the Orkney Islands [32], UK. Therefore, such curtailment events need to be accounted for in the energy community setting by including power flow (physical network/grid constraints) in the techno-economic analysis of individually-owned assets versus community-owned assets. The battery control mechanisms and power flow control through various HEMS schemes for the community energy can be same as the case of the prosumers.

Transactive energy communities

Energy communities can invest in either distributed individually-owned energy assets or jointly-owned community energy assets, and then communities can share or trade electricity. A crucial aspect of a community energy models and projects is that they often involve sharing of some joint resources and assets. One approach is to facilitate P2P sharing in the case of individually-owned assets, whereas another approach consists in creating a community energy coalition in the case of community-owned assets, where an aggregator or community energy operator distributes the benefits within the community. The coalitional model of the energy communities often involve jointly-owned energy assets such as community-owned wind turbines, solar PVs and/or shared battery storage. An important challenge that such energy community schemes raise is the need for reaching agreements that ensure fair allocation of revenues and benefits earned by jointly-owned assets. State of the art approaches for redistribution (sharing) of benefits from jointly-owned community energy assets among energy communities are described in the following Section 2.3.

Local energy markets allow energy communities to trade electricity to other members of the community, through a specific market mechanism [29]. Market mechanisms can either implement a full peer-to-peer (P2P) market, which ensures that a community member "A" is

trading electricity to another community member "*B*", with solutions such as in automated negotiations schemes [19], or can implement a peer-to-community (P2C) scheme, in which case electricity from a specific community member is traded to the community, without knowing exactly who will benefit from this electricity, such as what is achieved through double auction market clearing mechanisms [30]. A comprehensive study on the recent trends and the state-of-the art energy trading models for the energy communities is presented in the Section 2.4. First, the review of the state-of-the-art in energy sharing models is presented in the following subsection. Energy coalition and investment in the jointly-owned community energy assets are the recent trends, and there has been a growing effort in developing a fair redistribution or energy sharing mechanism. Hence, in this thesis, the focus has been on energy sharing mechanisms from jointly-owned community assets instead of P2P sharing mechanisms.

2.3 Sharing of energy in energy communities

Energy community projects often involve jointly-owned assets such as community-owned wind turbines or shared battery storage. Yet, this raises the question of how these assets should be controlled – often in real time, and how the energy outputs jointly-owned assets should be shared fairly among community members (prosumer agents), given not all members have the same size, energy needs or demand profiles. Game theory provides an insightful analytical and conceptual framework along with mathematical tools to study and analyse the complex interaction among independent rational players (in the context of this thesis, the households/agents) [37]. Cooperative (or coalitional) game theory has been identified as a useful tool in designing incentive mechanisms and business models in decentralized energy systems. In a cooperative/coalitional game, players form coalitions to maximise a common objective for mutual benefit. Then, the benefit is distributed equally or fairly among themselves using incentive-based solution concepts, such as the Shapley value [38].

In the context of energy communities characterized with renewable energy systems, coalitional game theory has been identified as a promising solution for energy sharing schemes [149], cost allocation [150], and benefit redistribution [151, 152] schemes among the community members. For instance, Alam *et al*. [40] proposed an energy exchange mechanism in rural communities that aimed to reduce battery usage and where an approximated Shapley value was used for the distribution of benefits among the households. Although they have proposed that the approximated Shapley value improves the computational time as compared to the original Shapley value, it still poses a significant computational challenge with the increase in the number of agents in the coalition.

Recently, Moncecchi *et al*. [153] have proposed a two-level benefit distribution scheme based on coalitional game theory. At the first level, the benefit is distributed to a group of community members. Then, at the second level, the benefit is distributed proportionally to individual members. While various operational scenarios were studied, only few players (nine community groups only) were considered in the coalition formation. Similarly,

Longxi Li [154] have proposed a cost-sharing scheme developed according to the Shapley value method. However, only four players are considered, thereby raising the issue of computational tractability and hence the practical application of the proposed redistribution mechanism is limited. Likewise, Chakraborty *et al*. [155] investigated the sharing of storage systems among consumers in a ToU pricing scheme using cooperative game theory. The sharing mechanism is illustrated using only five households which raises the issue of scalability and practicality as the household number increases in the coalition. Moreover, storage is considered ideal thereby neglecting the degradation aspect of the battery. In the work of Marzband *et al*. [156], cooperation among energy communities was studied in order to reduce the annual electricity cost, and profit redistribution mechanisms based on various solution concepts from cooperative game theory such as, Shapley, Nucleolus, and Merge and Split are proposed. Furthermore, Robu *et al*. [157] considered coalition formation for minimizing group buying risk. Here, consumers cooperate to form a group to buy electricity under one or several tariffs. Lately, a blockchain-based coalitional formation algorithm for trading energy was proposed by Thakur & Breslin [158].

A more recent study by Tveita *et al*. [159] compared annual electricity cost allocation among prosumers and consumers using solution concepts from cooperative game theory. Both Nucleolus and Shapley solution concepts were used to determine the annual electricity cost deviations as key asset parameters vary. While various operational scenarios were studied, only four players were considered, thereby raising scalability issues associated with increasing players and effects on coalition formation. Likewise, Chiş and Koivunen [160] have proposed a coalitional cost-game optimization of a portfolio of energy assets using Shapley value as the underlying redistribution method, modelling a realistic case study of 9 households. Safdarian *et al*. [161] have used the Shapley value for coalition-based value sharing in energy communities consisting of 24 apartments in southern Finland. Vesperman *et al*. [162] have also used number of solution concepts such as the Nucleolus and Shapley values in the market design of a local energy communities ranging in size from 4 up to 16 prosumers. Various energy, cost, and profit redistribution schemes based on coalitional game theory can also be found in [163–166]. All these recent works shows that the incentive-based solution concepts, such as the Shapley value is proposed as a promising redistribution mechanism. However, in most of the work reviewed, their numerical case studies consider only a small number of agents (up to $\sim$20), to keep the computation of the exact Shapley value tractable. Yet, realistically sized energy communities have more members, e.g., there are usually 50-200 consumers behind a substation/LV transformer in Europe [167], or potentially even more sharing an asset such as a large community wind turbine.

Hence, one of the major challenges in redistribution schemes based on coalition game theory is the issue of scalability. Specifically, when determining the solution concepts such as Shapley values in a coalition, the computation becomes highly complex and time-consuming as the number of players increases in the coalition. Moreover, most of the existing redistribution frameworks are developed without considering network constraints, in which case the computation becomes more challenging. Thus, there is

still a need to develop a redistribution mechanism that is fair, but also provides tractable computational performance that scales well with the increasing number of members in the energy community coalition, while considering operational network constraints. In the case of energy communities with individually-owned energy assets, prosumers can also share resources through specific local market mechanism such as P2P energy trading markets. Such emerging LEM solutions are reviewed in the following section 2.4.

2.4 Electricity trading in energy communities

Trading of energy between large producers, utility companies and consumers with established wholesale and retail markets is current practice; however, P2P energy trading and sharing between prosumers, consumers and the established electricity markets is a trending topic within the industry and research community. P2P energy trading is an emerging local market arrangement in distribution networks, in response to the challenges posed by the increasing penetration of distributed generation from renewable energy sources and the increasing electricity retail prices with decreasing feed-in tariff rates. The direct energy trading among consumers and prosumers is called peer-to-peer energy trading, which is developed based on the "P2P economy" concept (also known as sharing economy) [168]. In this section 2.4, literature survey is mainly focussed on the following aspects of P2P:

- Overall P2P architecture adopted including P2P agents modelling schemes.
- Various P2P market and incentive mechanisms, and state-of-the-art business models.
- Application of game theoretic modeling in P2P, focussed on coalitional game theory.

2.4.1 Overall P2P architecture adopted

P2P energy trading involves various entities such as consumers, prosumers, microgrids and the utility grid. In a normal power system, microgrids consisting of consumers and prosumers are connected to a distribution networks, and multiple distribution networks are connected to a transmission network [169]. Based on this power system framework, Long *et al*. [170] and Zhang *et al*. [171] proposed three hierarchical levels of P2P. The proposed architecture is further extended and presented by Abdella & Shuaib [169] as:

1. **Intra-microgrid trading:** P2P energy trading takes place between prosumers, consumers and utility in the same microgrid (within microgrid).
2. **Inter-microgrid trading:** P2P energy trading is conducted between multiple microgrid connected to same distribution network.
3. **Distribution level trading:** Energy trading takes place between multiple microgrid connected at different distribution networks.

Most of the P2P energy trading frameworks are based on the intra-microgrid trading architecture, so far inter-microgrid and distribution level P2P trading has not been discussed or implemented [169]. Furthermore, in the work of Long *et al*. [170] and Zhang *et al*. [171], a group of microgrids under the same distribution network is also defined as cell. Most of the existing P2P energy sharing studies and practical projects involve coordinators. However, in some decentralized blockchain-based papers and projects the coordinators are played by machine code automated algorithms rather than conventional intermediaries run by a human mediator. The structure of P2P energy trading and sharing reported in the literature can be categorized into two major groups as proposed by Jogunola *et al*. [172]:

1. **Centralized structure [173, 5, 174–180]:** In this architecture, a central entity acts as mediator between different producers and consumers. The various terms used for central coordinator are: Energy Sharing Provider (ESP) [173], Energy Sharing Coordinator [5], Central Unit [177], Elecbay [179, 178], P2P Market Operator (P2PMO) [180].

2. **Decentralized/distributed structure [181, 182, 158]:** Prosumers and consumers trade energy directly without the central mediator. Most of the literature on decentralised structure is based on blockchain-based distributed ledger technology [183, 158, 182]. Decentralised/distributed architecture provides faster mechanism for local balancing of energy demand and generation. It also, provides optimization benefits in terms of cost reduction from transportation and direct transaction between neighbours [172]. However, the major challenge for this type of P2P structure is the lack of adequate control over energy transactions. For example, there is no assurance that a buyer will get the right amount of energy purchased. Scaling and privacy issues are the most challenging aspect of decentralize/distributed structured P2P architecture [169].

In P2P trading models, generally an intelligent agent is modeled as controlling the individual home (prosumer/consumer) resources. This agent acts on behalf of the household to maximise the identified utility. Community is formed by connecting all the individual households through individual agents which is collectively refereed as multi-agent system. Such, agent modelling schemes are presented in the work of [40, 181, 5, 174, 182, 175, 184, 185]. The various assets coordinated by household agent are:

- Renewable energy generators which mostly includes solar PVs and wind turbine.
- Household demand load.
- Energy storage system: battery and EV.
- HEMS is also included in the work of Guerrero *et al*. [181] and Han *et al*. [184].

An example of P2P multi-agent system (MAS) is as follows, following what was implemented in several papers, such as Zhou *et al*. [5]. The topology of the P2P trading model is centrally controlled structure. The proposed framework includes three types of agents

and the dynamic behaviour and characteristics of these agents are defined though three corresponding models. Three types of agent are:

1. **Prosumer agent (PA):** Represents the independent individual households. Characterized by a specified decision-making model concerning its own demand and assets.

2. **Energy sharing coordinator agent (CA):** Coordinator coordinates between prosumer agents and retailer agent. Characterised by pricing model. CA manages the local energy trading among the prosumers and serve a aggregator to the grid by communicating with the retailer agent, which is done through implementation model.

3. **Retailer agent (RA):** Represents the grid. Considered as passive agent who simply sells/buys energy to/from CA based on the requested amount at pre-announced retail/export price. CA could also initiate demand response programs.

Three models defining the dynamic characteristics of agents are:

1. **Decision making model for the PA:** All the actions taken by PA is defined in decision making model. Household level optimization and control strategies including, scheduling of generation and demand, and corresponding demand response programs are defines in this model.

2. **Pricing model from the CA:** Local pricing scheme for trading among individual prosumers are defined. Grid export and import pricing schemes are defined in this model.

3. **Implementation model for interactions between agents:** P2P market mechanism is defined in the implementation model. Specific trading rules and regulations are also defined in this model.

2.4.2 P2P market mechanisms

In most of the literature, P2P energy trading and sharing is exclusively formulated as a game or an optimization. Bayram *et al*. [186] have classified P2P market mechanism based on the architecture as follows:

1. **Distributed optimization based mechanism:** Applicable for centralized structure. If the energy trading involves a central controller who coordinates trades among different entities, then it is proposed that the appropriate framework would be to use single objective maximization tool such as convex, stochastic, or swarm optimization to maximize social welfare.

2. **Game theoretic based mechanism:** Applicable for decentralized/distributed structure. Suitable for trade scenario involving multiple peers, who are either

interested to optimize their own utilities or form coalition to optimize the mutual benefit. Simulation based solutions are proposed to model the behaviour of the multiple agents involved in the energy trading. Appropriate and suitable incentive mechanism can be designed based on game theoretic models, which encourages peers to participate in the energy trading.

Sousa *et al*. [29] has categorized P2P markets based on the degree of decentralization and P2P topology as follows:

1. **Full P2P market:** Trading based on decentralized/distributed P2P structure.
2. **Community-based market:** Trading based on centralised P2P structure.
3. **Hybrid P2P market:** Combination of full and community-based P2P market.

Detailed comparisons among the three different markets are elaborated in the literature. A well structured design in community-based market allows the community manager to provide services to the grid operators as an aggregator. Abdella & Shuaib [169] has classified trading model based on the demand response optimization techniques as; centrally controlled models, incentive-driven models, cooperative-based and non-cooperative based game theoretic models. Primarily, the P2P market mechanism in all the proposed classification are based on topology, objectives of the peers, and incentive mechanisms. As presented in [186, 187, 183] the major trading mechanisms are discussed below:

1. **Auction based mechanism [181, 182, 5, 188, 189]:** This trading mechanism is normally designed for competitive peers where every peer participates in auction for energy trade. Auction theory is an analytical framework that matches peers interested in trading, rather than holding any of the traded commodity itself. The trading mechanism is related to distributed optimization based P2P market mechanism.
2. **Stackelberg game-based mechanism [190–192]:** Trading mechanism suitable for self-oriented peers, who want to maximize their own utility by participating in the P2P trade. This market mechanism consists of a leader who announces the prices of the energy and set of followers. A central controller or aggregator is usually the leader. The trading mechanism is related to game theoretic based P2P market mechanism.
3. **Coalition formation-based mechanism [158, 185, 189, 184]:** Applicable for cooperative peers who are willing to form a coalition to increase their mutual benefit. Fair and equal distribution of the benefits among peers are normally achieved through Shapley value and core solution concept techniques. The trading mechanism is also related to game theoretic based P2P market mechanism.

Optimization based P2P market mechanism

In most of the existing P2P business models, the network/grid constraints is not included in the trading mechanisms. This has shifted the research focus and efforts in P2P business

models. However, the recent research trend is on the integration of the network constraints P2P trading mechanisms. This is mostly achieved by including the power flow equations in the market optimization constraints. Recently, Guerrero *et al*. [13] have proposed a simplified version of AC Optimal Power Flow (AC OPF) for continuous double auctions, using voltage sensitivity coefficients and power transfer distribution factors (PTDF). Likewise, Wang *et al*. [193] and Han *et al*. [194] have proposed Distributed Locational Marginal Prices (DLMP) for P2P markets to promote energy trades that contribute to voltage and power losses regulation. Similarly, most of the current works that consider grid constraints also include an additional cost for energy transactions that is proportional to the power losses [13, 193–195]. Furthermore, another emerging active area of research is the integration of disruptive and distributed enabling technologies such as blockchain and smart contracts into P2P trading mechanisms [42]. Distributed ledger technologies (DLT) such as smart contracts in blockchain have emerged as one of the key driver for decentralized P2P markets. Smart contracts consist in programs running on a blockchain that are executed in a distributed way. In P2P energy trading applications, smart contracts can be used to execute specific functions. Normally, smart contracts first receive and process the bids, offers and money deposit from the stakeholders (prosumers and consumers).Then, smart contracts have been used to clear a P2P market. Various DLT-based market clearing mechanisms are proposed in the literature. For instance, Han *et al*. [194] and Khalid *et al*. [196] have used heuristic approaches to match buyers with sellers. While, Lasla *et al*. [197] and Kang *et al*. [198] have implemented auction mechanisms without grid constraints to clear the P2P market. Likewise, Leeuwen *et al*. [199] have used smart contract to clear the market by including the power flow constraints. In heuristic-based clearing mechanism, the smart contract usually matches buyers and sellers and validates a transactions as the bids are placed. In distributed optimization-based market clearing mechanism, the optimization problem is solved in a distributed way, using methods such as primal-dual gradient [200], alternating direction method of multipliers (ADMM) in which the global optimization problem is broken into smaller pieces that do not require all the information of the original problem and can be solved in a distributed way. A smart contract is used to coordinate a distributed AC OPF optimization using ADMM, where each node solves its sub-problem offline. Finally, smart contracts can also be used in the settlement phase of a market, where they can coordinate the monitoring of energy delivered and consumed by the households. Hence, by nature, smart contracts facilitate decentralization of energy markets as they remove the dependency in a third party operator, and replace it by distributed nodes achieving the same functions in a decentralized way.

Game theoretic based P2P market mechanism

Game theory provides an insightful analytical and conceptual framework along with mathematical tools to study and analyse a complex interaction among independent rational players (for instance, peers in P2P) [201]. It is broadly classified into two main branches:

1. **Non-cooperative game theory:** Mathematical formulation is based on strategies. Equilibrium based solution concept, mostly solution addressed in terms of Nash equilibrium.

2. **Cooperative game theory:** Mathematical formulation is based on coalition among the players. Incentive based solution concept, mostly solution addressed in terms of Shapley value, core, Nash bargaining and Pareto optimality.

In this section, in order to align with the identified objectives, literature survey is focussed more in application of cooperative(coalitional) game theory in P2P energy trading. In a cooperative game players communicate among themselves and form coalition to maximise the common objective for mutual benefit. Then, the benefit is distributed equally and fairly among themselves using solution concepts such as Shapley value and core. Overall battery usage is reduced by P2P energy trading based on coalitional game theory in [40], blockchain based coalitional formation algorithm for trading energy is proposed in [158]. P2P energy trading schemes based on coalitional game theory is presented in [172, 169, 39, 186]. An insightful general step-wise procedure for designing P2P energy trading mechanism based on cooperative game theory is presented by Tushar *et al*. [39] as follows:

- **Step-1:** Choose a suitable architecture for the P2P community.
- **Step-2:** Identify an appropriate utility function for each agent that clearly captures the benefit of coalition. Check if the utility function holds the property of superadditivity.
- **Step-3:** Examine for the existence of core in the coalition formation.
- **Step-4:** Conduct a stability test. Ensure to make the coalition stable by designing a suitable revenue distribution mechanism that lies in a core if a core is non-empty.
- **Step-4:** Design a fair and equal revenue distribution mechanism. Solution concepts such as Shapley value, Banzhaf Index (fairness criterion), the core (coalitional stability), Nucleolus (based on the notion of deficit), Kernel and Stable set are normally used.

One of the major challenges in P2P energy trading scheme based on coalition game theory is the issue of scalability. While determining the Shapley value, the computation becomes large and complex as the number of players increases in the coalition [39, 40]. To address this challenge, a significant work has been reported in literature. Most of the work is based on using the sampling techniques to approximate the Shapley value. In the work of Castro et al. [202], the Shapley value is approximated by a sampling based method that achieves a polynomial processing-time, which is implemented in the ApproShapley. Instead of using a normal Shapley value, an Asymptotic Shapley value is proposed by Lee *et al*. [175]. In work of Misra *et al*. [203], approximation is conducted by deriving differential equations from the axioms of Shapley value. Alam *et al*. [40] has adopted the sampling algorithm presented in [202]. Still, there are significant challenges associated

with sampling-based approach in a larger settings, as it requires large number of samples to obtain a reasonable approximation of the true Shapley value, which increases the computation cost considerably. Furthermore, application of sampling-based methods in energy communities is limited as they may not produce consistent result if they need to be return for verification purposes [38]. The results are normally inconsistent as approximation calculation is performed using random samples, which generates slightly different results even on the same data.

As highlighted by most of the available literature, an energy communities can share and trade electricity. However, exchanges of electricity is different from any other exchange of goods. It requires physical network (grid) lines to allow the exchanges of electricity. Technical limits of the physical network such has low voltage (LV) distribution grid can have severe impact on the way the electricity is shared and traded in energy communities. Therefore, the physical network constraints must be included in electricity trading models. The state-of-the-art in modelling of physical network constraints is explained in the following Section 2.5.

2.5 Modelling of physical network constraints

The physical network (the LV distribution grid) is an essential entity that allows the exchange of energy in the settings of the energy communities. Recently, several approaches have been proposed to integrate the network constraints such as electric cables thermal limits and voltage excursions in the market structures and trading strategies of the energy communities. Several approaches can be used to model a grid and assess the impact of integrating the DERs connected to the low voltage distribution network. Power flow approaches aim to determine the power flow, voltages and currents at every bus of the grid. The inputs of these approaches are usually the loads and producers characteristics, such as their forecasted consumption and production power, or current. A proper assessment of the different types of the electrical grid and needs of the energy communities are crucial in determining the type of method to be used in calculating the power flow and voltages. In this section, different state of the art power flow approaches are presented.

2.5.1 Linear models of electrical grids

The power flow problem models the non-linear relationships among power injected at each bus, demand power, bus voltages and angles, and circuit parameters. In most of the applications, the non-linear models are approximated with suitable assumptions to facilitate the use of fast load-flow solutions. However, the application of these linear approximated approaches in LV distribution grids are limited as they often tend to neglect the active power losses. Different linear models proposed in the literature are:

1. **Impedance based model:** In this model, the voltage is assumed to be constant all the time. Current and voltage are related by fundamental Ohm's law as shown in the

Eq. (2.5)

$$[\mathbf{I}] = [\mathbf{Y}]\,[\mathbf{V}] \tag{2.5}$$

Where, $[\mathbf{Y}]$ is the admittance matrix of the network, $[\mathbf{I}]$ is the current flow in the network, and $[\mathbf{V}]$ is the voltage at every node of the network. In the impedance based model, it is assumed that the voltage does not vary, and that the current required by each load is given by:

$$I = \frac{S^*}{V} \tag{2.6}$$

Here, S is the apparent power of the load at each bus, and the superscript * corresponds to the complex conjugate [204]. Unfortunately, this type of approach gives errors of magnitude close to 10%, which is not suitable for the purpose of local energy markets that usually already rely on consumption and production forecasts which are another important cause of errors.

2. **Power based model linearisation:** In the power based model, the power balance is computed at every node of the grid. The apparent power that is consumed or produced at node i is given by:

$$S_i = P_i + jQ_i \tag{2.7}$$

Then, the overall power balance is summarized as shown by Eq. (2.8) .

$$\begin{aligned} P_i &= |V_i| \sum_j \left|V_j\right| \left|Y_{ij}\right| \cos(\delta_j - \delta_i + \gamma_{ij}) \\ Q_i &= -|V_i| \sum_j \left|V_j\right| \left|Y_{ij}\right| \sin(\delta_j - \delta_i + \gamma_{ij}) \end{aligned} \tag{2.8}$$

Where, $Y_{ij}e^{j\gamma_{ij}} = \underline{Y}_{ij}$ is the admittance of the connection between bus i and bus j, and P_i is the sum between the generated power (accounted for positively) and the consumed power at node i. The voltage at each bus i is defined by $\underline{V}_i = V_i e^{j\delta_i}$, with δ_i the voltage angle. To make such formulation linear, it is often accepted to simplify the sin and cos functions, considering that the angle difference between node i and node j can be neglected, which yields to the following expression, that corresponds to a DC power flow (direct current) assumption:

$$\begin{aligned} P_i &= |V_i| \sum_j \left|V_j\right| \left|Y_{ij}\right| \cos(\gamma_{ij}) \\ Q_i &= -|V_i| \sum_j \left|V_j\right| \left|Y_{ij}\right| \sin(\gamma_{ij}). \end{aligned} \tag{2.9}$$

Although this method is well suited for non-resistive network (transmission networks), it is not well applicable to LV distribution grids that are usually more resistive.

Therefore, for low voltage distribution grids where active and reactive power losses cannot be neglected, it is necessary to adopt a more comprehensive approach, based on non-linear formulations such as the one expressed in Eq. (2.8) .

2.5.2 Non-linear models of electrical grids

In the literature, distribution load flow approach and AC power flow approach (based on Eq. (2.8)) are the two main models implemented for non-linear power flow computations, as described below:

1. **Distribution load flow:** Distribution load flow approaches take advantage of the radial characteristics of distribution grids to make the resolution of every bus' voltage quicker [205]. Starting from the bus at the top of the network, the algorithm computes the voltage of each sub-level (noted $i+1$) one after the other using the following equations:

$$\begin{aligned} P_{i,i+1} &= P_{i-1,i} - r_{i,i+1}\frac{P_{i-1,i}^2 + Q_{i-1,i}^2}{V_i^2} - P_{i+1} \\ Q_{i,i+1} &= Q_{i-1,i} - x_{i,i+1}\frac{P_{i-1,i}^2 + Q_{i-1,i}^2}{V_i^2} - Q_{i+1} \\ V_{i+1} &= \sqrt{V_i^2 - 2(r_{i,i+1}P_{i-1,i} + x_{i,i+1}Q_{i-1,i}) + (r_{i,i+1}^2 + x_{i,i+1}^2)\frac{P_{i-1,i}^2 + Q_{i-1,i}^2}{V_i^2}} \end{aligned} \tag{2.10}$$

   where level i is the parent level of level $i+1$ in the radial architecture, $r_{i,i+1}$ and $x_{i,i+1}$ are the line resistance and reactance between levels i and $i+1$, $P_{i,i+1}$ is the active power flowing from level i to level $i+1$, and P_{i+1} is the active power consumed or injected by the assets installed at the considered node. Although this method is well adapted to radial distribution power flow, it requires a forward-backward process to entirely capture the power flow in each branch, as the first branch's power cannot be known exactly otherwise.

2. **AC power flow:** In the literature, Current-based and power-based methods are the two different types of AC power flow approaches implemented. In current-based method, the algorithm aims to solve Eq. (2.11).

$$[\mathbf{V}]_{N+1} = [\mathbf{Y}]^{-1}[\mathbf{I}]([V_N]) \tag{2.11}$$

   where N is the iteration step of the resolution algorithm. This algorithm consists in initializing all voltages at a value of 1 per unit, then compute the current injection at each node from Eq. (2.5), Eq. (2.6), or from the constant current consumed/produced by the asset installed at the considered node, depending on the ZIP type of the asset (constant impedance, constant power or constant current respectively). The resulting current vector is then reinjected into Eq. (2.11) until the voltage has converged. While, in power-based method, the algorithm aims to solve Eq. (2.8), knowing what

is the power injected/consumed at each node of the grid. However, this requires to make some assumptions for nodes with large generation assets, such that the voltage amplitude is regulated, which is a weak assumption in transmission grids. Also, similar to the current based method, it requires to fix the voltage value to 1 per unit at one bus of the grid, called the Slack bus, which is often the bus at which the power injected is the greatest (connection with the main grid, or largest power plant modelled). Then, mathematical methods to solve Eq. (2.8) are either Gauss-Seidel or Newton-Raphson using the Jacobian matrix of the grid impedance [206]. Normally, the Newton-Raphson numerical approach allows a quicker convergence.

Power-based non-liner AC power flow approach is the most commonly used method. For instance, Guerrero *et al*. [181] have used Newton-Raphson power flow approach to determine the voltage sensitivity coefficients for the peer-to-peer (P2P) energy trading mechanism. Similarly, Azim *et al*. [145] have used power based method using IEEE 8500-node distribution test feeder to estimate the losses associated with P2P transactions. Furthermore, Couraud *et al*. [147] have studied the impact of fully decentralized reactive power control on low distribution network using the power based non-linear AC power flow approach. Recently, Tevar-Bartolome *et al*. [148] have assessed the impact of the distributed PV penetration on the LV distribution network using the planning-oriented load flow solver based on non-linear AC power flow approach. Likewise, Grzanic *et al*. [207] formulated a distribution network model using Newton-Raphson power flow method to study the impact of electric vehicle (EV) penetration on the LV distribution network. These various power flow approaches are formulated to account the network constraints such as power balance, line capacity and voltage excursions. However, most of the existing studies on the techno-economic analysis of individually-owned versus centrally-shared community-owned assets (renewable generator, battery storage) have not considered the network constraints. These energy assets might be prevented from exporting/consuming to/from the grid due to network constraints.

2.6 Key findings (main research gaps)

Chapter 2 presented the literature review relevant to the topic of this thesis. At first, a literature survey on smart local energy system (SLES) was presented. SLES such as energy communities and LEM are emerging as new methods to coordinate distributed energy assets in a local area and provide new financial incentives [4]. Generally, potential benefits of SLES includes opportunities for revenue generation or cost reduction for end-users and local communities and enable market access to small-scale generation and storage, which may unleash the value of demand-side flexibility and improve wider network and system management, but depend on the market design. There are also challenges and risks associated with the adoption of SLES, most importantly coalitions in energy communities and LEMs need to be adopted by end-users. Hence, the key to successful deployment is to place the consumers at the centre of the energy revolution and to design

solutions that are tailored to local communities and end-user needs, while achieving desired decarbonisation [43].

The decarbonization targets and the development of renewable and low carbon technologies are changing the electricity systems in UK and worldwide. The sustainable implementation of these changes in the energy markets can be achieved only if the consumers/prosumers are rightly incentivised. Similarly, the integration of the system, transmission and distribution network operators in the overall local energy portfolio is crucial for the successful and practical operation of the SLES. The current gaps and needs for unlocking the potential of SLES are evident from the various relevant reports and publications:

- *"Unlock value of customer actions and assets"*, Energy Digitisation Taskforce report-Delivering a Digitalised Energy System [12].
- *"....the design of our retail market has led to instability and a race-to-the-bottom on price, without providing incentives for consumers to invest in decarbonization or the demand flexibility that our future system desperately needs"*, Tony Blair Institute for Global Change report-Powering Ahead: The Need to Reform UK Energy Markets [208].
- *"..a capability gap in social factors within multi-agent energy system modelling"*, UKERC Briefing paper 2: Strengths and Weakness of Energy Modelling in the UK [209].
- *"..current Supplier Hub Model Review should provide the mechanism for consumers to engage with the market"*, University of Exeter, Energy Policy Group-Unlocking Local Energy Markets [210].
- *"Transition of Distribution Network Operator (DNO) to Distribution System Operator (DSO) is critical for the successful operation of Local Energy Markets"*, University of Exeter-Policy and Regulatory Barriers to Local Energy Markets in Great Britain [211].
- *"... the current regulatory incentives for network companies to adopt demand side or flexible operational approaches to solve network constraints are clearly developed than the incentives for long-term capital investments"*, CATAPULT Energy Systems-The policy and regulatory context for new Local Energy Markets [212].

In addition to the challenges faced by DSOs leading to local generation and load curtailments, financial incentives for renewable energy production such as feed-in tariffs are being reduced considerably, which impacts the pace of energy transition. Hence, the current energy market settings and regulatory frameworks do not offer the right incentives to consumers for adoption of the low-carbon energy assets. This is increasingly leading to a need for establishing a consumer-centric business models (incentives) with substantial innovation in the way the local networks are managed and balanced. In this context, how

SLES are designed and shared, are open research questions that require novel modelling paradigms that place end-users in the centre of the decision-making for the energy system.

In most of the literature reviewed, studies show that the community battery storage system offers higher benefits as compared to individual household distributed batteries. However, most of existing studies do not consider the battery degradation cost when determining the optimal battery capacity. The battery lifetime depends on the charge/discharge cycles, which in turn are shaped by the control scheme. Thus, there is a need to accurately estimate the depreciation of the battery from the operating profiles and therefore assess the operational cost and overall economic value of the integrated renewable energy system. Furthermore, although higher benefits can be achieved by investing in jointly-owned community energy assets, how to redistribute these benefits among the individual households in the community still remains a key open question, of both research and practical interest. Current energy communities usually employ algorithms based on proportionality of consumption to redistribute the benefits from the community-owned generator assets. However, such methods are not fair, and not applicable in the case of energy storage assets, where the proportionality of the asset usage does not apply. Hence, there is a need to design an efficient and fair redistribution mechanisms that applies to both community-owned renewable generator and storage assets, while incorporating the asset's degradation, and the physical network and operational constraints.

Furthermore, installation of renewable generator (solar PV/wind turbine) or batteries in the grid changes power flows, and might create congestions, voltage excursions, or line overheating. In such cases, the grid operator might consider the need for an Active Network Management (ANM) to remotely control the injection of distributed renewable generator and storage assets. Therefore, due to this congestion/voltage excursion, assets might be prevented from exporting/consuming to/from the grid, reducing the benefits from their owners. For instance, when the grid is constrained with voltage excursions, then the exports form PV/wind turbine and exports/imports from/to battery can be curtailed. Therefore, such curtailment events need to be accounted for in the energy community setting by including power flow (physical network/grid constraints) in the techno-economic analysis. For example, in most of the prior literature, the studied models of energy communities do not consider the impact of physical network constraints in the assessment of the techno-economic benefits of community-owned energy assets compared to individually-owned energy assets. Moreover, most of existing redistribution frameworks are developed without considering network constraints, in which case the computation cost becomes even more challenging. hence, there is an urgent need to develop practically applicable redistribution mechanism that is scalable and computationally tractable.

One of the major challenges in P2P energy trading scheme based on coalition game theory is the issue of scalability. Specifically, when determining the solution concepts such as Shapley values in a coalition, the computation becomes highly complex and time-consuming as the number of players increases in the coalition. Moreover, most of the existing redistribution frameworks are developed without considering network constraints, in which case the computation becomes more challenging. Thus, there is

still a need to develop a redistribution mechanism that is fair, but also provide tractable computational performance that scales well with the increasing number of members in the energy community coalition, while considering operational network constraints. These challenges are addressed in the following Chapters 3, 4, and 5.

Although innovative P2P transactive models are proposed as a promising solutions for SLES, implementation of a fair market clearing mechanism still remains as one of the biggest technical challenges of the P2P energy trading schemes. Moreover, there is still a need to study the impacts of a community's characteristics on the profitability of P2P transactive schemes. For instance, local P2P energy trading market may not be profitable if all the members of the community own a larger energy asset. There is a significant knowledge gap on such sensitivity study on identifying the right or suitable characteristics of the community that makes the P2P local market profitable for the community. Furthermore, there is need to study the self-sufficiency of the community with and without local P2P markets, particularly the kind or markets that are determined in terms of import/export from the grid and P2P local markets. These issues are further investigated in the following Chapter 6.

Chapter 3

Modelling the control of energy assets for a single prosumer

Chapter 3 focuses on the modelling of the real-time control of energy assets for a single prosumer. In this chapter, a comprehensive model of a single prosumer is proposed with the objective to determine the benefits a prosumer can expect from owning a Renewable Energy System (RES) and/or a Battery Energy Storage System (BESS). As highlighted in chapter 2, the management of integrated renewable energy systems (consisting of renewable generator and storage) requires a careful consideration of assets' cost, sizing and operation, such as to maximize their Remaining Useful Lifetime (RUL), and hence return on investment. Technically, for instance, the depth to which a battery is discharged, the discharge current and the chemistry used has a direct effect on its remaining useful lifetime. This translates into a considerable impact on the total cost of operation and maintenance of the battery, especially as energy storage is one of the most expensive component of an integrated renewable energy system. Moreover, the frequent charging and discharging operations leads to cyclic ageing and incurs an extra cost as it accelerates the depreciation of the battery. Along with the fact that batteries' lifetime is comparatively shorter than that of renewable generators, this highlights the importance of using an appropriate battery control mechanism to extend the system's useful life. In this chapter, a rule-based battery control algorithm is proposed for maximization of behind the meter self-consumption, which considers the effect of battery life degradation. Furthermore, pricing schemes along with a comprehensive analysis and power generation profile from wind turbine an solar PV, and demand profile for a prosumer is presented in this chapter. These pricing schemes, renewable generation and demand profiles are adopted in the community settings of this thesis. Finally, this chapter also describes a techno-economic study of energy assets, and discusses future scenarios in which assets would become more profitable to a prosumer.

Part of the research work presented in Chapter 3 were published in peer-reviewed scientific paper [213].

3.1 Research contributions

The state of the art in modelling the prosumer were presented in detail in chapter 2. In this thesis, a prosumer model is presented to study the techno-economic benefits of investment in energy assets such as renewable generator (wind/solar PV) and battery assets. With respect to the scientific publications found in the literature review, the main contribution of this work relates to the development of real-time battery control algorithm for optimal scheduling of prosumer (end-user) renewable energy production and consumption. This rule-based battery control algorithm maximizes behind the meter self-consumption of the prosumer and it considers the effect of physical assets life degradation in the overall techno-economic analysis. As shown in section 2.2.2 of chapter 2, most of existing studies do not consider the battery degradation cost when determining the optimal battery capacity. The battery lifetime depends on the charge/discharge cycles, which in turn are shaped by the control scheme. Work presented in this chapter aims to accurately estimate the depreciation of the battery from the operating profiles and therefore assess the operational cost and overall economic value of the integrated renewable energy system consisting of RES and BESS. The methods developed provide a useful control strategy for a single prosumer for optimal scheduling of the renewable generation and battery storage that maximizes local consumption and decreases the simple payback period of storage assets to make them profitable. The major contribution of this work is that the optimization formulation (real-time control algorithm) integrates consideration of battery lifespan by accurately computing the DoD of each discharge half-cycle experienced by the battery, which is not fully addressed by the state of the art formulations.

In summary, the research contributions of the work presented in chapter 2 that progress beyond the state of the art are:

- This work models the control of prosumer energy assets from an economic and technical perspective with an unprecedented level of details. This includes, incorporating real state-of-the-art battery control and degradation functions, using real commercially-available, dynamic tariffs from the UK market, as well as a whole year of high-granularity demand and renewable generation data.

- A real time rule-based battery control algorithm is proposed. The control scheme consists of operational real-time decisions to charge or discharge the battery, and this if-then rule based control strategy includes several objectives, such as local bill reduction, and maximization of self-consumption.

- The key novel feature of the proposed framework is an integration of battery degradation model with renewable energy optimization. To achieve this, the control scheme employs a battery state of health degradation model based on the battery depth of discharge in each control cycle. The proposed control algorithm takes into consideration the battery's depreciation cost, which is determined by the accurate enumeration of battery cycles, including partial cycling i.e. battery cycles that do not start or end at 100% of SoC.

- A comprehensive techno-economic study of benefits provided by energy assets connected behind-the-meter for a single prosumer is presented for both fixed and dynamic tariffs. The proposed real-time battery control algorithm is implemented using different parameters (battery characteristics, prices, production and demand time-series) that can be changed in order to realize a sensitivity study on the profitability of a DERs at a prosumer level.
- The proposed control scheme, experimental and the economic study of the single prosumer (including the sensitivity analysis) is validated using a real case study from large-scale ReFLEX (Responsive Flexibility) smart energy demonstrator project based on the islands of Orkney, Scotland, UK [8], one of the UK's largest smart local energy demonstrator project.

The detail modelling of the control of energy assets for a single prosumer is presented in the following sections.

3.2 Methodology

A prosumer is an owner of various DERs, and is able to generate electricity as well as consume electricity [5]. Figure 3.1 shows the basic prosumer model, such models typically involve distributed renewable electricity generation-usually wind or solar PV, battery energy storage system and flexible/non-flexible demand normally installed behind-the-meter (power that can be used directly without passing through the utility grid meter [214]). Generally, prosumer's aim is to maximize behind-the-meter self-consumption from local renewable generation to make DERs more profitable.

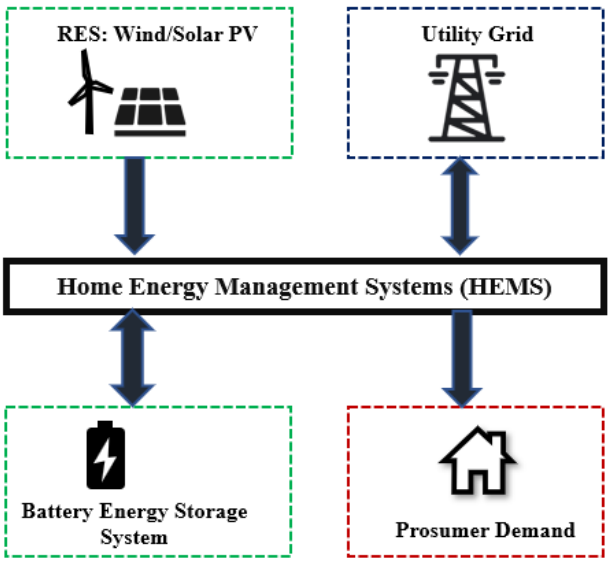

Figure 3.1: Prosumer model.

In the methodology employed, a prosumer model is utilized to examine the techno-economic advantages associated with investing in energy assets, including renewable

generators (wind/solar PV) and battery assets. This is illustrated in Figure 3.1. To achieve this, there is a need to use a simulated control of assets by implementing appropriate control algorithm considering the real time-series generation and demand data, simulated for different electricity pricing schemes. First, the model inputs are presented. This model inputs includes modelling of a real time-series data of production (wind/solar PV), prosumer demand and electricity pricing schemes (fixed tariff & dynamic ToU tariff). Then a comprehensive prosumer model with battery control mechanisms are described. Finally, a comprehensive techno-economic study is presented to determine the benefits offered by energy assets to prosumers, taking into account the degradation of physical assets and operational constraints.

3.3 Model data input

3.3.1 Demand profile data

Regarding the demand data available for simulation, a collection of energy demands of households connected to a smart grid during the Thames Valley Vision project [215] are utilized. The Thames dataset by Scottish & Southern Electricity Networks contains consumption data for 220 UK Elexon profile class-1 and class-2 households over a timespan of a year (from January 2017 to December 2017). Demand data consist of half hourly consumption load in watt-hour (Wh). In this thesis, the demand dataset for 200 houses of class-1 profile, which corresponds to domestic unrestricted customers, was used for the prosumer model. Two hundred households have been classified as either small or

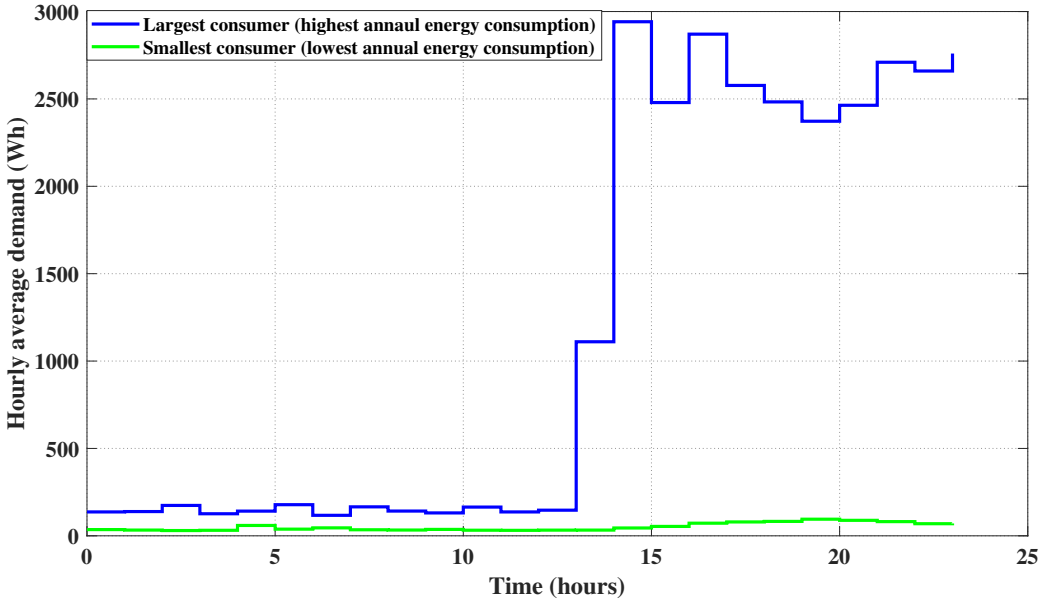

Figure 3.2: Hourly average demand of largest consumer (highest annual consumption) and smallest consumer (lowest annual energy consumption)

large consumers based on their annual energy consumption. Among these households,

the demand range varies significantly, ranging from the lowest annual consumption of 1001 kWh to the highest annual consumption of 18736 kWh. In order to determine the community demand, the individual demands of all 200 households are aggregated, providing an overall representation of the energy consumption within the community.

To analyse the energy consumption patterns of the highest consumer, lowest consumer, and the overall community, the average hourly demand for each category is computed. This provides insights into their respective energy usage throughout the day. Figure 3.2 showcases the average hourly demand for the highest consumer and lowest consumer. This figure enables a visual comparison of their energy consumption patterns, highlighting the peak and off-peak periods. The highest consumer's demand represents the household with the most significant energy usage in a year, while the lowest consumer's demand depicts the household with the lowest annual energy consumption.

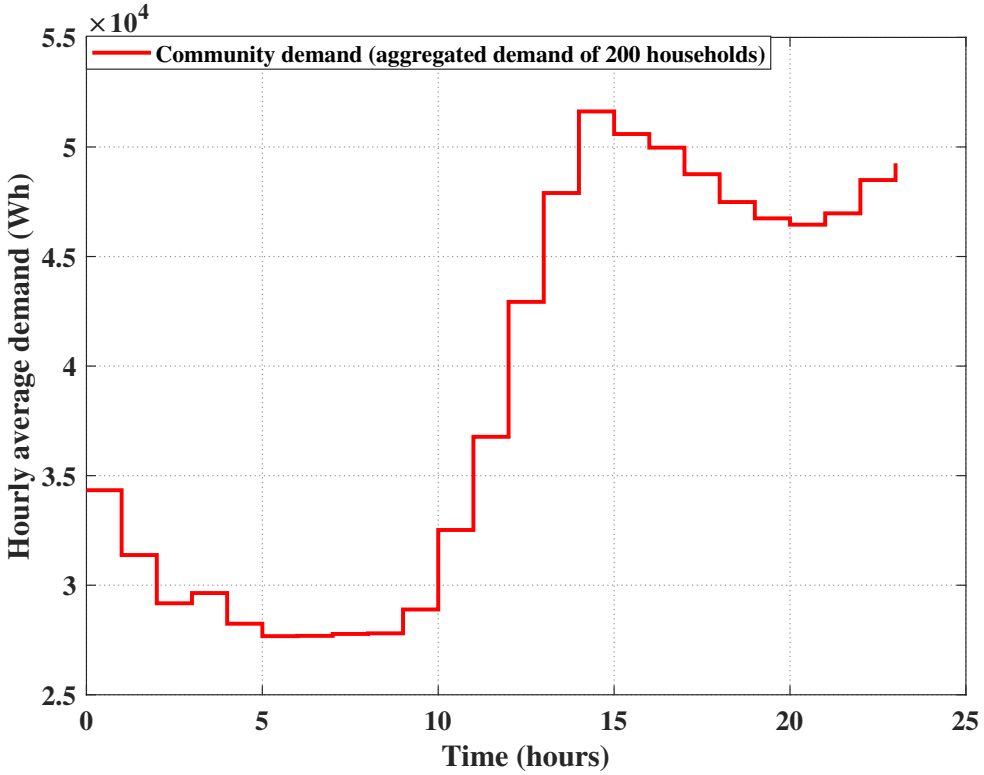

Figure 3.3: Hourly average demand of the community (aggregated demand of 200 households))

In Figure 3.3, the average hourly demand for the community is displayed. This plot illustrates the collective energy usage of all 200 households within the community. It showcases the overall energy demand over the course of a day, allowing for the identification of peak hours and general consumption trends. These figures provide valuable insights into the energy consumption patterns of different consumer types within the community. By comparing the average hourly demands for the highest consumer, lowest consumer, and community demand, a comprehensive understanding of energy usage variations can be obtained. These insights are crucial for designing effective energy management strategies and optimizing resource allocation within the community.

In this thesis, the utilization of demand data from the Thames Valley region in the South of England, rather than Orkney, was primarily driven by practical considerations. Specifically, it was found that the ReFLEX project, which had just commenced in Orkney, required more time to collect a sufficient amount of data from the installed smart meters. Meanwhile, comprehensive demand data from the Thames Valley area was readily available. Given the importance of having a substantial dataset for meaningful analysis, the decision was made to leverage the existing data from the Thames Valley region. This dataset provided a robust foundation for studying demand patterns, consumption behaviours, and other relevant factors within a real-world context.

On the other hand, for assessing the renewable generation potential of PV and wind resources, the decision was made to rely on Orkney's data. Known for its abundant renewable energy resources, Orkney provided a suitable setting to investigate the feasibility and optimization of integrating renewable energy sources into the local energy system. By combining the available demand data from the Thames Valley with the renewable generation data from Orkney, this thesis aims to contribute valuable insights into renewable energy systems. The broader objective is to enhance our understanding of renewable energy integration in different geographical contexts, ultimately facilitating the adoption and optimization of sustainable energy solutions worldwide. Furthermore, it is important to emphasize that throughout this thesis, a high priority has been given to the development of a robust methodology. While the dataset used is crucial for analysis, the focus has primarily been on ensuring rigorous research methods and sound analytical techniques to generate reliable and meaningful insights for the integration of renewable energy systems.

3.3.2 Wind speed and power model data

Real wind data from the UK Met Office Integrated Data Archive System (MIDAS) [216] provided by British Atmospheric Data Centre (BADC) was used for the analysis. The MIDAS dataset consist of meteorological observations from weather stations located at various parts of the UK. Wind data from the Kirkwall airport weather station located in Orkney, Scotland was specifically chosen to align with the objective of setting a local community energy system based on ReFLEX project [8]. Wind data obtained consist of hourly mean wind speed measured from anemometers at a nominal height of 10 m above the ground and ground is 26 m above sea level, rounded to the nearest knot (1 Kn = 0.5144 m/s). Wind data was cleaned and the missing data was replaced by double spline interpolation function. Similar methods adopted by Fruh [217, 218] and Andoni et al. [219] are applied for converting wind speed to power.

A power curve was adopted based on an Enercon E-33 [220] wind turbine of 330 kW rated capacity and a hub height of 50 m. The wind turbine has cut-in speed of 3 m/s and cut-out speed of 25 m/s. Logarithmic shear profile is used to extrapolate wind speed in m/s

from nominal anemometer height(Z^a) to nominal wind turbine hub height(Z^h):

$$U^h = U^a \frac{log\frac{Z^h}{Z^0}}{log\frac{Z^a}{Z^0}} \tag{3.1}$$

where, U^h is the wind speed at hub height, U_a is wind speed at anemometer height and Z^o is the surface roughness. Z^a = 26 m, Z^h = 50 m and the surface roughness Z^0 = 0.03 m (as adopted in [217–219]) are used in estimating the wind speed at hub height. The power curve of the Enercon E-33 wind turbine was used in estimating the power output of the wind turbine, and the generated power was normalised to the rated capacity or nominal power output. Then, the intermediate values of the estimated power are approximated by a sigmoid function with parameters a = 0.7526 s/m and b=8.424 m/s as per the Eq. (3.2).

$$f(u,a,b) = \frac{1}{1+e^{-a(u-b)}} \tag{3.2}$$

Wind power estimated in kW was converted to W and one hour resolution data is converted to half hourly data (using double spline interpolation function). Conversion of wind power was performed to make it compatible with the resolution of demand data. The wind power estimated from the power curve of the Enercon E-33 wind turbine is shown in Figure 3.4.

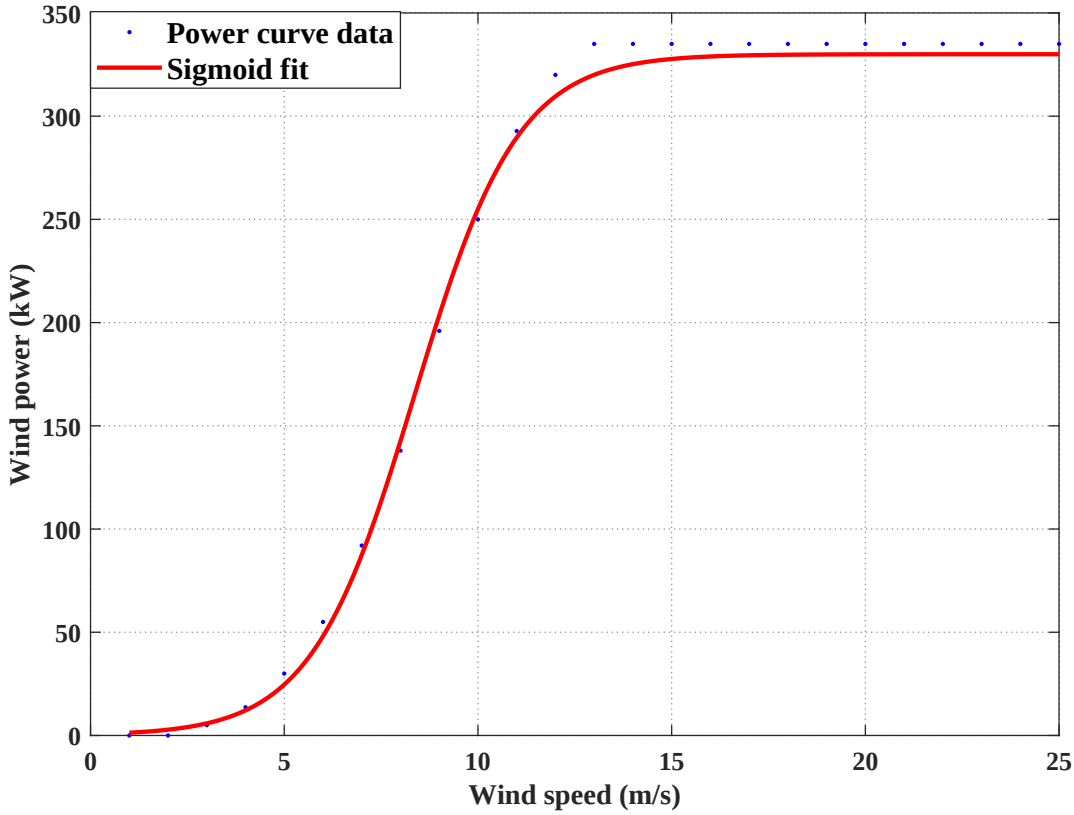

Figure 3.4: Power curve of Enercon E-33 wind turbine and best sigmoid fit function based on Eq. 3.2.

3.3.3 Solar radiation and PV power data

Similar to wind generation data, for the analysis we have used a real solar radiation data from the UK Met Office Integrated Data Archive System (MIDAS) [221] provided by British Atmospheric Data Centre (BADC). The MIDAS dataset consists of meteorological observations from weather stations located at various parts of the UK. In this thesis, solar irradiance data collected by station located at Kirkwall, Orkney is used.

The UK hourly solar radiation data contain the amount of solar irradiance received during the hour ending at the specified time. All sites report 'global' radiation amounts. This is also known as 'total sky radiation' as it includes both direct solar irradiance and 'diffuse' irradiance as a result of light scattering. To optimize energy production, solar panels are commonly angled in accordance with the latitude of the installation site. This practice enables the panels to effectively capture sunlight throughout the year by aligning them perpendicular to the sun's rays at noon during the equinoxes. In the case of Kirkwall, Orkney, which has a latitude of approximately 59 degrees north, a recommended tilt angle for solar PV panels would typically range from 60 to 65 degrees from the horizontal plane. This steeper tilt compensates for the reduced sunlight during the winter months and ensures efficient solar energy generation in the region.

The process of estimating solar PV power generation involves converting hourly solar radiation data from kilojoules per square meter (kJ/m^2) to watts per square meter (W/m^2). This conversion establishes a direct correlation between solar radiation intensity and potential power output. The data is then normalized, taking into account the system's efficiency and panel area, to ensure a more accurate estimation of actual power generation. To align the solar PV power data with the resolution of the demand data (i.e., half-hourly intervals), a conversion from hourly resolution to half-hourly resolution is performed. This adjustment enables a consistent analysis and comparison of the solar PV power data with the demand data. The resolution adjustment is typically achieved using double spline interpolation, which estimates power values at intermediate time points based on the available hourly data. By following these steps, the solar radiation data is effectively transformed into solar PV power data at a compatible resolution, allowing for accurate analysis and comparison with the demand data.

3.3.4 Tariff structure data

In this thesis, the focus was not on the consideration of the feed-in tariff (export tariff). Instead, two types of pricing schemes for energy imports from the main utility grid were taken into account. Export tariff to the grid was not included as many developed countries worldwide (such as the UK or the EU), guaranteed feed-in-tariffs (FITs) for renewable electricity generated by small DERs are being phased out as a support mechanism, i.e. they are gradually reduced or are well below retail tariffs available from large operators [34]. For instance, in the UK, FITs are no longer available to producers of any size since 31^{st} March 2019 [15]. A fixed and a dynamic time of use (ToU) import tariffs were considered as described below:

- **Fixed tariff:** a fixed tariff of 16 pence/kWh was adopted after comparing the fixed electricity prices offered by various UK-based electricity suppliers using web-tools in price comparison site Money Supermarket [222]. This website is one of the several price comparison sites approved and accredited by the Office of Gas and Electricity Markets (Ofgem) [223], the government regulator for the electricity and downstream natural gas markets in UK.

- **Dynamic tariff (ToU):** the dynamic ToU tariff was based on Agile Octopus [224] offered by Octopus Energy, a UK-based electricity supplier. Agile Octopus tariff consist of a maximum price of 35 pence/kWh, an average price of 15.9 pence/kWh, and a minimum of 2.8 pence/kWh. Both the fixed and dynamic ToU pricing schemes corresponds to real tariffs applied in 2022.

3.3.5 Unitary cost of energy assets

In this thesis, a battery cost of 150 £/kWh was assumed based on 2022 Lithium-ion battery forecasts estimated by BloombergNEF [225, 226]. According to BloombergNEF [226] and PV Europe-Energy Storage [227], battery costs are expected to drop even further in the following years with an estimated cost of less than $100/kWh expected in 2023. The chosen battery cost of 150 £/kWh for the year 2022 is consistent with the Lithium-ion battery cost forecasts for 2022 and 2025 published in the McKinsey quarterly report [228]. A cost of 1100 £/kW for solar PV generation capacity, and 1072 £/kW for wind generation capacity was assumed based on the production and installation cost of solar PV and wind turbines according to EIA, Annual Energy Outlook 2022 [229]. These costs reflects the average values of levelized cost of electricity (LCOE) and levelized avoided cost of electricity (LACE) for solar PV generating technologies entering service in 2025.

3.4 Model overview

The model of a single prosumer includes the following assets owned by the prosumer:

1. Wind turbine or solar PV.
2. Battery.
3. Non-flexible loads.

A power flow diagram of the single prosumer model is shown in Figure 3.5. The overall power balance of the system at any given time t is given by:

$$p^{\text{grid}}(t) = d(t) - p^{\text{bat}}(t) - g^{\text{wind/solar}}(t), \quad \forall t \in [0,T] \tag{3.3}$$

where T corresponds to the end of the considered time period for the operation of the system. For example, if the operation window $[0,T]$ consists of a full calendar year with half-hourly time steps, then $|[0,T]| = 365 \times 48 = 17520$ time steps. $g^{\text{wind/solar}}(t)$ is the power (or energy as fixed time interval is considered) generated by the renewable generator (either wind turbine or a solar PV installation). $p^{\text{grid}}(t)$ represents the power that a prosumer can buy/sell power from/to the grid. $p^{\text{bat}}(t)$ represents the power of the storage system, which is considered negative when the battery is charging (battery considered as load), and positive when the battery is discharging (battery considered as generator). $d(t)$ is the power consumed by the prosumer.

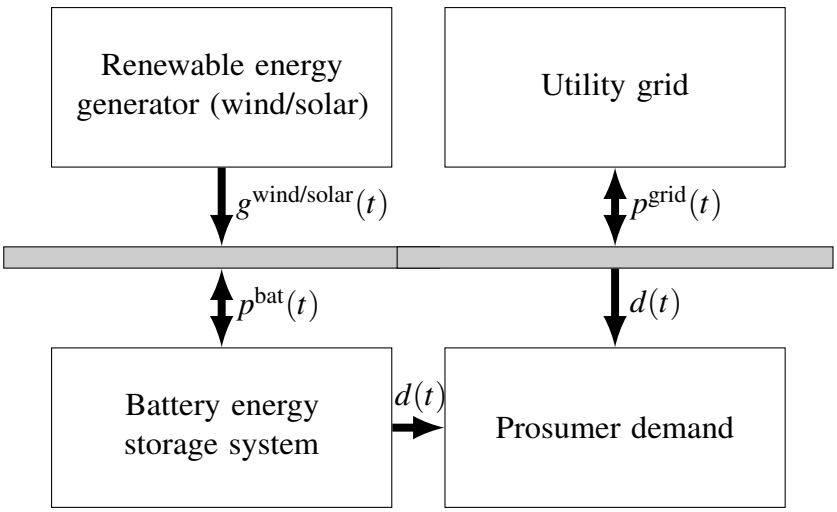

Figure 3.5: Power flow diagram of the single prosumer model.

The battery is used to store the excess power from the intermittent power source (wind or solar). The prosumer demand $d(t)$ is considered inflexible and needs to be satisfied at all times by these three power sources (RES, BESS and the utility grid). The control algorithm for the battery to meet the demand $d(t)$ with these three power sources is defined in the following subsection.

3.4.1 Battery modelling and control algorithm

The operation of the battery is constrained by the state of charge (SoC) levels, and a maximum power ($p^{\text{bat,max}}$) that the battery can be charged or discharged at, which corresponds to its maximum C-rating. At any given time t of a charging phase, the battery is charged with an efficiency (η^c) until it reaches the maximum battery capacity ($SoC^{\max}$). Charging constraints are defined as:

$$SoC(t) \leq SoC^{\max} \tag{3.4}$$

$$p^{\text{bat}}(t) \leq p^{\text{bat,max}} \tag{3.5}$$

Similarly, the battery can be discharged with an efficiency (η^d) until it reaches its minimum battery capacity ($SoC_{\min}$). Discharging constraints are defined as:

$$SoC(t) \geq SoC^{\min} \tag{3.6}$$

$$p^{\text{bat}}(t) \leq p^{\text{bat,max}} \tag{3.7}$$

The minimum battery capacity corresponds to the maximum allowable depth of discharge (DoD). A battery control scheme consists of operational real-time decisions to charge or discharge the battery. In this subsection, a *rule-based battery control* algorithm is proposed. The primary objective of this algorithm is to charge the battery during periods of power surplus and discharge the battery during periods of power deficit. The algorithm can be described as follows:

If $g^{\text{wind/solar}}(t) > d(t)$, there is *excess of power* generated from the intermittent source. The control strategy of the battery dictates the following:

i If $SoC(t) \leq SoC^{\max}$ and $p^{\text{bat}}(t) \leq p^{\text{bat,max}}$ then the excess power is stored in the battery (charging operation, $p^{\text{bat}}(t) < 0$).

ii If the battery is full ($SoC(t) > SoC^{\max}$) or if available power is greater than the maximum acceptable charging power ($p^{\text{bat}}(t) > p^{\text{bat,max}}$), then the prosumer sells the excess power to the utility grid at a selling price equal to $\tau^s(t)$.

The resulting SoC profile and the energy exported $e^s(t)$ to the grid during the identified duration of excess generation are determined as:

$$p^{\text{bat}}(t) = -\min\left(\min\left(\left[g^{\text{wind/solar}}(t) - d(t)\right], p^{\text{bat,max}}\right), \frac{[SoC^{\max} - SoC(t-1)]}{\eta^c \Delta t}\right) \tag{3.8}$$

$$SoC(t) = SoC(t-1) - \eta^c p^{\text{bat}}(t)\Delta t \tag{3.9}$$

$$e^s(t) = \left[g^{\text{wind/solar}}(t) - d(t) + p^{\text{bat}}(t)\right]\Delta t \tag{3.10}$$

where Δt corresponds to the duration of the considered time step.

Similarly, if $g^{\text{wind/solar}}(t) < d(t)$, then there is a *deficit in power* supplied by the intermittent source and the battery will operate as follows:

i If $SoC(t) \geq SoC^{\min}$ and $p^{\text{bat}}(t) \leq p^{\text{bat,max}}$ then discharge the battery to meet the demand (discharging operation, $p^{\text{bat}}(t) > 0$).

ii If the battery energy or power are not enough (i.e $SoC(t) < SoC^{\min}$ or $p^{\text{bat}}(t) > p^{\text{bat,max}}$) to compensate the power deficit at this time step, the prosumer buys the remaining deficit power from the utility grid at a buying price equal to $\tau^b(t)$.

Hence, the SoC profile and energy imported $e^b(t)$ from the utility grid during the identified duration of deficit in energy are determined as:

$$p^{\text{bat}}(t) = min\left(min\left(\left[d(t) - g^{\text{wind/solar}}(t)\right], p^{\text{bat,max}}\right), \eta^d\left[SoC(t-1) - SoC^{\min}\right]\right) \quad (3.11)$$

$$SoC(t) = SoC(t-1) - \frac{p^{\text{bat}}(t)}{\eta^d} \cdot \Delta t \quad (3.12)$$

$$e^b(t) = \left[d(t) - g^{\text{wind/solar}}(t) - p^{\text{bat}}(t)\right]\Delta t. \quad (3.13)$$

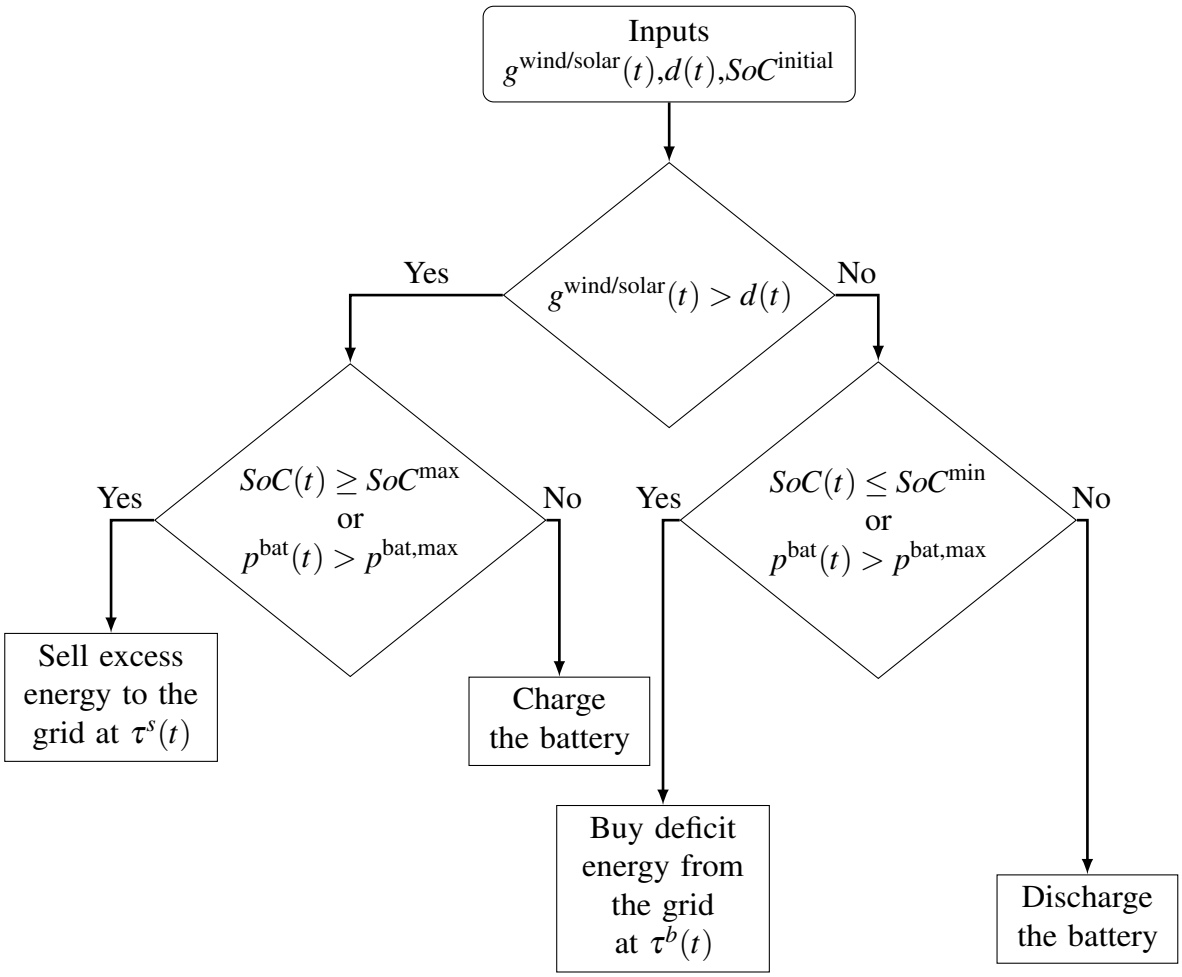

Figure 3.6: Flowchart of rule-based battery control strategy.

A flowchart of the proposed control strategy is shown in Figure 3.6. Algorithm 3.1 outlines this if-then rule based control strategy. The proposed control algorithm is generic in nature and can be easily extended to incorporate decisions based on price signals,

although our extensive experiments showed that incorporating current ToU price signals in the algorithm did not provide greater benefits to the prosumer.

Algorithm 3.1: Rule-based battery control algorithm

Input1: generation $g^{\text{wind/solar}}(t)$, demand $d(t)$, and grid price: $\tau^b(t)$,$\tau^s(t)$
Input2: battery specifications: η^c, η^d, SoC^{initial}, $SoC^{\max}$, $SoC^{\min}$, $p^{\text{bat,max}}$, rated capacity of the battery as variable input
for $t = 1 : T$ **do**
  $\forall t \in [0,T]$, excess of energy or deficit in energy is determined
  if $g^{wind/solar}(t) \geq d(t)$ **then**
    $$p^{\text{bat}}(t) = -min\left(min\left(\left[g^{\text{wind/solar}}(t) - d(t)\right], p^{\text{bat,max}}\right), \frac{[SoC^{\max} - SoC(t-1)]}{\eta^c \Delta t}\right)$$
    When, $SoC(t) \leq SoC^{\max}$ and $p^{\text{bat}}(t) \leq p^{\text{bat,max}}$
    Charging the battery ($p^{\text{bat}}(t) < 0$):
    $SoC(t) = SoC(t-1) - \eta^c p^{\text{bat}}(t)\Delta t$
    When, $SoC(t) > SoC^{\max}$ or $p^{\text{bat}}(t) > p^{\text{bat,max}}$
    Sell excess energy to the grid at $\tau^s(t)$:
    $e^s(t) = \left[g^{\text{wind/solar}}(t) - d(t) + p^{\text{bat}}(t)\right]\Delta t$
  else
    $$p^{\text{bat}}(t) = min\left(min\left(\left[d(t) - g^{\text{wind/solar}}(t)\right], p^{\text{bat,max}}\right), \eta^d\left[SoC(t-1) - SoC^{\min}\right]\right)$$
    When, $SoC(t) \geq SoC^{\min}$ and $p^{\text{bat}}(t) \leq p^{\text{bat,max}}$
    Discharge the battery ($p^{\text{bat}}(t) > 0$):
    $SoC(t) = SoC(t-1) - \frac{p^{\text{bat}}(t)}{\eta^d} \cdot \Delta t$
    When, $SoC(t) < SoC^{\min}$ or $p^{\text{bat}}(t) > p^{\text{bat,max}}$
    Buy deficit energy from the grid at $\tau^b(t)$:
    $e^b(t) = \left[d(t) - g^{\text{wind/solar}}(t) - p^{\text{bat}}(t)\right]\Delta t$
  end
end
Output: $\forall t \in [0,T]$, $SoC(t)$, input to **rainflow cycle counting algorithm** used to calculate the battery depreciation factor, $e^s(t)$ energy exported to grid at a selling price equal to $\tau^s(t)$, and $e^b(t)$ energy imported from grid at a buying price equal to $\tau^b(t)$.

The performance of the *rule-based battery control strategy* was compared with an *optimisation-based battery control* [230] based on Mixed Integer Linear Programming (MILP) that determines the optimal battery schedules for a future period (day-ahead for example) based on forecasts of future renewable generation, demand and electricity prices. Figure 3.7 shows the comparison of the bill of a prosumer for different battery control algorithms, such as the proposed rule-based algorithm (in yellow), and two optimization based control algorithms with different time horizon. The first optimization control with the time horizon of 1 day corresponds to an optimization-based battery control approach where the optimization problem is solved to determine the optimal battery schedules for the next 24 hours (1 day). This strategy considers forecasts of renewable generation,

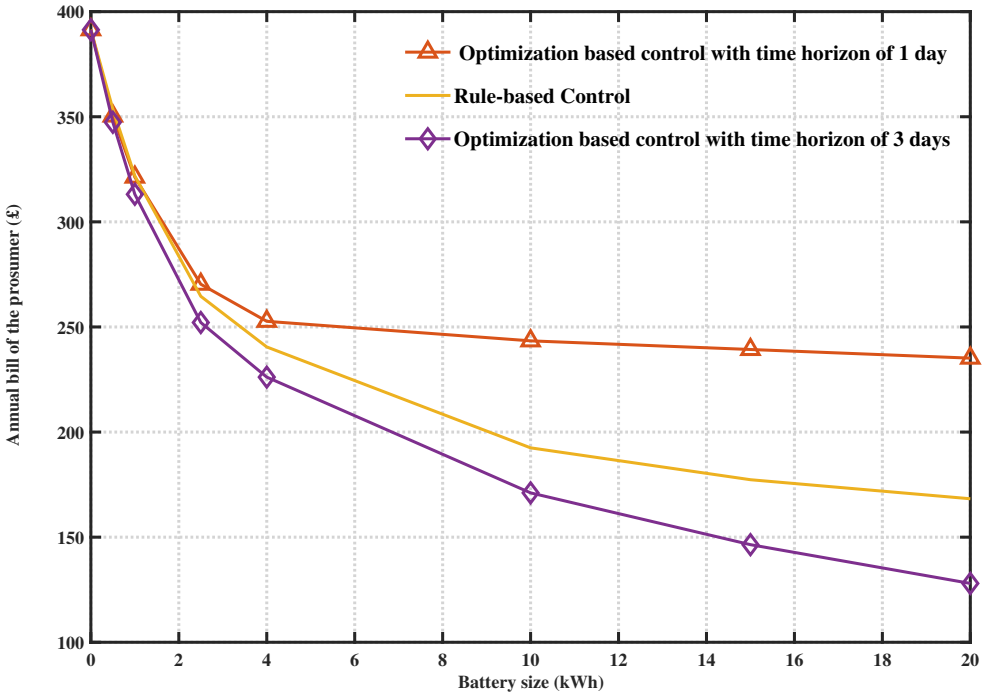

Figure 3.7: Comparison of the annual bill achieved for a prosumer using optimization based and rule-based control algorithms for batteries capacities ranging from 0 to 20 kWh.

demand, and electricity prices within a 24-hour time frame. The second optimization based control with time horizon of 3 days strategy is another optimization-based battery control approach with an extended time horizon. In this case, the optimization problem is solved to determine the optimal battery schedules for the next three days (72 hours). The forecasts of renewable generation, demand, and electricity prices are assumed to be accurate for this three-day period. The comparison of the prosumer's bill allows for an evaluation of the financial benefits obtained from each battery control strategy. It assesses the cost savings or other relevant metrics achieved by the rule-based approach compared to the optimization-based approaches with different time horizons. One can see that the longer the optimization time horizon is, the better the control decisions will be. However, this does not include the risk of forecast uncertainties.

The comparison demonstrated that longer optimization time horizons led to improved control decisions. However, this analysis did not account for the risk of forecast uncertainties. In the case where electricity import prices ($\tau^b(t)$) consistently exceeded electricity export prices ($\tau^s(t)$), both the rule-based battery control and the optimization based battery control for arbitrage yielded comparable benefits to the prosumer. However, the optimization based approach exhibited significantly greater complexity and uncertainty. Consequently, the thesis focused solely on the rule-based battery control scheme, as it provided satisfactory benefits without the added complexities associated with the optimization based approach.

3.4.2 Battery degradation for economic study

To determine the economic viability of integrated renewable energy systems that include battery energy storage system, it is important to assess the depreciation (degradation) of the battery, since the battery lifespan is much shorter than the one of other assets such as renewable generators [86, 85]. The useful battery lifetime depends on the frequency of charge/discharge cycles, and on the depth of discharge (DoD) [81]. Indeed, frequent deep charging and discharging operations lead to cyclic ageing inflicting additional costs, as the depreciation of the battery is accelerated [82]. Thus, there is a need to accurately estimate the depreciation of the battery to assess the operational cost and overall economic value of the battery energy storage system.

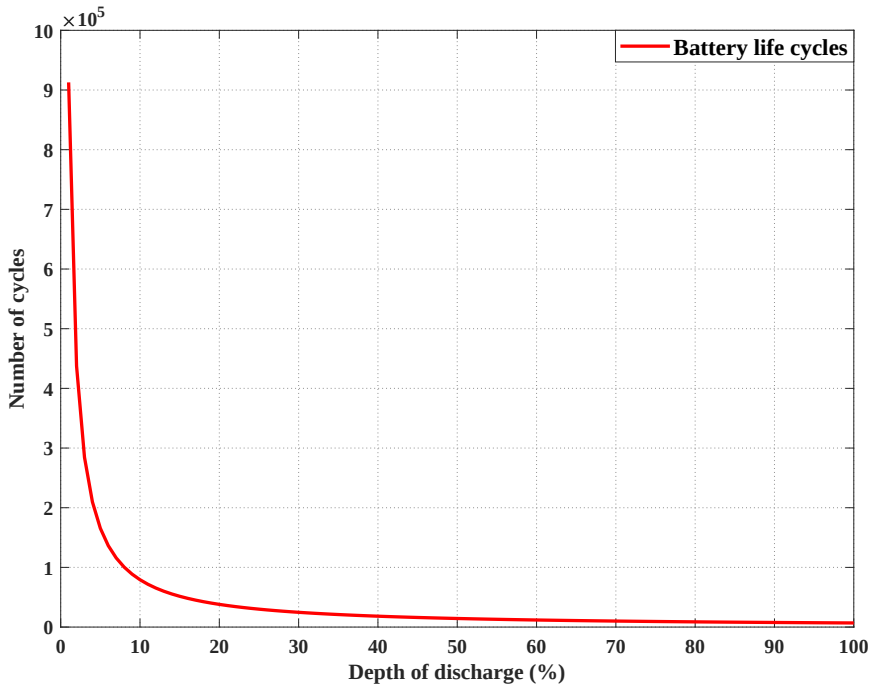

Figure 3.8: Li-ion battery life cycle data used in the modelling based on data from [86].

Calendar life refers to the number of years a battery is expected to last until it reaches its end of life (EoL). EoL is normally defined as a state of the battery when the maximum capacity of the battery reduces to 80% of its rated initial capacity. It is independent of its cycling behaviour, and thus it is normally regarded as constant [82]. Predominantly, the service life of the battery usually degrades when subjected to repeated charge/discharge cycles. Furthermore, battery life not only depends on total number of cycles, but also to the depth of discharge (DoD) of the cycles as specified by the manufacturers. Therefore, most of the emerging and existing battery degradation models assess the useful life of a battery by considering cyclic degradation [86, 84, 81, 85, 82, 87, 83, 69].

A battery cycle life corresponds to the number of charge/discharge cycles the battery can undergo based at a certain DoD as specified by the manufacturer. Typically, the number of cycles in a battery lifetime versus the cycle's DoD is specified in the battery data sheet as shown in Figure 3.8 . For instance, if the total number of permitted battery cycles is

2000 with 80% DoD, it means that every cycle from 100% state of charge (SoC) to 20% SoC consumes 1/2000 = 0.05% of the total life. Figure 3.8 shows that, as the DoD of the charging/discharging cycle increases, the expected cycle-life of the battery decreases. This means, a battery that is exposed to shallow charging/discharging cycles is expected to have a longer cycle-life than the battery that is exposed to deeper discharges [83]. It is important to note that the number of cycles versus DoD curve provided by manufacturers is obtained at specific temperature and C-rating.

A cycle is considered complete when the battery's depth of discharge returns to its initial point. Within these cycles, there are two types: *full cycles* and *half cycles*. Full cycles involve equal depths of discharging and charging, while half cycles consist of either a charging or discharging phase. Additionally, cycles can be further categorized as either *regular* or *irregular* based on the starting and ending state of charge (SoC) within the cycle. The specific definitions for regular and irregular cycles are as follows:

- *Regular cycles:* in this cycling process the starting SoC is 100%, then it is discharged to a certain SOC corresponding to a specific DoD and recharged back to 100% SoC. For example, 100% SoC-to-50% SoC-back to 100% SoC corresponds to 50% DoD cycle.

- *Irregular cycles:* in this case, the starting SoC is not other than 100% SoC, i.e. cycles start at any arbitrary SoC value. For example, 80% SoC-to-30% SoC-back to 80% SoC, which also corresponds to a 50% DoD cycle, relatively to the starting SoC.

In both cases, the DoD may be same, but the battery degradation is sensitive to the starting SoC. Note here that the number of cycles versus DoD specified in manufacturer data-sheets are based on regular cycles only. In real-life applications, the battery can hardly run regular cycles from 100% SoC to a specific DoD [85, 87]. Thus, an important aspect when integrating battery storage degradation in the economic analysis of a prosumer, is to assess the impacts of irregular cycles.

In this thesis, a *rainflow cycle counting algorithm* [98, 99] is adopted to count half and full cycles. Then, the algorithm is further modified to determine regular and irregular cycles. This algorithm was initially proposed by Socie and Downing [98] for material fatigue estimates, and has been widely used for extraction of full or partial cycles in battery degradation models [82, 86, 87, 85, 231]. In this thesis, the focus is solely on Lithium-ion battery technology. The battery cycle life data utilized in this study is sourced from [86]. Figure 3.8 shows the number of cycles, noted N_{cycles}, that a battery cell can perform before the battery capacity reduces to 80% of its initial capacity.

The input to the rainflow cycle counting algorithm is the SoC profile resulting from the simulated operation of Algorithm 3.1. Outputs include the number of cycles the battery experienced, which are classified by type (full or half cycles, regular or irregular) [86]. The number of cycles is also classified by their DoD and starting/ending SoC. The depreciation factor (DF) is then determined to estimate the battery lifetime.

The overall battery depreciation factor (DF), can be expressed as the sum of the depreciation from regular cycles (DF_r) and from irregular cycles (DF_i):

$$DF = DF_r + DF_i \tag{3.14}$$

Regular cycles can be combined into DoD bins of size Δ, where N^{DoD} is the maximum number of cycles at the given DoD specified by the battery manufacturer as shown in Figure 3.8, and n_r^{DoD} is the number of regular cycles observed within the range of $DoD \pm \frac{1}{2}\Delta$. With this, the contribution to the depreciation from regular cycles is determined as:

$$DF_r = \sum_{DoD=\frac{\Delta}{2}}^{100\%-\frac{\Delta}{2}} \frac{n_r^{DoD}}{N^{DoD}} \tag{3.15}$$

For, irregular cycles the depreciation factor is calculated with the following process, inspired from the work of Ke et al.[87]. The overall battery depreciation factor , DF, can be expressed as the contribution to the depreciation from each cycle. Since the data only provide information for regular cycles, an equivalent Depth of Discharge, DoD_{eq}, has to be defined.

For irregular cycles, the model assumes that the Depth of Discharge for an irregular cycle can be approximated by an equivalent Depth of Discharge for the highest SoC during a cycle, SoC_{max}, and the lowest SoC, SoC_{min}. The equivalent DoD is determined as:

$$DoD_{eq} = 100\% - SoC \tag{3.16}$$

where, $SoC = SoC_{max}$ or SoC_{min}.

Using the equivalent DoD and accounting for a full cycle with $m = 1$ and a half cycle with $m = \frac{1}{2}$, the contribution from irregular cycle j is determined as:

$$DF_j = m_j \times \left[\frac{1}{N\left(DoD_{j,\,min}^{eq}\right)} - \frac{1}{N\left(DoD_{j,\,max}^{eq}\right)} \right] \tag{3.17}$$

While this is derived for irregular cycles, it can also be applied to a full or half regular cycle assuming that N becomes infinite at zero DoD, and $1/N$ zero. The accumulated depreciation factor over J irregular cycles then becomes:

$$DF_i(J) = \sum_{j=1}^{J} DF_j \tag{3.18}$$

where J is the set of all irregular cycles.

3.5 Techno-economic study of prosumer energy assets

The main aim of the techno-economic study is to determine the benefits provided by energy assets (renewable generation capacity and storage) to prosumers, subjected to physical assets degradation and operational constraints. To achieve this, the presented Algorithm 3.1 is implemented by considering the different pricing schemes. A yearly energy bill savings (reduction of annual electricity bill of prosumer), which is a fairly intuitive indicator, is used to determine the economic value offered by energy assets to a prosumer. The resulting bills for a single prosumer are then compared in order to identify what parameters have the greatest impact on the energy assets profitability.

Broadly speaking, the yearly bill of a prosumer $b(T)$ can be expressed as the sum of the cost of the annual energy consumption and the depreciation cost of the assets c^A, minus the sum of revenues earned by exports to the grid, as shown below:

$$b(T) = \sum_{1}^{T} e^b(t)\tau^b(t) - \sum_{1}^{T} e^s(t)\tau^s(t) + c^A(T) \tag{3.19}$$

where the energy import $e^b(t)$ at time step t is given by Eq. (3.13), and the energy export $e^s(t)$ at time step t is given by Eq. (3.10). However, as many countries have reduced or removed export prices under the form of feed-in tariffs, our analysis will not include revenues from energy export. Hence, the yearly bill without feed-in tariff is determined as:

$$b(T) = \sum_{1}^{T} e^b(t)\tau^b(t) + c^A(T) \tag{3.20}$$

In Eqs. (3.19) and (3.20), c^A represents the depreciation cost which is due to the usage of the asset within the considered period. For example, for a considered period T equal to one year in which the asset is used following the manufacturer's recommendations, $c^A(T)$ corresponds to the annualized cost of the asset, given as follows:

$$c^A(T) = \frac{\text{Asset cost}}{\text{Life time (in years)}} \tag{3.21}$$

Taking into consideration the depreciation inflicted by battery operation and control Algorithm 3.1, the computation of the depreciation cost c^A must be updated as follows:

$$c^A(T) = \max\left(\frac{1}{\text{DF}}, \frac{\text{Asset cost}}{\text{Life time (in years)}}\right) \tag{3.22}$$

3.6 Experimental results for the case of a single prosumer

3.6.1 Techno-economic study of asset sizing

Initially, it is crucial for the prosumer to determine the appropriate capacity of energy assets to be installed. In this study, an optimal size was chosen for both the renewable generator (wind turbine, solar PV) and battery storage energy assets. To determine the optimal capacity that minimizes the billing expression defined in Eq. (3.20), a sensitivity analysis was conducted on the energy assets' capacity. This analysis allows for an investigation of the optimal sizing of the energy assets. To illustrate the sensitivity analysis, a prosumer with an annual demand of 7888 kWh (as discussed in Section 3.3.1) was considered. The simulations were conducted for two pricing schemes: a flat tariff of 16 pence/kWh [222] and the dynamic Agile Octopus ToU tariff [224] (as described in Section 3.3.4).

The optimal size of energy assets is determined based on achieving the minimal simple payback period. In this thesis, the process of determining the optimal capacities of the energy assets follows a step-by-step approach, as outlined below:

i **Optimal renewable generator only:** Initially, the focus is on determining the optimal capacity for the renewable generator (such as wind turbines or solar PV panels) without considering any storage. This step establishes the baseline for understanding the optimal capacity of the renewable generator alone.

ii **Optimal renewable generator and optimal battery storage capacity:** Building upon the previous step, the optimal capacity of the battery storage system (BESS) is determined by integrating it with the previously determined optimal capacity of the renewable generator. It is important to note that this thesis assumes the prosumer has already invested in the optimal renewable generator, and the battery storage is added to enhance the existing generation capacity. However, if the renewable generator and battery storage are considered as a new investment, the optimal capacity of the renewable generator may differ when combined with battery storage.

For both types of energy assets (renewable generators and batteries), the investment cost and degradation resulting from their operation are taken into account. The computation of the simple payback period for each energy asset involves simulations utilizing the battery control Algorithm 3.1 over a one-year period. Furthermore, the yearly bill of a prosumer without any energy assets (referred to as the baseline yearly bill) is determined. This baseline yearly bill serves as a reference for comparing the savings or benefits achieved from investing in generation and storage assets.

To elaborate further, the subsequent subsections of this thesis will detail the specific methodologies used to determine the optimal renewable generator capacity in the absence of storage and the subsequent calculation of the optimal battery capacity when integrated with the established renewable generator. The logical progression through these chapters ensures a comprehensive understanding of the varying optimal capacities for different

energy asset configurations. First, the optimal renewable generator capacity is determined as described in the following subsection.

Optimal renewable generator (wind turbine, solar PV) without battery storage assets

In the given scenario, it is assumed that the prosumer has the option to own either a solar PV or a wind turbine renewable generator. In this case, only the investment cost of the renewable generator is taken into consideration. The depreciation cost resulting from the operation of the renewable generator is not included, as it is assumed that the operations of the generator follow the manufacturer's guidelines. Furthermore, it is assumed that every prosumer owns a renewable generator with a rated power equal to the optimal rated power specifically determined for that prosumer. This represents the most conservative scenario for individual renewable generators, whether it is a solar PV or a wind turbine. Optimal rated capacity of the renewable generator corresponds to that rated power that achieves the minimum annual bill given by Eqs. (3.20). Simulations are performed for one year, without a battery energy storage system, and for both flat and ToU pricing schemes.

Pricing scheme	**Optimal wind turbine**			
	Optimal capacity (kW)	**Annual bill with optimal wind (£)**	**Annual bill without assets (baseline) (£)**	**Annual saving (£)**
Flat tariff	4.1	680	1262	582
ToU tariff	4.2	672	1274	601

Table 3.1: Prosumer optimal wind turbine capacity, and the corresponding annual bill and saving for both the flat tariff of 16 pence/kWh [222] and dynamic Agile Octopus ToU tariff [224].

Pricing scheme	**Optimal solar PV**			
	Optimal capacity (kW)	**Annual bill with optimal PV (£)**	**Annual bill without assets (baseline) (£)**	**Annual saving (£)**
Flat tariff	3.4	1090	1262	172
ToU tariff	3.4	1077	1274	196

Table 3.2: Prosumer solar PV capacity, and the corresponding annual bill and saving for both the flat tariff of 16 pence/kWh [222] and dynamic Agile Octopus ToU tariff [224].

Results of an optimal renewable generator size, the corresponding annual bill and the saving for the prosumer are shown in Table 3.1 for wind turbine and Table 3.2 for solar PV, obtained for both the flat tariff and dynamic ToU tariff pricing schemes. Figure 3.9 shows the evolution of prosumer yearly bill as a function of wind turbine capacity and shows that the optimal capacity for this prosumer simulated for a fixed tariff is 4.1 kW. With this

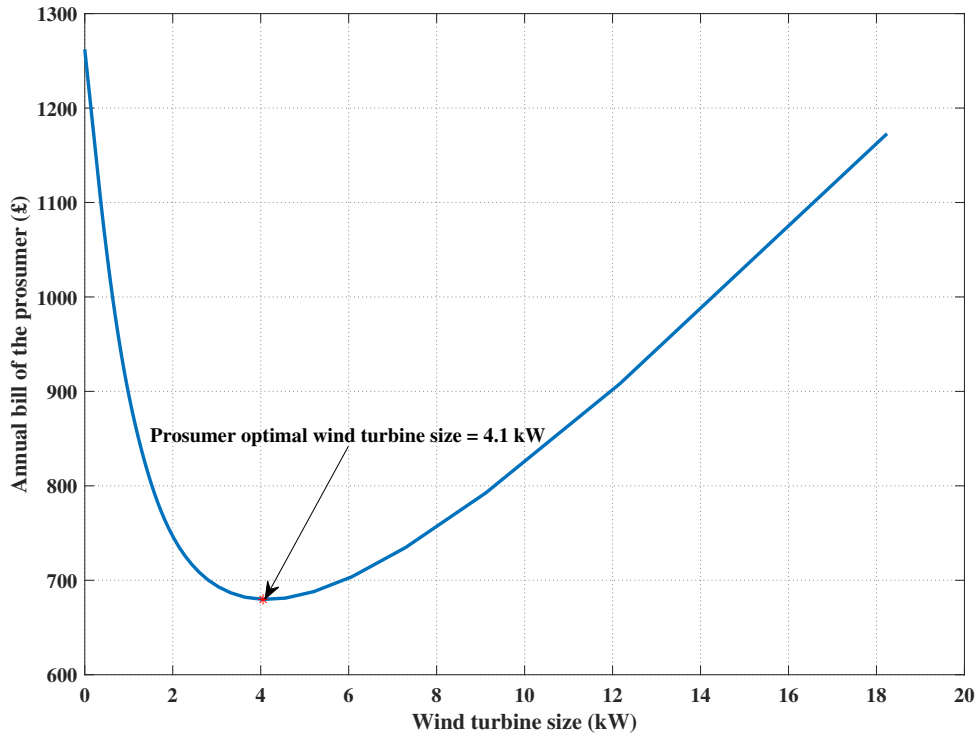

Figure 3.9: Annual bill versus wind turbine capacity for prosumer with annual demand of 7888 kWh simulated for the flat grid import tariff of 16 pence/kWh [222].

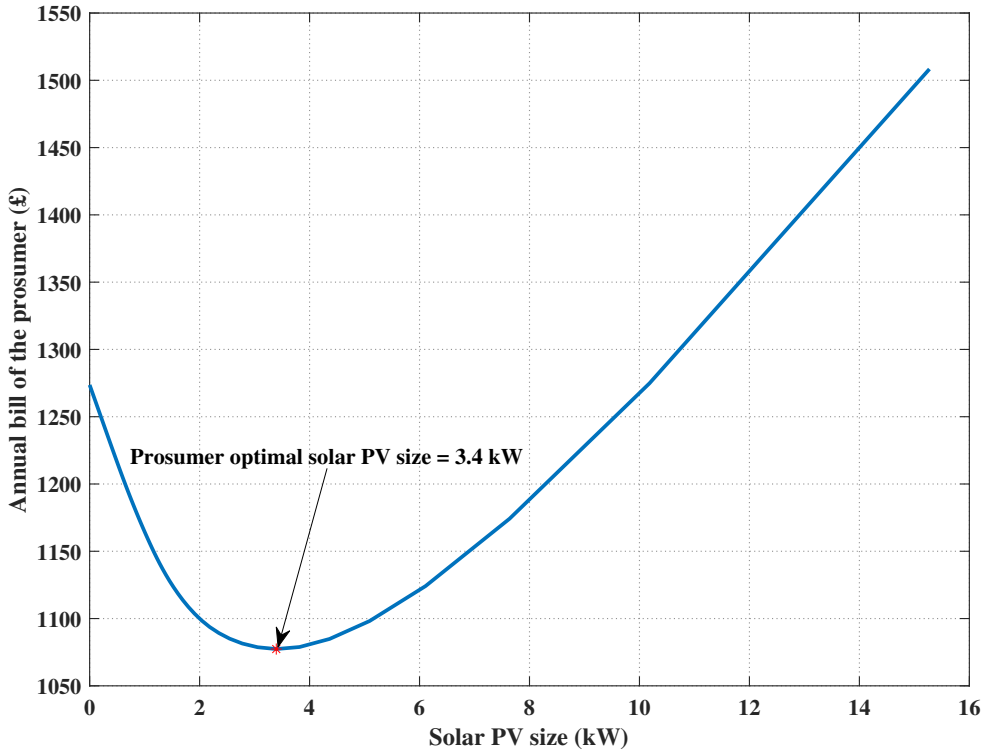

Figure 3.10: Annual bill versus solar PV capacity for prosumer with annual demand of 7888 kWh simulated for the dynamic Agile Octopus ToU grid import tariff [224].

optimal wind turbine, prosumer is able to save £582 yearly as compared to the baseline case without any energy assets (as shown in Table 3.1).

Similarly, Figure 3.10 shows the evolution of prosumer yearly bill as a function of solar PV capacity simulated for a dynamic ToU tariff. In this case, the optimal solar PV size obtained for the prosumer is 3.4 kW. With this optimal solar PV, prosumer is able to save £196 yearly as compared to the baseline case without any energy assets (as shown in Table 3.2).

Optimal battery storage capacity

In this scenario, it is assumed that the prosumer invests in battery storage systems in addition to the renewable generator (solar PV or wind turbine). The power ratings of the prosumer's renewable generator(s) are determined as the optimal ratings obtained in the previous Section 3.6.1, which considered renewable generators only without any storage assets. Similar to the case with the renewable generator only, the prosumer invests in a battery of the optimal size, taking into account the investment costs for both the battery and the optimal renewable generator. The depreciation factor of the battery is included to account for the battery usage cost, as defined in Eq. (3.14).

Pricing scheme	**Optimal battery (integrated with wind generator)**			
	Optimal capacity (kWh)	**Annual bill with optimal battery & wind (£)**	**Annual bill without assets (baseline) (£)**	**Annual saving (£)**
Flat tariff	13	601	1262	661
ToU tariff	12.8	591	1274	683

Table 3.3: Prosumer battery capacity, and the corresponding annual bill and saving for both the flat tariff of 16 pence/kWh [222] and dynamic Agile Octopus ToU tariff [224]. Prosumer battery integrated with wind generator.

Pricing scheme	**Optimal battery (integrated with solar PV generator)**			
	Optimal capacity (kWh)	**Annual bill with optimal battery & PV (£)**	**Annual bill without assets (baseline) (£)**	**Annual saving (£)**
Flat tariff	7	1044	1262	218
ToU tariff	6	1024	1274	249

Table 3.4: Prosumer battery capacity, and the corresponding annual bill and saving for both the flat tariff of 16 pence/kWh [222] and dynamic Agile Octopus ToU tariff [224]. Prosumer battery integrated with solar PV generator.

Simulations are performed for one year using the battery control Algorithm 3.1 for both the flat and dynamic ToU pricing schemes. Additionally, the battery depreciation cost is considered. The optimal rated capacity of the battery corresponds to the rated storage capacity that achieves the minimum annual bill, as determined by Eq. (3.20). The prosumer optimal battery capacity and corresponding annual bill are determined. Results of the optimal battery capacity obtained from battery integrated with the wind turbine renewable generator is shown in Table 3.3, and Table 3.4 for the battery integrated with solar PV renewable generator.

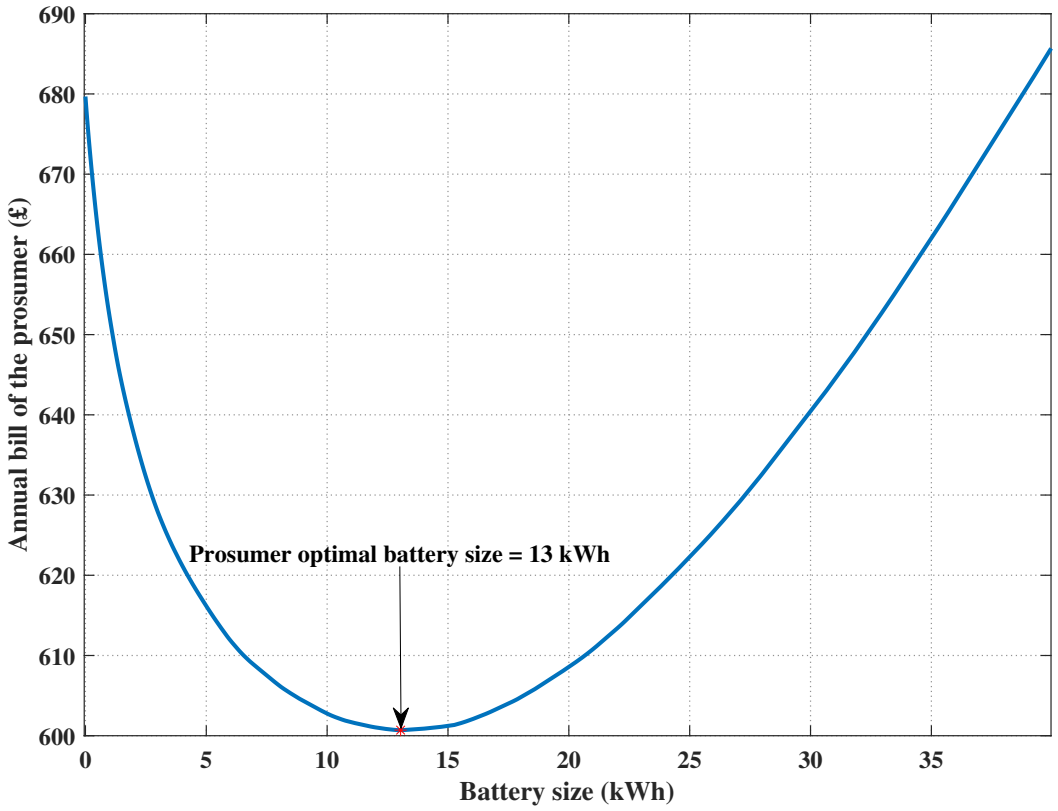

Figure 3.11: Annual bill versus battery capacity for prosumer with annual demand of 7888 kWh simulated for the flat grid import tariff of 16 pence/kWh [222] for a system of prosumer battery integrated with wind generator.

Figure 3.11 shows the evolution of prosumer yearly bill as a function of battery capacity and shows that the optimal capacity for this prosumer simulated for a fixed tariff is 13 kWh. Furthermore, for this prosumer, the optimal battery size is close to the battery capacity of a Tesla battery [232]. With this optimal battery and wind turbine, prosumer is able to save £661 yearly as compared to the baseline case without any energy assets (as shown in Table 3.3).

The unitary cost of the assets and electricity prices are important economic parameters that affect the profitability of energy assets owned by prosumer. The main aim of the techno-economic study of prosumer energy assets is to validate the proposed battery control Algorithm 3.1, and also determine what conditions make the adoption of energy

assets most profitable to prosumer. To achieve this, the proposed control algorithm was implemented for different economic parameters that were altered in order to investigate and realize a sensitivity study on the profitability of energy assets at a prosumer level. In an integrated renewable energy system, battery is the most expensive component and batteries' lifetime is comparatively shorter than that of renewable generators, this highlights the importance of using an appropriate battery control mechanism to extends the system's useful life. Hence, the sensitivity analysis is focussed more on the economic analysis of the flexibility provided by the battery energy storage systems.

Sensitivity analysis of the battery cost : a flat grid import tariff of 16 pence/kWh [222] as described in Section 3.3.4 is used for the sensitivity study. Figure 3.12 shows the evolution of the annual bill of a prosumer as a function of the size of the battery that the prosumer buys and for different battery costs. Simulation results clearly show that there is an optimal battery capacity that minimizes the annual bill, although the benefit in terms of bill reduction highly depends on the battery cost. Furthermore, one can see that the higher the cost of batteries is, the smaller the optimal battery capacity is. This information is extremely useful as it allows a company to size a prosumer's battery based on their particular consumption and production profiles. Nevertheless, it is worth noting that the bill reduction is still quite low (£190) even in the most advantageous case of a battery cost of 50 £/kWh.

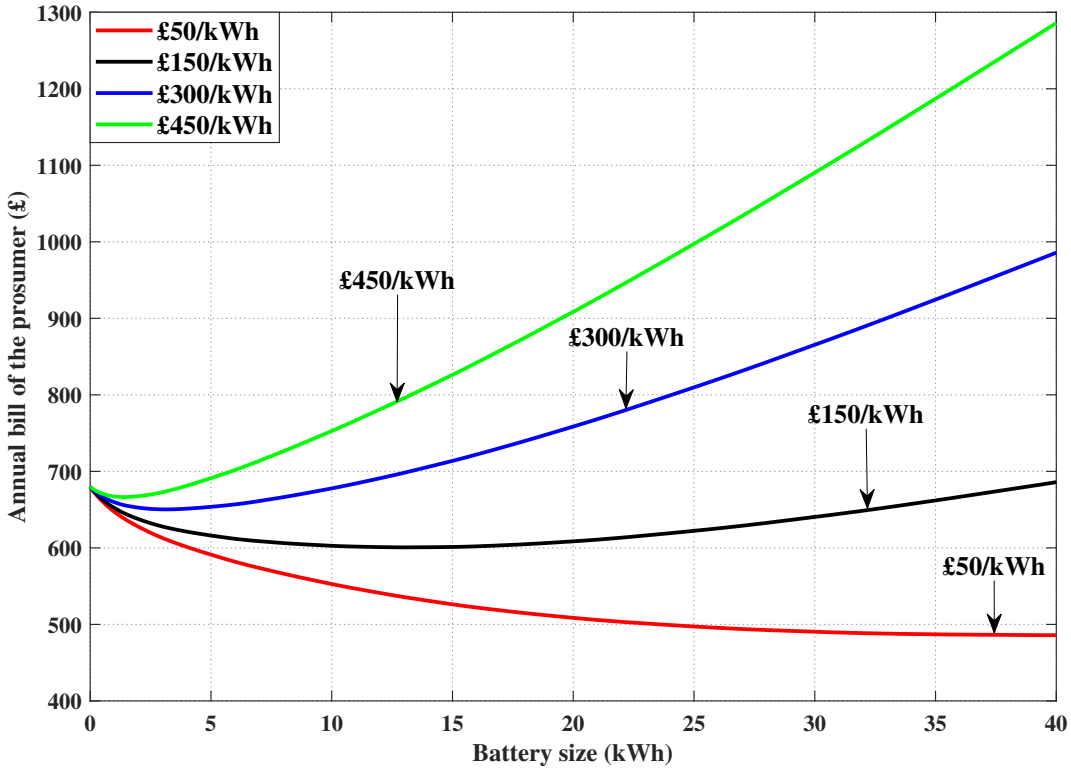

Figure 3.12: Prosumer annual bill versus battery capacity for different battery prices (£/kWh) simulated for the flat grid import tariff of 16 pence/kWh [222] for a system of prosumer battery integrated with wind generator.

Sensitivity analysis of the electricity price: the grid buying electricity price (τ^b) is the third parameter included in the economic analysis of the energy assets. To conduct the sensitivity analysis on the electricity price, a specific scenario was chosen, considering a battery cost of 150 £/kWh. This cost value is recommended in [225]. The selected scenario allows for an examination of how changes in electricity prices can impact the optimal sizing and performance of the energy storage system. The baseline electricity buying price is the flat grid import tariff of 16 pence/kWh, adopted after comparing the fixed electricity prices offered by various UK-based electricity suppliers using web-tools in price comparison site Money Supermarket [222]. This website is one of the several price comparison sites approved and accredited by the Office of Gas and Electricity Markets (Ofgem) [223], the government regulator for the electricity and downstream natural gas markets in UK.

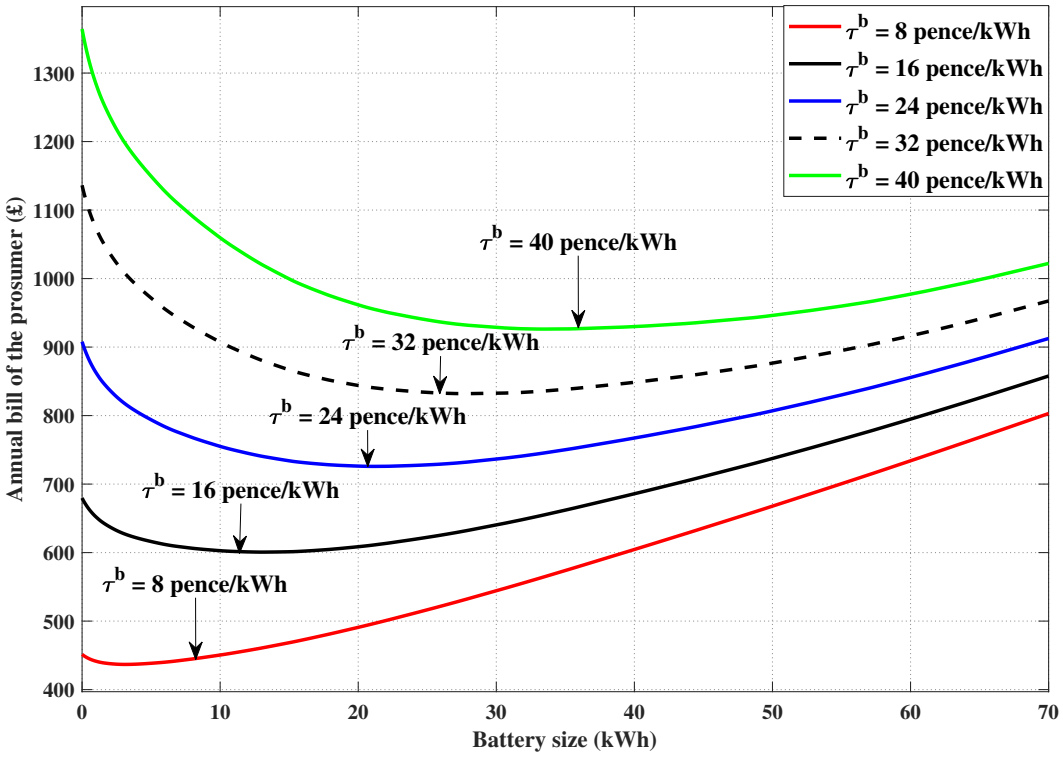

Figure 3.13: Prosumer annual bill versus battery capacity for different grid buying price (τ^b) with the battery cost of 150 £/kWh simulated for the flat grid import tariff, obtained from a system of battery integrated with wind generator.

The chosen baseline electricity buying price from grid is consistent with the average cost for the standard electricity in the UK as per the quarterly energy prices, quarter 2 (April to June) 2022 report [233] published by Department of Business, Energy & Industrial Strategy. Similar flat rate is adopted in the works of Zhou et al. [5], and Luth et al. [174]. To conduct the study, different scenarios were analysed, each one corresponding to a specific electricity buying price, as shown in Figure 3.13 . The simulation results shows that annual bills increase with the increase in electricity price. This increase in annual

bills is expected as the prosumer spends more money to satisfy his electricity consumption. Results show that the higher the price of electricity is, the more advantageous it is to install a battery system. For instance, for the scenario of a buying price equal to 40 pence/kWh, the decrease in annual bill is £438 with an optimal battery size of 33.5 kWh, while it is £14.68 in the case of a buying price of 8 pence/kWh and a battery capacity of 3.12 kWh.

3.7 Discussion of results and concluding remarks

Results from this techno-economic analysis shows that the increase of electricity prices along with the decrease of unitary cost of assets can make energy assets profitable for prosumers (as shown in Figure 3.12 and 3.13). Furthermore, as shown in Figure 3.9, 3.10 & 3.11, increasing the energy assets' capacity too much will increase the annual bill. Indeed, if a prosumer buys an energy asset that is much larger than the required size, the extra capacity will not be used, and will correspond to a loss of revenue.

The simulations show that with current market prices, the batteries are not profitable for most prosumers, unless economic parameters such as the battery cost and electricity price change, as it might be expected in the next decade [225]. The result is similar to the findings by Stelt et al. [14], who concluded that the economic feasibility of batteries depends largely on the battery cost, and that the current battery cost is found to be economically infeasible. Indeed, it is important to acknowledge that in the model described, no benefits or revenues resulting from energy or grid services provided by the battery have been taken into account. Services such as frequency regulation and demand response, which can be facilitated by the battery, have not been considered in the analysis. Including these additional benefits could further enhance the economic viability and value proposition of the energy storage system. Furthermore, prosumer is not able to obtain the maximum benefit from renewable generators (wind turbine, solar PV) as consumption is not the same time as the production. This mismatch between the renewable generation and consumption makes the renewable generators less profitable to the prosumer. Hence, there is a need to explore suitable optimization techniques to optimize the maximum benefits from usage of energy assets.

In this work, a model of a prosumer-based control algorithm was presented and assessed by incorporating the latest heuristics of battery state of health at a prosumer level. The control algorithm was implemented for different economic parameters that were altered in order to investigate and realize a sensitivity study on the profitability of energy assets at a prosumer level. Results from this work display a good performance of the rule-based scheduling when electricity import prices are relatively higher than export prices. The simulation analysis (based on real demand profiles, generation data, physical asset profiles and import prices in the United Kingdom at the time of writing) shows that investment in energy assets can be an economical feasible proposition, but this result depends on economic parameters of energy assets such as the unitary cost of the assets, the export prices of electricity, but also the type of services for which the assets can get revenues.

Chapter 4

Modeling energy assets ownership schemes in a community without network constraints

Chapter 4 focuses on a comparative study of benefits provided by DERs and BESS to prosumers between a scenario where every prosumer installs his own assets, which corresponds to the case presented in Chapter 3, and a scenario where prosumers join together to invest in community assets. Then, a novel approach is presented for redistributing the revenues generated by community assets to the members of the community. Energy community projects often involve jointly owned energy assets such as community-owned wind turbines, solar PVs and/or shared battery storage. While energy communities are a promising concept, a key challenge is how these assets can be efficiently controlled in real time, how the useful lifetime of the asset can be modelled and enhanced, and how the energy outputs from these jointly-owned assets should be shared fairly among community members, given that not all members have the same size, energy needs or demand profiles. Crucially, such real-time control and fair sharing of energy must also consider the physical assets degradation and operational constraints.

To address these challenges, this chapter introduces novel algorithms for intelligent control of energy assets and redistribution mechanisms. These methods lead to more fair and equitable strategies for dividing joint gains, utilizing tools from distributed AI (specifically, the multi-agent systems) and cooperative game theory. First, the study compare the case when individual households invest in their own home energy assets (renewable generator, storage) versus investing in a larger jointly-owned community energy asset. Through the case study presented in this thesis, the advantages of a collectively-owned or pooled energy assets approach are demonstrated. Next, several practical and computationally efficient mechanisms are proposed to fairly distribute the outputs from these jointly-owned assets among the households of the community.

Part of the research work presented in Chapter 4 were published in peer-reviewed scientific paper [213].

4.1 Research contributions

A comprehensive literature review on the state-of-the-art in community energy modelling and benefits redistribution mechanisms was presented analytically in the previous Chapter 2 (Section 2.2 & 2.3). As highlighted in Chapter 2, there is an urgent need for methods to increase energy access, resilience and reliability of communities. One way is for the community to invest in its own energy generation assets like solar PV and wind turbine, and battery energy storage systems. But, this raises the question of discovering benefits/drawbacks when investment in energy assets is performed individually or jointly on a community level. In other words, renewable generators and storage could be installed either individually at a household level, or jointly-owned, which all households in the community could use on a pre-agreed sharing basis. Hence, there is a need for a comprehensive method to study the techno-economic benefits of investment in jointly-owned community energy assets versus individually-owned distributed energy assets considering the physical assets degradation and operational constraints.

A literature survey on previous techno-economic analyses of such schemes reveals that community-owned assets could provide more savings (higher benefits) compared to distributed individually-owned assets. For instance, studies show that the community battery storage system offers higher benefits as compared to individual household distributed batteries [33, 16, 34–36, 136–141]. However, most of the existing studies on comparison of individually-owned assets versus centrally located community-owned assets, while considering both the renewable generation and battery, have not included the battery degradation cost in their techno-economic analysis. The battery lifetime depends on the charge/discharge cycles, which in turn are shaped by the control scheme. Thus, there is a need to accurately estimate the depreciation of the battery from the operating profiles and therefore assess the operational cost and overall economic value of the integrated renewable energy system.

Furthermore, although higher benefits can be achieved by investing in community assets, how to redistribute these benefits among the individual households in the community still remains a key open question, of both research and practical interest. Hence, there is a significant knowledge gap in how to design efficient and fair redistribution mechanisms to incentivize energy communities to invest in joint renewable energy assets, especially when incorporating physical asset constraints or the physical degradation during use of community assets.

This Chapter 4 provides a redistribution mechanism based on the marginal contribution of an individual household in the benefits from the community-owned assets, incorporating physical assets degradation. The mechanism proposed uses principles from mechanism design and cooperative game theory. Game theory provides an insightful analytical and conceptual framework along with mathematical tools to study and analyse the complex interaction among independent rational players (in our case the households) [37]. Cooperative (or coalitional) game theory has been identified as a useful tool in designing incentive mechanisms and business models in decentralized energy systems. In a cooperative game,

players form coalitions to maximise a common objective for mutual benefit. Then, the benefit is distributed equally or fairly among themselves using incentive-based solution concepts, such as the Shapley value. One major challenge faced by community energy scheme utilising coalition game theory is the issue of scalability [39, 40]. Specifically, when determining the Shapley values in a coalition, the computation becomes highly complex and time-consuming, as the number of players increases in the coalition. To address this computational challenges, in this thesis a more computationally tractable (and hence more practically applicable) redistribution mechanism based on the marginal contribution of each players is proposed. Another gap identified in the literature, is that techno-economic analysis of individual versus community assets is mostly focused on battery and solar PV only, and wind turbines have not been adequately investigated. Inclusion of wind-battery systems though is very important, especially in a country with remarkable wind resources like the UK.

Given the above challenges, the study in this thesis utilises real commercially-available, dynamic tariffs from the UK market, as well as a whole year of high-granularity demand and renewable generation data and develop a mechanism for fair redistribution of benefits from jointly-owned community energy assets to individual members (agents/households) of the energy communities. Findings of this work are related to a number of strands including community energy system research and cooperative game-theoretic applications for energy systems, but also to the area of electrical engineering and physical asset health monitoring of batteries. In more detail, the specific contributions of the work presented in Chapter 4 advance the state-of-the-art are:

- First, in this work, a principled model of community investment and sharing of energy assets is presented. The focus is on renewable generation and battery storage for both fixed and dynamic time of use (ToU) tariffs. The approach incorporates a comprehensive data-driven analysis to quantify the savings achieved through community-owned energy assets in comparison to individually-owned ones.

- Secondly, the incorporation of physical battery degradation into community energy optimization models is addressed, along with its impact on redistribution schemes. To achieve this, a battery state of health degradation model is employed, which relies on the battery depth of discharge in each control cycle.

- Thirdly, an investigation and proposal of redistribution schemes for sharing the benefits of community energy assets are conducted, drawing on principles from cooperative game theory. Cooperative game theory is an established methodology utilized for designing redistribution schemes in various practical domains [37, 40]. These redistribution schemes are assessed in different scenarios and based on multiple criteria, encompassing costs and financial benefits to each prosumer, as well as correlation with intermittent renewable output.

- Lastly, the savings achieved by the proposed redistribution schemes are discussed concerning various sizes of prosumers. Additionally, an assessment is conducted to

evaluate the fairness of these schemes and their impact on the potential uptake of renewable energy within energy communities.

The energy community is initially modelled based on the description provided in the following section.

4.2 Energy community setting

In this scenario, a community of 200 prosumers is taken into consideration, each having real half-hourly demand profiles derived from the dataset provided by the Thames Valley Vision End Point Monitor project [215]. These 200 demand profiles are further aggregated [35] to represent a single community demand profile. A community is formed by connecting all individual prosumers or individual agents into a system that is collectively referred to as a multi-agent system.

In this work, the first aim is to compare two configurations of energy communities. One configuration will consider the community as 200 individual agents, each one of them with their own consumption and local production, but without financial nor energy interaction between them. In such configuration, agents import electricity from the grid when their assets cannot cover their own consumption, whereas they can export electricity to the grid when they have production surplus. The second configuration corresponds to the case of an energy community in which agents invest together in jointly-owned community assets, such as community-owned wind or solar production, and community batteries. The demand of agents is considered inflexible. A renewable generator (either wind turbine or a solar PV installation), a battery energy storage system and the utility grid are the three power sources considered for satisfying the inflexible demand at all times. A power flow diagram of an agent or of the energy community considered as a whole is shown in Figure 4.1.

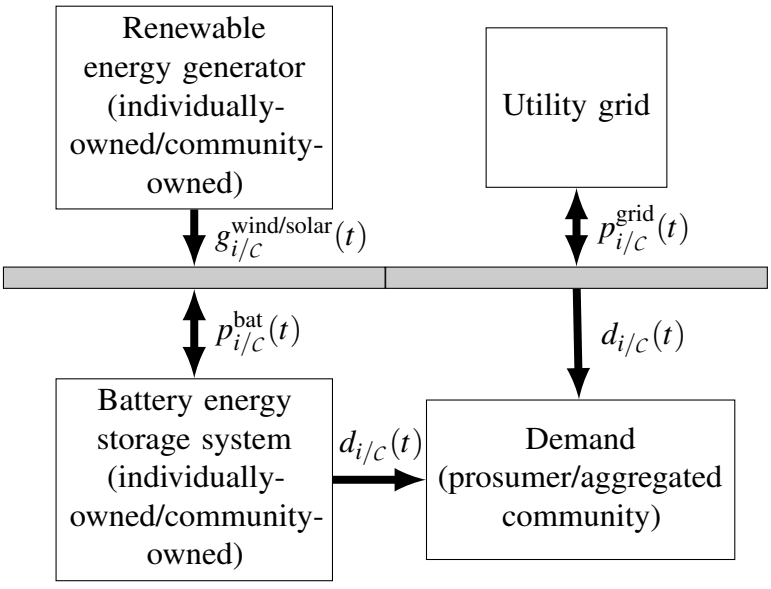

Figure 4.1: Power flow diagram of the energy community model.

An energy community model comprises a group of individual prosumers (agents) connected to a low-voltage distribution network. Specifically, for an agent i with $i = 1..N$ and $N = 200$ in the context of this thesis, $g_i(t)$ represents the generation from the intermittent renewable source and $d_i(t)$ the demand at time $t \in [0,T]$. The energy bill of agent i at time t is represented by $b_i(t)$, whereas if the considered period T is equal to one year, then $b_i(T)$ represents the total annual bill as outlined by Eq. (3.20).

The community $\mathcal{C}$, i.e. the set of all agents i, is formally defined as $\mathcal{C} = \{A_i \mid i \in [1,N]\}$ where $N = 200$ agents. Accordingly, $g_{\mathcal{C}}(t)$ and $d_{\mathcal{C}}(t)$ represent the generation and demand of the community $\mathcal{C}$ at time t. Similarly, the community bill at time t is represented by $b_{\mathcal{C}}(t)$, and the annual bill is given by $b_{\mathcal{C}}(T)$.

The overall power balance at any given time t of an agent i or of the energy community $\mathcal{C}$ is given by:

$$p_{i/\mathcal{C}}^{\text{grid}}(t) = d_{i/\mathcal{C}}(t) - p_{i/\mathcal{C}}^{\text{bat}}(t) - g_{i/\mathcal{C}}^{\text{wind/solar}}(t) \tag{4.1}$$

where $g_{i/\mathcal{C}}^{\text{wind/solar}}(t)$ is the power generated by the renewable generator, that can be individually owned, or owned by the community. $p_{i/\mathcal{C}}^{\text{grid}}(t)$ represents the power that an agent or that the community can buy/sell from/to the grid. $p_{i/\mathcal{C}}^{\text{bat}}(t)$ represents the power of the storage system (individually-owned, or centrally located and owned by the community), which is considered negative when the battery is charging (battery considered as a load), and positive when the battery is discharging (battery considered as a generator). $d_{i/\mathcal{C}}(t)$ is the power consumed by an agent or by the community considered as a whole, i.e the aggregated demand power of 200 agents.

The model inputs, battery control Algorithm 3.1, battery depreciation aspects and the economic setting of the single prosumer model described in Chapter 3 are applied to the community setting. The consideration in this study involves either a prosumer or the entire community owning a wind turbine or a solar PV renewable generator, along with a battery energy storage system, as outlined in Section 3.4 of Chapter 3. The cost of energy assets are assumed to be 150 £/kWh for the battery [225], 1100 £/kW for solar PV [229] generation capacity and 1072 £/kW for the wind turbine [229] generation capacity. As outlined by Eq. (3.20), the annual bill for agent i and the community $\mathcal{C}$ are defined as:

$$b_i(T) = \sum_{1}^{T} e_i^b(t)\tau^b(t) + c_i^A(T). \tag{4.2}$$

$$b_{\mathcal{C}}(T) = \sum_{1}^{T} e_{\mathcal{C}}^b(t)\tau^b(t) + c_{\mathcal{C}}^A(T). \tag{4.3}$$

where, $e_i^b(t)\tau^b(t)$ is the cost of energy imports from the utility grid by agent i at time t and $c_i^A(T)$ is the depreciation cost of assets owned by agent i in the considered period T. Similarly, $e_{\mathcal{C}}^b(t)\tau^b(t)$ is the cost of energy imported from the utility grid by the community as a whole at time t and $c_{\mathcal{C}}^A(T)$ is the depreciation cost of jointly-owned community assets for the considered period T.

This chapter introduces an energy community model that explores the advantages of community-owned energy assets compared to individually-owned ones, while also considering asset degradation functions. To evaluate the benefits of installing various assets, including a comprehensive battery degradation model, an approach based on real-time series data from a community is proposed. This approach compares the benefits of community-owned assets to those expected from individually-owned assets, while accounting for physical asset degradation constraints. Subsequently, a redistribution model for community benefits is proposed using using the methodology and principles from cooperative (or coalitional) game theory [234], particularly focusing on the concept of marginal value. The outlined energy community modeling approach is summarized in Figure 4.2.

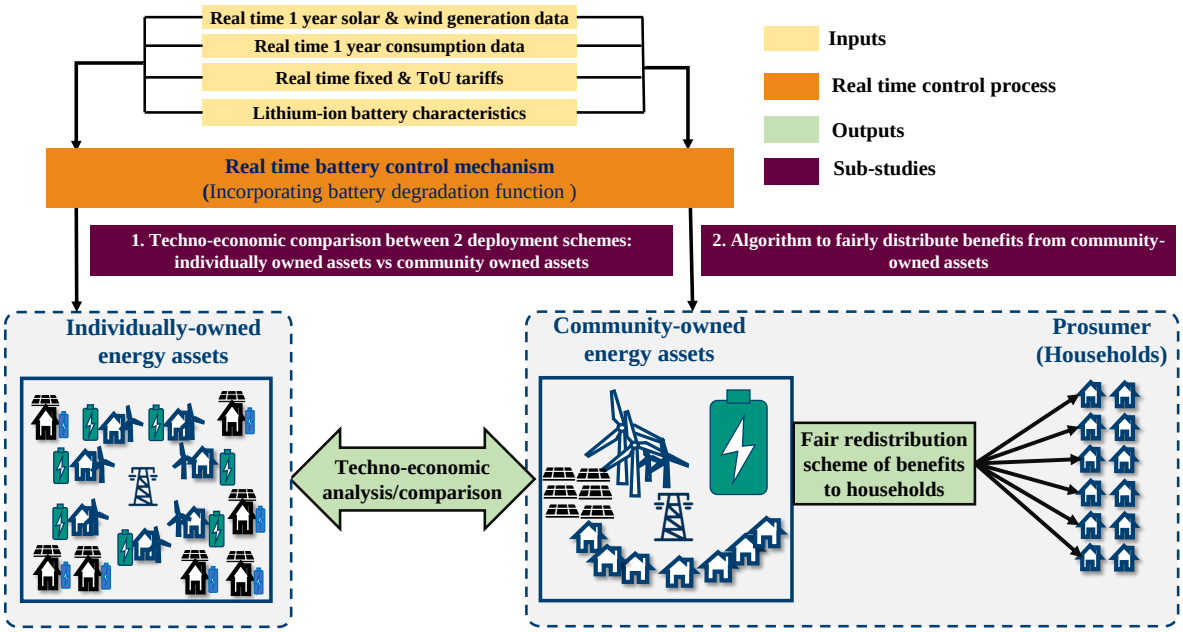

Figure 4.2: Overview of the energy community modeling approach.

First, the comparison of technical and economic benefits of investment in individually-owned or community-owned energy assets is assessed as described in the following Section 4.3.

4.3 Comparison of yearly bills obtained from investment in distributed individually-owned assets with jointly-owned community energy assets

Energy communities are able to maximize the behind-the-meter self-consumption by investing in the individual or jointly-owned community-shared renewable energy assets. In order to assess the most profitable investment options, the benefits (savings) obtained from the investment in the distributed individually-owned assets are compared to the benefits

obtained from the investment in the jointly-owned community-shared assets. The yearly savings are determined by comparing annual bills after investing in the assets (as described by Eqs. (4.2) and (4.3)) with the yearly bills before the assets were installed (i.e. without assets).

First, a baseline scenario is defined. In this baseline scenario, yearly bills for individual agents and the community are computed without generation or storage assets (renewable generator and BESS) for both the flat tariff of 16 pence/kWh [222] and dynamic Agile Octopus ToU tariff [224]. Table 4.1 shows the community annual bill ($b_C(T)$) and the sum of individual agents annual bills ($\sum_{i=1}^{N} b_i(T)$, where $N = 200$). It can be observed that without these local assets, annual bills are equal, which can be expected as the community represents the aggregated demand profiles of the individual agents. This baseline scenario is used for comparing the savings (benefits) from investing in generation and storage.

Without assets (baseline)	**Flat tariff**	**ToU tariff**
	Annual bill (£)	**Annual bill (£)**
Sum of individual agents yearly bills	134455	143923
Community yearly bill	134455	143923

Table 4.1: Baseline scenario: the sum of individual agents yearly bills and community yearly bill without the assets (renewable generator and battery) for both the flat tariff of 16 pence/kWh [222] and dynamic Agile Octopus ToU tariff [224].

4.3.1 Individual renewable generator vs community renewable generator without storage

First, the benefits provided by a community renewable generator are compared to those offered by individually-owned distributed renewable generators, without considering any storage system. It is assumed that the prosumer or the community can own either a solar PV or a wind turbine renewable generator. In this scenario, only the investment cost of the renewable generator is considered. Also, the study assumes the operations of the renewable generator follow the manufacturer operations. Hence, the depreciation cost of the renewable generator operation is not included. Furthermore, it is assumed that every prosumer owns a renewable generator with a rated power equal to the optimal rated power for this prosumer, which is the most conservative scenario for individual renewable generators (solar PV or wind turbines). Optimal rated capacity of the renewable generator corresponds to that rated power that achieves the minimum annual bill given by Eqs. (4.2) and (4.3). Simulations are performed for one year, without a battery energy storage system, and for both flat and ToU pricing schemes (similar to the case with single prosumer as described in Section 3.6.1 of Chapter 3).

The sum of individual agents optimal renewable generator capacities and the corresponding sum of individual annual bills are determined. Similarly, the community optimal renewable generator capacity and the corresponding annual bill are determined. Results

of these optimal renewable generator capacities and the corresponding annual bills are shown in Table 4.2 for wind turbine and Table 4.3 for solar PV renewable generator. The computation of the simple payback period for renewable generator is based on simulations using the battery control Algorithm 3.1 for one year.

Assets	Flat tariff		ToU tariff	
	Optimal capacity (kW)	Annual bill (£)	Optimal capacity (kW)	Annual bill (£)
Sum of individual agents optimal wind turbines	484	76339	518	80543
Community optimal wind turbine	405	64792	456	68448

Table 4.2: Sum of individual agents optimal wind turbine capacities, sum of individual agents annual bills, and community optimal wind turbine capacity and corresponding annual bill for both the flat tariff of 16 pence/kWh [222] and dynamic Agile Octopus ToU tariff [224].

Assets	Flat tariff		ToU tariff	
	Optimal capacity (kW)	Annual bill (£)	Optimal capacity (kW)	Annual bill (£)
Sum of individual agents optimal solar PV's	258	122557	297	129589
Community optimal solar PV	309	117092	347	123154

Table 4.3: Sum of individual agents optimal solar PV capacities, sum of individual agents annual bills, and community optimal solar PV capacity and corresponding annual bill for both the flat tariff of 16 pence/kWh [222] and dynamic Agile Octopus ToU tariff [224].

Result shows that the the community-owned renewable generator provides more savings (higher benefits) compared to distributed individually-owned renewable generators. For instance, as shown in Table 4.2, jointly-owned community wind turbine provide a substantially lower annual bill for both the fixed tariff and ToU tariff pricing schemes as compared to individually-owned distributed wind turbines. Similarly, community-owned solar PV leads to greater reduction in annual electricity bill compared to individually-owned solar PV's as shown in Table 4.3.

4.3.2 Individual battery vs community battery

In this scenario, it is assumed that the agents invest in battery storage systems, and compare the benefits of individual versus community batteries. The renewable generator (solar PV or wind turbine) power rating for individuals and for the community are the optimal ratings obtained in the previous Section 4.3.1 with renewable generators only. Similarly, it is assumed that each agent (individuals or the community) invest in a battery of the optimal

size, as described in Subsection 3.6.1 of Chapter 3 (for the case with single prosumer). Furthermore, the investment costs for the battery and the optimal renewable generator are considered. The depreciation factor of the battery is included to account for the battery usage cost based on Eq. (3.14). Simulations are performed using the battery control Algorithm 3.1 for one year for both the pricing schemes and with consideration of the battery depreciation cost. Optimal rated capacity of the battery corresponds to that rated storage capacity that achieves the minimum annual bill given by Eqs. (4.2) and (4.3).

The sum of individual agents optimal battery capacities and corresponding sum of individual annual bills are determined. Similarly, the community optimal battery capacity and the corresponding annual community bill are estimated. Results of the optimal battery capacity obtained from battery integrated with the wind turbine is shown in Table 4.4, and Table 4.5 from battery integrated with the solar PV renewable generator.

Assets	**Flat tariff**		**ToU tariff**	
	Optimal capacity (kWh)	**Annual bill (£)**	**Optimal capacity (kWh)**	**Annual bill (£)**
Sum of individual agents optimal batteries	1596	63158	1723	64877
Community optimal battery	1342	57389	1690	59136

Table 4.4: Sum of individual agents optimal battery capacities, sum of individual agents annual bills, and community battery capacity and corresponding annual bill for both the flat tariff of 16 pence/kWh [222] and dynamic Agile Octopus ToU tariff [224] obtained from battery integrated with **wind turbine renewable generator**.

Assets	**Flat tariff**		**ToU tariff**	
	Optimal capacity (kWh)	**Annual bill (£)**	**Optimal capacity (kWh)**	**Annual bill (£)**
Sum of individual agents optimal batteries	513	118488	602	122419
Community optimal battery	642	113790	620	117307

Table 4.5: Sum of individual agents optimal battery capacities, sum of individual agents annual bills, and community battery capacity and corresponding annual bill for both the flat tariff of 16 pence/kWh [222] and dynamic Agile Octopus ToU tariff [224] obtained from battery integrated with **solar PV renewable generator**.

Similar to the renewable generator case, results show that the community battery provides more savings (higher benefits) compared to the distributed individually-owned batteries. As shown in Table 4.4, while using the wind power generation only, community battery provides a substantially lower annual bill and hence the higher savings for both the fixed tariff and ToU tariff pricing schemes as compared to distributed individually-owned

batteries. Similarly, while using the solar PV generation only, higher benefits (lower annual bill) is obtained from community-owned battery as shown in Table 4.5.

4.3.3 Discussion of results

The main aim of the economic study of the energy community is to determine the benefits provided by assets (renewable generation capacity and storage) to prosumers and energy community as a whole, subjected to physical assets degradation constraints. To achieve this, the presented Algorithm 3.1 is implemented by considering the different pricing schemes. A yearly energy bill savings, which is a fairly intuitive indicator, is used to compare the economic performance of investments in individually-owned assets and community-owned assets. Results from the techno-economic analysis (as shown in Table 4.2, 4.3, 4.4 & 4.5) shows that the community-owned assets provide a substantially lower annual bill and hence the higher savings (higher benefits) for both the fixed tariff and ToU tariff pricing schemes as compared to distributed individually-owned energy assets. The advantages from community-owned assets are multiple. First, community assets require a lower capacity for the same services, hence potentially a lower cost. Second, community assets achieve lower annual energy bills for both pricing schemes considered in the study.

For instance, the community wind turbine provides more savings (higher benefits) compared to distributed individually-owned wind turbines. These results highlight multiple advantages that can be obtained by investing in the community wind turbine. Firstly, a community wind turbine requires a substantially lower optimal capacity for the same services. Secondly, lower annual bill is achieved by investing in the community wind turbine for both the flat tariff and dynamic ToU tariff. Similar to the wind power case, results show that the community battery provides more savings (higher benefits) compared to the distributed individually-owned batteries. Multiple advantages can be expected from investing in a community battery. First, community battery requires a lower optimal rated capacity while providing the same service (for the case obtained using the wind turbine generator only). Second, a lower annual bill is achieved by investing in a community battery in both cases of a flat and dynamic ToU tariffs. However, it is important to note that a consequent part of the financial savings obtained from community assets are attributed to the aggregation of the community consumption.

Furthermore, these economic results were obtained with the same unitary cost of the assets for the community-owned as for individually-owned, which might not be the case in real-world scenario, whereas in practice, the unitary cost of the community-owned asset might be lower due to economies of the scale effect. Thus, more savings can be obtained from community-owned assets by considering the economies of scale in the unitary cost of the assets. Therefore, community-owned assets generate benefits to the community. These results from the techno-economic analysis clearly shows the importance for determination of fair redistribution or allocation of benefits achieved in community projects. Moreover, although higher benefits can be achieved by investing in community assets, how to redistribute these benefits among the individual households in the community still remains a

key open question, of both research and practical interest. Hence, there is a significant knowledge gap in how to design efficient and fair redistribution mechanisms to incentivize energy communities to invest in joint renewable energy assets, especially when incorporating physical asset constraints or the physical degradation during use of community assets. To address these challenges, this thesis proposes a more computationally tractable (and hence more practically applicable) redistribution mechanism. This mechanism is based on the marginal contribution of each agent (in this case, households) of the community. The proposed redistribution mechanism is presented in detail in the following Section 4.4.

4.4 Mechanism design for fair redistribution of benefits achieved from jointly-owned community assets

Results from the techno-economic analysis described in Section 4.3 show that the community assets provide more savings (higher benefits) compared to distributed individually-owned assets. Hence, individual agents can improve their profitability of investment by joining forces, regrouping into communities and by co-investing in community assets. In the case of community owned assets, the revenues generated by the community-owned distributed generation system (renewable generator and BESS) can be distributed to the members of the community. However, this raises the key research question of how to fairly redistribute the energy outputs (and hence the financial benefits) from the community-owned assets to the individual members of the community. In this section, we present the fair redistribution scheme to fairly redistribute the benefits from the community-owned assets. Also, in order to test the advantages of the proposed redistribution mechanism, we present in this section the state-of-the-art redistribution methods, used in current practice in such projects, that will be used for comparison.

4.4.1 Mechanism for a fair redistribution

Community assets lead to a reduction in the electricity bills of all the members of the community. However, this raises the key question of how these financial benefits from the joint assets can be fairly shared between agents (households). In this section, we propose a new methodology for fair redistribution of cost savings from community energy assets that utilises the marginal contribution principle, often used in cooperative game theory.

Savings of the community after one year ($T = 1$ year), noted as $\Pi_C(T)$, are defined by the difference between the sum of all agents annual bills before the community assets were installed (which corresponds to the baseline scenario shown in Table 4.1), and $b_C(T)$ i.e. the energy bill for the whole community after one year with community assets. Hence, the community savings over time period T correspond to the bill reduction for the whole community over that period, as shown below:

$$\Pi_C(T) = \sum_{i=1}^{N} b_i^0(T) - b_C(T) \tag{4.4}$$

where $b_i^0(T)$ is the baseline bill for prosumer i before any asset was installed, which corresponds to the values displayed in Table 4.1. In order to compute a fair redistribution of the community savings among the individual agents, we propose to compute the contribution $\Theta_i(T)$ of each agent to these community savings. To compute the marginal contribution of an agent i, we remove agent i from the community of 200 agents (total community), and recompute the community savings consisted of 199 agents (reduced community). The *marginal contribution* $\Theta_i(T)$ of agent i is defined as the difference between the total community savings $\Pi_C(T)$ and the savings of the reduced community $\Pi_{C\setminus\{i\}}(T)$, as shown below:

$$\Theta_i(T) = \Pi_C(T) - \Pi_{C\setminus\{i\}}(T) \quad \forall i \in C \tag{4.5}$$

where C is the community of 200 households. Once the marginal contribution $\Theta_i(T)$ is computed for all the agents, we distribute community savings $\Pi_C(T)$ among the individual agents based on the following equation:

$$\Gamma_i(T) = \Pi_C(T)\frac{\Theta_i(T)}{\sum_{i\in C}\Theta_i(T)} \quad \forall i \in C \tag{4.6}$$

where $\Gamma_i(T)$ is the amount of money redistributed to agent i after period T.

Hence, the new bill of agent i for the time period T, noted $b_i^*(T)$ can be computed as follows:

$$b_i^*(T) = b_i^0(T) - \Gamma_i(T) \quad \forall i \in C \tag{4.7}$$

Intuitively explained, the marginal contribution $\Theta_i(T)$ of agent i represents the difference that an agent makes to the value of a given coalition in the community. Specifically, the marginal contribution $\Theta_i(T)$ is a metric that helps us understand how much each agent i contributes to the reduction of the energy bill and overall community savings, leading to an equal and fair redistribution of savings as shown by Eq. (4.7) . Existing coalitional game theory redistribution mechanism based on solution concepts like the Shapley value use marginal contributions at their core, but present issues of scalability as the number of agents in a coalition increases. Particularly, computing the Shapley value is computationally challenging [40, 235], as it requires the computation of the marginal contribution of each agent to every possible subset of a given coalition. The proposed redistribution mechanism $\Gamma_i(T)$ is faster as it computes only the marginal contribution $\Theta_i(T)$ of an agent i with respect to the grand coalition, therefore it scales better as the number of agents increases. The proposed sharing mechanism refereed as Method 1 based on marginal contribution, is aligned with the fundamental concept of cooperative game theory that concentrates on the division of payoffs from the community coalition, and not so much on what agents do to achieve those payoffs.

4.4.2 Implementation for a community with renewable generator only without battery storage

In Section 4.4.1, a method to redistribute benefits from community-owned assets was presented. To test the advantages of the proposed method (denoted below as Method 1), it is further compared with other state-of-the-art methods, denoted below as Methods 2, 3 and 4. In this section, the focus is on the case where the community owns a single renewable generator. Then, the following Section 4.4.3 addresses the case with a community renewable generator and a community battery. Energy bills of individual agents after redistribution of community savings from a community renewable generator can be computed by one of the methods listed below:

- **Method 1**: Individual bills are computed by Eq. (4.7), where redistribution is based on the marginal contribution of each agent.
- **Method 2**: Individual bills are estimated after the instantaneous community renewable generator power $g_C(t)$ is distributed among individuals based on their instantaneous demand $d_i(t)$. In other words, the renewable generator power allocated to agent i at each time step is determined as:

$$g_i(t) = g_C(t) \times \frac{d_i(t)}{\sum_{i \in C} d_i(t)} \tag{4.8}$$

  The bill of each agent i is computed by Eq. (4.2), where $g_i(t)$ replaces $g^{\text{wind/solar}}(t)$ in Eqs. (3.10) and (3.13).
- **Method 3**: Individual bills are estimated after the instantaneous community renewable generator power $g_C(t)$ is distributed equally among individuals, as shown below:

$$g_i(t) = \frac{g_C(t)}{N} \tag{4.9}$$

  with N the number of households in the community.
- **Method 4**: Individual bills are estimated after the instantaneous community renewable generator power $g_C(t)$ is distributed among the individuals based on their annual energy consumption, as shown below:

$$g_i(t) = g_C(t) \frac{\mathcal{E}_i(T)}{\sum_{i \in C} \mathcal{E}_i(T)} \tag{4.10}$$

  where $\mathcal{E}_i(T)$ corresponds to the annual energy consumption of agent i, and is given by:

$$\mathcal{E}_i(T) = \sum_{t=0}^{T} \left[e_i^b(t) - e_i^s(t) \right] \tag{4.11}$$

Finally, savings are determined by comparing the sum of annual bills over the community with the baseline total annual bill (without assets as shown in Table 4.1). First, we

implement the redistribution mechanism for the community with wind turbine generator only and then implement for the community with solar PV renewable generator only without storage.

Redistribution from community-owned wind turbine only

In this study, a community wind turbine with an optimal capacity of 405 kW for a flat tariff, and a 456 kW wind turbine for the case of dynamic ToU tariffs were considered. These correspond to optimal capacities obtained from the scenario with wind turbine only in Section 4.3.1 and shown in Table 4.2). The investment cost of the community wind turbine was assumed to be shared equally among the agents.

The sum of individual agents annual bills and total annual savings after redistribution based on the different methods are shown in Table 4.6 for a flat tariff, and Table 4.7 for a dynamic ToU tariff. Savings are determined as the difference between annual bills obtained from the considered redistribution method and the annual bills from the baseline scenario (as shown in Table 4.1).

Redistribution mechanism	**Sum of individual agent annual bills after redistribution (£)**	**Sum of individual agent annual bills without asset (baseline) (£)**	**Sum of individual agent annual savings (£)**
Method 1	64792	134455	69663
Method 2	64792	134455	69663
Method 3	81997	134455	52458
Method 4	76907	134455	57548

Table 4.6: Sum of individual agents annual bills and annual savings obtained from various redistribution mechanisms for flat tariff of 16 pence/kWh [222] for the scenario with community wind turbine only without battery.

Redistribution mechanism	**Sum of individual agent annual bills after redistribution (£)**	**Sum of individual agent annual bills without asset (baseline) (£)**	**Sum of individual agent annual savings (£)**
Method 1	68448	143923	75476
Method 2	68448	143923	75476
Method 3	85924	143923	57999
Method 4	80962	143923	62961

Table 4.7: Sum of individual agents annual bills and annual savings obtained from various redistribution mechanisms for Agile Octopus dynamic ToU tariff [224] for the scenario with community wind turbine only without battery.

Figure 4.3 shows the individual agents annual bills after redistribution in the case of a flat tariff pricing scheme. In this figure, on the X-axis we order the 200 agents (households)

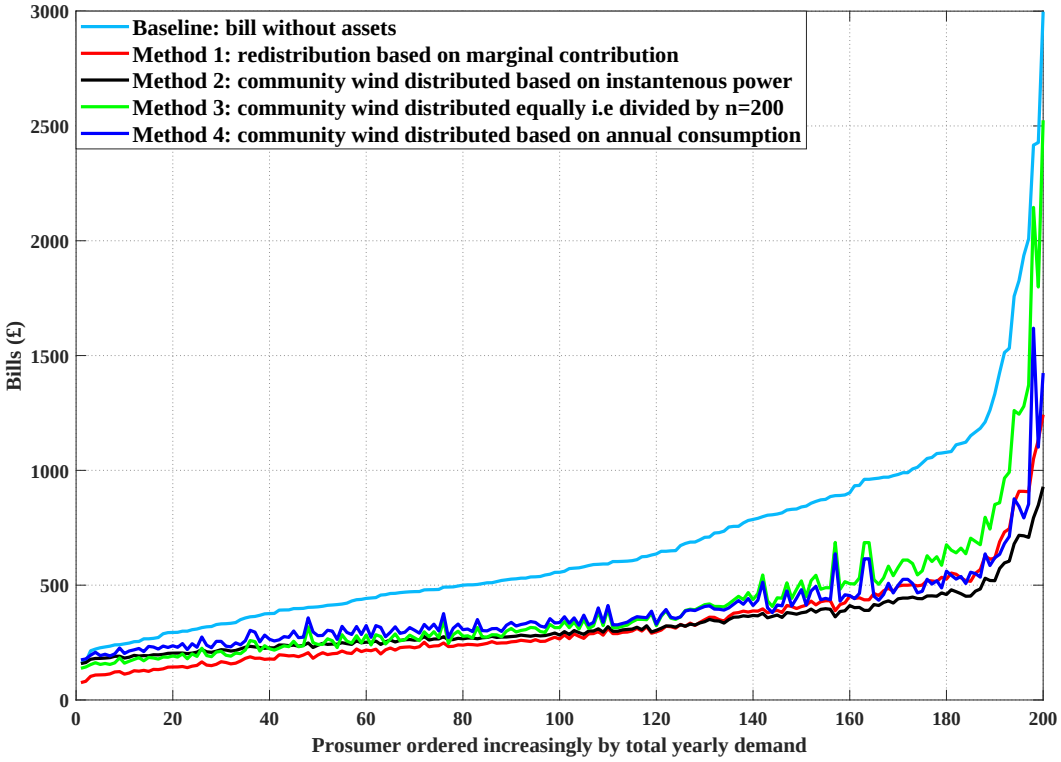

Figure 4.3: Individual agents yearly bills after redistribution for a flat tariff of 16 pence/kWh [222] obtained from community wind turbine only without battery.

in our case-study community increasingly by their total annual energy consumption (over all half-hourly periods in a year), while the Y-axis gives the annual energy bill of that agent. This representation is useful to investigate the fairness effects. Intuitively, even in the case when investing in community generation/storage assets is better for the community *on average*, the 4 different redistribution methods may lead to savings being distributed differently across small and larger agents.

Results for both pricing schemes are shown in Table 4.6 and 4.7. They clearly show that Method 1 and 2 yield the lowest bill for the whole community, and thus the greatest savings for almost every agent. Yet, Method 1 and Method 2 should undergo further comparison to evaluate the economic fairness in the redistribution scheme. The comparison between the two methods is illustrated using the flat tariff pricing scheme shown in Figure 4.4 .

The crossover point between the Method 1 and Method 2 curves shows that under Method 1 redistribution scheme, 67% of the agents can achieve lower annual bill, while only 33% of the agents obtain lower annual bills under the Method 2 mechanism. These agents (33%) correspond to households with higher annual consumption. However, according to Figure 4.3, agents with higher annual consumption are the agents who already obtain the highest bill reduction. Since the cost of the community wind turbine is shared equally among agents, irrespective of their demand profiles, we argue that, overall, it would be fairer to adopt the redistribution mechanism provided by Method 1, rather than Method 2.

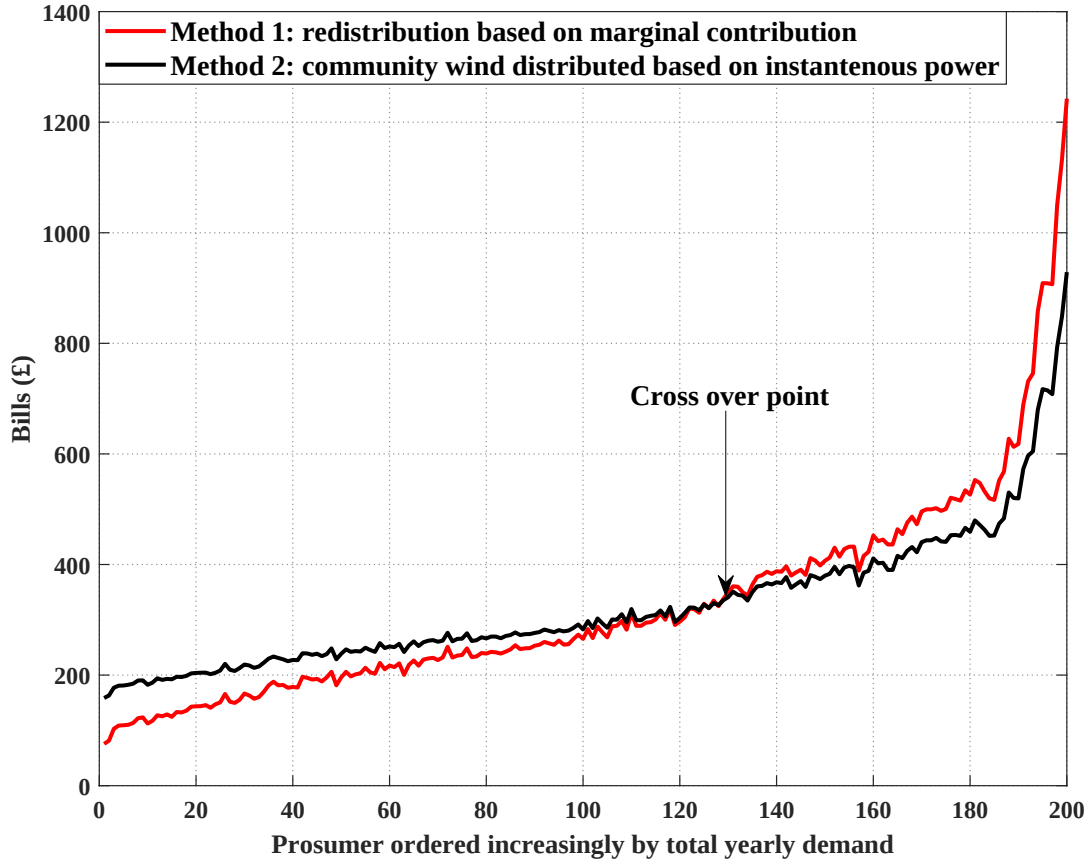

Figure 4.4: Individual agents yearly bills after redistribution based on Method 1 and Method 2 for a flat tariff of 16 pence/kWh [222] obtained from community wind turbine only without battery.

While it is true that the 1/3 of largest consumers would prefer Method 2, as shown in Figure 4.4, these large consumers already make the largest bill savings from joint assets in both methods, and in practice, having the 2/3 of the smallest households in the community also making noticeable savings is likely to lead to greater social acceptance of the scheme (both in financial terms and in terms of e.g. planning consent to install a wind turbine). Furthermore, it is worth mentioning that the electricity cost per kWh is strongly influenced by the correlation between the production $g_i(t)$ and the consumption $d_i(t)$ of the agent.

Sensitivity analysis of the electricity price: the economic fairness and robustness in the redistribution scheme is further evaluated by comparing Method 1 and Method 2 for different electricity buying prices (τ^b) for the flat grid import tariff, ranging from 8 pence/kWh to 24 pence/kWh as shown in Figure 4.5. The simulation results for each electricity import price clearly show that the bills curve for Method 1 and Method 2 cross at the exact same household number, as for the baseline tariff of 16 pence/kWh. Therefore, irrespective of the electricity buying prices, 67% of agents can achieve lower annual bills and thus higher annual savings under Method 1 redistribution scheme as compared to Method 2.

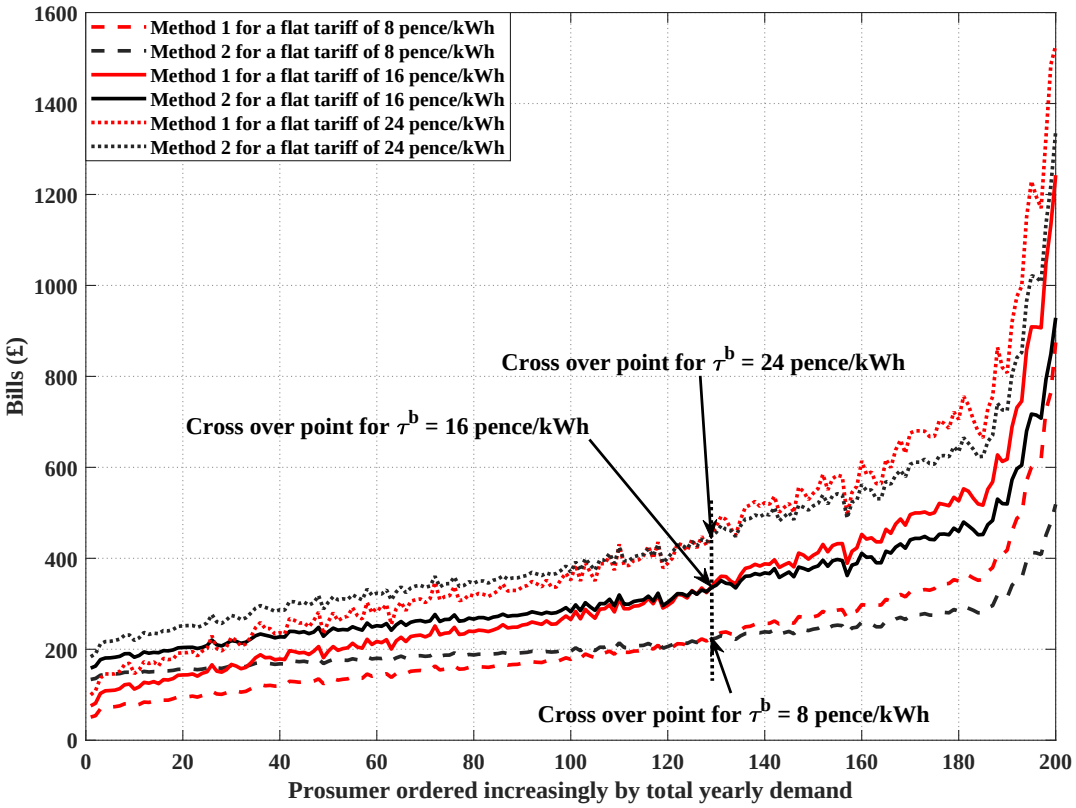

Figure 4.5: Individual agents yearly bills after redistribution based on Method 1 and Method 2 for different electricity buying prices (τ^b) for the flat grid import tariff.

Finally, Figure 4.6 shows the comparison between the Method 1 and Method 2 for the Agile Octopus dynamic ToU tariff. In Agile Octopus pricing scheme, the electricity import price varies with an average price of 15.9 pence/kWh, from minimum price of 2.8 pence/kWh to maximum price of 35 pence/kWh depending on the wholesale market prices. Similar to the case with flat tariff, the crossover point between Method 1 and Method 2 curves in Figure 4.6 clearly shows that more than 67% agents can achieve lower annual bills and thus higher savings under Method 1 redistribution scheme compared to Method 2. Therefore, the proposed redistribution scheme (Method 1) is fairer than Method 2 for all import prices studied.

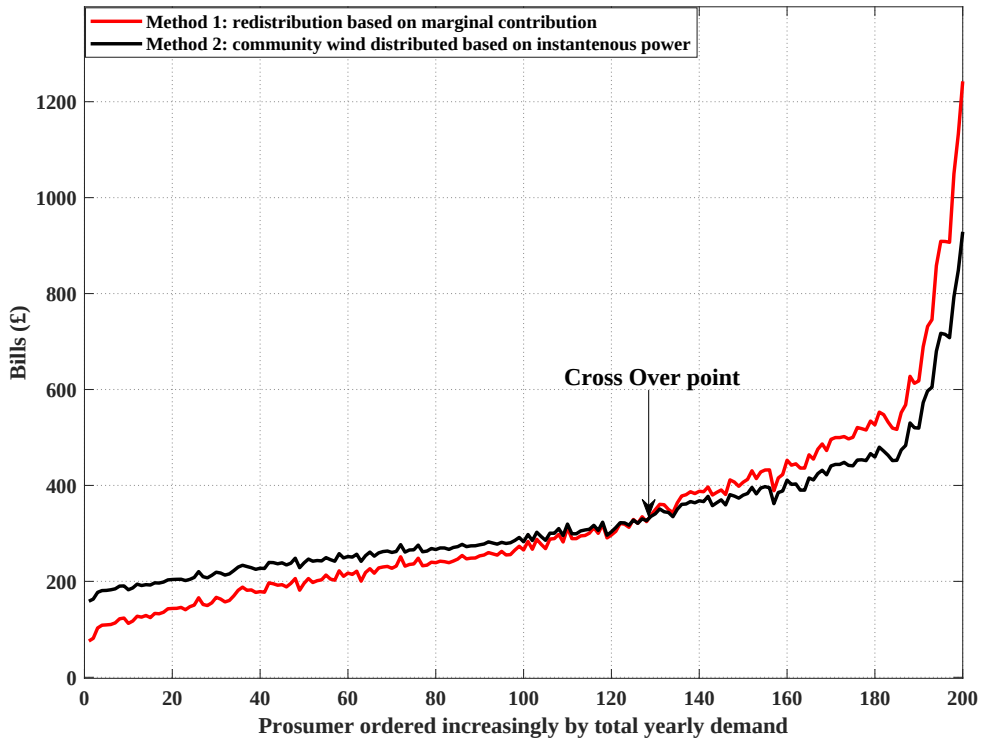

Figure 4.6: Individual agents yearly bills after redistribution based on Method 1 and Method 2 for the Agile Octopus dynamic ToU tariff [224] obtained from community wind turbine only without battery.

Redistribution from community-owned solar PV only

In this study, a community solar PV with an optimal capacity of 309 kW for a flat tariff, and a 347 kW solar PV for the case of dynamic ToU tariffs were considered. These correspond to optimal capacities obtained from the scenario with solar PV generator only in Section 4.3.1 and shown in Table 4.3). The investment cost of the community solar PV was assumed to be shared equally among the agents.

Redistribution mechanism	**Sum of individual agent annual bills after redistribution (£)**	**Sum of individual agent annual bills without asset (baseline) (£)**	**Sum of individual agent annual savings (£)**
Method 1	117092	134455	17363
Method 2	117092	134455	17363
Method 3	125097	134455	9358
Method 4	123464	134455	10991

Table 4.8: Sum of individual agents annual bills and annual savings obtained from various redistribution mechanisms for flat tariff of 16 pence/kWh [222] for the scenario with community solar PV only without battery.

The sum of individual agents annual bills and total annual savings after redistribution based on the different methods are shown in Table 4.8 for a flat tariff, and Table 4.9 for a

Redistribution mechanism	Sum of individual agent annual bills after redistribution (£)	Sum of individual agent annual bills without asset (baseline) (£)	Sum of individual agent annual savings (£)
Method 1	123154	143923	20770
Method 2	123154	143923	20770
Method 3	132282	143923	11642
Method 4	130471	143923	13452

Table 4.9: Sum of individual agents annual bills and annual savings obtained from various redistribution mechanisms for Agile Octopus dynamic ToU tariff [224] for the scenario with community solar PV only without battery.

dynamic ToU tariff. Savings are determined as the difference between annual bills obtained from the considered redistribution method and the annual bills from the baseline scenario (as shown in Table 4.1).

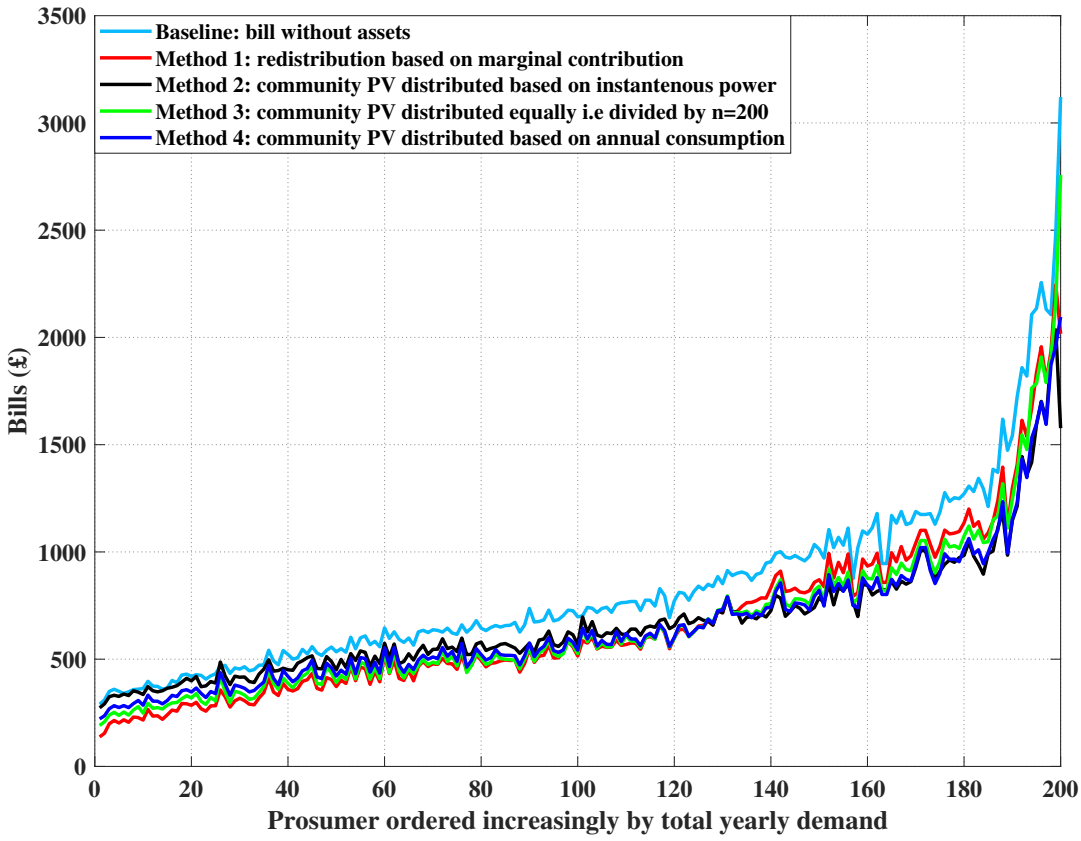

Figure 4.7: Individual agents yearly bills after redistribution for the Agile Octopus dynamic ToU tariff [224] obtained from community solar PV only without battery.

Figure 4.7 shows the individual agents annual bills after redistribution in the case of an Agile Octopus dynamic ToU tariff pricing scheme. Similar to the case with community-owned wind turbine, results from both the pricing schemes (as shown in Table 4.8 and 4.9) shows that Method 1 and 2 yield to the lowest bill for the whole community, and thus the

greatest savings for almost every agent. The comparison between Method 1 and Method 2 redistribution schemes that provided the lowest bill and hence the highest benefit for the community is illustrated in Figure 4.8 for the the Agile Octopus dynamic ToU tariff [224], and in Figure 4.9 for a flat tariff of 16 pence/kWh [222] pricing scheme.

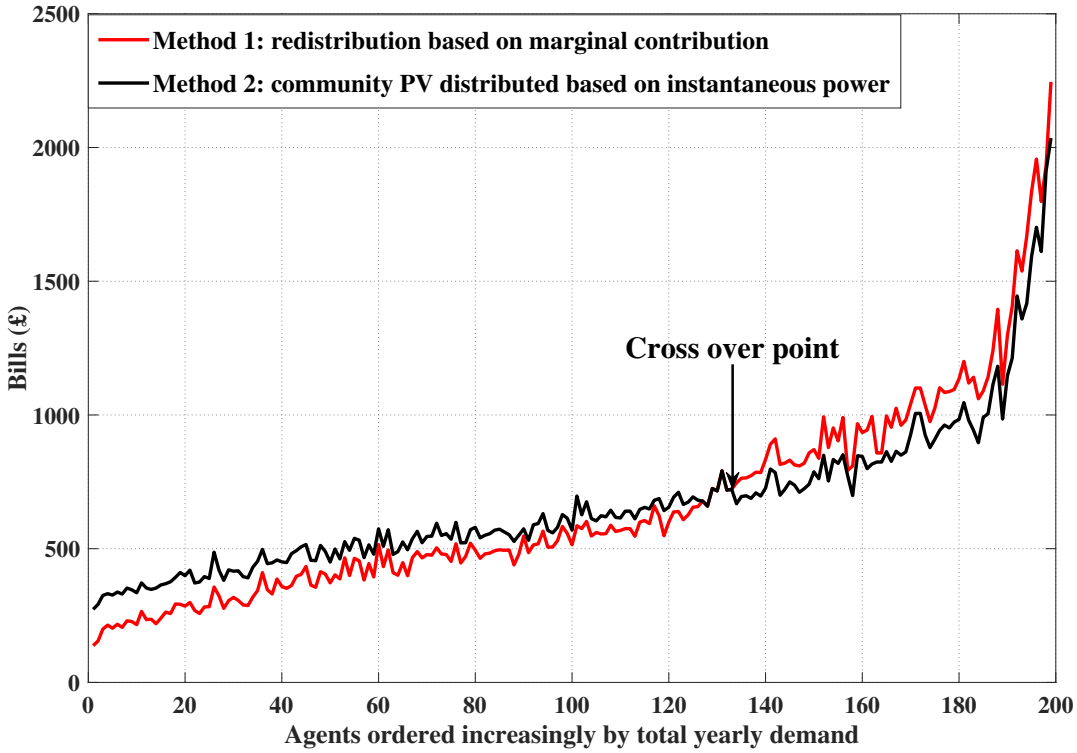

Figure 4.8: Individual agents yearly bills after redistribution based on Method 1 and Method 2 for the Agile Octopus dynamic ToU tariff [224] obtained from community solar PV only without battery.

Similar to the community wind turbine, the crossover point between Method 1 and Method 2 (as illustrated in Figure 4.8 & Figure 4.9) shows that the Method 1 the proposed redistribution method based on marginal contribution yields to a greater reduction of the annual bill for 67% of the community households compared to the Method 2 the state-of-the-art method. Hence, under the proposed marginal redistribution method, more households are able to decrease their annual bills than the existing state-of-art redistribution method. Practically, having 67% of households in the community, which are mainly small consumers, also benefiting from the proposed redistribution mechanism would lead to greater social acceptance, and hence to more communities forming coalitions to invest in jointly-owned renewable energy assets.

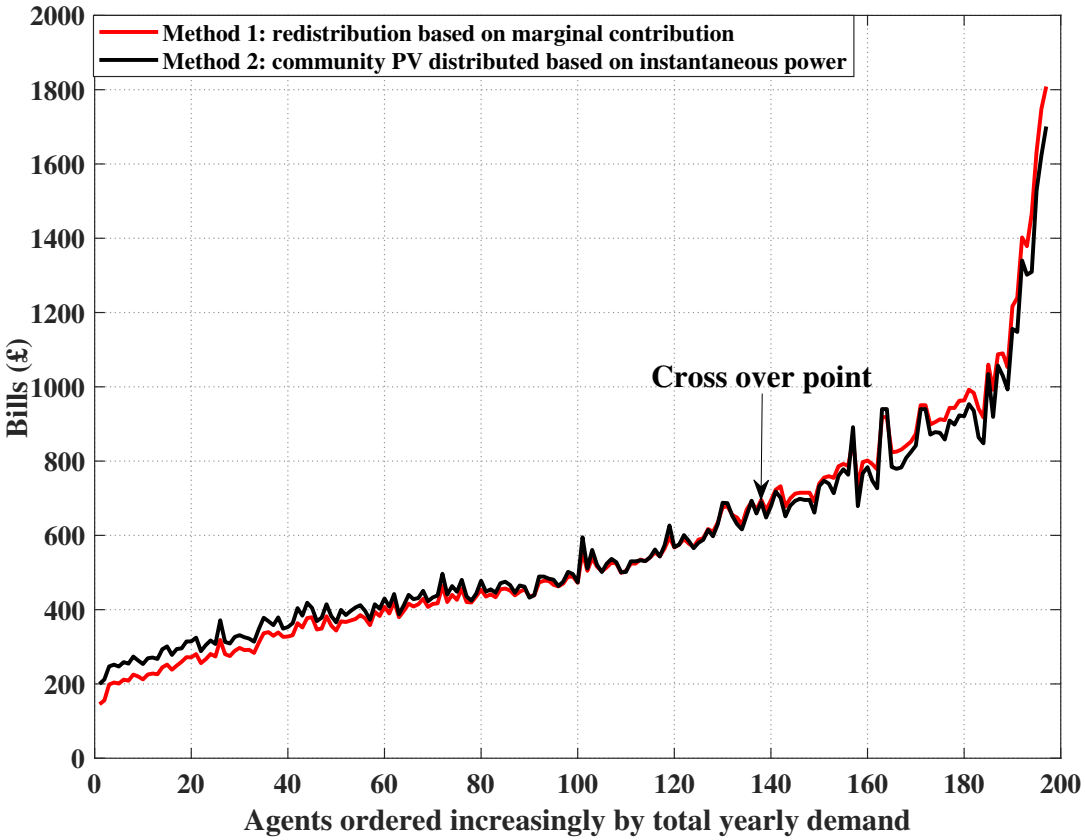

Figure 4.9: Individual agents yearly bills after redistribution based on Method 1 and Method 2 for a flat tariff of 16 pence/kWh [222] obtained from community solar PV only without battery.

4.4.3 Implementation for a community with renewable generator and battery

In this scenario, savings achieved from the community renewable generator and community battery along with the aggregation of the community consumption are redistributed based on the marginal contribution Method 1 only. Indeed, other methods as Method 4 cannot be implemented as they would require to assess the battery use for each prosumer (corresponding to a percentage of $g_C(t)$), which is not straightforward as the use of a battery can correspond to a discharge due to the household's consumption needs, but also to a charge due to the lack of consumption from the household. This is another key point that demonstrates the advantages of the proposed redistribution mechanism based on marginal contribution. Yet, there is still a need to redistribute fairly the benefits obtained from jointly-owned community renewable generator and storage assets. Hence, the proposed marginal cost redistribution method based on individual agents marginal contribution provides the equal and fair mechanism to redistribute the energy outputs (and hence financial benefits) from both the jointly-owned community renewable generator and battery assets.

In this study, we have considered investment costs for both the community-owned renewable generator and the community battery and performed an annual simulation based on the battery control algorithm 3.1 and pricing schemes, while also integrating the battery depreciation cost as in Eq. (3.14). Investment costs for community energy assets were shared equally among agents. Savings $\Pi_C(T)$ from the community renewable generator and community battery are redistributed among the agents based on their marginal contribution $\Theta_i(T)$, then the bills for individual agents are determined by Eq. (4.7). Finally, the savings are determined by comparing the sum of these annual bills over the community with the baseline total annual bill (without assets as shown in Table 4.1).

First, we implement the proposed redistribution the Method 1 based on marginal contribution for the scenario with community-owned wind turbine integrated with the community battery, and then implement for the scenario with community-owned solar PV integrated with community battery.

Redistribution from community-owned battery and community wind turbine

In the analysis for a flat tariff, an optimal community wind turbine capacity of 405kW and an optimal community battery capacity of 1342 kWh were considered. For dynamic ToU tariffs, we assumed an optimal community wind turbine of 456kW and a community battery of 1690 kWh (see Tables 4.2 and 4.4 obtained for the scenario with wind turbines only).

The overall sum of individual agents annual bills and total annual savings after redistribution based on Method 1 are shown in Table 4.10 for a flat tariff, and Table 4.11 for a dynamic ToU tariff pricing schemes.

Redistribution mechanism	**Sum of individual agent annual bills after redistribution (£)**	**Sum of individual agent annual bills without asset (baseline) (£)**	**Sum of individual agent annual savings (£)**
Method 1	57389	134455	77065

Table 4.10: Sum of individual agents annual bills and annual savings obtained from Method 1 for flat tariff of 16 pence/kWh [222] for the scenario with community wind turbine and community battery.

Redistribution mechanism	**Sum of individual agent annual bills after redistribution (£)**	**Sum of individual agent annual bills without asset (baseline) (£)**	**Sum of individual agent annual savings (£)**
Method 1	59136	143923	84787

Table 4.11: Sum of individual agents annual bills and annual savings obtained from Method 1 for Agile Octopus dynamic ToU tariff [224] for the scenario with community wind turbine and community battery.

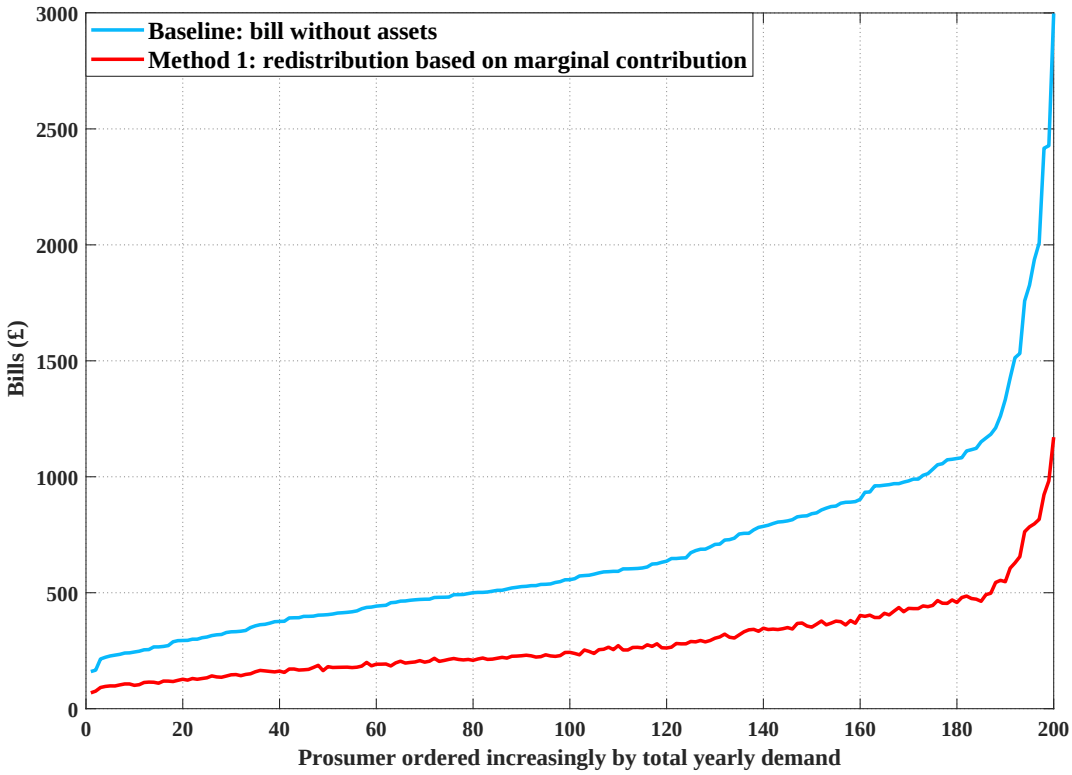

Figure 4.10: Individual agents yearly bills after redistribution based on Method 1 for a flat tariff of 16 pence/kWh [222] obtained from community wind turbine and community battery.

Figure 4.10 shows the individual agents annual bills after redistribution based on Method 1 for a flat tariff. In the case of the community-owned renewable generator only, various state-of-the-art Methods 2, 3 and 4 listed in this subsection, are available to allocate the wind power to individual agents. But, these methods are not applicable to community-owned batteries, as there is no clear method to split the power from the battery. Yet, there is still a need to assure fair sharing of the jointly-owned community renewable generator and storage resources. Hence, the proposed Method 1 based on the marginal contribution provides an equal and fair redistribution mechanism to distribute savings from both the community renewable generator and community battery.

Redistribution from community-owned battery and community solar PV

In this study, an optimal community solar PV capacity of 309kW and an optimal community battery capacity of 642 kWh were considered for a flat tariff pricing scheme, and an optimal community solar PV of 347kW and a community battery of 620 kWh was considered for a dynamic ToU tariff (see Tables 4.3 and 4.5 obtained for the scenario with solar PV only).

Similar to the case with community wind turbine and community battery, the overall sum of individual agents annual bills and total annual savings after redistribution based on Method 1 are shown in Table 4.12 for a flat tariff, and Table 4.13 for a dynamic ToU tariff pricing schemes.

Redistribution mechanism	Sum of individual agent annual bills after redistribution (£)	Sum of individual agent annual bills without asset (baseline) (£)	Sum of individual agent annual savings (£)
Method 1	113790	134455	20665

Table 4.12: Sum of individual agents annual bills and annual savings obtained from Method 1 for flat tariff of 16 pence/kWh [222] for the scenario with community solar PV and community battery.

Redistribution mechanism	Sum of individual agent annual bills after redistribution (£)	Sum of individual agent annual bills without asset (baseline) (£)	Sum of individual agent annual savings (£)
Method 1	117307	143923	26616

Table 4.13: Sum of individual agents annual bills and annual savings obtained from Method 1 for Agile Octopus dynamic ToU tariff [224] for the scenario with community solar PV and community battery.

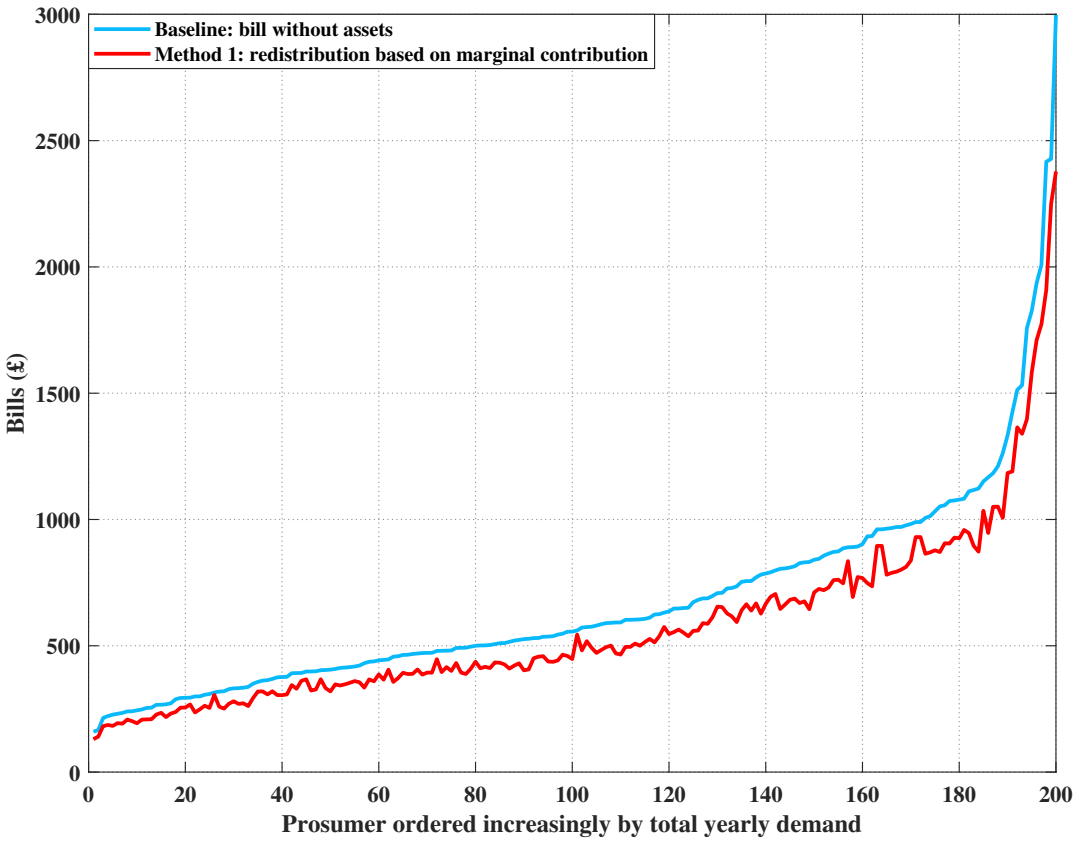

Figure 4.11: Individual agents yearly bills after redistribution based on Method 1 for a flat tariff of 16 pence/kWh [222] obtained from community solar PV and community battery.

The individual agents annual bills after redistribution based on Method 1 is shown in Figure 4.11 for fixed tariff and Figure 4.12 for dynamic ToU tariff pricing schemes. The proposed redistribution mechanism Method 1 which is based on the marginal contribution of each agent (key concept from coalitional game theory) is generic in nature and can be easily extended to incorporate other renewable generators. Hence, the sensitivity analysis of electric prices as applied to the case with the wind turbine also equally applies to the case with the solar PV renewable generator. As highlighted in the case with both community wind turbine and community battery, all the available state-of-the-art Methods 2, 3 and 4 listed in section 4.4.2 are not applicable to community-owned battery as there is no clear method to split the power from the battery. Hence, the proposed Method 1 based on marginal contribution provides an equal and fair redistribution mechanism to distribute savings from both the community-owned solar PV and community battery (as shown in Figure 4.11 & 4.12). This is another key point that demonstrates the advantages of the proposed redistribution mechanism based on the marginal contribution.

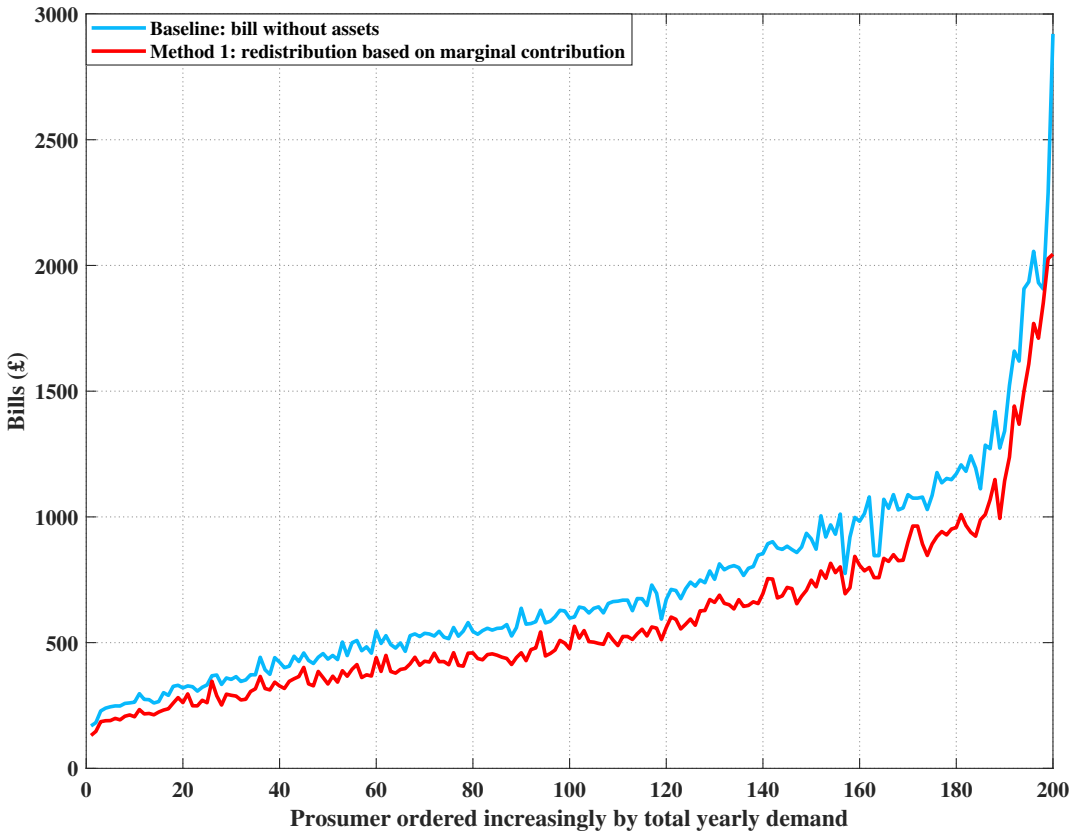

Figure 4.12: Individual agents yearly bills after redistribution based on Method 1 for an Agile Octopus dynamic ToU tariff [224] obtained from community solar PV and community battery.

4.4.4 Discussion of results

In this section, a novel algorithm is proposed for the fair redistribution of benefits obtained from community-owned assets. The algorithm demonstrates favourable redistribution and computational advantages when compared to existing state-of-the-art methods used to share the output of jointly-owned community energy assets. The proposed redistribution mechanism Method 1 is compared with existing redistribution and benefit allocation schemes for community-owned assets (state-of-the-art methods denoted as Method 2, 3 and 4).

Results from the comparison shows that, proposed method based on marginal contribution the Method 1 and the Method 2 based on instantaneous demand redistribution schemes provided the lowest annual bill and hence the highest saving for the community (as shown in Table 4.6, Table 4.7 & Figure 4.3 for community-owned wind generator, and Table 4.8, Table 4.9 & Figure 4.7 for community-owned PV generator). Then, the method 1 and method 2 were further compared to evaluate the economic fairness in the redistribution scheme. The crossover point (as shown in Figure 4.4, 4.5, 4.6, 4.8 & 4.9) between the two redistribution schemes shows that the proposed redistribution scheme Method 1 yields to a greater reduction of the annual bill for 67% of the community households compared state-of-the-art Method 2. Large consumers benefit slightly less under this scheme, but they still obtain the highest bill reduction in value as compared to households with lower demand profiles. Therefore, the proposed redistribution mechanism achieves a fairer redistribution leading to greater social acceptance, key to incentivise more communities to form coalitions and invest in jointly-owned renewable energy assets. Moreover, irrespective of the electricity buying prices, more agents could achieve consistently the lower annual bills and thus higher savings under Method 1 redistribution scheme as compared to Method 2.

Furthermore, the results based on 200 houses from the ReFLEX project [8], the UK's largest smart energy demonstration project shows that the proposed redistribution mechanism is generic in nature and is easily applicable to any type of community-owned assets, even the jointly-owned community battery storage assets; despite the apparent difficulty to assess how each member of the community takes advantage of assets.

4.5 Concluding remarks

In this work, a model of community investment and sharing of energy assets, encompassing renewable generation and battery storage, was thoroughly examined. The analysis was conducted within a market pricing regime that incorporated both fixed electricity tariffs and dynamic time of use (ToU) tariffs. An energy community model of a prosumer-based control algorithm was presented and assessed by incorporating the latest heuristics of battery state of health for both at an individual/prosumer level and at a community level. The control mechanism was implemented for both fixed electricity tariffs and dynamic ToU tariffs to compare the benefits obtained when an individual household invest in their own energy assets versus investing jointly in a community-owned energy assets.

To compare the economic performance of investments in community-owned assets and individually-owned assets, we considered an energy community of two hundred prosumers, that were all modelled by real time-series data of generation and consumption profiles from a community in UK for a full year. We computed yearly bills resulting from the proposed battery control algorithm and compared the reduction in yearly bills obtained by investment in individually-owned distributed energy assets with reduction due to investment in jointly-owned community energy assets.

Results from the techno-economic analysis show that community assets provide more savings (higher benefits) compared to distributed, individually-owned assets. The advantages from community assets are multiple. First, community assets require a lower capacity for the same services, hence potentially a lower cost. Second, community assets achieve lower annual energy bills for both pricing schemes considered in the study. The study highlighted the importance for determination of fair redistribution or allocation of benefits achieved in community projects. In this vein, we explored a number of benefit redistribution schemes (four methods in total, based on current practices). We proposed a method based on the marginal contribution of each prosumer, a key concept that assures fair distribution in coalitional game-theory. We showed that the proposed scheme achieved better performance than other methods, while also providing the additional advantage of being computationally tractable.

Chapter 5

Modeling energy asset ownership schemes in a community with network constraints

Chapter 5 presents an extension of the model developed in Chapter 4. The studies on the techno-economic analysis of individually-owned versus community-owned assets, and the marginal cost redistribution mechanisms proposed in the previous Chapter 4 have not considered the network constraints such as the local low-voltage (LV) grid characteristics, voltage limits and power ratings of electric cables and transformers. In practice however, the assets might be prevented from exporting/consuming to/from the grid due to network constraints, thereby reducing the associated benefits. For instance, when the grid is constrained with voltage excursions, then the exports form PV/wind turbine and exports/imports from/to battery can be curtailed. Hence, such curtailment events need to be accounted for in the energy community setting by including power flow (physical network/grid constraints) in the techno-economic analysis. Moreover, most of the existing redistribution frameworks (including the novel marginal cost redistribution method proposed in Chapter 4) are developed without considering network constraints, in which case the computation becomes more challenging. Thus, there is still a need to develop a redistribution mechanism that is fair, but also provide tractable computational performance that scales well with the increasing number of members in the energy community coalition, while considering operational network constraints.

To address these limitations, in this Chapter 5, the application of the rule-based battery control algorithm proposed in the previous Chapter 4 is extended by further incorporating the influence of battery life degradation, and the resultant increase in local renewable energy consumption within local operating constraints of the LV network. This chapter presents a model that first studies the techno-economic benefits of community-owned versus individually-owned energy assets considering the network/grid constraints. Then, using the methodology and principles from cooperative game theory, the novel fair redistribution mechanism introduced in our previous Chapter 4 is extended to include network operational constraints while being computationally tractable compared to the existing

state-of-the-art methods, and hence more practically applicable. Compared to prior work (presented in previous Chapter 4), in this chapter, we investigate in greater detail the complex interdependencies within the system, such as using real state-of-the art battery control which incorporates the power flow (physical network/grid constraints), and physical degradation of the asset into the community energy optimization models.

In this chapter, the energy community model incorporating the network constraints is illustrated using the solar PV renewable generator integrated with battery storage assets. However, the model is general and proposed methodologies are generic in nature and can be applied to any renewable generator such as wind turbine. Moreover, practically the solar PV renewable generators are the most distributed energy assets that are individually-owned by households. In such settings, a recent emerging approach to increase the benefits from the individually-owned assets such as solar PV is to share the joint resources and assets by facilitating peer-to-peer (P2P) or peer-to-community (P2C) local energy markets. In Chapter 6, the proposed community energy model is expanded to assess how peer-to-peer (P2P) or peer-to-consumer (P2C) market mechanisms, particularly with individually-owned assets, such as solar PVs, can enhance the benefits of the community scheme. This extension allows for a comparative analysis of the advantages of community-owned assets in contrast to individually-owned assets, both with and without the incorporation of P2P or P2C market mechanisms.

Research work presented in Chapter 5 was published in a peer-reviewed scientific paper [152].

5.1 Research contributions

A comprehensive literature review on the state-of-the-art in community energy modelling was presented analytically in the previous Chapter 2. The physical network (the LV distribution grid) is an essential entity that allows the exchange of energy in the settings of the energy communities. However, an important aspect that has often been neglected in existing research on energy community models is the relevance of the distribution grid's technical limits. Installation of renewable generator (solar PV/wind turbine) or batteries in the grid changes power flows, and might create congestions, voltage excursions, or line over-heating. In such cases, the grid operator might consider the need for an active network management to remotely control the injection of distributed renewable generator and storage assets. Therefore, due to this congestion/voltage excursion, assets might be prevented from exporting/consuming to/from the grid, reducing the benefits from their owners. For instance, when the grid is constrained with voltage excursions, then the exports form PV/wind turbine and exports/imports from/to battery can be curtailed as it is currently the case in Orkney Islands [236], UK. Therefore, such curtailment events need to be accounted for in the energy community setting by including power flow (physical network/grid constraints) in the techno-economic analysis. For example, in most of the prior literature, the studied models of energy communities do not consider the impact

of physical network constraints in the assessment of the techno-economic benefits of community-owned energy assets compared to individually-owned energy assets.

Furthermore, although most prior literature sources show that community-owned battery storage system offers higher benefits as compared to individually-owned distributed batteries [33, 16, 34–36], these studies often do not consider battery degradation cost. Also, although higher benefits can be achieved by investing in community assets, how to redistribute these benefits among the individual households in the community still remains a key open question, of both research and practical interest. Current energy communities usually employ algorithms based on proportionality of consumption to redistribute the benefits from the community-owned generator assets. However, such methods are not fair, and not applicable in the case of energy storage assets, where the proportionality of the asset usage does not apply. Hence, there is a need to design an efficient and fair redistribution mechanisms that applies to both community-owned renewable generator and storage assets, while incorporating the asset's degradation, and the physical network and operational constraints.

In the context of decentralized energy systems, coalitional game theory has been identified as a promising solution for designing incentive mechanisms for community energy trading and sharing. In a cooperative game, players form coalitions to maximise a common objective for mutual benefit. Then, the benefit is distributed equally or fairly among themselves using incentive-based solution concepts, such as the Shapley value. Existing coalitional game theory redistribution mechanism based on concepts like the Shapley value use marginal contributions at their core, but present issues of scalability as the number of agents in a coalition increases [40, 235]. Moreover, most of existing redistribution frameworks are developed without considering network constraints, in which case the computation cost becomes even more challenging.

To address the above challenges, this Chapter 5 presents a model that first studies the techno-economic benefits of community-owned assets versus individually-owned energy assets considering the network/grid constraints. In order to assess the benefits from installing various assets including a comprehensive model of battery degradation, we propose an approach based on real time-series data of a community, and compare the benefits provided by community-owned assets with the benefits expected from individually-owned assets, considering operational network constraints. Then, using the methodology and principles from cooperative game theory, the novel fair redistribution mechanism introduced in our previous Chapter 4 is extended to include network operational constraints while being computationally tractable compared to the existing state-of-the-art methods, and hence more practically applicable.

More specifically, this chapter presents a methodology for real-time control of energy community assets from an economic and technical perspective. Compared to prior work we investigate in greater detail the complex interdependencies within the system, such as using real state-of-the art battery control which incorporates the power flow (physical network/grid constraints), and physical degradation of the asset into the community energy optimization models. Moreover, the research in this study includes a full model of power

flows in a LV distribution network describing an energy community, and – as a first - the effect of network constraints and curtailment imposed by the system operator to maintain LV network operational compliance is modelled. This is coupled to both the algorithm for the smart control of the battery and generation source, but also extends to the redistribution algorithm. This represents a significant and novel contribution to the current state-of-the-art.

In summary, the research contributions of the work presented in Chapter 5 that progress beyond the state of the art are:

- This chapter presents a techno-economic comparison between two configurations of energy communities connected to a low-voltage distribution network. First, a configuration with individually-owned distributed energy assets, such as solar PV and residential batteries. Then, a second configuration in which distributed energy assets are jointly owned by the community, and installed in a single location. The proposed two configurations of energy communities are compared by studying the economic impacts of installing various energy assets on the grid for both fixed and dynamic time of use (ToU) tariffs.

- In this work, power flow (physical network/grid constraints), and physical battery degradation are incorporated into community energy optimization models, including the effect of network constraints on redistribution schemes. To achieve this objective, a battery state of health degradation model is utilized, which relies on the battery depth of discharge in each control cycle, while simultaneously ensuring that the bus voltages remain within permissible limits. This represents a considerable extension of prior work of control and sharing of assets in energy communities, which do not – or very rarely consider physical LV network constraints in their modeling (including the novel marginal cost redistribution method proposed in Chapter 4)

- This chapter presents a fair and computationally tractable redistribution scheme for sharing the benefits obtained from community-owned energy assets subjected to physical network constraints, based on principles from cooperative game [37, 40], and its advantageous is tested and verified by comparing with the state-of-the-art redistribution mechanisms.

- The proposed energy community model is validated using a real case study from the ReFLEX (Responsive Flexibility) project that aims to develop a large-scale demonstrator for community energy integration in Orkney, Scotland, UK [8].

Firstly, the power flows in an LV network that describe the energy community are modelled in the subsequent section.

5.2 LV Network model

Two configurations of energy communities were compared in Chapter 4. In the first configuration, community comprised of 200 individual agents are considered, each one of them with their own consumption and local production, but without financial nor energy interaction between them. In such configuration, agents import electricity from the grid when their assets cannot cover their own consumption, whereas they can export electricity to the grid when they have production surplus. The second configuration corresponds to the case of an energy community in which agents invest together in jointly-owned community energy assets, such as wind or solar production, and community batteries. The demand of agents is considered inflexible. A renewable generator (either wind turbine or a solar PV installation), a battery energy storage system and the utility grid are the three power sources considered for satisfying the inflexible demand at all times. A power flow diagram of an agent or of the energy community considered as a whole was shown in Figure 4.1 in the previous Chapter 4. As described (defined by Eq. 4.1), the overall power balance at any given time t of an agent i or of the energy community C is given by:

$$p^{\text{grid}}_{i/C}(t) = d_{i/C}(t) - p^{\text{bat}}_{i/C}(t) - g^{\text{PV}}_{i/C}(t) \tag{5.1}$$

where $g^{\text{PV}}_{i/C}(t)$ is the power generated by the solar PV generator, that can be individually owned, or owned by the community. $p^{\text{grid}}_{i/C}(t)$ represents the power that an agent or that the community can buy/sell from/to the grid. $p^{\text{bat}}_{i/C}(t)$ represents the power of the storage system (individually-owned, or centrally located and owned by the community), which is considered negative when the battery is charging (battery considered as a load), and positive when the battery is discharging (battery considered as a generator). $d_{i/C}(t)$ is the power consumed by an agent or by the community considered as a whole, i.e the aggregated demand power of 200 agents.

However, the power flow diagram proposed in Figure 4.1 does not include physical constraints such as electric cables thermal limits and voltage excursions. Therefore, in energy communities with important renewable production, such as the Orkney Islands considered in the ReFLEX project [8], agents may be prohibited from exporting power at particular times, due to electric cables overheat. As a result, network constraints (technical limits of the electrical grid) must also be added to the energy community model described by Figure 4.1. To include physical constraints such as network constraints, we have considered a 13-bus radial distribution system to connect all agents of the community. This network model is adapted from the IEEE 13-bus network [237].

In this chapter, the primary objective is to compare two configurations of energy communities that consider the incorporation of network constraints. First, a configuration with individually-owned distributed generation assets, such as solar PV and residential batteries. Households are randomly aggregated among the 13-buses, as presented in Figure 5.1. Then, a second configuration in which distributed generation assets are owned by the community, and installed in a single location. Figure 5.2 shows the location of assets

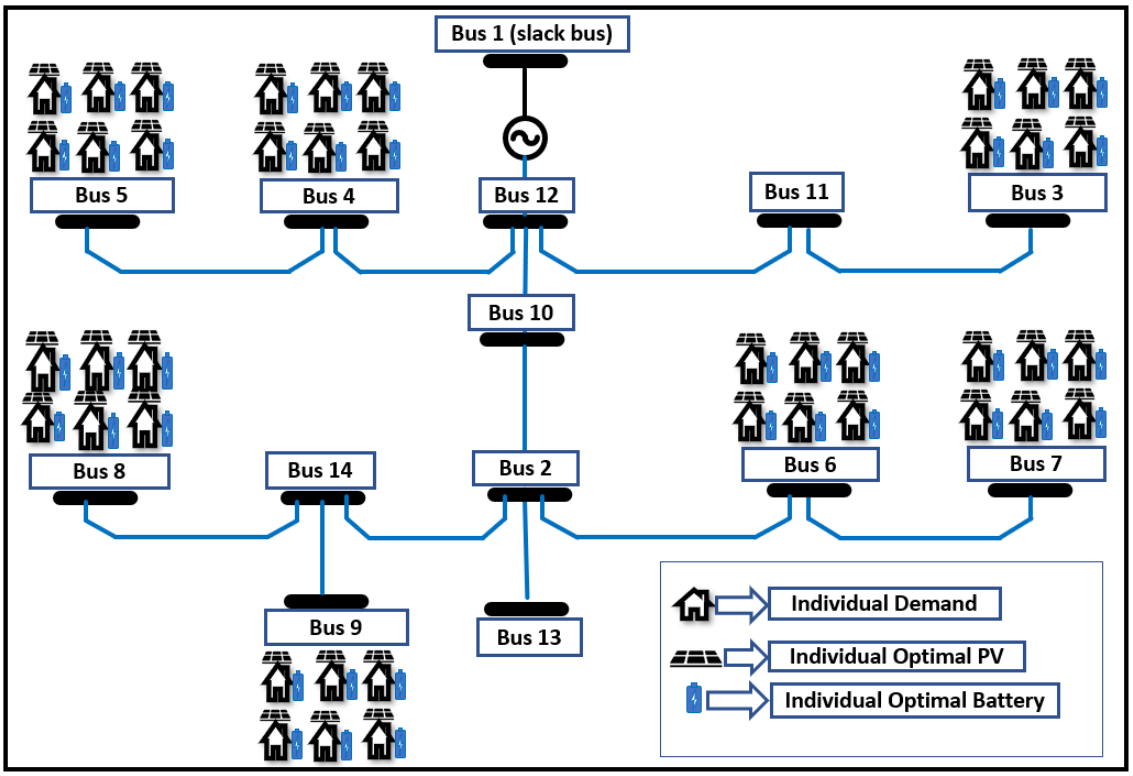

Figure 5.1: Electric network used in simulations with grid constraints for individually-owned assets.

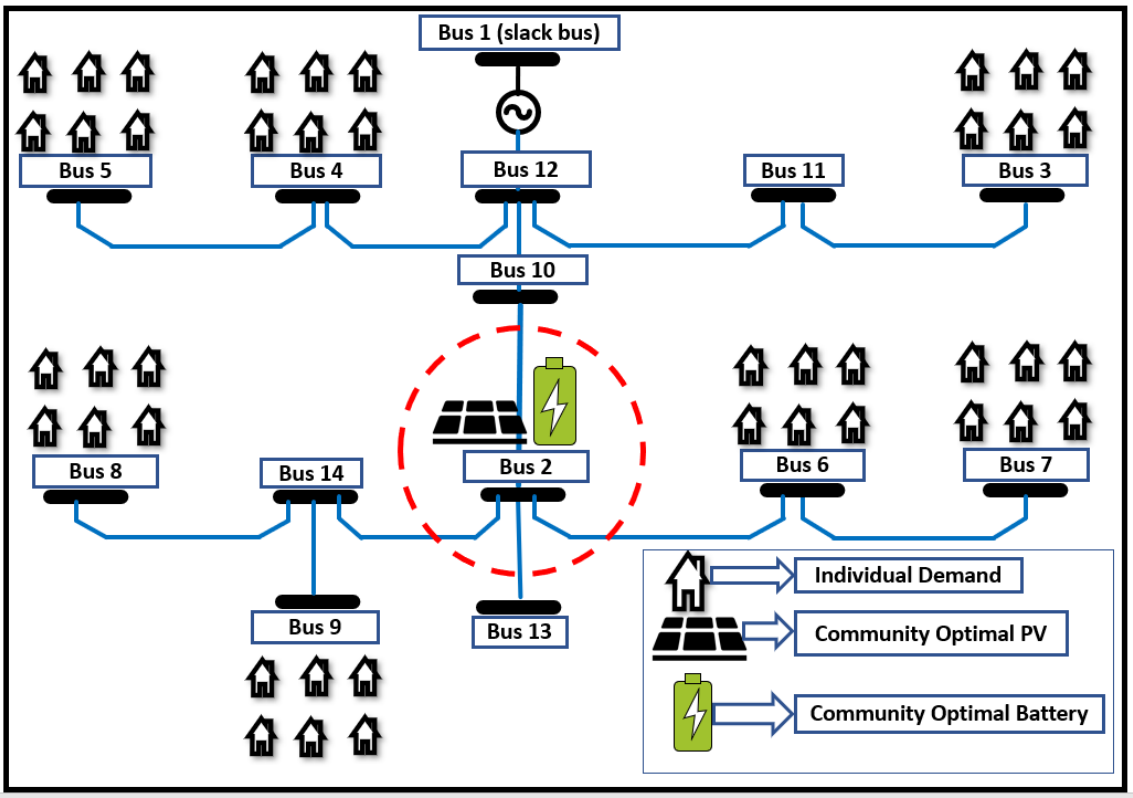

Figure 5.2: Electric network used in simulations with grid constraints for centrally located community-owned assets.

and households in the configuration of centrally located, community-owned generation and storage assets.

Community-owned assets are connected to a unique bus without load, that was chosen to be in a central location of the grid, in order to reduce the risk of constraining the grid. Bus 1 (slack bus) represents the main connection to the transmission grid, and its voltage is set to reference voltage of 1 p.u with the base voltage of 236 V. Power flow in this

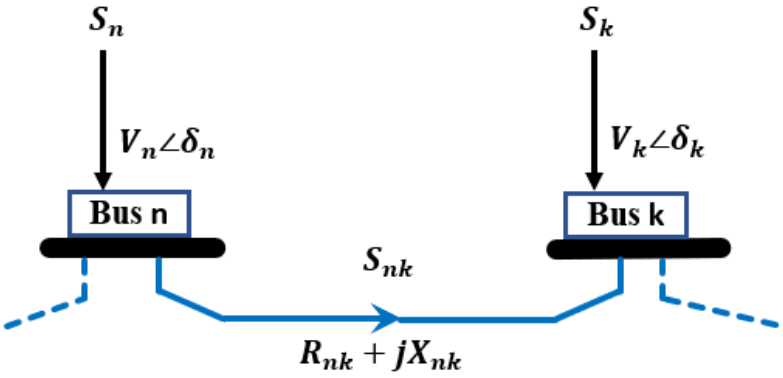

Figure 5.3: Power balance at a bus of the electric grid.

13 bus grid model is computed for every time interval considered in our simulations in order to determine the voltages and power (active and reactive) flowing at every bus. The power flow computation follows a power approach in which the apparent power balance is stated for every bus of the grid, as shown in Figure 5.3. We define, $S_n = P_n + jQ_n$ the apparent power that is consumed or produced at bus n. $Z_{nk} = R_{nk} + jX_{nk}$ is the impedance (admittance, $Y_{nk} = 1/Z_{nk}$) of the line between bus n and bus k and $S_{nk} = P_{nk} + Q_{nk}$ is the apparent power flowing between bus n and bus k. The power balance equations are summarized in Eq. 5.2.

$$\begin{aligned} P_n &= |V_n| \sum_k |V_k|\,|Y_{nk}|\,cos(\delta_k - \delta_n + \gamma_{nk}) \\ Q_n &= |V_n| \sum_k |V_k|\,|Y_{nk}|\,sin(\delta_k - \delta_n + \gamma_{nk}) \end{aligned} \tag{5.2}$$

where $\overline{Y_{nk}} = Y_{nk}e^{j\gamma_{nk}}$ is the admittance of the line connection between bus n and bus k. P_n is the total active power produced and consumed at bus n, which is considered positive if produced and negative if the power is consumed. Similarly, Q_n is the total reactive power produced (positive) and consumed (negative) at bus n. The voltage at bus n is defined by $\overline{V_n} = V_n e^{j\delta_n}$, with δ_n the voltage angle. The line parameters and other related details considered in the 13-bus radial distribution system is provided in the Appendix A (adapted as provided in [237]). The power balance expressed in Eq. (5.2) is solved using the Newton-Raphson method, and gives the following two fundamental outputs:

i The voltage at each bus, in amplitude and phase.

ii The power (active and reactive) flowing through each bus.

Furthermore, in order to provide a techno-economic study that enables the comparison between the two configurations proposed (individually-owned and community-owned assets), we have considered one year of data for load consumption [215] and solar PV

production [221] with half-hourly time intervals, using Thames Valley Vision data for both flat tariff [222] and Agile Octopus dynamic ToU [224] pricing schemes (as described in Section 3.3 in Chapter 3). These 200 demand profiles are further aggregated [35] to represent a single community demand profile. Power flows were computed for the whole year. Also, we have linearly increased the power consumption of each household in order to consider an energy community in which voltage profiles are already close but still within the UK's upper and lower admissible voltage limits of 1.1 per unit (p.u) and 0.94 p.u. respectively for the whole year. Therefore, this setting consists of a case of normal operation with acceptable voltage and congestion profiles, while allowing us to study the potential impacts of installing various assets on the grid. The control algorithm of distributed generation assets, including the remote control from the Distribution System Operator (DSO) to prevent voltage out-of-bounds excursions, is defined in the following section.

5.3 Battery control algorithm with voltage control mechanism

In this chapter, the battery control Algorithm 3.1 applied to the single prosumer model described in Chapter 3 and energy community setting (without network constraints) described in Chapter 4 is modified by incorporating the power flow (physical network/grid constraints) through voltage control mechanism.

A new battery control scheme consists of operational real-time decisions to charge or discharge the battery, based on the difference between the agent/community power consumption and its PV production. When the PV production exceeds the power consumed, the control scheme charges the battery if the bus voltage (V^{bus}) is within the permissible limits ($0.94p.u \leq V^{\text{bus}} \leq 1.1p.u$), until it reaches the full capacity. Any excess is exported and sold to the main grid, provided the V^{bus} is within the permissible limits. Whenever, the demand exceeds the PV production, the battery is discharged until it reaches its maximum allowable depth of discharge (DoD), provided the V^{bus} is within the permissible limits. Any remaining deficit is purchased and imported from the grid. The bus voltage is regulated within the safe permissible limits by controlling the export from the PV generator, and export/import from/to the battery assets.

As described in Section 3.4.1 of Chapter 3, the operation of the battery is constrained by the state of charge (SoC) levels, and a maximum power ($p^{\text{bat,max}}$) that the battery can be charged or discharged at, which corresponds to its maximum C-rating. In this work, Coulomb-counting method is used to estimate the SoC of the battery. The accuracy of this method depends mainly on how the current drawn from or to the battery is measured and on the nominal battery capacity [238]. In our study, the nominal battery capacity is updated at regular intervals of the simulation. This approach is similar to the solutions implemented in commercial batteries. A number of commercial battery manufacturers such as ABB [239] propose an updated Coulomb-counting method for SoC estimation.

At any given time t of a charging phase, the battery is charged with an efficiency (η^c) until it reaches the maximum battery capacity ($SoC^{\max}$). Charging constraints are defined as:

$$SoC(t) \leq SoC^{\max} \tag{5.3}$$

$$p^{\text{bat}}(t) \leq p^{\text{bat,max}} \tag{5.4}$$

Similarly, the battery can be discharged with an efficiency (η^d) until it reaches its minimum battery capacity ($SoC^{\min}$). Discharging constraints are defined as:

$$SoC(t) \geq SoC^{\min} \tag{5.5}$$

$$p^{\text{bat}}(t) \leq p^{\text{bat,max}} \tag{5.6}$$

The minimum battery capacity corresponds to the maximum allowable DoD.

In this section, a *rule-based battery control* algorithm is proposed, targeting the charging of the battery during power surplus and discharging the battery during power deficits, all while ensuring the bus voltage (V^{bus}) remains within acceptable limits. The algorithm can be described as follows:

If $g^{\text{PV}}(t) > d(t)$, there is *excess of power* generated from the PV generator. The control strategy of the battery dictates the following:

I If $SoC(t) \leq SoC^{\max}$ and $p^{\text{bat}}(t) \leq p^{\text{bat,max}}$ then the excess power is stored in the battery (charging operation), provided the $V^{\text{bus}}(t)$ due to bus power $P^{\text{bus}}(t)$ is within the permissible limits i.e $0.94p.u \leq V^{\text{bus}}(t) \leq 1.1p.u$. Where, $P^{\text{bus}}(t)$ is the total net active and reactive power of the bus at time t given by Eq. (5.2).

II If the battery is full ($SoC(t) > SoC^{\max}$) or if available power is greater than the maximum acceptable charging power ($p^{\text{bat}}(t) > p^{\text{bat,max}}$), then the agent/community sells the excess power to the utility grid at a selling price equal to $\tau^s(t)$, provided the $V^{\text{bus}}(t)$ due to bus power $P^{\text{bus}}(t)$ is within the permissible limits i.e $0.94p.u \leq V^{\text{bus}}(t) \leq 1.1p.u$.

The resulting SoC profile, power at bus $P^{\text{bus}}(t)$, and the energy exported $e^s(t)$ to the grid during the identified duration of excess generation are determined as:

$$p^{\text{bat}}(t) = -min(min([g^{\text{PV}}(t) - d(t)], p^{\text{bat,max}}), \frac{[SoC^{\max} - SoC(t-1)]}{\eta^c \Delta t}) \tag{5.7}$$

$$SoC(t) = SoC(t-1) - \eta^c p^{\text{bat}}(t)\Delta t \tag{5.8}$$

$$P^{\text{bus}}(t) = g^{\text{PV}}(t) - p^{\text{bat}}(t) \tag{5.9}$$

$$e^s(t) = \left[P^{\text{bus}}(t) - d(t)\right]\Delta t \tag{5.10}$$

where Δt corresponds to the duration of the considered time step.

III If the excess PV power available for charging the battery or for export to grid violates the safe voltage limit (i.e $0.94p.u \leq V^{\text{bus}}(t) \leq 1.1p.u.$), then the power export from the PV, and power import to battery are curtailed ($P^{\text{curtailed}}$) until the voltage is within the permissible limits, accordingly the $P^{\text{bus}}(t)$ is updated. When the generation from the PV is curtailed due to voltage violations, the demand is satisfied by importing energy ($e^b(t)$) from the utility grid at a buying price equal to $\tau^b(t)$. Whenever the $V^{\text{bus}}(t) > 1.1p.u$, the voltage is controlled as follows.

i If the battery is fully charged, then the export from PV is curtailed and the bus power is updated as:

$$P^{\text{bus}}(t) = P^{\text{bus}}(t) - P^{\text{curtailed}} \tag{5.11}$$

If the updated $P^{\text{bus}}(t) > 0$, then the excess energy is exported to the utility grid:

$$e^s(t) = \left[P^{\text{bus}}(t) - d(t)\right] \Delta t \tag{5.12}$$

If the updated $P^{\text{bus}}(t) < 0$, then the deficit energy is imported from the utility grid:

$$e^b(t) = \left[d(t) - P^{\text{bus}}(t)\right] \Delta t \tag{5.13}$$

ii If the battery is in the process of charging, then the power export from PV and power import to battery are curtailed, and the bus power is updated as:

$$p^{\text{bat}}(t) = -min(min([p^{\text{bat}}(t) + P^{\text{curtailed}}], p^{\text{bat,max}}), \frac{[SoC^{\max} - SoC(t-1)]}{\eta^c \Delta t}) \tag{5.14}$$

$$P^{\text{bus}}(t) = g^{\text{PV}}(t) - p^{\text{bat}}(t) \tag{5.15}$$

If the updated $P^{\text{bus}}(t) > 0$, then the excess energy is exported to the utility grid:

$$e^s(t) = \left[P^{\text{bus}}(t) - d(t)\right] \Delta t \tag{5.16}$$

If the updated $P^{\text{bus}}(t) < 0$, then the deficit energy is imported from the utility grid:

$$e^b(t) = \left[d(t) - P^{\text{bus}}(t)\right] \Delta t \tag{5.17}$$

Similarly, if $g^{\text{PV}}(t) < d(t)$, then there is a *deficit in power* supplied by the PV generator. During this time, the demand is satisfied by discharging the battery, provided the battery capacity is above the minimum SoC and the bus voltage (V^{bus}) is within the permissible limits. Otherwise, the deficit power is imported from the utility grid.

Figure 5.4 illustrates a comprehensive flowchart of the proposed control strategy, integrating network constraints. In the presence of excess renewable generation, the prosumer's objective is to sell all surplus energy. However, considering the physical network/grid limitations, such sales are restricted. Likewise, during periods of energy deficit, the prosumer's preference is to discharge the battery, yet network constraints prohibit it. These crucial aspects were not addressed in the previous Chapter 3 & 4. In this Chapter 5, these network constraints are addressed by introducing an additional voltage control mechanism, highlighted in blue within the Flowchart depicted in Figure 5.4. This inclusion enhances the overall effectiveness of the control strategy.

Algorithm 5.1 & 5.2 outlines this if-then rule based control strategy. Algorithm 5.1 demonstrates the proposed control strategy for battery management and voltage regulation when there is excess generation in the renewable system. On the other hand, Algorithm 5.2 showcases the optimization of deficits in renewable generation.

Most of the time the voltage excursion is characterized predominantly by over-voltage phenomenon (i.e high voltage violations $V^{\text{bus}}(t) > 1.1p.u$). Hence, the voltage control mechanism for the case with $V^{\text{bus}}(t) > 1.1p.u$ is only included in the control scheme. However, if the bus voltage violates the lower permissible limit ($V^{\text{bus}}(t) < 0.94p.u$) and $g^{\text{PV}}(t) > d(t)$, then the bus voltage can be controlled by limiting the battery charging until it is within the permissible limit. If $g^{\text{PV}}(t) < d(t)$, then the bus voltage can be controlled by increasing the reactive power production from the battery.

Whenever the bus voltage (V^{bus}) violates the permissible limits, then the gird is constrained, hence the exports from PV and exports/imports from/to battery are curtailed. This reduces the financial benefits offered by the assets. The economic parameters to assess and compare the benefits of community-owned assets with individually-owned assets is presented in the next section.

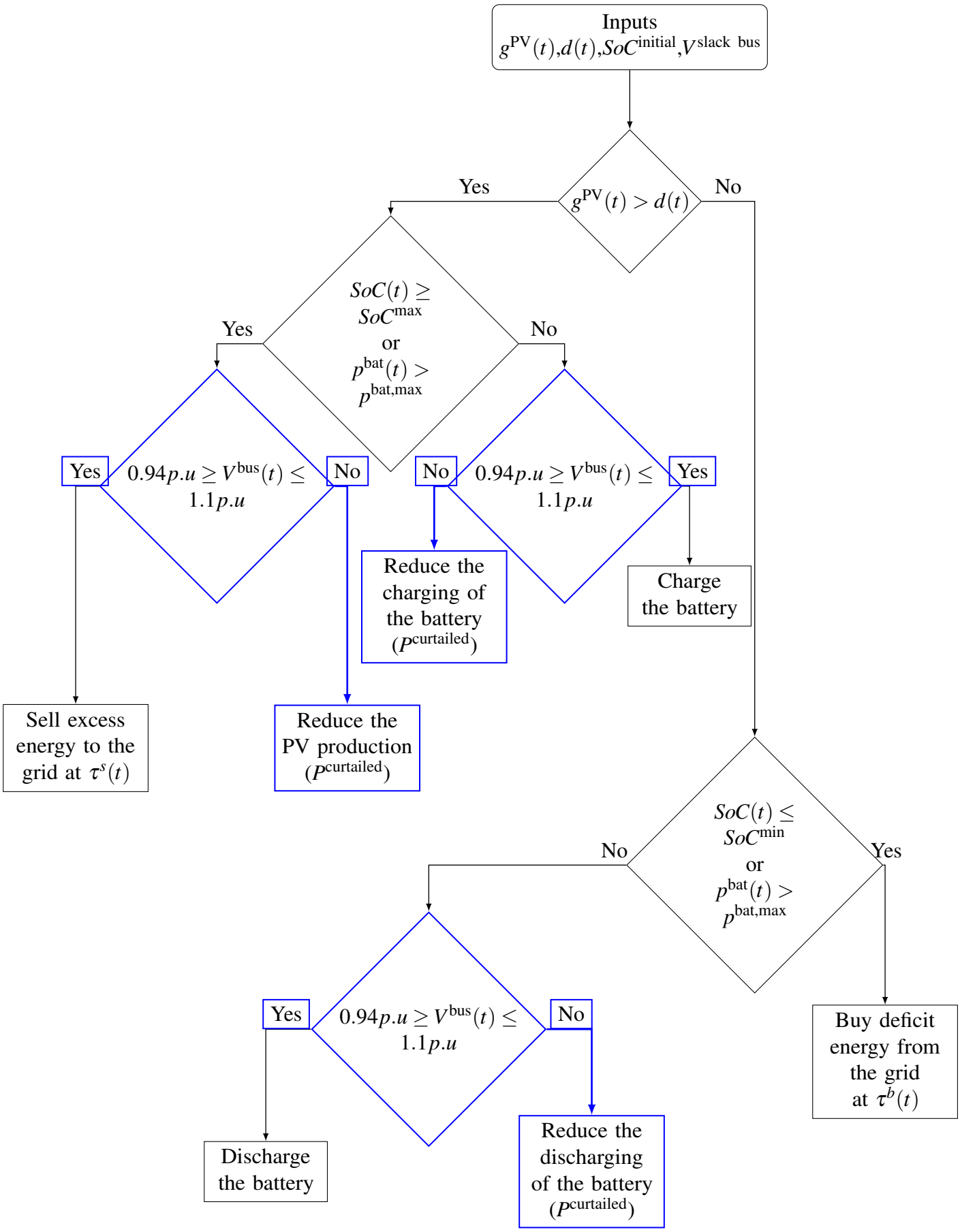

Figure 5.4: Flowchart of battery and voltage control scheme.

Algorithm 5.1: Battery control and voltage regulation algorithm for optimizing excess in renewable generation

Input: $g^{\text{PV}}(t)$, $d(t)$, $\tau^b(t)$,$\tau^s(t)$,η^c, η^d, $SoC^{\text{initial/max/min}}$,$p^{\text{bat,max}}$, $V^{\text{slack bus}} = 1p.u$
for $t = 1 : T$ **do**
  $\forall t \in [0,T]$, excess of energy or deficit in energy is determined
  if $g^{PV}(t) \geq d(t)$ **then**
    $$p^{\text{bat}}(t) = -min\left(min\left(\left[g^{\text{PV}}(t) - d(t)\right], p^{\text{bat,max}}\right), \frac{[SoC^{\max} - SoC(t-1)]}{\eta^c \Delta t}\right)$$
    When, $SoC(t) \leq SoC^{\max}$ and $p^{\text{bat}}(t) \leq p^{\text{bat,max}}$
    Provided, $0.94p.u \leq V^{\text{bus}}(t) \leq 1.1p.u$
    Charge the battery ($p^{\text{bat}}(t) < 0$):
    $SoC(t) = SoC(t-1) - \eta^c p^{\text{bat}}(t)\Delta t$
    $P^{\text{bus}}(t) = g^{\text{PV}}(t) - p^{\text{bat}}(t)$
    When, $SoC(t) > SoC^{\max}$ or $p^{\text{bat}}(t) > p^{\text{bat,max}}$
    Provided, $0.94p.u \leq V^{\text{bus}}(t) \leq 1.1p.u$
    Sell excess energy to the grid at $\tau^s(t)$:
    $e^s(t) = \left[P^{\text{bus}}(t) - d(t)\right]\Delta t$
    Voltage control mechanism:
    while $V^{bus}(t) > 1.1p.u$ **do**
      if $p^{bat}(t) \geq p^{bat,max} \,||\, SoC(t) \geq SoC^{max}$ **then**
        Export from PV is curtailed (production from PV is reduced):
        $P^{\text{bus}}(t) = P^{\text{bus}}(t) - P^{\text{curtailed}}$
        if $P^{bus}(t) > 0$ **then**
          $e^s(t) = \left[P^{\text{bus}}(t) - d(t)\right]\Delta t$
        else
          $e^b(t) = \left[d(t) - P^{\text{bus}}(t)\right]\Delta t$
        end
      else
        Import to battery is curtailed (charging of the battery is reduced):
        $$p^{\text{bat}}(t) = -min\left(min\left(\left[p^{\text{bat}}(t) + P^{\text{curtailed}}\right], p^{\text{bat,max}}\right), \frac{[SoC^{\max} - SoC(t-1)]}{\eta^c \Delta t}\right)$$
        $P^{\text{bus}}(t) = g^{\text{PV}}(t) - p^{\text{bat}}(t)$
        if $P^{bus}(t) > 0$ **then**
          Excess energy exported to grid at $\tau^s(t)$:
          $e^s(t) = \left[P^{\text{bus}}(t) - d(t)\right]\Delta t$
        else
          Deficit energy imported from grid at $\tau^b(t)$:
          $e^b(t) = \left[d(t) - P^{\text{bus}}(t)\right]\Delta t$
        end
      end
    end
  else
    Battery control and voltage regulation mechanism for optimizing the deficit in renewable generation is outlined in Algorithm 5.2
  end
end
Output: $\forall t \in [0,T]$, $SoC(t)$, $e^s(t)$, $e^b(t)$, $P^{\text{bus}}(t)$, $V^{\text{bus}}(t)$

Algorithm 5.2: Battery control and voltage regulation algorithm for optimizing deficits in renewable generation

Input: $g^{\text{PV}}(t)$, $d(t)$, $\tau^b(t)$,$\tau^s(t)$,η^c, η^d, $SoC^{\text{initial/max/min}}$,$p^{\text{bat,max}}$, $V^{\text{slack bus}} = 1p.u$
for $t = 1 : T$ **do**
  $\forall t \in [0,T]$, excess of energy or deficit in energy is determined
  if $g^{PV}(t) \geq d(t)$ **then**
    Battery control and voltage regulation for optimizing the excess in renewable genration is outlined in Algorithm 5.1
    Voltage control mechanism:
    Export from PV is curtailed (production from PV is reduced)
    Import to battery is curtailed (charging of the battery is reduced)
  else
    $p^{\text{bat}}(t) = min\left(min\left(\left[d(t) - g^{\text{PV}}(t)\right], p^{\text{bat,max}}\right), \eta^d\left[SoC(t-1) - SoC^{\text{min}}\right]\right)$
    When, $SoC(t) \geq SoC^{\text{min}}$ and $p^{\text{bat}}(t) \leq p^{\text{bat,max}}$
    Provided, $0.94p.u \leq V^{\text{bus}}(t) \leq 1.1p.u$
    Discharge the battery ($p^{\text{bat}}(t) > 0$):
    $SoC(t) = SoC(t-1) - \frac{p^{\text{bat}}(t)}{\eta^d} \cdot \Delta t$
    $P^{\text{bus}}(t) = g^{\text{PV}}(t) + p^{\text{bat}}(t)$
    Buy deficit energy from grid at $\tau^b(t)$:
    $e^b(t) = \left[d(t) - P^{\text{bus}}(t)\right]\Delta t$
    Voltage control mechanism:
    while $V^{bus}(t) > 1.1p.u$ **do**
      if $p^{bat}(t) \leq 0 \,||\, SoC(t) \leq SoC^{min}$ **then**
        When the battery is completely discharged, then any production from the PV is curtailed or reduced:
        $P^{\text{bus}}(t) = max\left(0, P^{\text{bus}}(t) - P^{\text{curtailed}}\right)$
        Deficit energy imported from grid at $\tau^b(t)$:
        $e^b(t) = \left[d(t) - P^{\text{bus}}(t)\right]\Delta t$
      else
        Export from battery is curtailed (discharging of the battery is reduced):
        $p^{\text{bat}}(t) = min\left(max\left(0, \left[p^{\text{bat}}(t) - P^{\text{curtailed}}\right]\right), \eta^d\left[SoC(t-1) - SoC^{\text{min}}\right]\right)$
        $P^{\text{bus}}(t) = g^{\text{PV}}(t) + p^{\text{bat}}(t)$
        Deficit energy imported from grid at $\tau^b(t)$:
        $e^b(t) = \left[d(t) - P^{\text{bus}}(t)\right]\Delta t$
      end
    end
  end
end
Output: $\forall t \in [0,T]$, $SoC(t)$,$e^b(t)$, $P^{\text{bus}}(t)$, $V^{\text{bus}}(t)$
$SoC(t)$, input to **rainflow cycle counting algorithm** used to calculate the battery depreciation factor
$e^s(t)$ energy exported to grid at a selling price equal to $\tau^s(t)$
$e^b(t)$ energy imported from grid at a buying price equal to $\tau^b(t)$
$P^{\text{bus}}(t)$ updated bus power
$V^{\text{bus}}(t)$ updated bus voltage

5.4 Techno-economic indicators

The main aim of the economic study of the energy community is to determine the benefits provided by assets (renewable generation capacity and storage) to prosumers, subjected to network and operational constraints. To achieve this, the presented Algorithm 5.1 & 5.2 are implemented by considering the different pricing schemes (as described in Section 3.3.4 of Chapter 3). A yearly energy bill savings, which is a fairly intuitive indicator, is used to compare the economic performance of investments in individually-owned assets and community-owned assets. In this section, we provide the key economic performance indicator adopted in the proposed comparative study.

The economic value of both community-owned assets and individually-owned assets can be assessed and compared by considering the reduction of the sum of the annual electricity bill of all the households from the energy community. The yearly bill $b(T)$ of an agent/community can be expressed as the sum of the cost of the annual energy consumption and the depreciation cost of the assets c^A, minus the sum of revenues earned by exports to the grid, as shown below:

$$b(T) = \sum_{1}^{T} e^b(t)\tau^b(t) - \sum_{1}^{T} e^s(t)\tau^s(t) + c^A(T) \tag{5.18}$$

where the energy import $e^b(t)$ at time step t is given by Eq. (5.19), with P^{house} the power imported (if positive) or exported (if negative) by the considered household.

$$e^b(t) = \left[d(t) - P^{\text{house}}(t)\right]\Delta t \tag{5.19}$$

Similarly, the energy export $e^s(t)$ at time step t is given by Eq. (5.20).

$$e^s(t) = \left[P^{\text{bus}}(t) - d(t)\right]\Delta t \tag{5.20}$$

However, as many countries have reduced or removed export prices under the form of feed-in tariffs, our analysis will not include revenues from energy export. Thus, the yearly bill without feed-in tariff is determined as:

$$b(T) = \sum_{1}^{T} e^b(t)\tau^b(t) + c^A(T) \tag{5.21}$$

Similar to the community settings described in Chapter 4, the model inputs, battery depreciation aspects and the economic setting of the single prosumer model described in Chapter 3 are applied to the community setting. As outlined by Eq. (3.20), the annual bill for agent i and the community $\mathcal{C}$ are defined as:

$$b_i(T) = \sum_{1}^{T} e_i^b(t)\tau^b(t) + c_i^A(T). \tag{5.22}$$

$$b_C(T) = \sum_{1}^{T} e_C^b(t)\tau^b(t) + c_C^A(T). \tag{5.23}$$

where, $e_i^b(t)\tau^b(t)$ is the cost of energy imports from the utility grid by agent i at time t and $c_i^A(T)$ is the depreciation cost of assets owned by agent i in the considered period T. Similarly, $e_C^b(t)\tau^b(t)$ is the cost of energy imported from the utility grid by the community as a whole at time t and $c_C^A(T)$ is the depreciation cost of jointly-owned community assets for the considered period T.

This chapter presents an energy community model that first studies the techno-economic benefits obtained from community-owned assets and individually-owned assets considering the network constraints, and compare it with the case without network constraints. Then, we present the fair redistribution scheme to fairly redistribute the benefits from the community-owned assets. Also, in order to test the advantages of the proposed redistribution mechanism, we present in this chapter the state-of-the-art redistribution method, used in current practice in such projects, that will be used for comparison. This proposed energy community modelling approach is summarized in Figure 5.5.

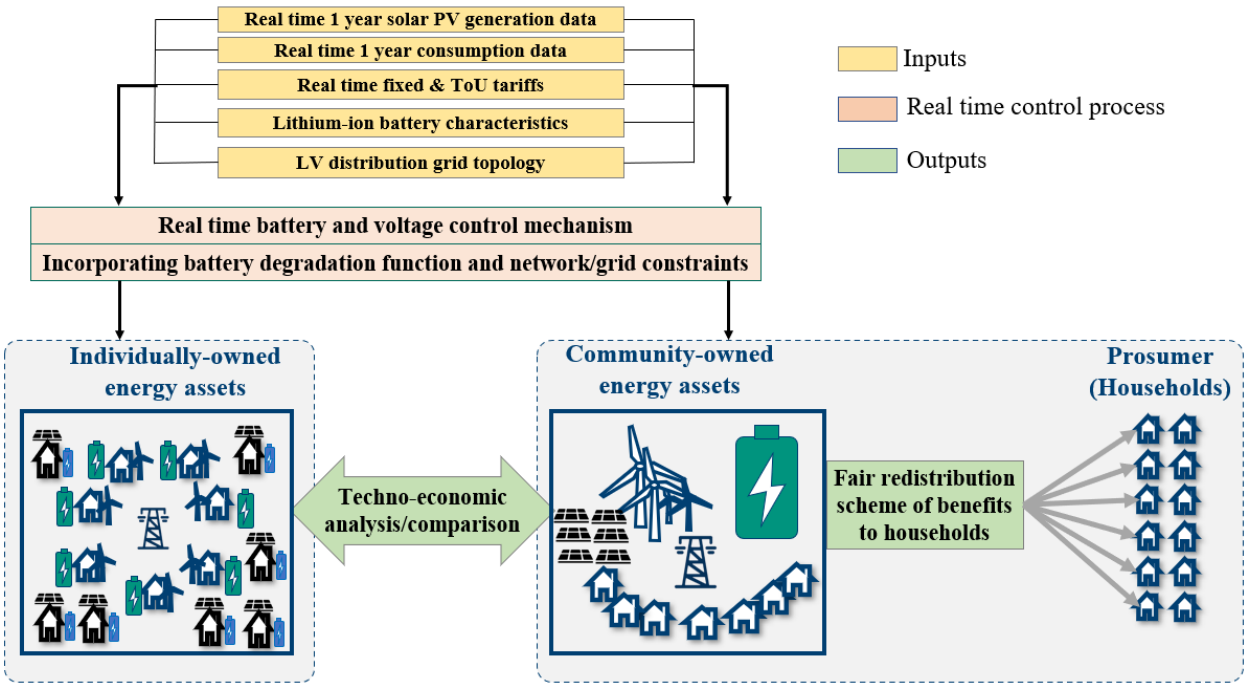

Figure 5.5: Overview of the energy community modeling approach incorporating the network constraints

Similar to the community settings (without network constraints) described in Chapter 4, the model input, tariff structures and unitary cost of energy assets described in Section 3.3 of Chapter 3 are used for analysis. In this setting, we consider prosumer or a community as a whole invest in a individually-owned distributed solar PV renewable generator along with a battery energy storage system as outlined shown in Figure 5.1, or invest in a jointly-owned community solar PV and community battery as shown in Figure 5.2. The cost of energy assets are assumed to be 150 £/kWh for the battery [225] and 1100 £/kW for solar PV [229] generation capacity. In this study, we chose to use an optimal size for both

individual assets and community assets that was obtained in Chapter 4. Results of the optimal assets sizing are shown in Table 4.3 for PV, and Table 4.5 for battery (that was obtained from battery integrated with solar PV renewable generator). An optimal size of PV or battery corresponds to the size that provides the minimal simple payback period.

The potential impacts of installing these various assets (with optimal capacities) on the grid, and the corresponding economic analysis is presented in the following section.

5.5 Comparison of yearly bills obtained from investment in distributed individually-owned assets with jointly-owned community energy assets with network constraints

As a reminder, the 13-bus grid model for the 200 households community with optimal capacity assets (as shown in Table 4.3 & 4.5) is shown in Fig. 5.1 & 5.2 as described in Section 5.2. Yearly bus voltages are computed every half-hour of the year by running power flow simulation over the network, with the given consumption and production profiles. Based on these voltage profiles, the impact of considering the grid on the profitability of DERs and battery energy storage system (BESS) is studied under various scenarios. The scenarios correspond to different assets installation schemes in the network. The yearly bills are computed under the various scenarios considering the network constraints, and then compared with the yearly bills computed without network constraints (as described in Chapter 4) in order to assess how grid constraints can impact the deployment of individual and community owned assets. Yearly bills are computed for both the fixed tariff of 16 pence/kWh using [222] and dynamic ToU Agile Octopus [224] tariff pricing schemes under various scenarios as presented in the following subsections.

5.5.1 Scenario 1: community without local renewable generation or battery assets (baseline scenario-no energy assets)

In this scenario, we only consider the demand of households, without any assets. This setting defines a *baseline scenario*, against which the other scenarios can be compared. The yearly bills with network constraints under this baseline scenario are computed for both the fixed and ToU tariffs, and compared with the yearly bills computed without network constraints. Table 5.1 shows the sum of individual agents annual bills and the community annual bill determined without any assets.

As described in Section 5.2, in the baseline scenario without any assets, the grid is not constrained as there is no voltage excursion nor cable overloading. Hence, the sum of individual annual bills and community annual bill are equal for both cases with and without network constraints. Furthermore, it can be observed that without assets, the community annual bill is equal to the sum of individual annual bills, which is expected as

Without assets (baseline)	With network constraint		Without network constraint	
	Fixed Tariff	ToU Tariff	Fixed Tariff	ToU Tariff
	Annual bill (£)	Annual bill (£)	Annual bill (£)	Annual bill (£)
Sum of individual agents yearly bills	134455	143923	134455	143923
Community yearly bill	134455	143923	134455	143923

Table 5.1: Economic comparison of individually-owned and community-owned assets under baseline scenario 1 (without assets) for both the fixed tariff of 16 pence/kWh [222] and dynamic Agile Octopus ToU tariff [224].

the community represents the aggregated demand profiles of the individual households, and there are no local renewable generation or battery storage assets.

5.5.2 Scenario 2: community with solar PV renewable generator asset only without battery

With only solar PV	With network constraint		Without network constraint	
	Fixed Tariff	ToU Tariff	Fixed Tariff	ToU Tariff
	Annual bill (£)	Annual bill (£)	Annual bill (£)	Annual bill (£)
Sum of individual agents yearly bills	122557	129589	122557	129589
Community yearly bill	119315	126371	117092	123154

Table 5.2: Economic comparison of individually-owned and community-owned assets under scenario 2 (PV only without battery) for both the fixed tariff of 16 pence/kWh [222] and dynamic Agile Octopus ToU tariff [224].

In this scenario, we consider the demand of households, with renewable generator asset only, without battery storage (in the experiments in this Chapter 5, the renewable generation is shared solar, but the model is general, hence this could also be a shared community wind turbine). The yearly bills with network constraints under this scenario are computed for both the fixed and ToU tariffs, and compared with the yearly bills computed without network constraints. Table 5.2 shows the sum of individual agents annual bills and community annual bill obtained under this scenario.

Figure 5.6 shows the yearly voltage distribution of the buses obtained for the network with individually distributed optimal solar PV's. Additionally, Figure 5.7 illustrates the yearly voltage profile of the most adversely impacted Bus-9. Here, it can be observed

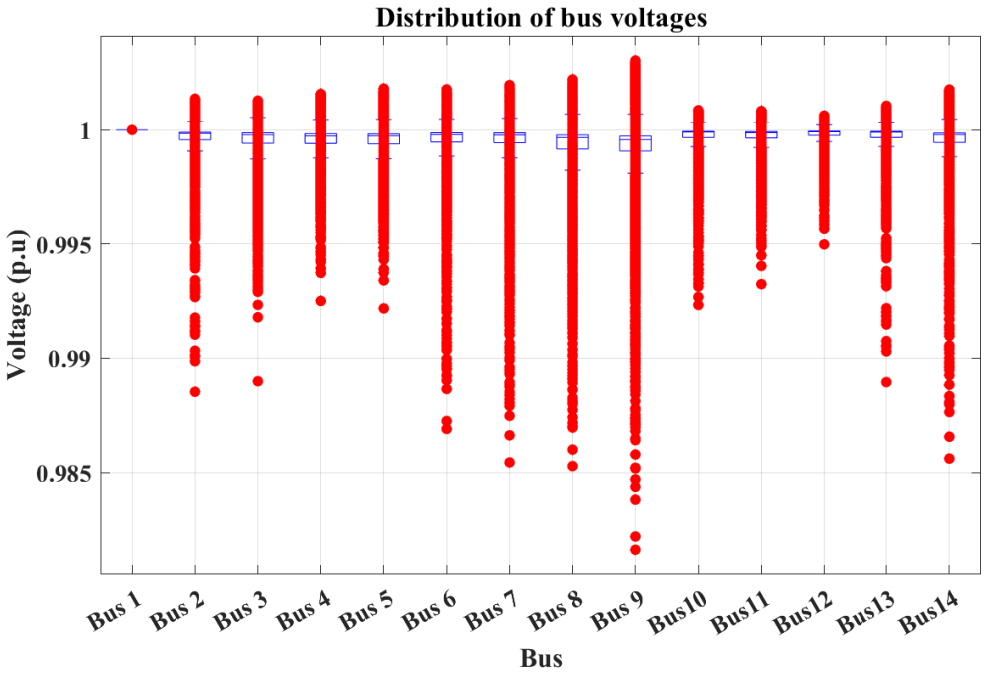

Figure 5.6: Yearly voltage distribution of the buses for the network with individually-owned optimal PV's without battery.

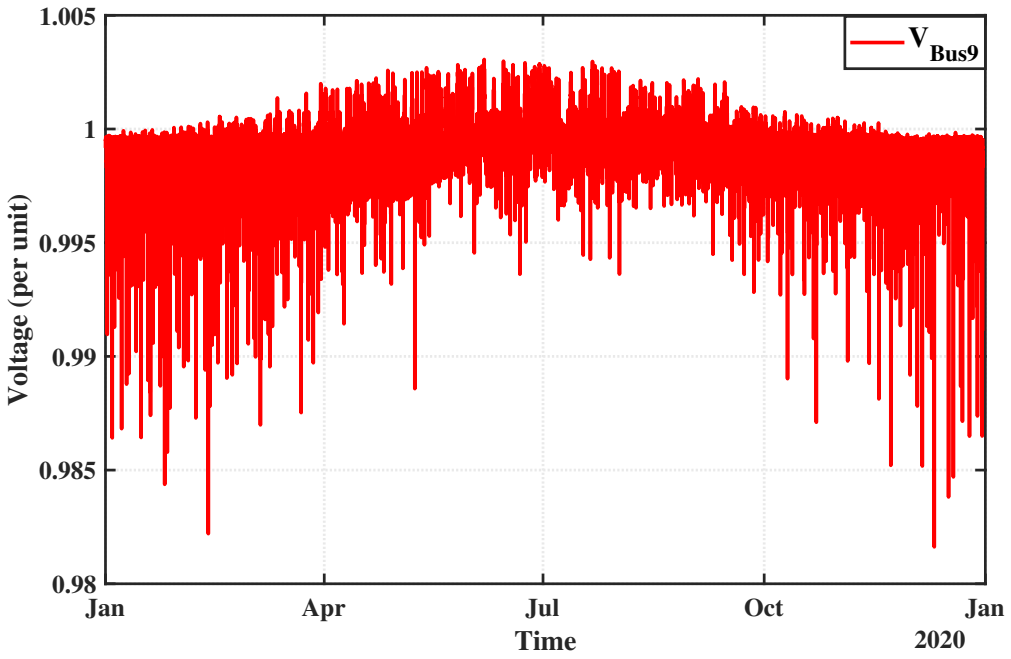

Figure 5.7: Yearly voltage profile of Bus-9 for the network with individually-owned optimal PV's without battery.

that there is a rise in voltage during the summer months due to high power production from solar PV, whereas voltages reduces during the winter months. However, the rise in the voltage is within the permissible limits. similarly, the voltage distribution of the remaining buses exhibits a consistent pattern, as depicted in Figure 5.6. Furthermore, it can be observed that the voltage distribution of Bus 1 is constantly at 1 p.u, this is expected as Bus 1 represents the slack bus the main connection to the transmission grid, and it voltage

is set to reference volatge of 1 p.u with the base voltage of 236 V. Hence, the exports from individual PV's are not curtailed. Thus, the sum of individual yearly bills computed with network constraints and without network constraints are equal (as shown in Table 5.2).

In contrast to the scenario with individually distributed assets, Figure 5.8 presents the yearly voltage distribution of the buses obtained for the network with centrally located community-owned, optimally-sized solar PV systems, assuming no curtailment by the grid. Furthermore, Figure 5.9 shows the yearly voltage profile of Bus-2, which is one of the most affected buses in this configuration.

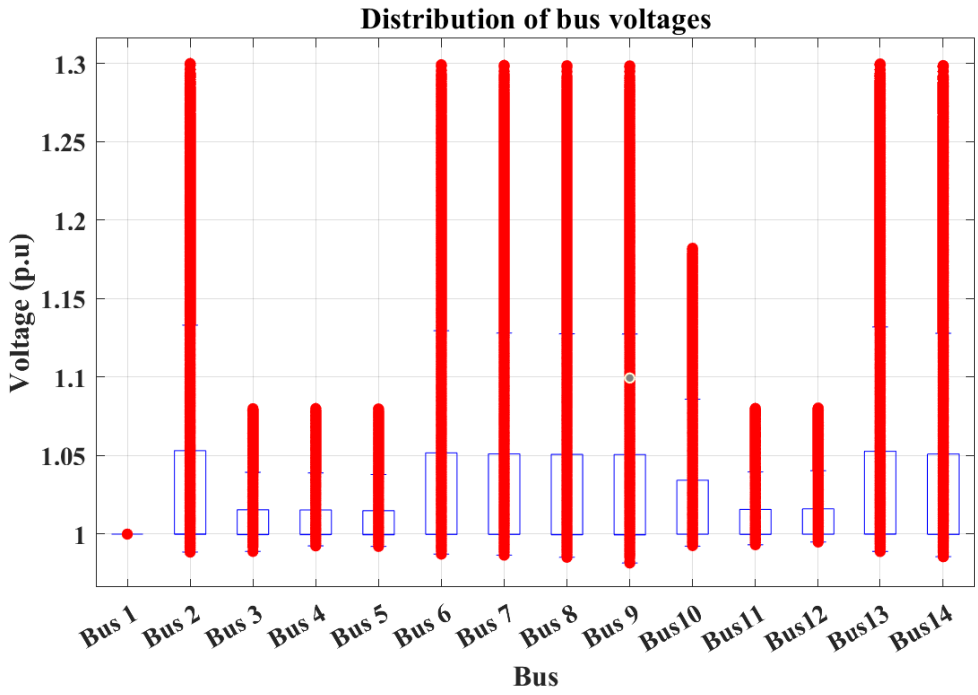

Figure 5.8: Yearly voltage distribution of the buses for the network with community-owned optimal PV only without voltage control mechanism.

Upon analysing Figure 5.8 and Figure 5.9, an important observation emerges. In the absence of control from the grid operator, it is evident that the bus voltages exceed the highest permissible limit of 1.1 per unit (p.u) ($0.94 \leq V^{\text{bus}} \leq 1.1$ p.u). This indicates that without grid intervention, the voltage levels at Bus-2, as well as other buses, rise beyond the acceptable range.

In practice, the grid operator would not allow such voltage excursions, and may curtail assets exporting too much power. In this case, the grid will curtail the community-owned asset every-time the voltage rise above 1.1 p.u. Figure 5.10 shows the yearly voltage distribution of the buses after implementing the voltage control mechanism by grid operator as described in Section 5.3.

This curtailment reduces the financial benefits offered by the community-owned solar PV. It can be observed in Table 5.2 that when the network constraints is considered the community annual bill increases by £2223 for flat tariff and by £3217 for ToU tariff compare to the case without network constraints. Thus, the overall saving of the energy community is reduced when grid operations are considered.

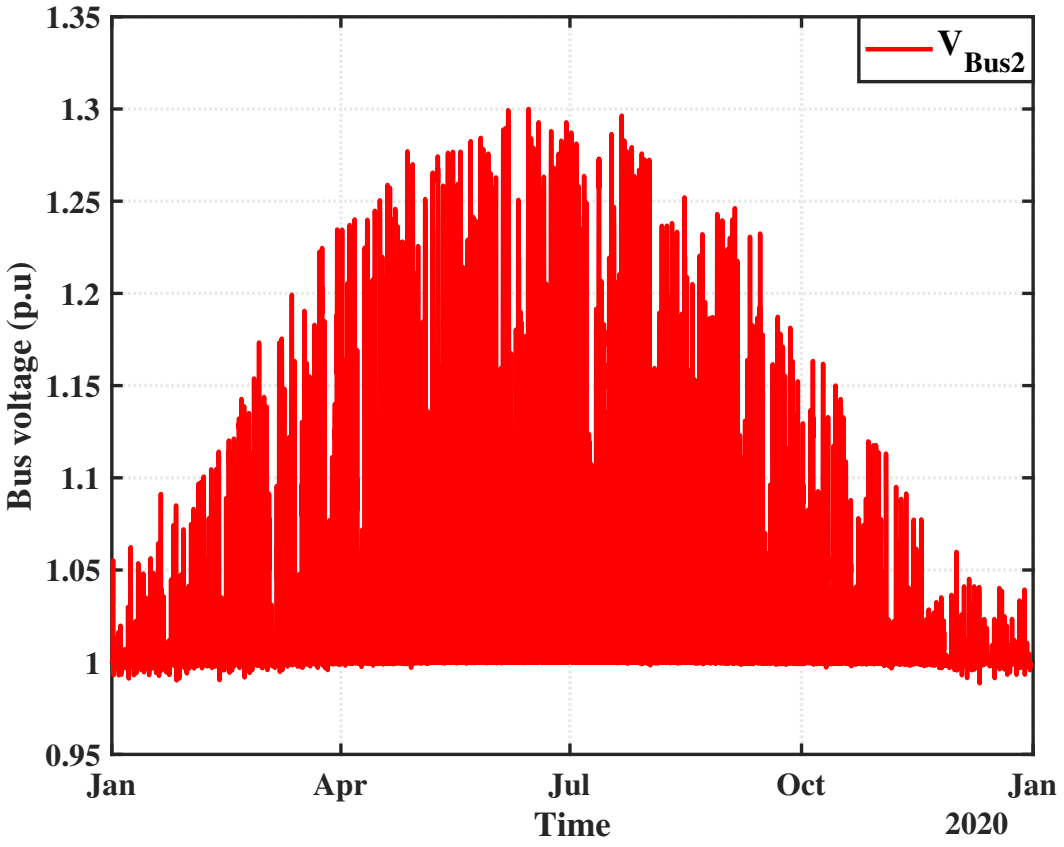

Figure 5.9: Yearly voltage profile of Bus-2 for the network with community-owned optimal PV only without voltage control mechanism.

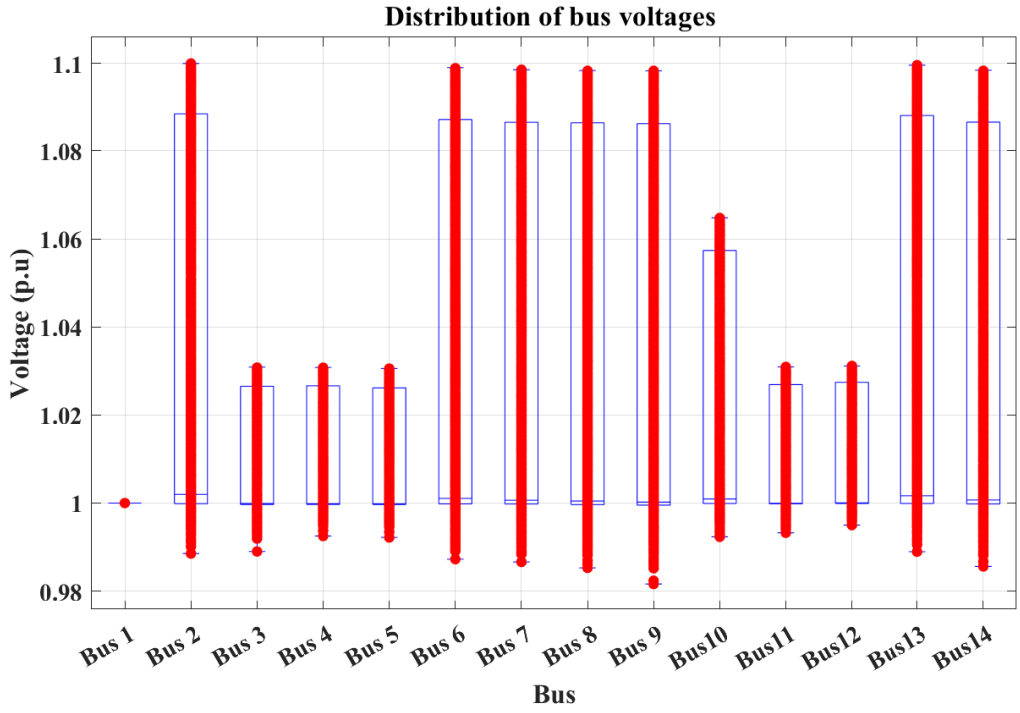

Figure 5.10: Yearly voltage distribution of the buses for the network with community-owned optimal PV only after implementing the voltage control mechanism.

5.5.3 Scenario 3: community with both solar PV renewable generator and battery storage assets

In this scenario, we consider the demand of households, with both renewable generator and the battery storage assets. The yearly bills with network constraints under this scenario are computed for both the fixed and ToU tariffs, and compared with the yearly bills computed without network constraints. Table 5.3 shows the sum of individual agents annual bills and community annual bill obtained under this scenario.

With both solar PV and battery	With network constraint		Without network constraint	
	Fixed Tariff	ToU Tariff	Fixed Tariff	ToU Tariff
	Annual bill (£)	Annual bill (£)	Annual bill (£)	Annual bill (£)
Sum of individual agents yearly bills	118488	122419	118488	122419
Community yearly bill	115664	121326	113790	117307

Table 5.3: Economic comparison of individually-owned and community-owned assets under scenario 3 for both the fixed tariff of 16 pence/kWh [222] and dynamic Agile Octopus ToU tariff [224].

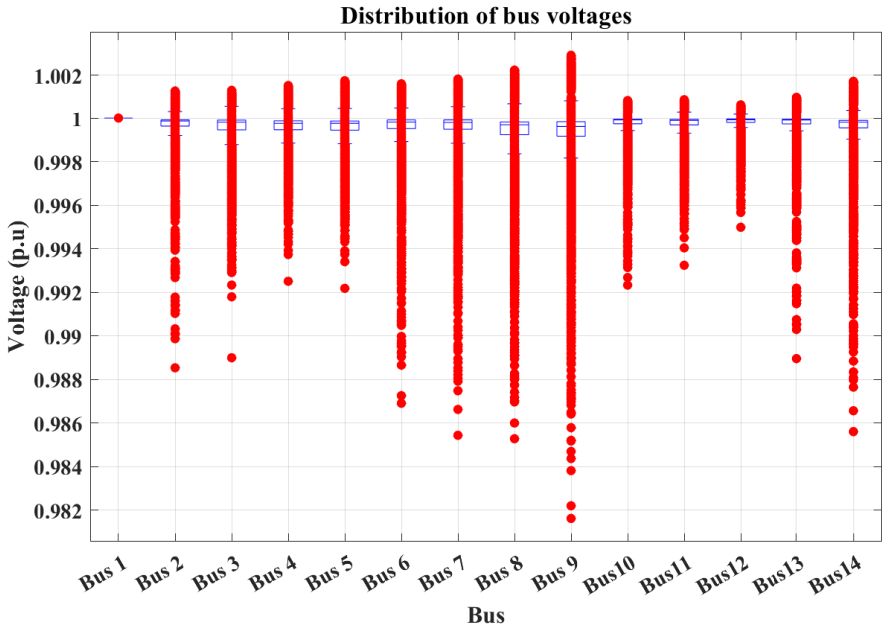

Figure 5.11: Yearly voltage distribution of the buses for the scenario with individually-owned optimal PV's and optimal batteries.

Figure 5.11 shows the yearly voltage distribution of the buses obtained for the network with individually distributed optimal solar PV's and optimal batteries. Additionally, Figure 5.12 depicts the yearly voltage profile of the most adversely impacted Bus-9. Similar to scenario 2, one can observe the rise in the bus voltages, and the seasonal effects in the

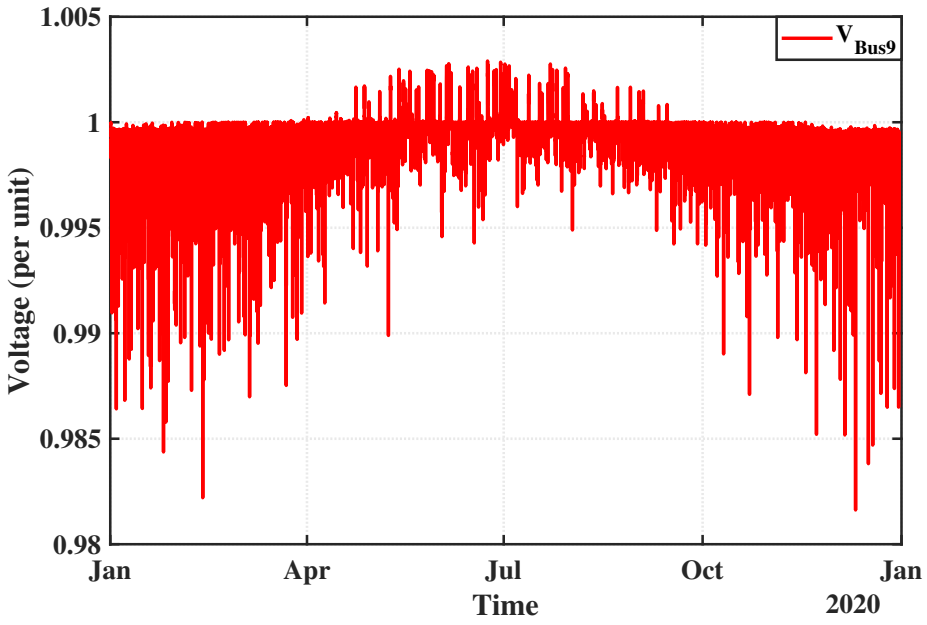

Figure 5.12: Yearly voltage profile of Bus-9 for the network with individually-owned optimal PV's and optimal batteries.

voltage profiles. In this scenario also, the rise in the voltages are within the permissible limits. As the voltages are within the thresholds, the grid is not constrained, hence the exports from the individual PV's and export/import from/to individual batteries are not curtailed. Thus, the sum of individual yearly bills computed with network constraints and without network constraints are equal as the grid is not constrained when both the individual PV's and batteries are installed (as shown in Table 5.3).

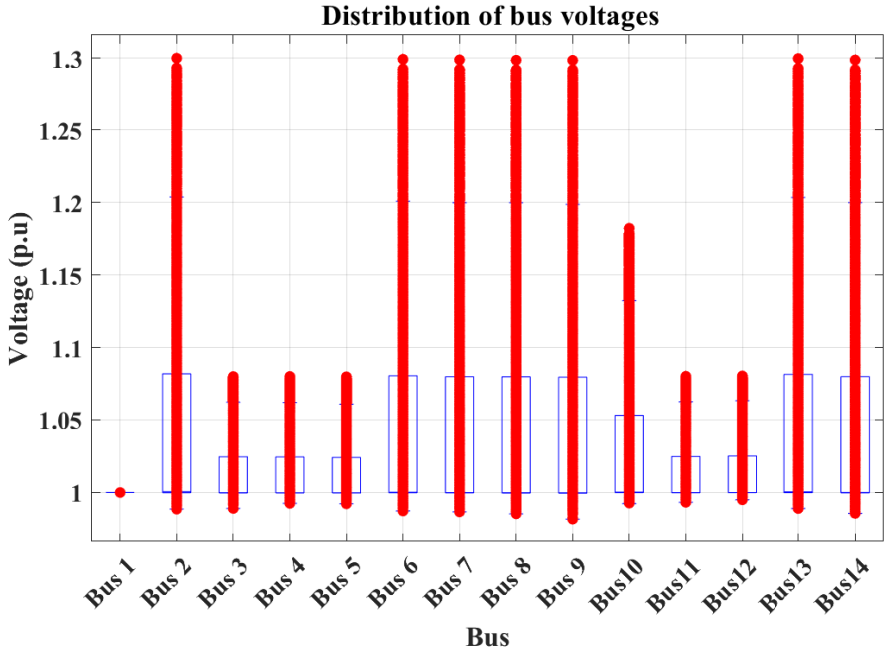

Figure 5.13: Yearly voltage distribution of the buses for the network with community-owned optimal PV and optimal battery assets without voltage control mechanism.

In the case with community-owned optimal PV and optimal battery, Figure 5.13 shows the yearly voltage distribution of the buses obtained for the network without implementing the voltage control mechanism. Furthermore, Figure 5.14 shows the yearly voltage profile of Bus-2, which is one of the most buses significantly impacted by voltage excursions caused by community-owed assets. Similar to the Scenario 2 with community PV only, the bus voltages rise above the 1.1 p.u the highest permissible limit.

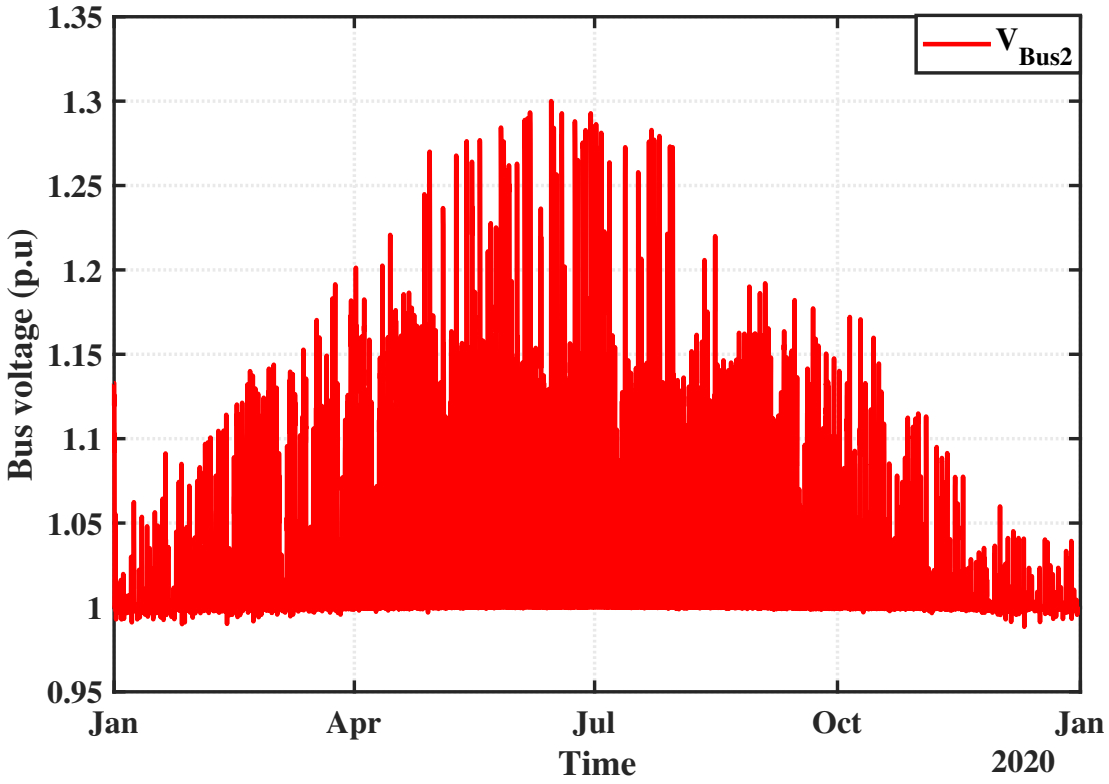

Figure 5.14: Yearly voltage profile of Bus-2 for the network with community-owned optimal PV and community battery without voltage control mechanism.

In such case, the grid operator will control the voltage by curtailing the export/import from/to community-owned assets as described in Section 5.3. Figure 5.15 shows the voltage profile of the buses after implementing the voltage control mechanism. This curtailment reduces the overall saving of the community. This effect can be observed in Table 5.3 , where the annual bill with network constraints is increased by £1874 for flat tariff and £4019 for ToU tariff as compared to yearly bill computed without network constraints.

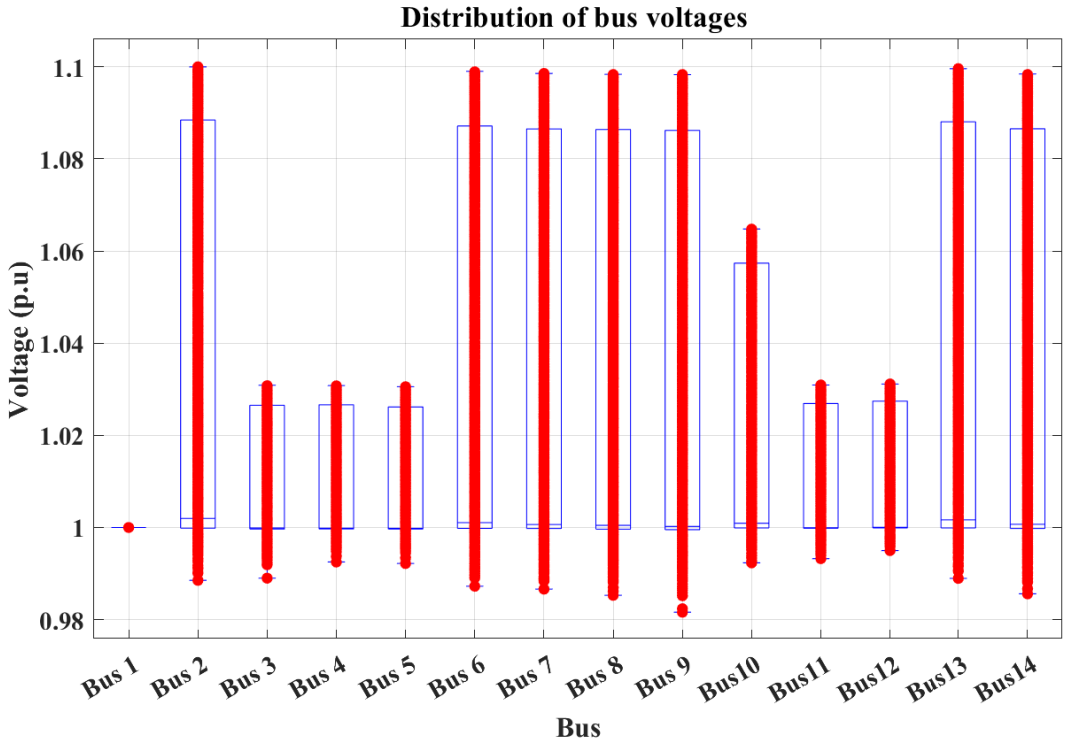

Figure 5.15: Yearly voltage distribution of the buses for the network with community-owned optimal PV and optimal battery after implementing the voltage control mechanism.

5.5.4 Discussion of results

Overall, for the community with individually-owned assets, the bus voltages remains within permissible limits. As the voltages are within the thresholds, export/import from/to the assets are not curtailed, and the bills in the scenarios with and without network constraints are identical.

Figure 5.8 and 5.13 show that there are voltage excursions in the grid when the community-owned assets are installed. In such case, the grid operator may curtail assets exporting/importing too much power. Hence, the community-owned assets gets curtailed every-time the voltage rise above 1.1 p.u. It is important to note that the voltage at bus 2 the location of community-owned PV and battery is not controlled. As shown in the Figure 5.2, the community-owned PV and battery are connected to bus 2 which makes the power export being concentrated at one location, thus with the community-owned assets the voltage rises more than in the scenario with individually-owned assets. Whenever the voltage rises above the permissible limit then the exports from PV and exports/imports from/to battery are curtailed until the voltage is within the threshold. In order to illustrate this curtailment effect, the yearly generation from community-owned solar PV with and without voltage control mechanism is shown in Figure 5.16.

Overall, we observe that, there is significant reduction in the production from community-owned PV because of curtailment due to voltage constraints. This reduces the financial benefits offered by the community-owned assets and limits the assets that can be further included in the network. Hence, the study shows that when the network (grid) constraints are incorporated then the benefits from the community assets are reduced. Therefore, when

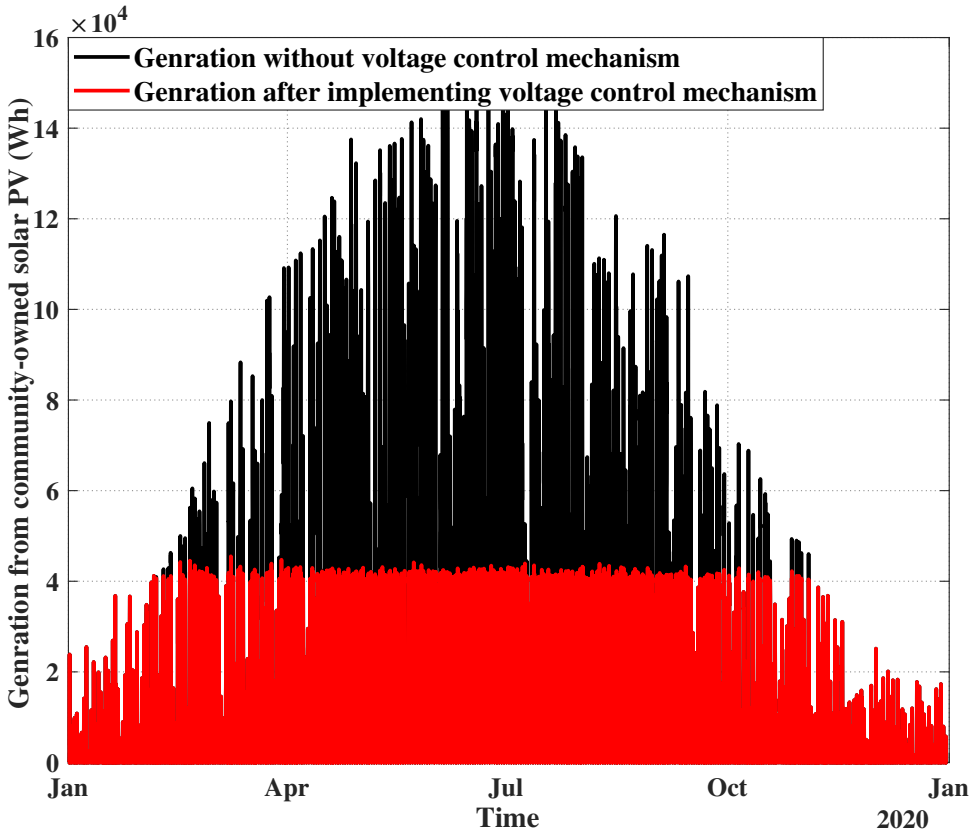

Figure 5.16: Yearly generation from community-owned solar PV with and without voltage control mechanism.

considering community assets, one should pay attention to the location of the assets and nature of the distribution grid considered. If the community assets are placed in a location where there is no grid issue, then there is a higher benefit.

While considering the network constraints, even though the benefits from the community-owned assets are reduced due to curtailment, still community-owned assets provide a substantially lower annual bill for both the fixed tariff and ToU tariff pricing schemes (as shown in Table 5.2 & 5.3). Furthermore, these economic results were obtained with the same unitary cost of the assets for the community-owned as for individually-owned, which might not be the case in real-world scenario, whereas in practice, the unitary cost of the community-owned asset might be lower due to economies of the scale effect. Thus, more savings can be obtained from community-owned assets by considering the economies of scale in the unitary cost of the assets. Therefore, community assets generate benefits to the community.

A key research question that still remains is how to redistribute fairly these benefits to the community members. There is still a considerable gap in both existing research and practice regarding what are the optimal and fair methods to redistribute the energy outputs (and hence financial benefits) from the jointly community-owned assets to their members, while incorporating the asset's degradation, and the physical network and operational constraints. This will be addressed next, in Section 5.6.

5.6 Fair redistribution of benefits achieved from community shared assets

For both the cases with and without network constraints, results from the economic analysis described in Section 5.5 show that community-owned assets lead to reduction in the annual electricity bill compared to individually-owned assets. Hence, individual agents can achieve more savings (higher benefits) by forming the community coalition and by investing in jointly-owned community assets.

In the case of community owned assets, the revenues generated by the community-owned distributed generation system (PV and battery) can be distributed to the members of the community. However, this raises the key research question of how to fairly redistribute the energy outputs (and hence the financial benefits) from the community-owned assets to the individual members of the community. Moreover, most of existing redistribution frameworks are developed without considering network constraints, in which case the computation cost becomes even more challenging. To address this computational challenge, we propose in this chapter a more computationally tractable (and hence more practically applicable) redistribution mechanism based on the marginal contribution of each agent (in our case household) of the community. We incorporate power flow (physical network/grid constraints), and physical battery degradation into community energy optimization models, including the effect of network constraints on redistribution schemes. To achieve this, we employ a battery state of health degradation model based on the battery depth of discharge in each control cycle, while maintaining the bus voltages within the permissible limits. This represents a considerable extension of prior work on redistribution mechanism (denoted as Method 1) to fairly redistribute the benefits from the community-owned assets presented in Chapter 4. Furthermore, in order to test the advantages of the proposed redistribution mechanism with network constraints, it is compared with the various state-of-the-art redistribution methods (Method 2, 3, & 4 presented in Chapter 4). We begin by describing the proposed marginal cost redistribution mechanism with network constraints in the following subsections.

5.6.1 Mechanism for a fair redistribution

A redistribution method without considering the network constraints was described in Section 4.4 of the previous Chapter 4. The proposed redistribution mechanism is based on the marginal contribution of each agent, a key concept in cooperative game theory. The marginal contribution $\Theta_i(T)$ of an agent i for the period T represents the difference that an agent makes to the value of a given coalition in the community. Specifically, the marginal contribution $\Theta_i(T)$ is a metric that assess how much each agent i contributes to the reduction of the energy bill of the community as a whole.

As a reminder, a marginal cost redistribution method (presented in previous Chapter 4) is again described in this section. Then, the proposed marginal cost redistribution method incorporating the network constraints is described in detail. Savings of the community

after one year ($T = 1$ year), noted as $\Pi_C(T)$, are defined by the difference between the sum of all agents annual bills before the community assets were installed (which corresponds to the baseline scenario without assets as shown in Table 4.1), and $b_C(T)$ i.e. the energy bill for the whole community after one year with community-owned assets. Hence, the community savings over time period T correspond to the bill reduction for the whole community over that period, as shown below:

$$\Pi_C(T) = \sum_{i=1}^{N} b_i^0(T) - b_C(T) \tag{5.24}$$

where $b_i^0(T)$ is the baseline bill (bill without assets) for prosumer i before any asset was installed. In order to compute a fair redistribution of the community savings among the individual agents, the contribution $\Theta_i(T)$ of each agent to these community savings is computed. To compute the marginal contribution of an agent i, we remove agent i from the community of 200 agents (total community), and recompute the community savings of this virtual community of 199 agents (reduced community). The *marginal contribution* $\Theta_i(T)$ of agent i is defined as the difference between the total community savings $\Pi_C(T)$ and the savings of the reduced community $\Pi_{C\setminus\{i\}}(T)$, as shown below:

$$\Theta_i(T) = \Pi_C(T) - \Pi_{C\setminus\{i\}}(T) \quad \forall i \in C \tag{5.25}$$

where C is the community of 200 households. Once the marginal contribution $\Theta_i(T)$ is computed for all the agents, we distribute community savings $\Pi_C(T)$ among the individual agents based on the following equation:

$$\Gamma_i(T) = \Pi_C(T)\frac{\Theta_i(T)}{\sum_{i\in C}\Theta_i(T)} \quad \forall i \in C \tag{5.26}$$

where $\Gamma_i(T)$ is the amount of money redistributed to agent i after period T.

Hence, the new bill of agent i for the time period T, noted $b_i^*(T)$ can be computed as follows:

$$b_i^*(T) = b_i^0(T) - \Gamma_i(T) \quad \forall i \in C \tag{5.27}$$

The computation of the marginal cost redistribution method in a setup that considers network constraints is computationally expensive as it requires to recompute the marginal contribution of every agent, which requires power-flow computation for every time step of the considered period (e.g. one year). Hence, for larger network, the redistribution mechanism by marginal cost redistribution method may not be computationally tractable.

To address this computational challenge while considering the network constraints, we propose an *approximation method*. First, we compute the agents i new bill $b_i^{*(\neg)}(T)$ for the case without network constraints using the Eq. (5.27) as expressed in Eq. (5.28):

$$b_i^{*(\neg)}(T) = b_i^0(T) - \Gamma_i(T) \quad \forall i \in C \tag{5.28}$$

Then, we compute the difference between community yearly bill *with network constraints* ($b_C^{\mathrm{NC}}(T)$) and community yearly bill *without network constraint* ($b_C^{\neg}(T)$). Finally, the equal part of the computed difference in the bill is distributed equally among the agents by adding to the new bill $b_i^{*(\neg)}(T)$ obtained using Eq. (5.28). Finally, the new bill of agent i with network constraints ($b_i^{*(\mathrm{NC})}(T)$) is determined as expressed in Eq. (5.29).

$$b_i^{*(\mathrm{NC})}(T) = b_i^{*(\neg)}(T) + \frac{b_C^{\mathrm{diff}}}{N} \tag{5.29}$$

where $N = 200$ agents (households) in our case. b_C^{diff} is the difference between community yearly bill considering network constraints and community yearly bill without network constraints as expressed in Eq. (5.30).

$$b_C^{\mathrm{diff}} = b_C^{\mathrm{NC}}(T) - b_C^{\neg}(T) \tag{5.30}$$

To test the advantages of the proposed marginal cost redistribution method with network constraints, we compare its benefits with the various state-of-the-art redistribution Methods 2, 3 and 4 described in Section 4.4.2 of Chapter 4. On comparison, the proposed marginal cost redistribution method with network constraints and the Method 2 the instantaneous power redistribution method (with network constraints) was able to achieve lowest bill for the whole community, and thus the greatest savings for almost every agent. Hence, the proposed redistribution mechanism is only compared with the Method 2 the state-of-the-art instantaneous power redistribution method [240]. In this method, an instantaneous PV power $g_C^{\mathrm{PV}}(t)$ produced by community-owned PV generator is distributed among individual agents based on their instantaneous demand $d_i(t)$. In other words, the PV power allocated to agent i at each time step is determined as:

$$g_i^{\mathrm{PV}}(t) = g_C^{\mathrm{PV}}(t) \times \frac{d_i(t)}{\sum_{i \in C} d_i(t)} \tag{5.31}$$

Then, the new bill of each agent i is computed using Eq. (5.22). First, we implement for the case with community-owned generator only, without storage asset. Then, redistribution of cost savings from both the community-owned generator and storage is implemented.

5.6.2 Implementation for a community with solar PV only

The investment cost of community PV was assumed to be shared equally among the agents, but the revenues are not equally distributed. As described in Section 5.6.1, using Eq. (5.29) the new yearly energy bills ($b_i^{*(\mathrm{NC})}(T)$) of individual agents after redistribution of community savings from a community-owned solar PV is computed by marginal cost redistribution method with network constraints. This method is the approximated version that is computationally tractable. The new yearly bills obtained using approximated marginal cost redistribution method are compared with the new yearly bills obtained using marginal cost redistribution method without approximation. The comparison between the redistribution mechanism *with approximation* and *without approximation* is shown in Figure 5.17 for the fixed tariff [222] and Figure 5.18 for the dynamic ToU Tariff [224].

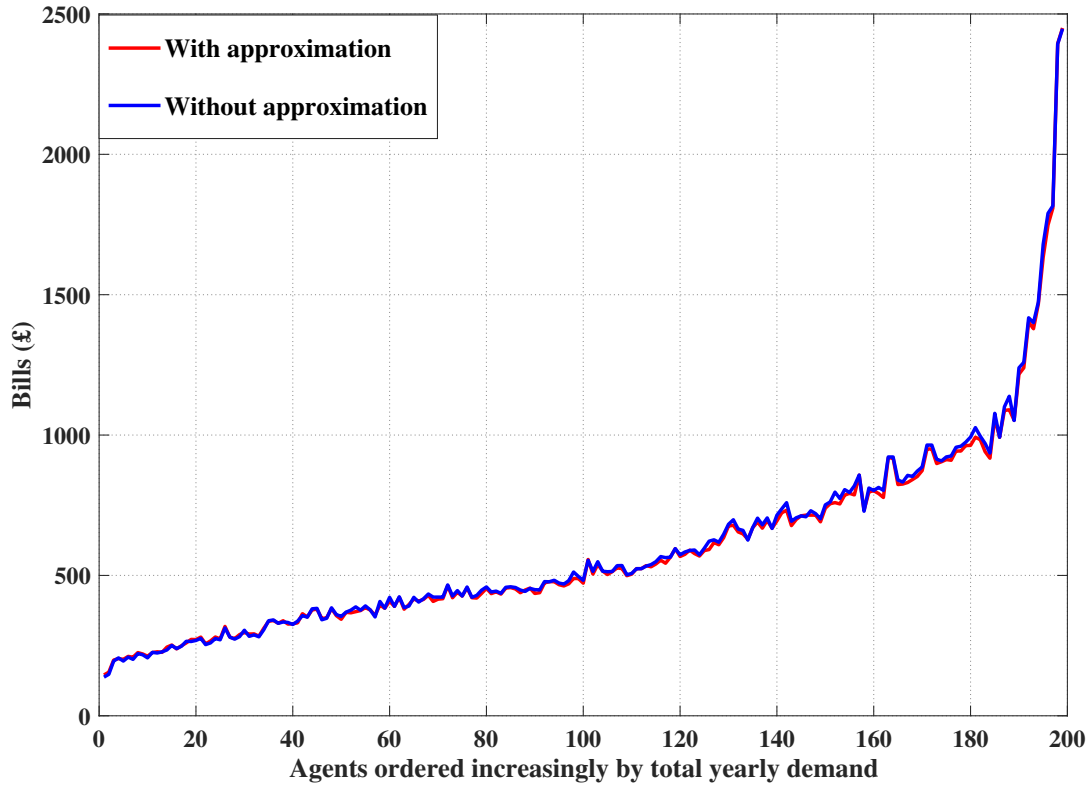

Figure 5.17: Comparison between the individual agents yearly bills obtained after redistribution by approximated marginal cost redistribution method with redistribution mechanism without approximation for a fixed tariff of 16 pence/kWh [222].

For fixed tariff, the individual agents yearly bills obtained after redistribution by approximated marginal cost redistribution method is similar to results obtained by redistribution mechanism without approximation, with the correlation coefficient of 99.99% (as shown by Figure 5.17). Similarly, for dynamic ToU tariff the results are similar with the correlation coefficient of 99.98% (as shown by Figure 5.18). Hence, while considering the network constraints, approximated marginal cost redistribution method can be used to redistribute the benefits from community owned assets, as it is much more computationally tractable. In Figure 5.17 & 5.18 , on the X-axis we order the 200 agents (households) of the considered

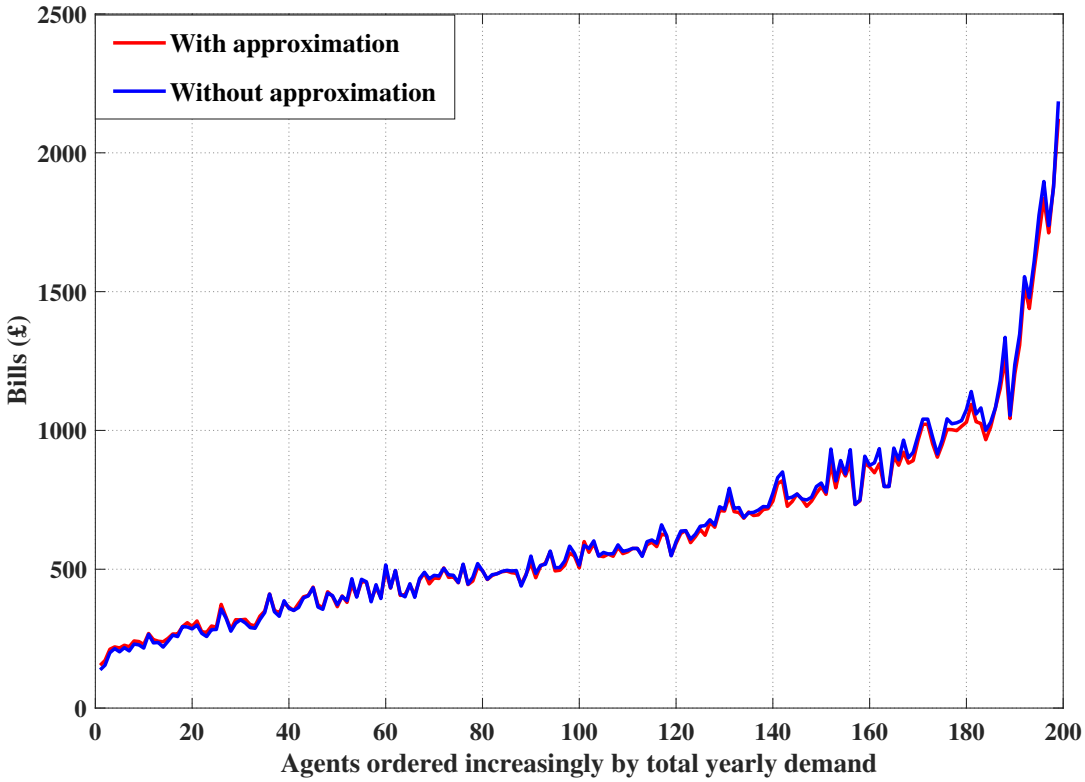

Figure 5.18: Comparison between the individual agents yearly bills obtained after redistribution by approximated marginal cost redistribution method with redistribution mechanism without approximation for the dynamic ToU Agile Octopus tariff [224].

community in increasing order by their total annual energy consumption. The Y-axis gives the annual energy bill of each agent. This representation is useful to evaluate the economic fairness in the redistribution scheme among the small and larger consumers.

In order to test the advantages of the proposed redistribution mechanism the marginal cost redistribution method with network constraints, we compare its benefits with the instantaneous power redistribution method that was described in Section 5.6.1 which corresponds to the state-of-the-art redistribution mechanism (based on current practice).

Figure 5.19 shows the individual agents annual bills after redistribution by marginal cost redistribution method and instantaneous power redistribution method in the case of the dynamic ToU Agile Octopus [224] tariff pricing scheme.

Similar to the case with the community settings without network constraints (as presented in Chapter 4), the crossover point between the redistributed bill curves in Figure 5.19 clearly shows that, with marginal cost redistribution method 67% of the agents can achieve lower annual bill than instantaneous power redistribution method (these are the lower total annual bill, hence smaller consumers), while with state-of-the-art method only 33% of the agents obtain lower annual bills (hence this scheme benefits mainly larger consumers, with larger annual demand). Hence, under the proposed marginal cost redistribution method with network constraints, more agents are able to decrease their annual bill than the instantaneous power redistribution method with network constraints.

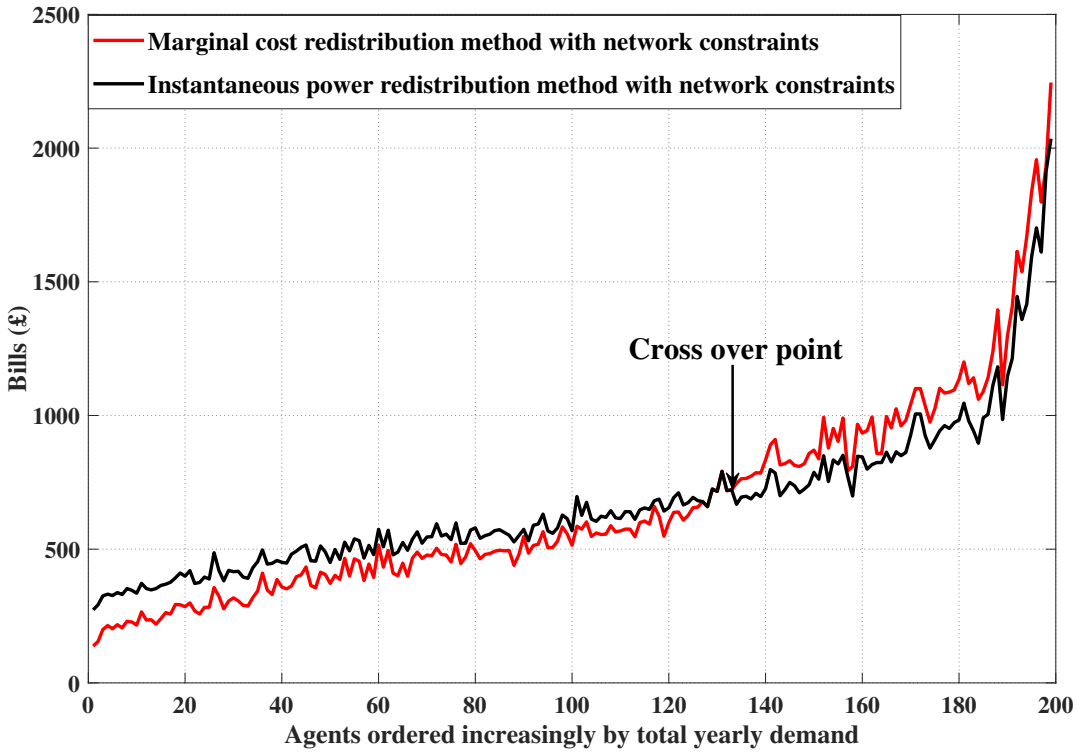

Figure 5.19: Individual agents yearly bills after redistribution by marginal cost redistribution method and instantaneous power redistribution method, with network constraints for the dynamic ToU Agile Octopus tariff [224].

While it is true that large consumers benefit slightly less under our scheme (because, of course, the total community bill is equal in both cases), these agents with higher demand profiles are the agents who already obtain the highest bill reduction as compared to agents with lower demand profiles as illustrated in the Figure 5.20. Therefore, the proposed redistribution mechanism achieves a fairer redistribution as compared to currently practised redistribution scheme. Practically, having the 67% of agents in the community (including many smaller consumers) also benefiting from the proposed redistribution mechanism would lead to greater social acceptance, and hence more likely to join the coalition to invest in the jointly-owned community assets.

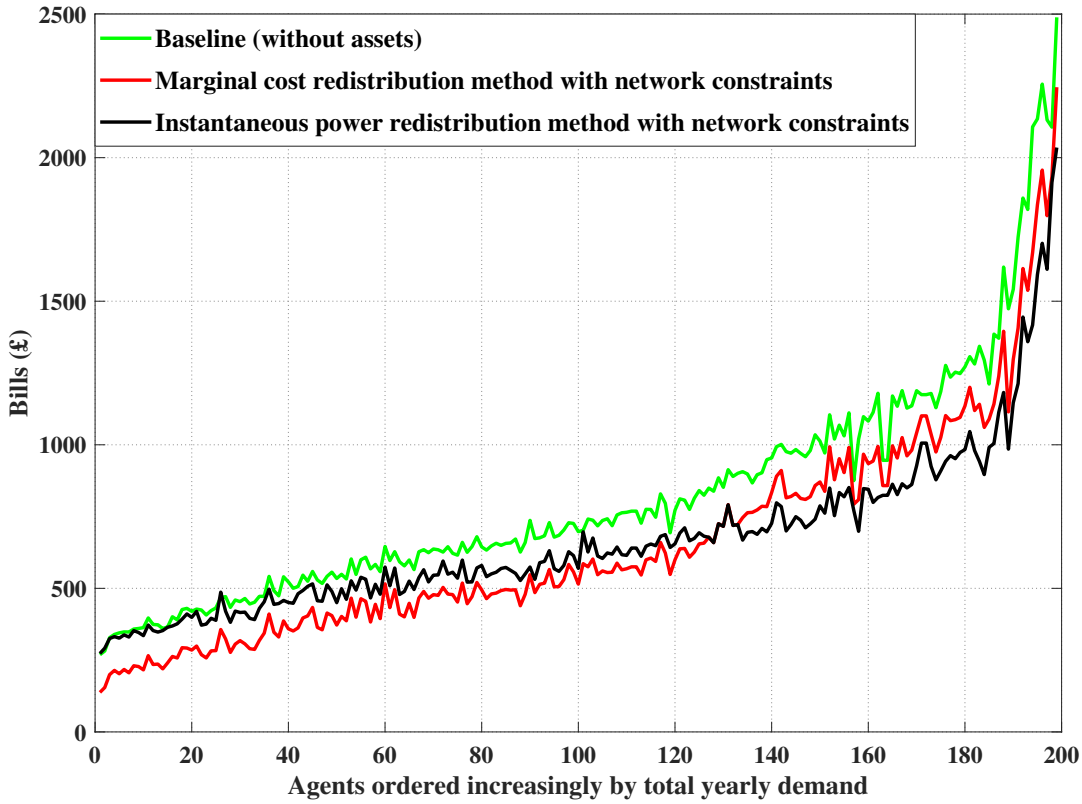

Figure 5.20: Individual agents yearly bills without assets (baseline), and yearly bills after redistribution by marginal cost redistribution method and instantaneous power redistribution method, with network constraints for the dynamic ToU Agile Octopus tariff [224].

5.6.3 Implementation for a community with solar PV and battery

In this scenario, the savings (benefits) achieved from both the community-owned solar PV and community-owned battery are redistributed by marginal cost redistribution method with network constraints only. Investment costs for the community energy assets were shared equally among the agents. Figure 5.21 shows the individual agents annual bills after redistribution in the case of the dynamic ToU Agile Octopus [224] tariff pricing scheme.

In the literature, the instantaneous power redistribution method is only used for solar power or wind, but it cannot be used for communities with batteries, as it is not easy to determine who used more the battery assets than others. This is another key point that demonstrates the advantages of the proposed redistribution mechanism based on marginal contribution. Yet, there is still a need to redistribute fairly the benefits obtained from jointly-owned community renewable generator and storage assets.

Hence, the proposed marginal cost redistribution method based on individual agents marginal contribution provides the equal and fair mechanism to redistribute the energy outputs (and hence financial benefits) from both the jointly-owned community solar PV and battery assets.

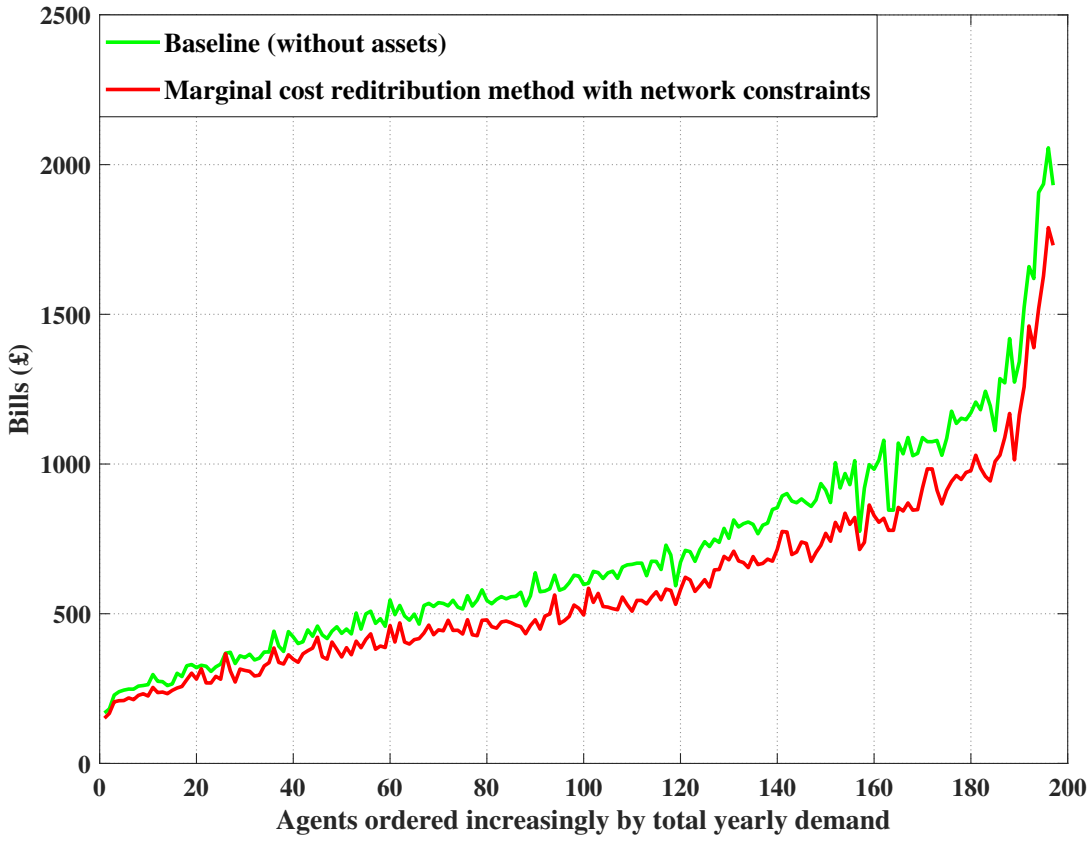

Figure 5.21: Individual agents yearly bills without assets (baseline) and yearly bills after redistribution by marginal cost redistribution method with network constraints for the dynamic ToU Agile Octopus tariff [224].

5.6.4 Discussion of results

In this section, we have proposed a novel algorithm to fairly redistribute among community members the benefits obtained from community owned assets. We have proposed an efficient and fair redistribution mechanisms that applies to both community-owned renewable generator and storage assets, while incorporating the asset's degradation, and the physical network and operational constraints.

In this chapter, we proposed a marginal cost redistribution method with network constraints. This method is the approximated version that is computationally tractable. The new yearly bills obtained using approximated marginal cost redistribution method are compared with the new yearly bills obtained using marginal cost redistribution method without approximation. The comparative study between the redistribution mechanism with approximation and without approximation clearly shows that the results are similar with an correlation coefficient of 99.99% for fixed tariff and 99.98% for dynamic ToU tariff (as shown in Figure 5.17 & 5.18). Hence, while considering the network constraints, approximated marginal cost redistribution method can be used to redistribute the benefits from community owned assets, as it is much more computationally tractable and more scalable. Thus, marginal cost redistribution with network constraints is more practically

applicable with respect to modelling the economic sharing of joint assets in community energy systems.

Moreover, to test the advantageous and to evaluate the economic fairness in the redistribution scheme, the proposed marginal cost redistribution method with network constraints is compared with the current state-of-the-art redistribution methods. Result from this comparative study shows that proposed marginal cost redistribution method yields to a greater reduction of the annual bill for 67% of the community households compared state-of-the-art methods (as shown in the Figure 5.19). Large consumers benefit slightly less under this scheme, but they still obtain the highest bill reduction in value as compared to households with lower demand profiles (as illustrated in the Figure 5.20). Therefore, the proposed redistribution mechanism achieves a fairer redistribution leading to greater social acceptance, key to incentivise more communities to form coalitions and invest in jointly-owned renewable energy assets.

Furthermore, all the available state-of-the-art redistribution methods applicable for jointly-owned community renewable generators only. Current energy communities usually employ algorithms based on proportionality of consumption to redistribute the benefits from the community-owned generator assets. However, such methods are not fair, and not applicable in the case of jointly-owned battery energy storage assets, where the proportionality of the asset usage does not apply as there is no clear method to split the power from the battery. Hence, the proposed redistribution method based on marginal contribution provides an equal and fair redistribution mechanism to distribute savings from both the community-owned renewable generator and community storage such and community-owned battery. This is another key point that demonstrates the advantages of the proposed redistribution mechanism based on the marginal contribution.

5.7 Concluding remarks

In this Chapter 5, we have proposed a techno-economic modeling methodology that couple's battery control, battery degradation, community energy from RES with LV network operating constraints, with a fair redistribution optimisation of benefits to jointly owned assets. The control mechanism was implemented for both fixed electricity tariffs and dynamic ToU tariffs to compare the benefits obtained when an individual household invest in their own energy assets versus investing jointly in a community-owned energy assets. To compare the economic performance of investments in community-owned assets and individually-owned assets, we considered an energy community of two hundred prosumers, that were all modelled by real time-series data of generation and consumption profiles from a community in UK for a full year. We computed yearly bills resulting from the proposed battery control algorithm and compared the yearly bills computed with and without network constraints to assess how network/grid constraints can impact the deployment of individual and community-owned assets.

Experimental results from our study (based on real input data from the UK) show that, overall, the operation of individually-owned distributed assets are less impacted by grid

constraints than the operation of community-owned assets. Indeed, when generation is not located close enough to consumption, it might lead to local over-voltage that could result in curtailment by the distribution system operator of export from community-owned assets. This curtailment reduces the overall saving of the community, which illustrates the importance of considering the physical grid constraints in the energy community schemes. However, even with curtailment due to grid constraints, the economic comparison between community-owned assets and individually-owned assets still shows that community-owned assets provides better benefits to energy communities for both tariffs schemes studied.

Next, for energy communities with community-owned assets, we developed a practically applicable and computationally efficient redistribution mechanism to fairly share the energy and associated financial benefits from community-owned assets between the community members. This redistribution mechanism is based on the marginal contribution of each member, which is a key concept from coalitional game theory that looks at rewarding members based on the value they provide to the community. We showed that the proposed redistribution mechanism is applicable to any type of community-owned assets, even storage assets; despite the apparent difficulty to assess how each member takes advantage of assets.

A crucial aspect of a community energy models and projects is that they often involves sharing of some joint resources and assets. One approach is to facilitate peer-to-peer (P2P) or peer-to-community (P2C) trading in the case of individually-owned assets, whereas another approach consists in creating a community energy coalition in the case of community-owned assets, where an aggregator or community energy operator distributes the benefits within the community (as shown in this Chapter 5 and the previous Chapter 4). In the next Chapter 6, we extend the energy community model by exploring how P2C market mechanisms with individually owned assets can increase the benefits of such community energy scheme, and how such a setting compares to community-owned assets.

Chapter 6

Peer-to-Community (P2C) Energy Trading Framework for Energy Community

In the case of community settings with individually-owned energy assets presented in Chapter 4 and 5, the techno-economic study was conducted without considering local energy markets such as Peer-to-Peer (P2P) or Peer-to-Community (P2C) energy markets. Indeed, it was shown in previous chapters that jointly owned community energy assets are more profitable than individually owned energy assets in a "business as usual" configuration in which individual households do not share energy. Then, we proposed a novel algorithm to fairly distribute the benefits from these community owned assets. However, for the sake of completeness, we should now also consider novel mechanisms such as local energy markets that can increase the profitability from individually-owned energy assets. As a matter of fact, community with individually-owned assets can share the resources and benefits through local P2P or P2C energy markets. Furthermore, while considering the network constraints, as highlighted in Chapter 5, we highlighted that in an already constrained network, there could be a significant reduction in the production from jointly-owned community PV generator because of curtailment due to voltage constraints. This reduces the financial benefits offered by community-owned assets and limits the assets that can be further included in the network. However, in the case of a community with distributed individually-owned energy assets, the bus voltages in the same community remained within the permissible limits. While staying within acceptable voltage thresholds, local energy market mechanisms can provide a novel opportunity to make renewable energy assets more profitable, and thus incentivise investments into low carbon technologies.

This Chapter 6 presents a model of energy community with local P2C market mechanism in order to complete the comparison between individually-owned assets and community-owned assets. To fully capture the potential and limitations from P2C market mechanisms, we conducted a sensitivity study on different parameters such as the adoption rate of renewable energy assets in the community. A non-uniform pricing scheme is proposed in the P2C market mechanism and the outcomes are studied for three different types of P2C

sellers simulated under different community settings and tested for various scenarios of local generation and consumption. This chapter presents a multi-unit auction based P2C market clearing mechanism and the techno-economic performance of the individual agents and community as a whole is studied by determining the reduction in the yearly bill and the final savings achieved from local P2C market. Finally, The battery control algorithm as proposed in the previous chapters is extended to incorporate the proposed P2C market mechanism.

6.1 Research contributions

Novel decentralised energy frameworks, such as energy communities, LEMs and SLES, are emerging as promising solutions to coordinate generation, storage, and demand-side flexibility in a local area. Trading of energy between large producers, utility companies and consumers with established wholesale and retail markets is current practice; however, local P2C or P2P energy trading and sharing between prosumers, consumers and aggregators is a trending topic within the industry and research community. A comprehensive literature review on the state-of-the-art in P2P and P2C market mechanisms was presented analytically in the previous Chapter 2. As highlighted in the literature review, there is still a need for establishing a consumer-centric business model such as local peer-to-peer energy trading markets and energy coalitions to optimize the consumption and storage of renewable energy within the local community, and the trade of energy and services locally and outside the community. Furthermore, these emerging local markets need to provide a fair mechanism to incentivise and engage consumer/prosumer in the energy transition.

This Chapter 6 presents a local P2C market framework based on centrally operated mechanism, in which a community aggregator determines each trade's characteristics (price and quantity) by running a multi-unit auction. In a multi-unit auction market clearing mechanism, the market operator clears the market by computing the clearing price that maximizes the social welfare of the community. In our case, the proposed multi-unit auction market clearing mechanism is focused on achieving the fair allocation of total energy available for P2C market among the sellers and the buyers. There are indeed auctions every half-hourly of the operation, but there is one multi-unit auction where the price (pence) per unit (kWh) is averaged for each unit. In the proposed P2C market mechanism, we assume every consumer must satisfy their energy demand (either from the grid or the local P2C market), and averaging over the multiple units of price is the fairest way to share the cost for that market.

In summary, the research contributions of the work presented in Chapter 6 are:

- This chapter presents a framework for a Peer-to-Community (P2C) local market mechanism. The dynamics of the P2C market mechanism is studied for three different type of P2C sellers (non-uniform pricing scheme) and tested for three different types of community settings (mix of prosumers and consumers) under different rates of renewable energy adoption.

- A fair allocation scheme for the total energy available in the P2C market is proposed, aimed at incentivizing households to actively participate in local energy initiatives. An equal split ratio method is proposed to fairly distribute the energy total energy available from P2C market among the buyers. In the case of sellers, the framework is designed such that the cheapest seller gets the first priority to sell to the P2C local market the excess energy available at any operation time period.

- A market clearing mechanism based on a multi-unit auction is proposed for the P2C market. In this market clearing approach, all the bids of the prosumer sellers gets the price they have asked if selected. Then, the prosumer buyer in the P2C market pays a weighted average of the bids selected, starting from the cheapest P2C selling prices (prosumer seller bids ranked from cheapest to most expensive price ranges). Hence, P2C market clearing mechanism is designed such that, at excess times, the proposed market clears at a price lower than grid price (if prosumers bids are bellow the grid price). However, at deficit times, market may clear at grid import price (grid offering infinite quantity of energy, all the energy will be sold at the grid price).

- A techno-economic comparison is presented, analyzing the investment in individually-owned assets both with and without the P2C market mechanism, in contrast to jointly-owned community assets. The profitability of the proposed P2C market mechanism is tested for different settings of the community, and further tested to explore and assess the suitability of P2C frameworks in terms of import/export from/to the grid and local P2C market using the minutely real-time simulation versus half-hourly P2C market clearing time interval simulation.

- Finally, the proposed energy community model with local P2C market mechanism is validated using a real case study from the ReFLEX (Responsive Flexibility) project that consists in a large-scale demonstrator for community energy integration in Orkney, Scotland, UK [8].

6.2 Community setting

Similar to the community settings presented in Chapter 4 and 5, the model inputs (demand and generation data), tariff pricing schemes and the unitary cost of the energy assets presented in Section 3.3 of Chapter 3 are applied to the community settings. In this Chapter 6, we propose a P2C market mechanism for a community to trade and share resources and benefits with the prosumers with individually-owned energy assets. We consider that all prosumers invest in a distributed solar PV renewable generator and a battery storage energy assets. In this study, we chose to use an optimal size for both individually-owned solar PV's and batteries assets that was obtained in Chapter 4 (as shown in Table 4.3 for PV, and Table 4.5 for battery (that was obtained from battery integrated with solar PV renewable generator)). An optimal size of PV or battery corresponds to the size that provides the minimal simple payback period.

For this community with P2C market model, the study mainly focusses on exploring the suitable characteristics that makes the community with P2C local markets profitable as compared to the previous setting of the community with jointly-owned assets. To understand the dynamics of P2C market mechanisms, we have considered different settings of the community based on the percentage of distributed assets owned by the individual households/agents as follows:

- **Community setting 1:** all 200 households-prosumers with individually-owned optimally-sized PV's and optimal batteries (same setting as the community model presented in Chapter 4 and 5)
- **Community setting 2:** 100 households-prosumers with individually-owned optimally-sized PV's and optimal batteries, and 100 households-consumers without assets
- **Community setting 3:** 67 households-prosumers with individually-owned optimally-sized PV's and optimally-sized batteries, 33 households-prosumers with individually-owned PV's only, and 100 households-consumers without assets

The three presented setting of the community consist of mixture of prosumers with both PV's and batteries, prosumer with PV's only and finally the consumers without any assets. Therefore, this setting consists in a realistic scenario to better understand the dynamics of P2C market mechanisms, while allowing us to study the techno-economic comparison of individually-owned assets with and without P2C market mechanism versus jointly-owned community assets.

In this community settings, during the period of deficit energy, the households/agents can satisfy their energy demand by importing either from the P2C market or from the utility grid. However, during the period of excess generation, agents can export through P2C market only, as we have not considered an export tariff to the grid. Hence, the selling price of the P2C market is crucial in generating an healthy competition among the sellers, where agents offer their excess generation at different selling prices. One of the possible strategy of P2C sellers can be to set a higher per-unit price (close to 100% the default grid import price), and get paid more if the demand is very high, but risk sometimes to not sell the excess energy if the demand is low. Another strategy can be to set a lower per-unit price, and get paid less per unit, but this low-cost seller will have priority in selling, even when demand is lower or medium. Hence, it is better to have different types of P2C sellers, so that various parameters can be measured to explore the profitability of P2C market mechanism for different sellers under various scenarios of local generation and consumption. In order to understand the true dynamics of P2C market mechanisms with different selling prices, we have identified three different categories of P2C sellers as follows:

- **Low price sellers:** randomly (uniformly distributed) generated selling price from 10% of grid import price to 30% of grid import price
- **Medium price sellers:** randomly (uniformly distributed) generated selling price from 31% of grid import price to 70% of grid import price

- **High price sellers:** randomly (uniformly distributed) generated selling price from 71% of grid import price to 100% of grid import price

The grid import tariff sets the baseline (highest price boundary) for the import pricing schemes in P2C market, as otherwise rational prosumers would prefer to buy from the grid (i.e. utility company), rather than from other prosumers in the community. As discussed above, the selling prices for the different categories of the P2C sellers are randomly distributed based on the percentage of grid import price. In this P2C market, the grid is also a bidder and mostly set-up as a last option as compared to the local agents with excess generation. Price dynamics of this community setting is such that, at deficit times, the P2C market clears at grid import price (utility grid offering infinite quantity of energy all the times), and at excess times, the P2C market clear a price lower than the grid import price.

Furthermore, for the three identified different community settings consisting of three different sellers distribution, the profitability of P2C market mechanism is studied by determining the yearly bills with and without P2C market mechanism for different ratios of PV adoption within the community. These ratio range from 0 to 1, where 1 corresponds to the situation where the community is fully autonomous from annual energy point of view. The ratio of PV adoption is given by:

$$PVRatio = \frac{\text{Total community yearly PV generation}}{\text{Total community yearly Demand}} \tag{6.1}$$

When the $PVRatio$ is equal to one, this means that the community annual energy demand is equal to the community PV generation (same setting as the community model presented in Chapter 4 and 5). The amount of generation is changed to determine the profitability for different types of P2C sellers. For instance, if the renewable generation is higher than demand, in this case, low-price sellers will always sell the energy, and high price sellers will very rarely sell the energy. On the other hand, if the amount of renewable energy is low, then it would be a better strategy for the seller to set high selling price which is much closer to grid import price. Hence, by changing the PV generation, the profitability of the P2C market mechanism is studied at different constraint settings in terms of total generation versus total demand (as defined by Eq. (6.1)).

In order to assess the impact of each P2C market configuration, we will consider indicators such as the yearly energy bill savings, which is a fairly intuitive indicator to compare the techno-economic performance of the community with jointly-owned assets versus individually-owned assets with and without P2C market mechanisms. First, the individual households/agents optimize their own self-consumption from their energy assets and then trade the energy locally through P2C markets. Figure 6.1 shows the general setting of the proposed P2C energy trading model which is implemented to study the profitability of the three categories of P2C sellers for different ratios of PV generation to demand. The P2C model consist of mainly two stages:

i **Stage 1:** Individual prosumer battery control optimization.

ii **Stage 2:** P2C market mechanism.

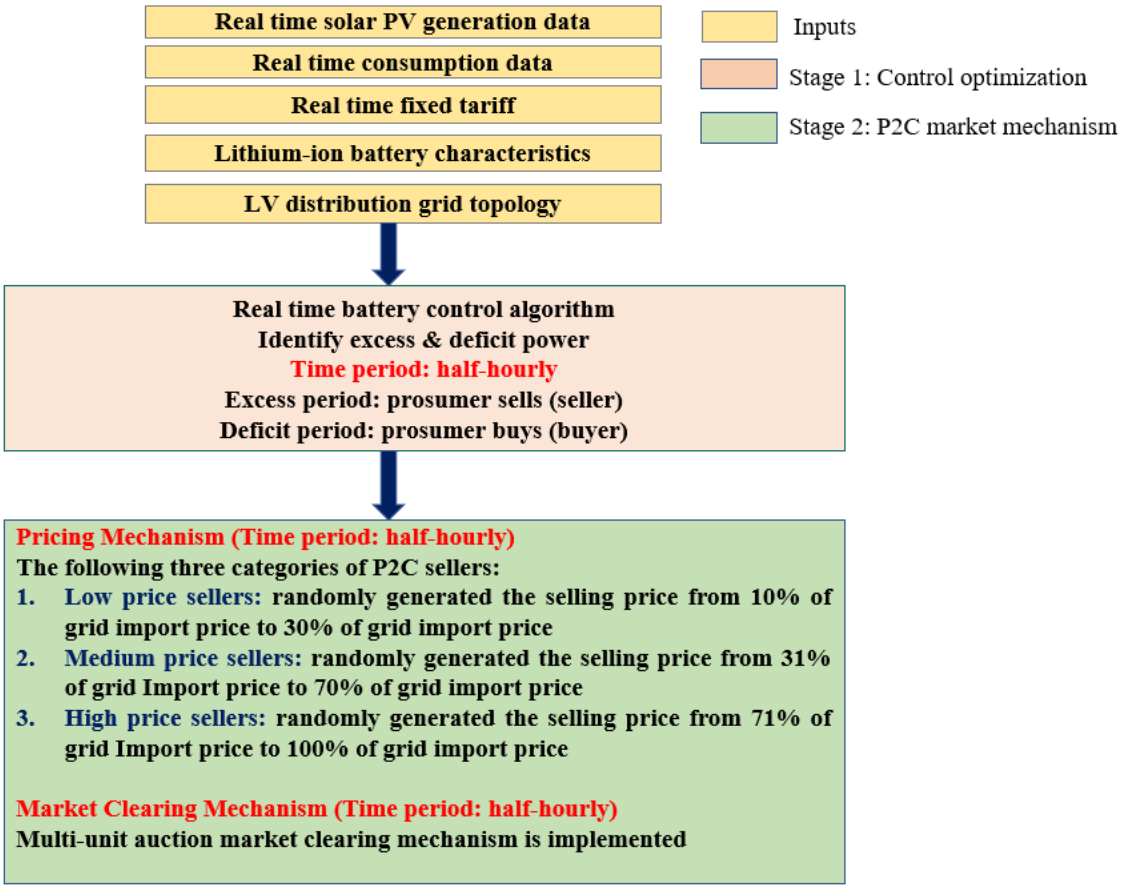

Figure 6.1: Overview of P2C modelling approach

Next, the various stages of the proposed P2C model depicted in Figure 6.1 are described. The explanation commences with a detailed account of "Stage 1," presented in Section 6.3.

6.3 Individual prosumer battery control optimization

Similar to the community settings presented in Chapter 4 and 5), the battery control Algorithm 3.1 applied to the single prosumer model described in Chapter 3 is extended by incorporating the P2C market mechanism. As described in Section 3.4.1 of Chapter 3, the operation of the battery is constrained by the state of charge (SoC) levels, and a maximum power ($p^{\text{bat,max}}$) that the battery can be charged or discharged at, which corresponds to its maximum C-rating.

At any given time t of a charging phase, the battery is charged with an efficiency (η^c) until it reaches the maximum battery capacity ($SoC^{\max}$). Charging constraints are defined as:

$$SoC(t) \leq SoC^{\max} \tag{6.2}$$

$$p^{\text{bat}}(t) \leq p^{\text{bat,max}} \tag{6.3}$$

Similarly, the battery can be discharged with an efficiency (η^d) until it reaches its minimum battery capacity ($SoC^{\min}$). Discharging constraints are defined as:

$$SoC(t) \geq SoC^{\min} \tag{6.4}$$

$$p^{\text{bat}}(t) \leq p^{\text{bat,max}} \tag{6.5}$$

The minimum battery capacity corresponds to the maximum allowable DoD. In this chapter, a rule-based battery control algorithm is implemented. The battery control scheme consists of operational real-time decisions to charge or discharge the battery, based on the difference between the prosumer power consumption and its own PV production. The control strategy is similar to the case with the single prosumer presented in Chapter 3 and community setting in Chapter 4 & 5. In this community model with P2C market mechanism, for every operational time period Δt (half-hourly in our case), each individual prosumer optimizes control of its own battery, then the following parameters are determined for all the prosumers:

1. **Excess power ($P^{\text{excess}}(t)$):** prosumer sells (seller) at excess time period. The algorithm can be described as follows:

   If $g^{\text{PV}}(t) > d(t)$, there is *excess of power* generated from the renewable generator. The control strategy of the battery dictates the following:

   i Excess power is stored in the battery (charging operation).

   ii If the battery is full or if available power is greater than the maximum acceptable charging power, the prosumer sells the excess power $P^{\text{excess}}(t)$ to the local P2C market.

   The resulting SoC profile and the excess power exported $P^{\text{excess}}(t)$ to the local P2C market during the identified duration of excess generation are determined as:

$$p_i^{\text{bat}}(t) = -min\left(min\left(\left[g^{\text{PV}}(t) - d(t)\right], p^{\text{bat,max}}\right), \frac{[SoC^{\max} - SoC(t-1)]}{\eta^c \Delta t}\right) \tag{6.6}$$

$$SoC_i(t) = SoC(t-1) - \eta^c p^{\text{bat}}(t)\Delta t \tag{6.7}$$

$$P_i^{\text{excess}}(t) = \left[g^{\text{PV}}(t) - d(t) - p^{\text{bat}}(t)\right]\Delta t \tag{6.8}$$

   where Δt corresponds to the duration of the considered time step.

2. **Deficit power ($P^{\text{deficit}}(t)$):** prosumer buys (buyer) at deficit time period. Similarly, the algorithm can be described as follows:

   if $g^{\text{PV}}(t) < d(t)$, then there is a *deficit in power* supplied by the intermittent source and the battery will operate as follows:

   i Discharge the battery to meet the demand.

ii If the battery energy or power are not enough to compensate the power deficit at this time step, the prosumer buys the remaining deficit power $P^{\text{deficit}}(t)$ from the local P2C market. Finally, if the deficit demand is not met from P2C market, then the prosumer buys from the utility grid.

Hence, the SoC profile and deficit power imported $P^{\text{deficit}}(t)$ from the local P2C market or utility grid during the identified duration of deficit in power are determined as:

$$p_i^{\text{bat}}(t) = min\left(min\left(\left[d(t) - g^{\text{PV}}(t)\right], p^{\text{bat,max}}\right), \eta^d \left[SoC(t-1) - SoC^{\text{min}}\right]\right) \quad (6.9)$$

$$SoC_i(t) = SoC(t-1) - \frac{p^{\text{bat}}(t)}{\eta^d} \cdot \Delta t \quad (6.10)$$

$$P_i^{\text{deficit}}(t) = \left[d(t) - g^{\text{PV}}(t) + p^{\text{bat}}(t)\right] \Delta t. \quad (6.11)$$

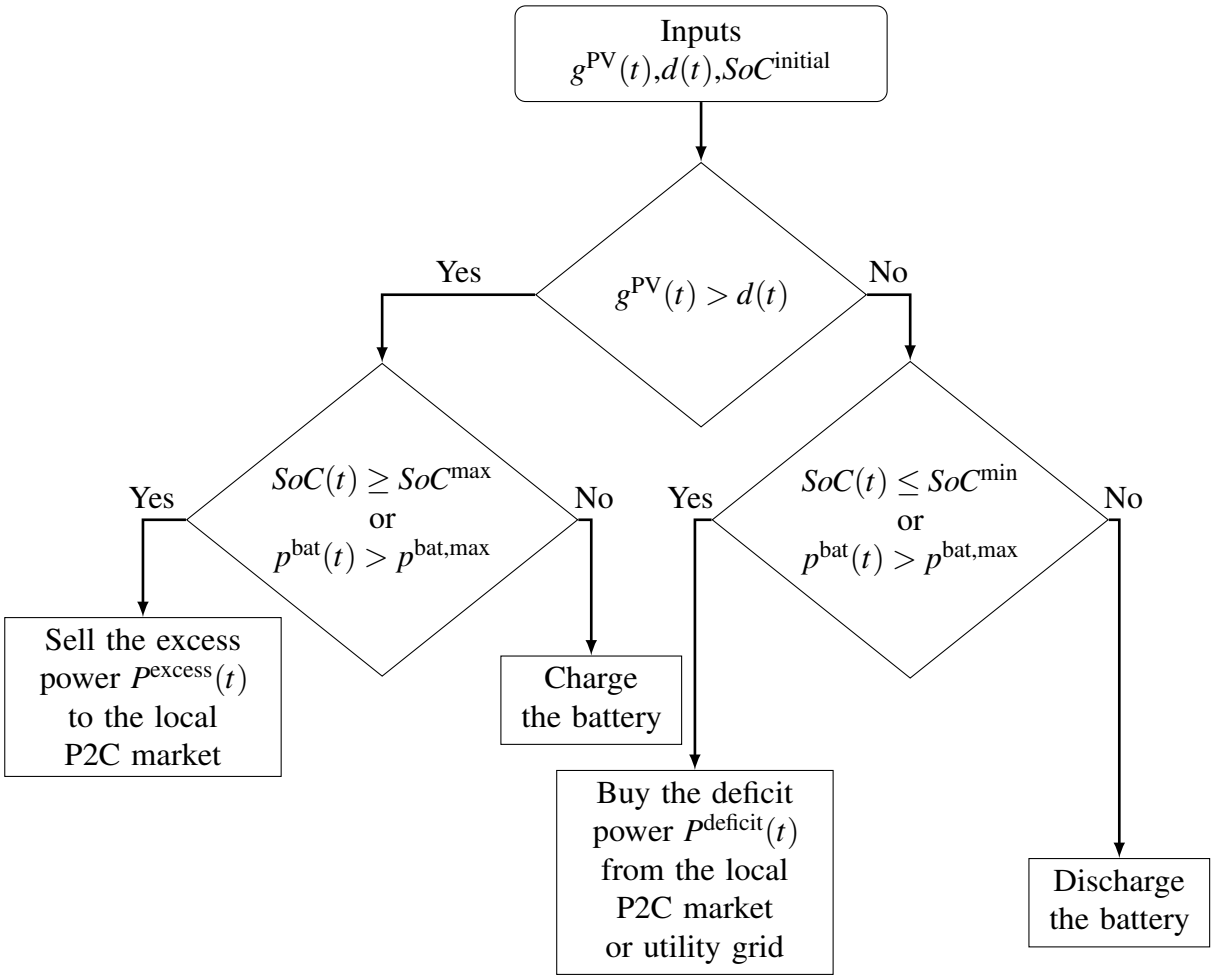

Figure 6.2: Flowchart of an individual prosumer battery control strategy.

Next, for every operational time period Δt (half-hourly in our case), the excess and deficit energy for all the households/agents of the community is determined. Specifically, for an agent i with $i = 1..N$ and $N = 200$ in our case, at time $t \in [0, T]$, $P_i^{\text{excess}}(t)$ represents the excess power and $P_i^{\text{deficit}}(t)$ the deficit power. As expressed in the community settings

in Chapter 4 and 5, the community $\mathcal{C}$, i.e. the set of all agents i, is formally defined as $\mathcal{C} = \{A_i \mid i \in [1,N]\}$ where $N = 200$ agents. Accordingly, $P_{\mathcal{C}}^{\text{excess}}(t)$ and $P_{\mathcal{C}}^{\text{deficit}}(t)$ represent the excess and deficit power of the community $\mathcal{C}$ at operational time t. At every operational time period, both $P_{\mathcal{C}}^{\text{excess}}(t)$ and $P_{\mathcal{C}}^{\text{deficit}}(t)$ cannot be greater than zero in the same time (in absolute value). Either one has to be zero if the other one is not zero.

Then, the excess power is exported in the local P2C market, and deficit power is either imported from local P2C market or from the utility grid (mostly preferred as the last option). The variables $P_{\mathcal{C}}^{\text{excess}}(t)$ and $P_{\mathcal{C}}^{\text{deficit}}(t)$ of the community at that particular operational time period are the essential inputs to the P2C market the stage 2 (detail description presented in the next Section 6.4) of the proposed P2C model. A flowchart of the proposed battery control strategy is shown in Figure 6.2. Algorithm 6.1 outlines this if-then rule based control strategy incorporating the P2C market mechanism.

Algorithm 6.1: Individual prosumer battery control algorithm

Input 1 : generation $g^{\text{PV}}(t)$, demand $d(t)$, and grid import price: $\tau^{b}(t)$
Input 2 : battery specifications: η^{c}, η^{d}, SoC^{initial}, $SoC^{\max}$, $SoC^{\min}$, $p^{\text{bat,max}}$, rated capacity of the battery as variable input
Input 3 : bids from P2C sellers: low, medium and high price
for $t = 1 : T$ **do**
  $\forall t \in [0,T]$, excess of energy or deficit in energy is determined
  if $g^{PV}(t) \geq d(t)$ **then**
    $p^{\text{bat}}(t) = -min\left(min\left(\left[g^{\text{PV}}(t) - d(t)\right], p^{\text{bat,max}}\right), \frac{\left[SoC^{\max} - SoC(t-1)\right]}{\eta^{c}\Delta t}\right)$
    $SoC(t) = SoC(t-1) - \eta^{c} p^{\text{bat}}(t)\Delta t$
    $P^{\text{excess}}(t) = \left[g^{\text{PV}}(t) - d(t) - p^{\text{bat}}(t)\right]\Delta t$
  else
    $p^{\text{bat}}(t) = min\left(min\left(\left[d(t) - g^{\text{PV}}(t)\right], p^{\text{bat,max}}\right), \eta^{d}\left[SoC(t-1) - SoC^{\min}\right]\right)$
    $SoC(t) = SoC(t-1) - \frac{p^{\text{bat}}(t)}{\eta^{d}} \cdot \Delta t$
    $P^{\text{deficit}}(t) = \left[d(t) - g^{\text{PV}}(t) + p^{\text{bat}}(t)\right]\Delta t$
  end
end
Output 1 : $\forall t \in [0,T]$, $SoC(t)$:- input to **rainflow cycle counting algorithm** used to calculate the battery depreciation factor
Output 2 : $\forall t \in [0,T]$, $P^{\text{excess}}(t)$:- input to P2C market mechanism
Output 3 : $\forall t \in [0,T]$, $P^{\text{deficit}}(t)$:- input to P2C market mechanism

In this setting, the excess power of each agent is sold to P2C market only and export to the grid is not considered in the current model. On the other hand, the deficit power is bought from both the P2C market and grid. First, the deficit power is bought from the local P2C market and any other remaining deficit power is satisfied by importing from the grid which offers infinite power.

Similar to the community settings described in Chapter 4 and 5, the model inputs, battery depreciation aspects and the economic setting of the single prosumer model

described in Chapter 3 are applied to the this community setting with the P2C market mechanism. Next, the pricing schemes, the fair allocation of energy among P2C sellers and buyers, and the multi-unit auction P2C market clearing mechanisms are described in the following Section 6.4.

6.4 Peer-to-Community (P2C) market mechanisms

Smart local energy system (SLES) have emerged as a solution to allow prosumers (i.e households/agents with micro renewable generation and/or storage) to generate extra revenues by selling production surpluses, and provide consumers (agents without energy assets) access to electricity at a lower cost than the standard grid tariff. In SLES, local energy markets can either allow consumers to buy electricity directly from a producer/prosumer (Peer-to-peer (P2P)), or from an aggregator (Peer-to-community (P2C)). In this chapter, we provide a community-based market mechanism in which peers (consumer and prosumer/producer) buy or sell energy from/to community. The local P2C market is based on centrally operated mechanism, in which a community aggregator determines each trade's characteristics (price and quantity) by running a multi-unit auction. The community aggregator can be either a Distribution System Operator (DSO) or a dedicated market operator.

As described in Section 6.3, for every operational time period, prosumer who are the agents with energy production assets are considered seller during the periods with excess generation, and the same prosumer is considered buyer during the periods of deficit in local generation. Consumer who are the agents without any assets are considered buyers for all the times. The utility grid is also considered as the bidder where the grid import tariff sets the baseline for the P2C market seller bids. A multi-unit auction market clearing mechanism is proposed, in which the market operator clears the market by computing the clearing price that maximizes the social welfare of the community. In our case, the proposed multi-unit auction market clearing mechanism is focused on achieving a fair allocation of total energy available for P2C market among the sellers and the buyers. There are indeed auctions every half-hourly of the operation, but there is one multi-unit auction where the price (pence) per unit (kWh) is averaged for each unit. In the proposed P2C market mechanism, we assume every consumer must satisfy their energy demands (either from the grid or the local P2C market), and averaging over the multiple units of price is the fairest way to share the cost for that market.

In this community model with P2C market mechanism, a fixed grid import tariff of 16pence/kWh [222] is considered.The P2C market dynamics is studied for three different categories of P2C sellers simulated for various settings of the community. Essentially, there are five mechanisms that constitute the proposed P2C market, and these mechanisms are explained in detail in the following sections.

6.4.1 Non-uniform P2C pricing scheme

In this community setting with local P2C market mechanism, a non-uniform pricing scheme is proposed where all the sellers in P2C local market have non-uniform selling prices. Similar to the community setting presented in Chapter 4 and 5, in our analysis the power export to gird is not considered. Hence, the dynamics of the P2C market will hugely depend on the pricing strategy of the P2C sellers. The non-uniform pricing schemes enables us to study the profitability of P2C market mechanism for different sellers under various scenarios of local generation and demand. In this non-uniform pricing scheme, the sellers in the P2C local market have different selling prices. This different selling prices are generated as a percentage of the grid import price (τ^b) and the P2C sellers are categorized into three different categories as follows:

- **Low price sellers:** randomly generated the selling price from 10% of grid import price to 30% of grid import price (τ^b). The selling prices for this category of low price sellers are defined by a range of 10% to 30% of τ^b as shown in Eq. (6.12).

$$\tau^{\text{LowPrice}} = [0.1 : 0.3]\tau^b(£/kWh) \tag{6.12}$$

- **Medium price sellers:** randomly generated the selling price from 31% of grid import price to 70% of grid import price (τ^b). The selling prices for this category of low price sellers are defined by a range of 31% to 70% of τ^b as shown in Eq. (6.13).

$$\tau^{\text{MediumPrice}} = [0.31 : 0.7]\tau^b(£/kWh) \tag{6.13}$$

- **High price sellers:** randomly generated the selling price from 71% of grid import price to 100% of grid import price (τ^b). The selling prices for this category of low price sellers are defined by a range of 71% to 100% of τ^b as shown in Eq. (6.14).

$$\tau^{\text{HighPrice}} = [0.71 : 1]\tau^b(£/kWh) \tag{6.14}$$

In this non-uniform pricing scheme, the selling prices in the P2C market consists of the set of these low, medium and high selling prices, noted as $\tau^{\text{P2C}} = \left\{\tau^{\text{LowPrice}}, \tau^{\text{MediumPrice}}, \tau^{\text{HighPrice}}\right\}$, $pence/kWh$. Then, the households/agents are randomly allocated into different categories of P2C sellers. For instance, the distribution of selling prices ($pence/kWh$) for the community of 200 agents is shown in Eq. (6.15).

$$\tau_C^{\text{P2C}} = \left\{\tau_1^{\text{LowPrice}} \ldots\ldots \tau_{67}^{\text{LowPrice}}, \tau_1^{\text{MediumPrice}} \ldots\ldots \tau_{67}^{\text{MediumPrice}}, \tau_1^{\text{HighPrice}} \ldots\ldots \tau_{66}^{\text{HighPrice}}\right\} \tag{6.15}$$

According to Eq. (6.15), the 200 households are randomly allocated into different categories of P2C sellers as follows:

- 67 households: Low price sellers
- 67 households: Medium price sellers

- 66 households: High price sellers

At specific operational times, the P2C sellers have random selling prices which is within the boundaries of the low, medium or high categories. Next, the determination of total energy available for import/export from/to P2C market and the utility grid is presented in the following subsection.

6.4.2 Determination of total energy available from P2C market

As described in Section 6.3, first individual households/agents optimize their own self-consumption for every operational time period Δt (half-hourly in our case). After applying the battery control Algorithm 6.1, the excess and deficit power for all the agents of the community is determined. Specifically, for an agent i with $i = 1..N$ and $N = 200$ in our case, at time $t \in [0,T]$, $P_i^{\text{excess}}(t)$ represents the excess power and $P_i^{\text{deficit}}(t)$ the deficit power. Using this individual parameters, we determine the total excess power ($P_{\text{Total}}^{\text{excess}}(t)$) and total deficit power ($P_{\text{Total}}^{\text{deficit}}(t)$) for all the agents of the community as follows:

$$P_{\text{Total}}^{\text{excess}}(t) = \sum_{i=1}^{N} [P_i^{\text{excess}}(t)]\Delta t \tag{6.16}$$

$$P_{\text{Total}}^{\text{deficit}}(t) = \sum_{i=1}^{N} [P_i^{\text{deficit}}(t)]\Delta t \tag{6.17}$$

where Δt corresponds to the duration of the considered operational time step. Next, we determine $P_{\text{Total}}^{\text{P2C}}(t)$ the total power available for trade in the P2C market as follows:

If $P_{\text{Total}}^{\text{deficit}}(t) > P_{\text{Total}}^{\text{excess}}(t)$, the $P_{\text{Total}}^{\text{P2C}}(t)$ is determined as:

$$P_{\text{Total}}^{\text{P2C}}(t) = P_{\text{Total}}^{\text{excess}}(t) \tag{6.18}$$

At this operational time period, there is deficit in local generation. The total power available from the P2C market ($P_{\text{Total}}^{\text{P2C}}(t)$) is not able to meet the total demand of the community. Hence, the community imports the remaining power from the grid. Eq. (6.19) shows the total power imported from the utility grid.

$$P_{\text{Total}}^{\text{Grid Import}}(t) = P_{\text{Total}}^{\text{deficit}}(t) - P_{\text{Total}}^{\text{P2C}}(t) \tag{6.19}$$

Similarly, if $P_{\text{Total}}^{\text{deficit}}(t) \geq P_{\text{Total}}^{\text{excess}}(t)$, the $P_{\text{Total}}^{\text{P2C}}(t)$ is determined as:

$$P_{\text{Total}}^{\text{P2C}}(t) = P_{\text{Total}}^{\text{deficit}}(t) \tag{6.20}$$

At this operational time period, there is an excess of power generated from the solar PV generator. Community is able to meet the total deficit demand from the P2C market, and any excess power is exported to the grid. Eq. (6.21) shows the total power imported from the utility grid.

$$P_{\text{Total}}^{\text{Grid Export}}(t) = P_{\text{Total}}^{\text{excess}}(t) - P_{\text{Total}}^{\text{P2C}}(t) \tag{6.21}$$

However, in this community setting we have only considered the import tariff of the grid and export tariff is not considered in the techno-economic analysis. One of the most important aspect that need to be considered is the fair allocation of $P^{\text{P2C}}_{\text{Total}}(t)$ the total energy available from P2C market among the sellers and the buyers. The proposed fair allocation schemes are explained in the following subsection. We begin by describing the fair allocation of total energy available from P2C market among the P2C sellers.

6.4.3 Fair distribution of total energy available for P2C market among the P2C sellers

At every operational time period, the P2C sellers (excess energy) are sorted and ranked from the cheapest to most expensive price sellers. Then, $P^{\text{P2C}}_{\text{Total}}(t)$ the total energy available for the P2C market is distributed such that the cheapest seller gets the first priority to sell the excess energy available at that operational time period to P2C local market. The non-uniform pricing scheme and the allocation of P2C sellers into three different categories of P2C sellers is defined by Eq. (6.15). For this pricing scheme, the K represents the set of indices of the cheapest to most expensive ranked sellers allocated in τ^{P2C}_{C}, such that $K \in R$, $R = x|1 < x < N$, and $N = 200$ in our case. Then, the proceeding step-wise process involved in the fair distribution of total energy available for P2C market among the sellers is present as follows:

Step 1: At every specific operational time period, the cheapest P2C seller gets the first priority to sell the excess power through P2C market. Specifically, for the agent i ranked K^{th} based on the τ^{P2C}_{C}, the total power exported through P2C market is determined as shown below:

$$P^{\text{P2C Export}}_{i}(t) = min\left(P^{\text{excess}}_{i}(t,K), P^{\text{deficit}}_{\text{Total}}(t)\right) \tag{6.22}$$

Step 2: However, if the total deficit power for the whole community at that operational time is not met from the first cheapest seller, then the second cheapest seller is chosen to sell the excess power to the P2C market, and the total remaining total deficit energy is updated as follows:

$$P^{\text{deficit}}_{\text{remaining}}(t) = P^{\text{deficit}}_{\text{Total}}(t) - P^{\text{P2C Export}}(t) \tag{6.23}$$

Then, the total power exported through P2C market is updated as:

$$P^{\text{P2C Export}}_{i}(t) = min\left(P^{\text{excess}}_{i}(t,K), P^{\text{deficit}}_{\text{remaining}}(t)\right) \tag{6.24}$$

Step 3: If the total deficit power is not satisfied and still there are agents with excess power to sell for P2C market, then the Eq. (6.23) is updated and the next cheapest seller is chosen by updating the Eq. (6.24). These steps are repeated until the total deficit power is fully satisfied or the excess energy are fully sold for the P2C market.

The excess power not sold through P2C market can be sold to the utility grid, but in our case grid export tariff is not considered so it is not sold to grid. For the agent i, the

power exported to the grid is computed as shown below:

$$P_i^{\text{Grid Export}}(t) = P_i^{\text{excess}}(t,K) - P_i^{\text{P2C Export}}(t) \tag{6.25}$$

The fair distribution of total power available form the P2C market among the P2C buyers is described in the next subsection.

6.4.4 Fair distribution of total energy available from P2C market among the P2C buyers

At every operational time period, the total energy available for P2C market is distributed equally among the P2C buyers (deficit energy). For fair redistribution of the energy available from P2C market, first, the buyers are sorted and ranked from the smallest to largest deficit energy required at that operational time period. Then, the total energy available from P2C market is distributed equally among the buyers by *equal split ratio*. If there is any surplus energy in the equal distribution, then this surplus energy is further distributed among the buyers with larger deficit energy. In some of the proposed peer-to-peer trading schemes, the energy available form the P2C market is distributed among buyers by the proportional to the size of the demand of each buyer. However, this distribution scheme benefits only to the large consumers (higher annual consumption) and smaller consumers do not benefit from the local P2C market. Since the import tariff from the local P2C market are cheaper than the standard grid tariff, irrespective of agents/households demand profiles, we argue that, overall there should be a much fairer mechanisms to distribute the total energy available from P2C market among the potential buyers.

To implement the proposed equal split ratio distribution method, for every operational time period, the P2C buyers are sorted and ranked from the smallest to largest deficit energy required based on the computation defined in $P_C^{\text{deficit}}(t)$. For this deficit energy required, the L represents the set of indices of the smallest to largest demand ranked buyers as computed in $P_C^{\text{deficit}}(t)$, such that $L \in R$, $R = x|1 < x < N$, and $N = 200$ in our case. Initially, the total number of P2C buyers (N_{Buyers}) is determined for that operational time period. Then, the proceeding step-wise process involved in the fair distribution of total energy available for P2C market among the buyers is present as follows:

Step 1: $P_{\text{Total}}^{\text{P2C}}(t)$ the total energy available from P2C market is distributed equally among the buyers by the ratio of $P_{\text{Total}}^{\text{P2C}}(t)$ to N_{Buyers} at operational time t. Specifically, for the agent i ranked L^{th} based on the $P_C^{\text{deficit}}(t)$, the total power that will be granted (imported) from P2C market from P2C market is determined as shown below:

$$P_i^{\text{P2C Import}}(t) = min\left(P_i^{\text{deficit}}(t,L), \frac{P_{\text{Total}}^{\text{P2C}}(t)}{N_{\text{Buyers}}}\right) \tag{6.26}$$

Step 2: However, for an agent, if the total deficit energy required at that operational time period is less than the equal split that was allocated to the buyer, than the difference between the agent's required power and the equally distributed power is further allocated among the

other buyers with higher consumption demands by keeping track of the remaining excess power ($P_i^{\text{remaining excess}}(t)$). Hence, Eq. (6.26) is modified as shown below:

$$P_i^{\text{P2C Import}}(t) = min\left(P_i^{\text{deficit}}(t,L), \frac{(P_i^{\text{remaining excess}}(t) + P_{\text{Total}}^{\text{P2C}}(t))}{N_{\text{Buyers}}}\right) \tag{6.27}$$

The remaining excess power is updated as:

$$P_i^{\text{remaining excess}}(t) = P_i^{\text{remaining excess}}(t) + max(0, \frac{P_{\text{Total}}^{\text{P2C}}(t)}{N_{\text{Buyers}}} - P_i^{\text{P2C Import}}(t)) \tag{6.28}$$

Step 3: The surpluses are regrouped and distributed equally among the remaining buyers with higher deficit demand. These steps are repeated until the total energy available for the P2C market are distributed equally among the P2C buyers. These step-wise process of the proposed equal split ratio distribution method is illustrated in Figure 6.3.

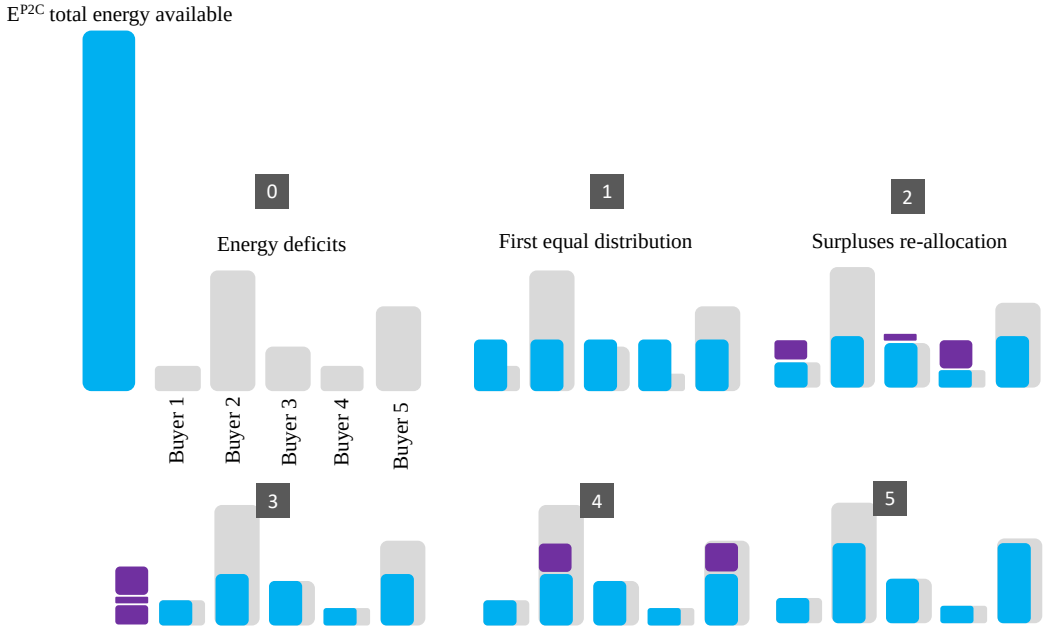

Figure 6.3: Illustration of step-wise equal split ratio method for equal distribution of the total energy available for P2C market among the buyers.

The proposed distribution method based on an equal split ratio achieves a greater degree of fairness in the allocation of cheaper energy from the P2C market, since it allows to distribute the energy available from P2C market equally among all the buyers initially (irrespective of the demand profiles) and then any surpluses are redistributed to those buyers who consume more. Any deficit power that are not met from the P2C market is fulfilled by importing from the utility grid. For the agent i, who has not met his demand after this P2C energy/power distribution scheme, the power imported from grid is computed as shown below:

$$P_i^{\text{Grid Import}}(t) = P_i^{\text{deficit}}(t,L) - P_i^{\text{P2C Import}}(t) \tag{6.29}$$

Then, a P2C market clearing price is determined after the distribution of total energy available for P2C market among the sellers and buyers. A multi-unit auction market

clearing mechanism is proposed, in which the market operator clears the market by computing the clearing price that maximizes the social welfare of the community. The proposed multi-unit auction P2C market clearing mechanism is presented in the next subsection.

6.4.5 A multi-unit auction P2C market clearing mechanism

For every operational time period, prosumers are agents with energy assets. They are considered as seller during the periods with excess generation, and the same prosumer is considered as buyer during the periods of deficit in local generation. Consumer are agents without any energy assets. They are considered as buyers for all the times. The utility grid is also considered as a bidder where the grid import tariff sets the baseline for the P2C market seller bids. P2C market clearing mechanism is designed for half-hourly time period. In this thesis, a multi-unit auction market clearing mechanism is proposed. In this market clearing approach, all the bids of the prosumer sellers get the price they have asked if selected. Then, buyers in the P2C market pay a weighted average of the bids selected, starting from the cheapest P2C selling prices (prosumer seller bids ranked from cheapest to expensive price ranges as defined in Eq. (6.15)). Hence, P2C market clearing mechanism is deigned such that, at energy (or power) excess times, market clears at a price lower than grid price. However, at deficit times, market may clear at grid import price depending on the proportion of energy/power that is supplied by the grid (utility grid offering infinite quantity of energy).

At any given time t of the operational time period (half-hourly in our case), if $P^{\text{deficit}}_{\text{Total}}(t) < P^{\text{P2C}}_{\text{Total}}(t)$, at this period the total requested power/energy for all the agents of the community is less than the total power/energy available for the P2C market. The total cost of energy exported to the P2C market is computed Using Eq. (6.22):

$$e^{\text{P2C}}_{\text{Total}}(t) = \sum_{i=1}^{N} P_i^{\text{P2C Export}}(t)\,\tau_i^{\text{P2C}} \tag{6.30}$$

where τ_i^{P2C} is the selling price of the agent i (as defined in Eq. (6.15)) of the non-uniform pricing scheme of the local P2C market. The selling prices are sorted and ranked from the cheapest to most expensive prices. Then, the P2C market clearing price per unit is determined as:

$$\tau^{\text{P2C}}_{\text{clearing price}}(t) = \frac{e^{\text{P2C}}_{\text{Total}}(t)}{P^{\text{deficit}}_{\text{Total}}(t)} \tag{6.31}$$

Hence, Eq. (6.31) represents the price per unit, computed from the weighted average of the P2C sellers bids selected, starting from the cheapest P2C selling prices.

If $P^{\text{deficit}}_{\text{Total}}(t) > P^{\text{P2C}}_{\text{Total}}(t)$, at this operational time period, the total energy available from the P2C market is not sufficient to meet the total deficit demands of the community. Any deficit energy that are not met from the P2C market is fulfilled by importing from the utility grid. The total cost of importing the remaining energy from the grid is computed

using Eq. (6.29):

$$e^{\text{Grid}}_{\text{Total}}(t) = \sum_{i=1}^{N} P_i^{\text{Grid Import}}(t)\tau^b \tag{6.32}$$

where τ^b is the grid import tariff and is same for all the agents of the community. In this scenario, both the bids from the P2C sellers and the gird are considered, and the P2C market clearing price per unit is determined as:

$$\tau^{\text{P2C}}_{\text{clearing price}}(t) = \frac{\left[e^{\text{P2C}}_{\text{Total}}(t) + e^{\text{Grid}}_{\text{Total}}(t)\right]}{P^{\text{deficit}}_{\text{Total}}(t)} \tag{6.33}$$

Hence, Eq. (6.33) represents the weighted average of the P2C sellers bids selected (if the price is below the grid import price, starting from the cheapest P2C selling prices), and the grid's bid (grid offering infinity quantity of energy). At certain operation time period if the there is no power available from the P2C market ($P^{\text{P2C}}_{\text{Total}}(t) = 0$), then the P2C market clears at the grid import price of τ^b.

The P2C buyers pay the P2C market clearing price per unit $\tau^{\text{P2C}}_{\text{clearing price}}(t)$ (as shown by Eq. (6.31) and Eq. (6.33)) which is the weighted average of the P2C sellers bids selected. Algorithm 6.2 outlines the proposed P2C market mechanism described in subsection 6.4.1 to 6.4.5.

Next, with this pricing scheme the P2C market dynamics of three different categories of low, medium and high P2C sellers is studied by determining the yearly bills with and without P2C market for the different ratios of the total yearly community PV generation as defined in Eq (6.1). Therefore, the yearly energy bill savings, which is a fairly intuitive indicator, is used to compare the economic performance of investments in individually-owned assets with and without local P2C market. The yearly bill $b_i(T)$ of an agent i can be expressed as the sum of the cost of the annual energy import from P2C market, sum of cost of import from the grid and the depreciation cost of the assets c^A, minus the sum of revenues earned by exports to the local P2C market, as shown below:

$$\begin{aligned} b_i(T) = \sum_{1}^{T} P_i^{\text{P2C Import}}(t)\tau^{\text{P2C}}_{\text{clearing price}}(t) + \sum_{1}^{T} P_i^{\text{Grid Import}}(t)\tau^b \\ - \sum_{1}^{T} P_i^{\text{P2C Export}}(t)\tau^{\text{P2C}}_{\text{clearing price}}(t) + c^A(T) \end{aligned} \tag{6.34}$$

where, at time step t, the energy import $P_i^{\text{P2C Import}}(t)$ from P2C market is given by Eq. (6.27), the energy import $P_i^{\text{Grid Import}}(t)$ from grid is given by Eq. (6.29), and the energy export $P_i^{\text{P2C Export}}(t)$ to P2C market at time step t is given by Eq. (6.22). Similar to the settings described in Chapter 3, 4 and 5, in Eq. (6.34) the c^A represents the depreciation cost which is due to the usage of the asset within the considered period. For example, for a considered period T equal to one year in which the asset is used following the manufacturer's recommendations, $c^A(T)$ corresponds to the annualized cost of the asset,

Algorithm 6.2: Local peer-to-community (P2C) market mechanisms

Input 1 : prosumer excess power $P_C^{\text{excess}}(t)$, prosumer/consumer deficit power $P_C^{\text{deficit}}(t)$

Input 2 : grid import price: $\tau^b(t)$, bids from P2C sellers: τ_C^{P2C}

for $t = 1 : T$ **do**

  $\forall t \in [0, T]$, total energy available for P2C market is determined

  $P_{\text{Total}}^{\text{excess}}(t) = \sum_{i=1}^{N} [P_i^{\text{excess}}(t)] \Delta t$

  $P_{\text{Total}}^{\text{deficit}}(t) = \sum_{i=1}^{N} [P_i^{\text{deficit}}(t)] \Delta t$

  if $P_{Total}^{deficit}(t) \geq P_{Total}^{excess}(t)$ **then**

    $P_{\text{Total}}^{\text{P2C}}(t) = P_{\text{Total}}^{\text{excess}}(t)$

    $P_{\text{Total}}^{\text{Grid Import}}(t) = P_{\text{Total}}^{\text{deficit}}(t) - P_{\text{Total}}^{\text{P2C}}(t)$

  else

    $P_{\text{Total}}^{\text{P2C}}(t) = P_{\text{Total}}^{\text{deficit}}(t)$

    $P_{\text{Total}}^{\text{Grid Export}}(t) = P_{\text{Total}}^{\text{excess}}(t) - P_{\text{Total}}^{\text{P2C}}(t)$

  end

  Allocation of total energy available for P2C market among the P2C sellers:

  $K = \left\{ \tau_{\text{cheapest}}^{\text{P2C}} : \tau_{\text{expensive}}^{\text{P2C}} \right\}$ represents the set of indices of the cheapest to most expensive ranked sellers allocated in τ_C^{P2C}

  for $K = \left\{ \tau_{cheapest}^{P2C} : \tau_{expensive}^{P2C} \right\}$ **do**

    $P_i^{\text{P2C Export}}(t) = min\left(P_i^{\text{excess}}(t,K), P_{\text{Total}}^{\text{deficit}}(t)\right)$

    $P_{\text{remaining}}^{\text{deficit}}(t) = P_{\text{Total}}^{\text{deficit}}(t) - P^{\text{P2C Export}}(t)$

    $P_i^{\text{P2C Export}}(t) = min\left(P_i^{\text{excess}}(t,K), P_{\text{remaining}}^{\text{deficit}}(t)\right)$

    $P_i^{\text{Grid Export}}(t) = P_i^{\text{excess}}(t,K) - P_i^{\text{P2C Export}}(t)$

  end

  Allocation of total power available from P2C market among the P2C buyers:

  $L = \left\{ P_{\text{smallest}}^{\text{deficit}} : P_{\text{largest}}^{\text{deficit}} \right\}$ represents the set of indices of the smallest to largest demand buyers as computed in $P_C^{\text{deficit}}(t)$

  for $L = \left\{ P_{smallest}^{deficit} : P_{largest}^{deficit} \right\}$ **do**

    $P_i^{\text{P2C Import}}(t) = min\left(P_i^{\text{deficit}}(t,L), \frac{(P_i^{\text{remaining excess}}(t) + P_{\text{Total}}^{\text{P2C}}(t))}{N_{\text{Buyers}}}\right)$

    $P_i^{\text{remaining excess}}(t) = P_i^{\text{remaining excess}}(t) + max(0, \frac{P_{\text{Total}}^{\text{P2C}}(t)}{N_{\text{Buyers}}} - P_i^{\text{P2C Import}}(t))$

    $P_i^{\text{Grid Import}}(t) = P_i^{\text{deficit}}(t,L) - P_i^{\text{P2C Import}}(t)$

  end

  P2C market clearing mechanism:

  if $P_{Total}^{deficit}(t) < P_{Total}^{P2C}(t)$ **then**

    $e_{\text{Total}}^{\text{P2C}}(t) = \sum_{i=1}^{N} P_i^{\text{P2C Export}}(t) \tau_i^{\text{P2C}}$

    $\tau_{\text{clearing price}}^{\text{P2C}}(t) = \frac{e_{\text{Total}}^{\text{P2C}}(t)}{P_{\text{Total}}^{\text{deficit}}(t)}$

  else

    $e_{\text{Total}}^{\text{Grid}}(t) = \sum_{i=1}^{N} P_i^{\text{Grid Import}}(t) \tau^b$

    $\tau_{\text{clearing price}}^{\text{P2C}}(t) = \frac{\left[e_{\text{Total}}^{\text{P2C}}(t) + e_{\text{Total}}^{\text{Grid}}(t)\right]}{P_{\text{Total}}^{\text{deficit}}(t)}$

  end

end

Outputs: $\sum_1^T P_i^{\text{P2C Import}}(t), \sum_1^T P_i^{\text{Grid Import}}(t), \sum_1^T P_i^{\text{P2C Export}}(t)$

given as follows:

$$c^A(T) = \frac{\text{Asset cost}}{\text{Life time (in years)}} \tag{6.35}$$

In this chapter, a detailed Lithium-ion *battery degradation model* presented in Chapter 3 is used to determine the battery depreciation factor (DF) to estimate the battery useful lifetime. Taking into consideration the depreciation resulting from the battery operation and Algorithm 6.1, the computation of the depreciation cost c^A in Eq. (6.34) is updated as follows:

$$c^A(T) = \max\left(\frac{1}{\text{DF}}, \frac{\text{Asset cost}}{\text{Life time (in years)}}\right) \tag{6.36}$$

Techno-economic comparison of individually-owned assets with and without P2C market mechanism versus jointly-owned community assets is presented in the following Section 6.5. In the same section, a sensitivity study is presented to understand the true dynamics of the proposed P2C market mechanism, and to determine the characteristics of the community settings that make local P2C market schemes profitable to the households and the community as a whole.

6.5 Economic study of communities with individually-owned assets with P2C market

In this community setting with local P2C market mechanism, we consider the individual households invest in an individually-owned distributed solar PV renewable generator along with a battery energy storage system. Similar to the community settings described in Chapter 4 and 5, the model input, tariff structures and unitary cost of energy assets described in Section 3.3 of Chapter 3 are used for analysis. The cost of energy assets are assumed to be 150 £/kWh for the battery [225] and 1100 £/kW for solar PV [229] generation capacity. The economic performance of investment in this individually-owned energy assets is compared with the investment in jointly-owned community energy assets (centrally-shared community assets as described in Chapter 5 considering network constraints). In this study, we chose to use an optimal size for both individual assets and community assets that was obtained in Chapter 4. Results of the optimal assets sizing are shown in Table 4.3 for PV, and Table 4.5 for battery (that was obtained from battery integrated with solar PV renewable generator). An optimal size of PV or battery corresponds to the size that provides the minimal simple payback period.

In this community model with P2C market mechanism, a fixed grid import tariff of 16pence/kWh [222] is considered. The P2C market dynamics is studied for three different categories of P2C sellers simulated for various settings of the community as shown below:

- **Community setting 1:** all 200 households-prosumers with individually-owned optimal PV's and optimal batteries (same setting as the community model presented in Chapter 4 and 5). In this setting, the 200 prosumers are randomly allocated into different categories of P2C sellers (non-uniform pricing scheme) as follows:

i Low price sellers: 67 households

ii Medium price sellers: 67 households

iii High price sellers: 66 households

- **Community setting 2:** 100 households-prosumers with individually-owned optimal PV's and optimal batteries, and 100 households-consumers without assets. In this setting, the 100 prosumers are randomly allocated into different categories of P2C sellers (non-uniform pricing scheme) as follows:

  i Low price sellers: 34 households

  ii Medium price sellers: 33 households

  iii High price sellers: 33 households

- **Community setting 3:** 67 households-prosumers with individually-owned optimal PV's and optimal batteries, 33 households-prosumers with individually-owned PV's only, and 100 households-consumers without assets. In this setting, the 67 prosumers (both PV & battery) and 33 prosumers (Pv only) are randomly allocated into different categories of P2C sellers (non-uniform pricing scheme) as follows:

  i Low price sellers (prosumer with PV & battery): 23 households

  ii Medium price sellers (prosumer with PV & battery): 22 households

  iii High price sellers (prosumer with PV & battery): 22 households

  iv Low price sellers (prosumer with PV only): 11 households

  v Medium price sellers (prosumer with PV only): 11 households

  vi High price sellers (prosumer with PV only): 11 households

The main aim of the techno-economic study of the energy community is to determine the profitability of the local P2C market mechanism for the different settings of the community. However, only *Community setting 1* is used for the techno-economic comparison of the investment in jointly-owned community energy assets versus individually-owned assets with and without P2C market mechanism. This choice was made because community settings 1 is the only scenario with the same settings as the community with jointly-owned energy assets presented in Chapter 4 and 5. This comparison of economic performance in the investment of community assets versus individually-owned assets with P2C market mechanism for different PV ratios is presented in the following subsection. The comparison between P2C market in community setting 1 and community with jointly-owned energy assets is presented in Section 6.5.1. The comparison between all the community settings, all with P2C market mechanism is presented in Section 6.5.2.

6.5.1 Communities with P2C markets versus jointly-owned energy assets

To provide a comprehensive comparison study between both community types (with individual assets and P2C market vs jointly owned assets), we will compare the benefits of P2C for different amount of PV installed. The demand of the community is kept constant but the generation from renewable generator PV is increased or decreased to obtain different $PVRatio$ as defined by Eq. (6.1). The profitability of the local P2C market mechanism, and the dynamics of the non-uniform pricing schemes are studied for the different PV ratios. If the $PVRatio$ is equal to one, this means that the community demand is equal to community PV generation (same setting as the community model presented in Chapter 4 and 5). If the $PVRatio = 2$ means that the total community yearly generation is twice the total community yearly demand. Similarly, If the $PVRatio = 0.5$ means that the total community yearly PV generation is half the total community yearly demand. The different PV ratios are chosen to study the real pricing dynamics among the three different low, medium and high P2C sellers in the local P2C market. The optimal capacities of individually-owned and community-owned energy assets (solar PV and battery) obtained for various PV ratios are shown in Table 6.1 & 6.2.

Assets	**Community assets size**	**Sum of individual agents assets' capacities**			
	Ratio = 0.37	**Ratio = 0.25**	**Ratio = 0.4**	**Ratio = 0.5**	**Ratio = 1**
PV (kW)	309	209	335	419	838
Battery (kWh)	642	513	513	513	513

Table 6.1: Comparison of jointly-owned community asset capacity and individually-owned assets' capacities for PV ratio = 0.25, 0.4, 0.5 & 1.

Assets	**Community assets size**	**Sum of individual agents assets' capacities**			
	Ratio = 0.37	**Ratio = 1.5**	**Ratio = 2**	**Ratio = 2.5**	**Ratio = 3**
PV (kW)	309	1256	1675	2094	2513
Battery (kWh)	642	513	513	513	513

Table 6.2: Comparison of jointly-owned community asset capacity and individually-owned assets' capacities for PV ratio = 1.5, 2, 2.5 & 3

The yearly bills of the individual agents are computed under various PV ratios with P2C market mechanism, and then compared with the yearly bills computed using the jointly-owned community assets. Yearly bill for the individual with P2C market mechanism is defined by Eq. (6.34). The yearly bills of community with jointly-owned assets corresponds to the yearly bills obtained by considering the network constraints as defined by Eq. (5.23) in Chapter 5. Yearly bills with P2C market mechanism is also obtained by considering

the grid constraints, but as specified in Chapter 5, there is no over-voltage. Similar to the community settings in Chapter 4 and 5, the baseline yearly bills corresponds to the yearly bills computed for individual agents and community without generation or storage energy assets. Table 4.1 shows the baseline bills for both the flat tariff of 16 pence/kWh [222] and dynamic Agile Octopus ToU tariff [224]. However, in this chapter with P2C market mechanism we will be referring to the fixed tariff pricing scheme only.

The community annual bill obtained from jointly-owned assets and the sum of individual households bills computed with and without P2C market mechanism are shown in Table 6.3 for PV ratio equal to 0.4, 0.5 & 1, and Table 6.4 for PV ratio equal to 1.5, 2 & 2.5.

	Community yearly bill (£)	**Sum of individual agents yearly bills (£)**					
Assets	**Ratio = 0.37**	**Ratio = 0.4**		**Ratio = 0.5**		**Ratio = 1**	
Adoption		**With P2C**	**No P2C**	**With P2C**	**No P2C**	**With P2C**	**No P2C**
PV Only	119315	117156	123006	118074	124316	130619	137231
PV & Battery	115664	115926	116977	115584	116801	124797	126271

Table 6.3: Economic comparison of jointly-owned community assets and individually-owned assets with and without P2C market for PV ratio equal to 0.4, 0.5 & 1

	Community yearly bill (£)	**Sum of individual agents yearly bills (£)**					
Assets	**Ratio = 0.37**	**Ratio = 1.5**		**Ratio = 2**		**Ratio = 2.5**	
Adoption		**With P2C**	**No P2C**	**With P2C**	**No P2C**	**With P2C**	**No P2C**
PV Only	119315	148371	154769	168149	174214	188924	194659
PV & Battery	115664	140904	142423	159523	161030	179397	180888

Table 6.4: Economic comparison of jointly-owned community assets and individually-owned assets with and without P2C market for PV ratio equal to 1.5, 2 & 2.5

As shown in Table 6.3, the community yearly bill obtained from jointly-owned community PV only is £119315. The minimum sum of individual agents yearly bills obtained with P2C market mechanism is £117156. This is obtained at the PV ratio equal to 0.4. Otherwise the community assets provides greater benefit. For the case without P2C the sum

of individual agents yearly bills obtained are much higher for all the ratios as compared to the community yearly bill.

Similarly, the community yearly bill obtained from jointly-owned community PV and battery is £115664. The minimum sum of individual agents yearly bills obtained with P2C market mechanism is £115584. This shows that individually-owned assets with P2C market mechanism offer slightly more benefit when the PV ratio is equal to 0.5. Otherwise, the community-owned assets offer more benefits as compared to individually-owned assets with and without P2C market mechanism.

For the PV ratio equal to 1.5 and above, the sum of individual agents yearly bills obtained are higher than the bills obtained without any assets as shown in Table 6.4. This clearly shows that at higher PV ratios, there is an increasing cost, but there is no further increase in the benefits. The reason for this is solar PV does not produce at the right times, and the control algorithm of the battery does not allow to sell electricity outside the production times. Agents/prosumers produce more electricity than needed, but agents cannot sell it, so there is no increase in the overall benefits.

Next, we present the the comparison of the profitability of the P2C market mechanism for all the community settings.

6.5.2 Impacts of the community's characteristics on the P2C scheme profitability

When the ratio of total yearly PV generation is increased then the PV capacity also increases and correspondingly the yearly bills also increased, which can prevent us from accurately study the impact of the community configuration. Hence, the cost of the assets are not considered while determining the yearly bills for different ratios of PV in the sensitivity study presented in this section. This is to allow us to study the real pricing dynamics among the three different low, medium and high P2C sellers. Here, the cost of the assets i.e yearly cost of battery and PV is not included in the yearly bills determined. For different ratios of PV generation, the yearly bills for three categories of P2C sellers are computed for the three different community settings 1 , 2 & 3. First, the results obtained for the community setting 1 is presented.

Community setting 1: all 200 households-prosumers with individually-owned optimal PV's and optimal batteries

The Figure 6.4 and Table 6.5 show the total yearly bills of Low, Medium & High Price P2C Sellers obtained with and without P2C market mechanism for different PV ratios. The total baseline bills obtained without assets for the Low, Medium & High Price P2C Sellers are included in Table 6.5 for comparison and analysis.

There is a significant reduction in the bills with the increase in the PV Ratio i.e PV generation is more than the demand as as shown in Figure 6.4 and Table 6.5. In this community setting 1, study shows that the High Price P2C Sellers are able to reduce more

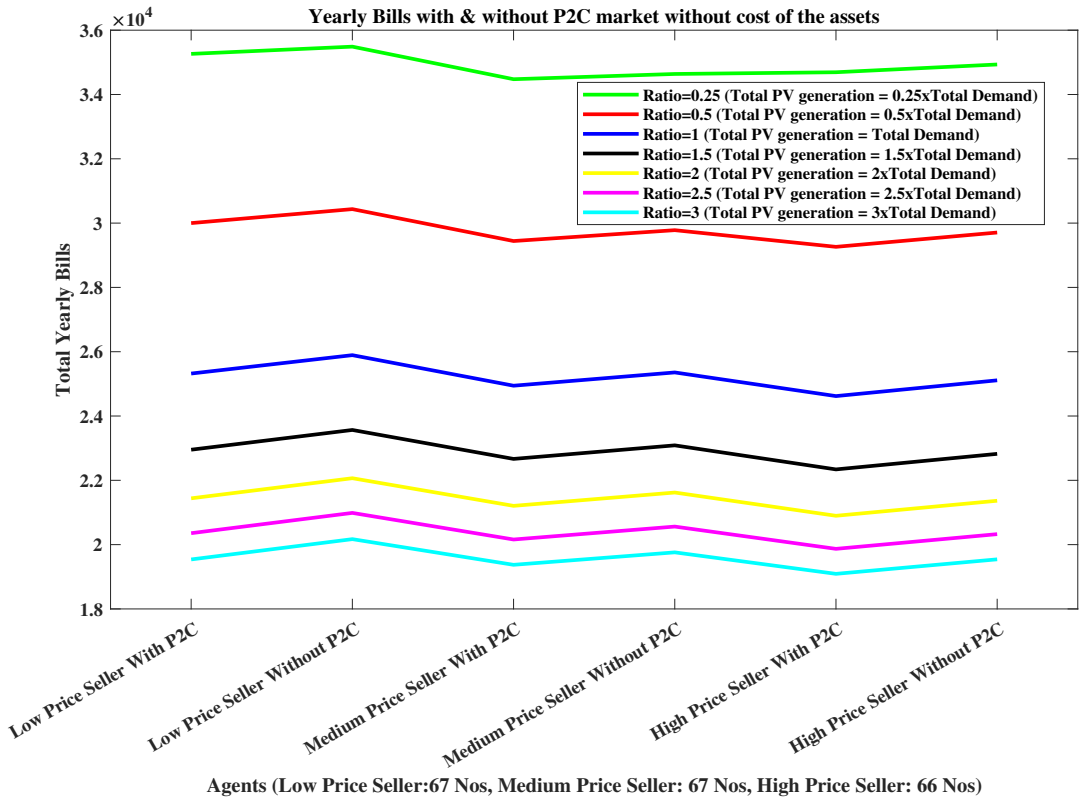

Figure 6.4: Comparison of total yearly bills for community setting 1.

Prosumers (Sellers)	Sum of individual agents yearly bills (£) PV Ratios 0.25	0.5	1	1.5	2	2.5	No Assets
Low Price_P2C	35263	30000	25321	22952	21440	20356	45356
Low Price _No P2C	35488	30435	25893	23566	22065	20987	45356
Medium Price_P2C	34475	29442	24943	22666	21206	20159	43991
Medium Price_No P2C	34638	29780	25355	23088	21620	20561	43991
High Price_P2C	34692	29262	24620	22339	20897	19869	45109
High Price _No P2C	34934	29707	25110	22823	21365	20326	45109

Table 6.5: Comparison of total yearly bills for community setting 1.

bills compare to Low & Medium Price P2C sellers, and Medium Price P2C Sellers are able to reduce the bills the least for all the different PV ratios (constrained scenarios-low to high

PV generation as compared to demand) as shown in Table 6.5. The reduction in the bills is computed comparing the bill obtained for different P2C sellers with the baseline (bills obtained without assets) bills. However, when we compare the cases with and without P2C market mechanism, there is no significant reduction due to P2C market mechanism for all the three low, medium and high P2C Sellers for all the PV ratios.

The reduction in the bill is mainly because each individual agent already have larger capacity PV (as the ratio increases) and optimal batteries that are used for maximizing the self-consumption. Hence, in this Community Setting 1 the study shows that the P2C market mechanism does not offer economic or financial benefits to the community if all the households invest in energy assets.

Community Setting 2: 100 households-prosumers with individually-owned optimal PV's and optimal batteries, and 100 households-consumers without assets

The Figure 6.5 and Table 6.6 show the total yearly bills of Low, Medium & High Price P2C Sellers, and consumers obtained with and without P2C market mechanism for different PV ratios. The total baseline bills obtained without assets for the Low, Medium & High Price P2C Sellers, and consumers are included in Table 6.6 for comparison and analysis.

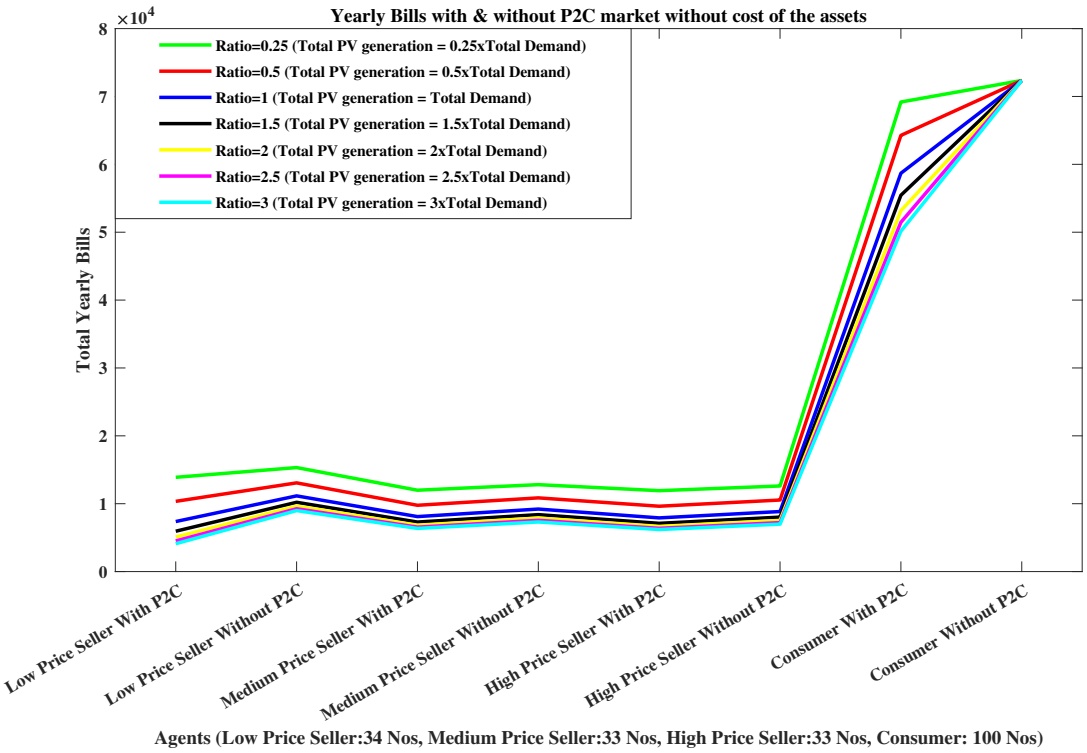

Figure 6.5: Comparison of total yearly bills for community setting 2.

Comparing to community setting 1, in this community setting 2, there is a significant reduction in the bills of low, medium and high price P2C sellers and consumer with P2C mechanism as compared to the case without P2C market mechanism as shown in Figure 6.5 and Table 6.6. In this community setting 2, study shows that the Low Price P2C Sellers are able to reduce more bills compare to Medium & High Price P2C sellers. This is due

Prosumers (Sellers) and Consumers	Sum of individual agents yearly bills (£) PV Ratios						
	0.25	0.5	1	1.5	2	2.5	Baseline
Low Price _P2C	13889	10347	7374	5944	5083	4513	22981
Low Price _No P2C	15324	13069	11152	10209	9640	9260	22981
Medium Price_P2C	11987	9767	8101	7298	6833	6550	19279
Medium Price_No P2C	12806	10859	9211	8390	7889	7552	19279
High Price_P2C	11919	9628	7909	7109	6654	6378	19837
High Price_No P2C	12612	10541	8845	8023	7538	7215	19837
Consumer_P2C	69184	64265	58689	55447	53168	51458	72358
Consumer_No P2C	72358	72358	72358	72358	72358	72358	72358

Table 6.6: Comparison of total yearly bills for community setting 2.

to the market mechanism. indeed, lower prices are chosen before. However, it could be that higher price make greater profit per unit and that at low PV ratio , they get energy to sell, so make more savings. In this setting also Medium Price P2C Sellers are able to reduce the bills the least for all the different PV ratios (constrained scenarios-low to high PV generation as compared to demand) as shown in Table 6.6. The study shows that there is an optimal price strategy depending on the community setting, or depending on the amount of PV generation (PV ratio).

Furthermore, the consumers are able to reduce bills more at the higher PV ratios, which is evident as the consumers are able to buy more energy from P2C market at higher PV ratios i.e more PV generation are available for P2C market.

Community Setting 3: 67 households-prosumers with individually-owned optimal PV's and optimal batteries, 33 households-prosumers with individually-owned optimal PV's only, and 100 households-consumers without assets

The Figure 6.6 and Table 6.7 show the total yearly bills of Low, Medium & High Price P2C Sellers, and consumers obtained with and without P2C market mechanism for different PV ratios.

Similar to community setting 2, in this community setting 3, there is also a significant reduction in the bills of low, medium and high price P2C sellers and consumer with P2C mechanism as compared to the case without P2C market mechanism as shown in Figure 6.6 and Table 6.7.

In this setting also, the low price P2C sellers are able to reduce more bills for all the PV ratios than all other sellers. This is due to the market mechanism. indeed, lower prices are chosen before. However, it could be that higher price make greater profit per unit and that at low PV ratio , they get energy to sell, so make more savings. Furthermore,

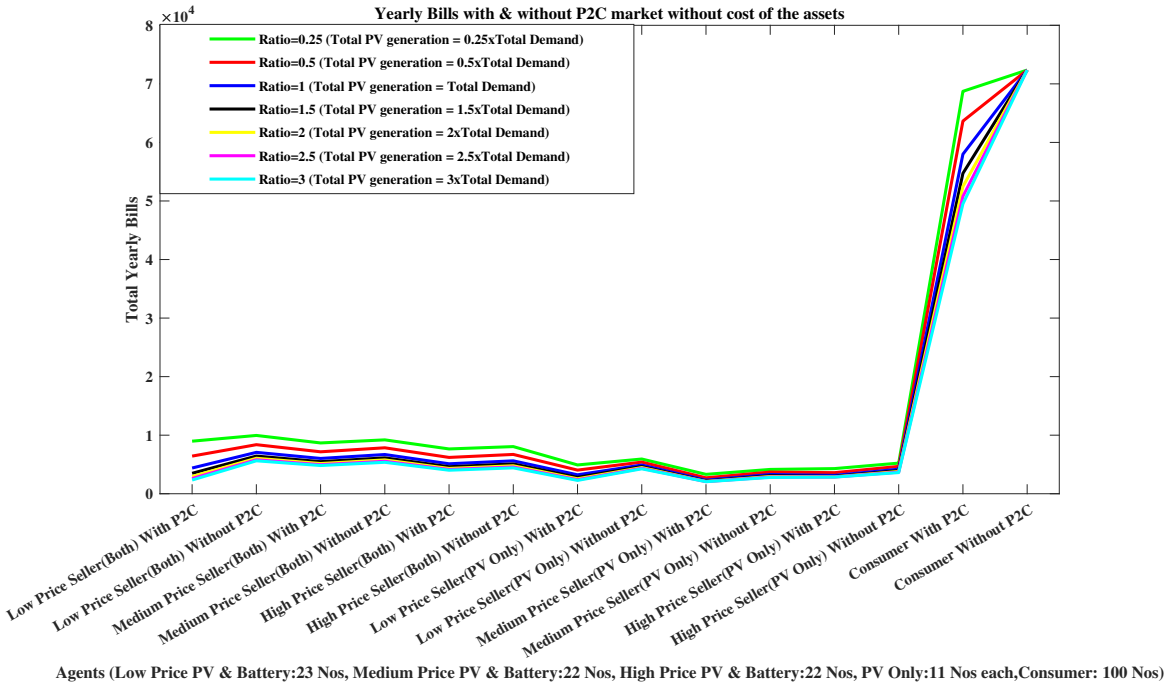

Figure 6.6: Comparison of total yearly bills for community setting 3.

Prosumers (sellers) and Consumers	Sum of individual agents yearly bills (£)						
	PV Ratios						
	0.25	0.5	1	1.5	2	2.5	No Assets
Low (PV & Battery)_P2C	8975	6427	4391	3488	2949	2596	15501
Low (PV & Battery)_No P2C	9956	8377	7066	6431	6052	5802	15501
Medium (PV & Battery)_P2C	8674	7161	6026	5477	5156	4956	13666
Medium (PV & Battery)_No P2C	9200	7846	6697	6125	5777	5542	13666
High (PV & Battery)_P2C	7649	6200	5113	4610	4320	4142	12696
High (PV & Battery)_No P2C	8051	6713	5618	5088	4774	4566	12696
Low (PV)_P2C	4916	4036	3232	2802	2552	2387	7479
Low (PV)_No P2C	5928	5402	4900	4639	4468	4347	7479
Medium (PV)_P2C	3309	2720	2324	2165	2097	2069	5613
Medium (PV)_No P2C	4151	3698	3284	3075	2944	2851	5613
High (PV)_P2C	4292	3598	3131	2955	2888	2855	7141
High (PV)_No P2C	5226	4669	4190	3951	3799	3692	7141
Consumer_P2C	68727	63644	57992	54721	52459	50789	72358
Consumer_No P2C	72358	72358	72358	72358	72358	72358	72358

Table 6.7: Comparison of total yearly bills for community setting 3.

the consumers are able to reduce more bills in this settings as compared to community setting 2 for all the PV ratios. This reduction could be because in this setting there are less prosumers with battery assets, so more energy are available in the P2C market for the consumers.

6.5.3 Discussion of results

In this section, we present the overall findings of the study on comparison between the community with P2C market versus jointly-owned assets, and the comparison of all the community settings with all P2C market mechanism. In Figure 6.5 & 6.6, consumers are also shown along with the P2C sellers (prosumers) to indicate the benefits obtained by consumers from P2C market compared the case without P2C market mechanism. The P2C local market mechanism is designed such that at the end of the P2C market, if there is energy import from grid, then it is ensured that there is no energy export to grid and vice-versa. Furthermore, the proposed P2C market does not provide any service/improvement to network/grid as demand response is not considered for the community. This is validated by ensuring that at every operation time period, the difference between the total deficit energy to buy and total excess energy to sell are always equal to the difference between the total imported energy from grid and total energy exported to grid as shown by Eq. (6.37).

$$P_{\text{Total}}^{\text{deficit}}(t) - P_{\text{Total}}^{\text{excess}}(t) = P_{\text{Total}}^{\text{Grid Import}}(t) - P_{\text{Total}}^{\text{Grid Export}}(t) \tag{6.37}$$

On comparison of total yearly bills with and without P2C Market mechanism, the study shows that there is no significant reduction in the bills due to P2C market mechanism for all the three Low, Medium and P2C sellers for all the PV Ratios. In the Community Setting 1, it is found that the energy traded within P2C local market is extremely low as compared to the grid imports resulting in the same yearly bills with and without P2C local market. This is mostly because each prosumer (household/agent) has already a larger capacity optimal battery and optimal solar PV for maximizing self-consumption. Furthermore, with the current rule-based battery control algorithm, it is unlikely that the users owning solar PV and battery will have surpluses to sell while there is no demand response or change in their usage of the battery depending on the market needs. Therefore, the profitability of the P2C market scheme was minimum for the Community Setting 1. It clearly shows that P2C scheme is not profitable if all the households/agents own energy assets such as PV and battery.

Hence, sensitivity study on the Community Setting 2 & 3 was conducted to understand the right community settings that make the P2C market scheme profitable for the community. Community Setting 2 & 3 show a more realistic community with diversity of assets (mixture of prosumers and consumers). The study shows that the reduction in the bills due to P2C market mechanism compared to the bills obtained without P2C market scheme is indeed greater for the Community Setting 2 & 3. Results shows that the Low Price P2C Sellers are able to reduce more bills compare to Medium & High Price P2C sellers for all the PV ratios for both the community settings 2 & 3. This can be

explained by the fact that in this specific market setting, priority is given to the low price sellers. Therefore, little energy quantity is awarded to higher price sellers, and despite their unitary price, the overall benefits are lower for sellers with higher prices. In the same time, consumers (agents without assets) are able reduce their yearly bills for all the PV ratios as compared to the case without P2C market mechanism for both the community settings 2 & 3. This shows that the right setting of the community is paramount to make local Peer-to-Community market schemes profitable to the community. Furthermore, study clearly shows that P2C scheme is less profitable if there is no demand response strategy in the community settings.

Next, we propose to study the difference between a real time vision and a half-hourly vision in terms of real imports/exports, and impacts on the grid. The sensitivity study on the energy community settings with local P2C market mechanism is further extended to explore and assess what kind of market that is determined in terms of import/export from the grid and local P2C market using the minutely real-time simulation versus half-hourly P2C market clearing time interval simulation. This comparison of P2C market with minutely real-time simulation versus half-hourly P2C market clearing time interval simulation in the following Section 6.6.

6.6 Economic study and comparison of P2C market with minutely real-time simulation versus half-hourly market clearing simulation

In this thesis, the community settings are operated based on the assumption of perfect knowledge of the future consumption and generation. However, in practice the future consumption and generation are forecasted on a half-hourly basis. While considering the half-hourly market clearing mechanism, the local P2C market makes us believe that the community will self-consume most of the electricity, and there is no need for the import from the grid. However, while looking closer (at a minute time frame), the community might not be self-sufficient at all as it actually does not always produce at the same time as it consumes. At this half-hourly clearing time, if the community imports from the grid then this rises the question around settlements in the energy market. When a half-hourly LEM states that the community is balanced, is it truly balanced when looking at a minutely time interval? Particularly, how much the grid services are used, and what kind of fees and payment to be settled for the grid services. In this section, to address this question, an economic study and comparison of P2C market with minutely real-time simulation versus half-hourly market clearing simulation is presented.

In this study, a recent demand profile and solar PV generation of 55 households with one minute resolution from the ReFLEX (Responsive Flexibility) project [8] is considered. The minutely resolution demand and generation data allows us to compare the households import/export from/to grid of P2C market with minutely real-time simulation versus half-hourly market clearing simulation. Furthermore, the one-minute resolution data was

preferred over half-hourly resolution demand data in order to determine the power flow accurately as the half-hourly demand represents the energy not the power. Similar to the community settings described in Chapter 4 and 5, we choose to use an optimal size for both solar PV generator and the battery storage corresponding to the minutely resolution demand and generation data. Every individual agent/prosumer owns his optimal PV size and optimal battery capacity. A summary of the model parameters is shown in Table 6.8. This model corresponds to the Community Setting 1 as presented in Section 6.2.

Parameters	P2C Model
Sum of individual agent monthly demand (kWm)	4177175
Sum of optimal individual PV's (kW)	62
Sum of optimal individual battery (kWh)	2053
Fixed tariff (pence/kWh)	16
Unitary cost of battery (£/kWh)	150
Unitary cost of PV generation (£/kW)	1100

Table 6.8: Optimal PV and optimal battery capacities, and other parameters of the P2C model simulated for 55 households

Here, we have assessed the difference in the import/export from/to the grid & P2C market using the minutely real-time simulation versus half-hourly P2C market clearing time interval simulation to understand the evolution of local markets. As described in previous Section 6.3, initially using the Algorithm 6.1, individual agents optimizes their own consumption. Then, during the excess generation, the excess power is exported to local P2C market, and during the deficit period, the remaining power is imported either from the P2C market or utility grid. Finally, using Algorithm 6.2, the same detail Peer-to-Community (P2C) market mechanisms described in Section 6.4 is used for the study of three different P2C sellers in an non-uniform pricing scheme of the local P2C market (as presented in Section 6.4.1). This model corresponds to the Community Setting 1, all 55 households-prosumers with individually-owned optimal PV's and optimal batteries. In this setting, the 55 prosumers are randomly allocated into different categories of P2C sellers (non-uniform pricing scheme) as follows:

i Low price sellers: 18 households

ii Medium price sellers: 18 households

iii High price sellers: 19 households

For a half-hourly market clearing simulation, the minutely demand and generation data is aggregated into half-hourly basis to determine the parameters such as import/export from/to grid, and import/export from/to P2C market. For a minutely real-time simulation, parameters such as import/export from/to grid, and import/export from/to P2C market are computed using the real-time minutely data. The final computed parameters are aggregated into half-hourly basis to compare with the parameters obtained from half-hourly market clearing simulation.

The study is mainly focussed on the comparison of energy imports from grid computed using half-hourly market clearing simulation with the imports from grid computed using minutely real-time simulation. Figure 6.7 shows the energy imported from grid using minutely real-time and half-hourly market clearing time period simulated for low-price seller of non-uniform pricing scheme. It can be observed that the imports from the grid not exactly the same. But very close for both the case with real-time minutely simulation and with half-hourly market clearing simulation. Similar result results are obtained for the high and medium price sellers.

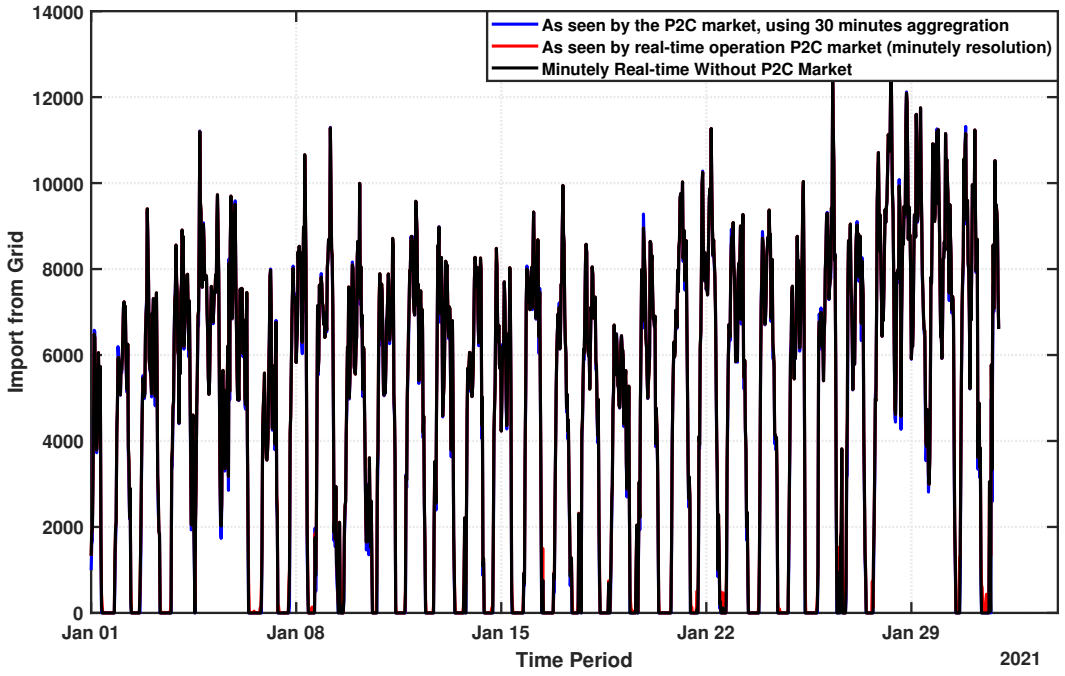

Figure 6.7: Import from grid computed using minutely real-time and half-hourly market clearing simulation.

6.6.1 Discussion of results

In this study, the comparison was made on the import from the grid as seen by the P2C market. The analysis involved using 30-minute aggregation and real-time minutely operation with and without P2C local market operation. The primary objective was to assess the self-sufficiency of the community in terms of energy consumption. The results from the study show that most of the time the imports from the grid are same in all the three scenarios(half-hourly clearing mechanism, minutely real-time with P2C market, and minutely real-time without P2C market) studied.

6.7 Concluding remarks

In this chapter, a local Peer-to-Community (P2C) market mechanism is proposed for a community. The main goal is to enable individual households to equitably share the resources and benefits derived from their investments in individually-owned energy assets. The proposed P2C model consists of mainly two stages. First, the individual households/agents optimizes their own self-consumption from energy assets and then trade the energy locally through P2C markets. The battery control mechanism is implemented to optimize their own consumption and production, and then the deficit and excess power are computed and proposed to be traded in the P2C market. The dynamics of the proposed P2C market mechanism is studied for three different types of P2C sellers (non-uniform pricing scheme) and tested for three different types of community settings (mix of prosumers and consumers) under different ratios of PV generation. We computed yearly bills resulting from the proposed algorithm of multi-unit auction P2C market clearing mechanism. The yearly bills were used for the techno-economic comparison of investment in individually-owned assets with and without P2C market mechanism versus jointly-owned community assets. The profitability of the proposed P2C market mechanism is tested for different settings of the community under different rates of renewable energy adoption.

Experimental results (based on the real input data from the UK) show that, the profitability of the P2C market scheme was minimum for the Community Setting 1 (all prosumers). It clearly shows that P2C scheme is not profitable if all the households/agents own energy assets such as PV and battery. On the other hand, the study shows that the reduction in the bills due to P2C market mechanism compared to the bills obtained without P2C market scheme is more for the Community Setting 2 & 3 (mixture of prosumers and consumers). Results show that the Low Price P2C Sellers are able to reduce more bills compare to Medium & High Price P2C sellers for all the PV ratios for both the community settings 2 & 3. Meanwhile, consumers (agents without assets) are able reduce their yearly bills for all the PV ratios as compared to the case without P2C market mechanism for both the community settings 2 & 3. The study show that the local P2C market mechanism can be profitable to the community only if it is integrated with suitable demand response strategies, and should possess the capability to change the usage of the battery depending on the market needs. Furthermore, the benefit of the P2C market mechanism is limited if there is no option to export to utility grid, and most importantly the profitability depends on the right settings of the community. Otherwise, the jointly-owned community energy assets provide higher benefits to the community.

Hence, the study shows that in a realistic community with diversity of assets, P2C local market mechanism are a tangible solution to provide a lower cost energy access, and thus setting of right pricing mechanisms and inclusion of demand response schemes are crucial in realizing the full benefit of smart local energy system integrating P2C markets. The results from the study also highlights the need for smart local energy system planning and simulation tools.

Finally, the results from the comparative study of P2C market with minutely real-time simulation versus half-hourly market clearing simulation shows that the import from the grid is same for all the three scenarios studied. This result helps us to validate that during half-hourly market clearing period, the community is self-sufficient from the local P2C market, and there is almost no import from the grid. Otherwise, there should be a balancing mechanism to pay for the energy and services provided by the grid. This would require an appropriate settlement mechanism in local energy markets.

Chapter 7

Conclusions and Future Work

7.1 Overview of results of the thesis

Energy communities formed by prosumers are increasingly becoming a promising solution to delivering sustainable energy systems that promote renewable integration and active participation of end-users. Energy community projects often involve jointly owned energy assets such as community-owned wind turbines, solar PVs and/or shared battery storage. Energy communities are a promising concept, that can enable better use of locally generated renewable energy. However, given that not all members have the same size, energy needs or demand profiles, a key challenges are how these assets can be efficiently controlled in real time, how the useful lifetime of the asset can be modelled and enhanced using AI, and how the energy outputs from jointly-owned community energy assets should be shared fairly among community members. Crucially, such real-time control and fair sharing of energy must also consider the technical constraints of the community, such as physical network/grid characteristics, voltage limits and electrical cable thermal limits. Energy community models and local energy solutions face numerous challenges to achieve successful rollout and adoption. Most importantly, these new business models need to be accepted by end-users and need to promote sustainable behaviour, value creation and active engagement. In this thesis, we argue that there are several key objectives that need to be met to achieve these goals.

In this thesis, a techno-economic modelling methodology is proposed that couples battery control, battery degradation, community energy from renewable energy sources (RES) with LV network operating constraints, and a fair redistribution optimization of benefits to jointly owned assets. The control mechanism was implemented for both fixed electricity tariffs and dynamic ToU tariffs to compare the benefits obtained when an individual household invest in their own energy assets versus investing jointly in a community-owned energy assets. To compare the economic performance of investments in community-owned assets and individually-owned assets, we considered an energy community of two hundred prosumers, that were all modelled by real time-series data of generation and consumption profiles from a community in UK for a full year. We computed yearly bills resulting from the proposed battery control algorithm and compared

the yearly bills computed with and without network constraints to assess how network/grid constraints can impact the deployment of individual and community-owned assets.

Next, in the context of energy communities with community-owned assets, a practically applicable and computationally efficient redistribution mechanism was developed. The primary aim was to ensure a fair distribution of energy and the associated financial benefits among the community members who own the assets. This redistribution mechanism is based on the marginal contribution of each member, which is a key concept from coalitional game theory that looks at rewarding members based on the value they provide to the community. It was demonstrated that the proposed redistribution mechanism is applicable to all types of community-owned assets, including storage assets. This was achieved despite the apparent challenge of accurately assessing how each community member benefits from these assets.

Finally, a framework of peer-to-community (P2C) local market mechanism is proposed as an alternative to investment in jointly-owned community energy assets in the case when the integration of the community assets are limited due to physical network/grid constraints. The local P2C market mechanism enable households to share and trade energy by investing in the distributed individually-owned energy assets. The profitability of the P2C market mechanism is studied for different constraint settings in terms of total generation versus total demand, and investigated how much each type of generator produced energy, how much they could sell locally (P2C) and produce profit. In summary, in this thesis we investigated a model of a community investment and sharing of energy assets, including renewable generation and battery storage in a market pricing regime of fixed electricity tariffs and dynamic time of use (ToU) tariffs. The main research works and key findings of this thesis is presented in the next section.

7.2 Summary of research work and key findings

The first part of the research work undertaken studied a model of a prosumer-based control algorithm was presented and assessed by incorporating the latest heuristics of battery state of health for both at an individual/prosumer level and at a community level. The control algorithm was implemented for different economic parameters that were altered in order to investigate and realize a sensitivity study on the profitability of batteries at the level of individual prosumers. Results from this work display a good performance of the heuristic-based scheduling when electricity import prices are relatively higher than export prices. The simulation analysis (based on real demand profiles, generation data, physical asset profiles and import prices in the United Kingdom at the time of writing) shows that investment in batteries can be an economical feasible proposition, but this result depends on economic parameters such as the cost of the battery, the export prices of electricity, but also the type of services for which the battery can get revenues. This output based on a large-scale study of 200 households is relevant for industrials and investors to confirm business models around battery use.

Next, the research work in this thesis studied the principled model of community investment and sharing of energy assets, such as renewable generation and battery storage for both fixed and dynamic time of use (ToU) tariffs. Specifically, the research work studied the techno-economic analysis of investment in distributed individually-owned energy assets versus investment in jointly-owned community energy assets. Results from the techno-economic analysis show that community assets provide more savings (higher benefits) compared to distributed, individually-owned assets. The advantages from community assets are multiple. First, community assets require a lower capacity for the same services, hence potentially a lower cost. Second, community assets achieve lower annual energy bills for both pricing schemes considered in the study. The study highlighted the importance for determination of fair redistribution or allocation of benefits achieved in community projects.

In this vein, various benefit redistribution schemes (four methods in total, based on current practices) were explored. Work in this thesis proposed a method based on the marginal contribution of each prosumer, a key concept that assures fair distribution in coalitional game-theory. It was demonstrated that the proposed scheme achieved better performance than other methods, while also providing the additional advantage of being computationally tractable. Hence, the proposed marginal cost redistribution method is fair, scalable, and more practically applicable. Results (based on real large-scale case study of 200 households) shows that the proposed redistribution method yields to a greater reduction of the annual bill for almost 67% of the community households compared state-of-the-art methods. This 67% fraction of the prosumer agents corresponds to households with lower annual consumption (small demand profiles). Although large consumers benefit slightly less under this proposed redistribution scheme, they still obtain the highest bill reduction in value as compared to households with lower demand profiles. Therefore, the proposed redistribution mechanism achieves a fairer redistribution leading to greater social acceptance, key to incentivising more communities to form coalitions and invest in jointly-owned renewable energy assets. Furthermore, current energy communities usually employ algorithms based on proportionality of consumption to redistribute the benefits from the community assets. However, such methods are not fair, and not applicable in the case of energy storage assets, especially community-owned batteries as it is not easy to determine who used more the battery assets than others. This is another key point that demonstrates the advantages of the proposed redistribution mechanism based on marginal contribution. Hence, the redistribution method proposed in this thesis fills a key knowledge gap by providing a fair redistribution method that applies to both community-owned renewable generator and storage assets.

The physical network (the LV distribution grid) is an essential entity that allows the exchange of energy in the settings of the energy communities. However, an important aspect that has often been neglected in existing research on energy community models is the relevance of the distribution grid's technical limits. In this thesis, a comprehensive model is provided to study the effect of such physical network and operational constraints in the energy community setting by including the power flow (network/grid constraints) in

techno-economic analysis of investment in distributed individually-owned energy assets versus jointly-owned community assets. Experimental results from our study show that, overall, the operation of individually-owned distributed assets are less impacted by grid constraints than the operation of community-owned assets. Indeed, when generation is not located close enough to consumption, it might lead to local over-voltage that could result in curtailment by the distribution system operator of export from community-owned assets. This curtailment reduces the overall saving of the community, which illustrates the importance of considering the physical grid constraints in the energy community schemes. However, even with curtailment due to grid constraints, the economic comparison between community-owned assets and individually-owned assets still shows that community-owned assets provides better benefits to energy communities for both tariffs schemes studied. Hence, this thesis work further studied the effect of physical network constraints on the redistribution schemes.

Subsequently, an approximated marginal cost redistribution method was developed to address the computational challenge while considering the network/grid constraints. The results showed that the individual agents yearly bills obtained after redistribution by approximated marginal cost redistribution method is similar to results obtained by redistribution mechanism without approximation, with the correlation coefficient of 99.99% for both the fixed and dynamic tariffs. Hence, while considering the network constraints, approximated marginal cost redistribution method can be used to redistribute the benefits from community owned assets, as it is much more computationally tractable particularly while considering the large realistically-sized community settings. This represents a significant contribution to the state-of-the-art of sharing resources in energy communities.

The last part of this thesis was devoted to the study of the profitability of the local peer-to-community (P2C) market mechanism for the households with individually-owned energy assets. The framework for the P2C market mechanism includes the method for achieving fairness and equity in the distribution pf total energy available for the local P2C market among the P2C buyers and sellers. A single market clearing price is obtained by running the multi-unit auction, where the price per unit is averaged for each unit. In the proposed P2C market mechanism, we assume every consumer must satisfy their energy demands (either from the grid or the local P2C market), and averaging over the multiple units of price is the fairest way to share the cost for that market. The study shows that in a realistic community with diversity of assets, P2C local market mechanism are a tangible solution to provide a lower cost energy access, and thus setting of right pricing mechanisms and inclusion of demand response schemes are crucial in realizing the full benefit of smart local energy system such as P2C markets. The results from the study also highlights the need for smart local energy system planning and simulation tools. Furthermore, this thesis studied the comparison of P2C market with minutely real-time simulation versus half-hourly market clearing simulation to validate if the community is self-sufficient during the aggregated half-hourly market clearing periods. To achieve this, the total energy import/export from/to grid during a minutely real-time simulation is compared with the total energy import/export from/to grid obtained during half-hourly market clearing

simulation. The results from the comparative study shows that the import/export from/to the grid is same for both the minutely real-time simulations and half-hourly clearing simulation. This result helps us to validate that during half-hourly market clearing period, the community is self-sufficient from the local P2C market, and there is no import from the grid. Otherwise, there should be a balancing mechanism to pay for the energy and services provided by the grid. This would require an appropriate settlement mechanism in local energy markets.

Finally, the proposed energy community model is implemented and validated using a real case study from the UK based large-scale smart energy demonstration project. To our best knowledge, this thesis models the control of energy community assets from an economic and technical perspective with an unprecedented level of detail. This includes for example, incorporating real state-of-the-art battery control and degradation functions, using real commercially-available, dynamic tariffs from the UK market, as well as a whole year of high-granularity demand and renewable generation data. Although, while the experiments and validation are based on the UK project, the proposed community energy methods are general in scope, and can apply to any country where such community energy schemes are undertaken. The concept of energy communities is equally important - arguably even more so - in developing countries, the proposed energy community models in this thesis can be more relevant to such developing countries, because energy users in such communities often have limited or no access to electricity from a central power grid, and hence rely on the community energy project for their power needs.

Overall, this thesis presented a model of the community investment in energy assets for both the fixed and dynamic tariffs. The work proposed a data-driven analysis to quantify the savings of community-owned versus individually-owned energy assets incorporating the physical assets degradation and network/grid constraints. Then, inspired by coalitional game theory methods, this thesis provides a novel algorithm to fairly redistribute among community members the benefits from community owned assets, which is shown to have desirable redistribution and computational benefits, compared to existing state-of-the-art methods for sharing output of community energy assets. This work is one of the first, to our knowledge, to integrate a battery depreciation model and power flow (network/grid constraints) into community energy optimization modelling. Data-driven monitoring of energy assets state of health is crucial for economically viable integration of local renewable generation, and the community energy model provides a very attractive application. Moreover, for researchers interested in cooperative game theory application in energy (which is a growing research area), the proposed model is one of the first to use such concepts in a community energy setting. Specifically, we propose a redistribution model for benefits in a community based on marginal value, a key concept in cooperative game theory. Next, the future directions of the research work identified for this thesis is presented in the following section.

7.3 Future work

The following directions are identified for future work consideration with regards to the work presented in this thesis:

- **Consideration of hybrid energy assets and further analysis of the proposed methodologies**

  In the existing energy community model, the focus is primarily on two main configurations: a solar PV generator combined with battery storage or a wind turbine along with battery storage. However, with the increasing involvement of prosumers and communities in sustainable energy solutions, there is an opportunity to explore and invest in hybrid renewable generators integrated with battery storage. These hybrid systems combine PV solar panels, wind turbines, and battery storage to create a more efficient and versatile energy solution. Therefore, in future endeavours, our aim is to enhance the energy community model by incorporating these hybrid energy assets. By expanding the scope to include hybrid renewable setups, we envision a more comprehensive and adaptable energy community model. Furthermore, in future work, the plan is to enhance the current community model and the proposed methodologies, specifically:

  i. Conduct sensitivity analysis of the location of the jointly-owned community energy assets in the LV distribution grid. In the current model, it is assumed that the jointly-owned community energy assets either PV or a battery storage is assumed to be located at the centre of the network. However, there is still a need to determine the optimal location of the community assets.

  ii. Accurately quantify the error made by using the lesser battery life models, especially in terms of difference between using calendar or Ah (ampere-hour) metrics and assuming one cycle per day at the given DoD (Depth of Discharge).

  iii. Accurately quantify the scaling of the proposed redistribution method

  iv. Identify the effect of correlation between generation and consumption on the proposed redistribution schemes.

  v. Conduct further analysis to asses the overall attractiveness and acceptability of the proposed redistribution method based on marginal contribution to different agents within the community, including those with higher decision-making power due to their wealth. This evaluation will consider various factors, such as economic considerations, decision-making power, and potential incentives that may influence stakeholders' perspectives. By quantifying these aspects, we aim to provide a comprehensive understanding of the method's viability and its alignment with diverse stakeholder interests.

- **Consideration of new revenue streams for energy assets**

  In the current heuristic-battery control algorithm, we have not considered the demand response or grid services to change the usage of battery depending on the market

needs. In future work, our study can be extended to consider new revenue flows though participation in energy and ancillary service markets, such as providing demand-side flexibility services to the distribution system operator. Local flexibility markets are identified as a promising low-cost solution to address the ever-increasing grid issues as an alternative option to expensive grid reinforcement and unnecessary curtailment of loads and renewable generation. Energy communities can leverage the controllable assets such as batteries to provide reliable flexibility for the energy and ancillary services markets.

- **Consideration of consumer preferences and needs**

  Future work will also consider to integrate consumer preferences and needs in the community optimization model to achieve realistic local-tailored solutions aligned to end-user needs. Energy is often treated as a homogeneous product; however, research indicates that end-consumers may experience preferences related to the energy source or destination, they may prefer several RES technologies over others or may prefer trading energy with peers from their community. Sustainable behaviour is influenced by end-user values, such as caring for convenience, individual interest or caring for others or the environment. These are normally referred as "side constraints" or "preference constraints" to the efficient market in efficient mechanism design [241]. In future work, it will be more interesting and practically important to compare what happens if such constraints are integrated with the local P2C or P2P market clearing mechanisms.

- **Consideration of uncertainty in the generation and demand**

  In this thesis, the community settings are operated based on the assumption of perfect knowledge of the future consumption and generation. However, in practice the future consumption and generation are forecasted, and there may be a great degree of uncertainty associated with these forecasted generation and demand profiles. Another potential future work is to extend the community energy models by considering the uncertainty in the generation and demand, particularly focussing on the accurate forecasting of at local level by taking into account the uncertainty in the renewable resources and demand side. Considering battery energy management systems, this translates into reasoning about the definitions of optimal decisions while also looking at forecast uncertainty to check the robustness of a proposed methods.

- **Model extension for multi energy vectors**

  Another potential future work is to consider extensions of our model that take into account other energy vectors and assets - such as transport and community-shared hydrogen fuel cells. In this context, green hydrogen is increasingly being explored as a promising energy storage solution, for renewable communities with excess renewable generation.

- **Development of other redistribution schemes**

While this thesis focuses on the key topic of marginal cost redistribution mechanism, there are many other fairness concepts that could be explored in energy applications, and it would be relevant to compare their outcome to proposed marginal cost redistribution method. Specifically, the promising solution concepts such as Shapley Values [242], least-core or the nucleolus based on coalitional game theory, have been explored less in energy applications. The application and adaptation of such fairness concepts in energy could be a fruitful area, for both research and practice, providing energy communities with the computational tools to make best use of shared energy assets. Furthermore, another promising avenues of future research is to encode such redistribution mechanisms into smart contracts executed on blockchain systems [131, 42].

- **Modelling other use cases**

  Finally, one direction of work we plan to pursue is exploring the use of our community energy control and redistribution methods for remote communities, or communities in developing countries or regions, such as those in sub-Saharan Africa or parts of Asia. In such settings, energy consumers often do not have access to a central power grid, or power grid supply is unreliable, hence community energy projects often provide the only way to access electricity [129, 243, 244]. The methods proposed in this thesis could also be very relevant for these settings, and we plan to explore their application to remote and developing regions communities in future work.

References

[1] OurWorld in Data, "Renewable Energy." https://ourworldindata.org/renewable-energy, 2023. [Date Accessed: 2023-02-25].

[2] UN Sustainable Development Goals, "Goal 7: Affordable and Clean Energy." https://www.un.org/sustainabledevelopment/energy/, 2023. [Date Accessed: 2023-02-25].

[3] Intergovernmental Panel on Climate Change (IPCC) Report, "Climate Change 2022: Mitigation of Climate Change ." https://www.ipcc.ch/report/sixth-assessment-report-working-group-3/, 2023. [Date Accessed: 2022-02-25].

[4] UK Government, "Energy white paper: Powering our net zero future." https://www.gov.uk/government/publications/energy-white-paper-powering-our-net-zero-future, 2020. [Date Accessed: 2022-09-05].

[5] Y. Zhou, J. Wu, and C. Long, "Evaluation of peer-to-peer energy sharing mechanisms based on a multiagent simulation framework," *Applied Energy*, vol. 222, pp. 993–1022, 2018.

[6] European Commission (EU), "'Fit for 55': delivering the EU's 2030 Climate Target on the way to climate neutrality." https://eur-lex.europa.eu/legal-content/EN/TXT/?uri=CELEX%3A52021DC0550, 2023. [Date Accessed: 2022-02-25].

[7] GOV.UK, "Biggest ever renewable energy support scheme opens." https://www.gov.uk/government/news/biggest-ever-renewable-energy-support-scheme-opens, 2023. [Date Accessed: 2022-02-25].

[8] European Marine Energy Centre (EMEC), "ReFLEX: Responsive Flexibility ." https://www.reflexorkney.co.uk/, 2022. [Date Accessed: 2022-09-10].

[9] E. Mengelkamp, J. Gärttner, K. Rock, S. Kessler, L. Orsini, and C. Weinhardt, "Designing microgrid energy markets: A case study: The brooklyn microgrid," *Applied Energy*, vol. 210, pp. 870 – 880, 2018.

[10] Grid-Friends project, "Schoonschip, North Amsterdam-The most sustainable floating district in Europe." https://schoonschipamsterdam.org/en/, 2023. [Date Accessed: 2023-02-27].

[11] Auroville, "Auroville-the City of Dawn." https://auroville.org/, 2023. [Date Accessed: 2023-02-27].

[12] CATAPULT Energy Systems, "Delivering a Digitalised Energy System." https://es.catapult.org.uk/report/delivering-a-digitalised-energy-system/, 2022. [Date Accessed: 2022-09-20].

[13] J. Guerrero, A. C. Chapman, and G. Verbič, "Decentralized P2P Energy Trading Under Network Constraints in a Low-Voltage Network," *IEEE Transactions on Smart Grid*, vol. 10, no. 5, pp. 5163–5173, 2019.

[14] S. van der Stelt, T. AlSkaif, and W. van Sark, "Techno-economic analysis of household and community energy storage for residential prosumers with smart appliances," *Applied Energy*, vol. 209, pp. 266–276, 2018.

[15] The Office of Gas and Electricity Markets(Ofgem), "About the FIT scheme-Closure of the FIT scheme." https://www.ofgem.gov.uk/environmental-and-social-schemes/feed-tariffs-fit, 2022. [Date Accessed: 2022-09-15].

[16] S. Dong, E. Kremers, M. Brucoli, R. Rothman, and S. Brown, "Improving the feasibility of household and community energy storage: A techno-enviro-economic study for the UK," *Renewable and Sustainable Energy Reviews*, vol. 131, p. 110009, 2020.

[17] EnergyREV, "What is a smart local energy system?." https://www.energyrev.org.uk/news-events/blogs/what-is-a-smart-local-energy-system/, 2022. [Date Accessed: 2022-09-06].

[18] R. Ford, C. Maidment, C. Vigurs, M. J. Fell, and M. Morris, "Smart local energy systems (sles): A framework for exploring transition, context, and impacts," *Technological Forecasting and Social Change*, vol. 166, p. 120612, 2021.

[19] C. Etukudor, B. Couraud, V. Robu, W.-G. Früh, D. Flynn, and C. Okereke, "Automated negotiation for peer-to-peer electricity trading in local energy markets," *Energies*, vol. 13, no. 4, 2020.

[20] European Commission, "Best practices on Renewable Energy Self-consumption: Delivering a New Deal for Energy Consumers." https://ec.europa.eu/energy/sites/ener/files/documents/1_EN_autre_document_travail_service_part1_v6.pdf, 2022. [Date Accessed: 2022-09-12].

[21] Community Energy Scotland, "Community Energy Projects and Innovations." https://communityenergyscotland.org.uk/projects-innovations/, 2023. [Date Accessed: 2023-02-25].

[22] E. Commission, J. R. Centre, A. Uihlein, and A. Caramizaru, *Energy communities : an overview of energy and social innovation*. Publications Office, 2020.

[23] Scottish Government, "The future of energy in Scotland: Scottish energy strategy." https://www.gov.scot/publications/scottish-energy-strategy-future-energy-scotland-9781788515276/documents/, 2017. [Date Accessed: 2022-09-05].

[24] UK Government, "The Grand Challenges, Industrial Strategy: building a Britain fir for the future." https://www.gov.uk/government/publications/industrial-strategy-the-grand-challenges/industrial-strategy-the-grand-challenges, 2022. [Date Accessed: 2022-09-05].

[25] ReFLEX, "Energy Superhub Oxford (ESO)." https://energysuperhuboxford.org/about-the-project/, 2022. [Date Accessed: 2022-09-10].

[26] Project LEO, "Local Energy Oxfordshire)." https://project-leo.co.uk/, 2022. [Date Accessed: 2022-09-10].

[27] J. Lowitzsch, C. Hoicka, and F. van Tulder, "Renewable energy communities under the 2019 european clean energy package – governance model for the energy clusters of the future?," *Renewable and Sustainable Energy Reviews*, vol. 122, p. 109489, 2020.

[28] Energy Regulatory Commission (CRE), France, "Criterion of geographical proximity for extended collective self-consumption." https://www.cre.fr/Documents/Deliberations/Avis/projet-d-arrete-modifiant-l-arrete-du-21-novembre-2019-fixant-le-critere-de-proximite-geographique-de-l-autoconsommation-collective-etendue, 2022. [Date Accessed: 2022-09-15].

[29] T. Sousa, T. Soares, P. Pinson, F. Moret, T. Baroche, and E. Sorin, "Peer-to-peer and community-based markets: A comprehensive review," *Renewable and Sustainable Energy Reviews*, vol. 104, pp. 367–378, 2019.

[30] H. Kim, H. Choi, H. Kang, J. An, S. Yeom, and T. Hong, "A systematic review of the smart energy conservation system: From smart homes to sustainable smart cities," *Renewable and Sustainable Energy Reviews*, vol. 140, p. 110755, 2021.

[31] Findhorn Ecovillage, "Community-owned wind turbines, Findhorn Wind Park." https://ecovillagefindhorn.org/index.php/renewable, 2023. [Date Accessed: 2023-02-27].

[32] SSEN,Active Network Management, "Orkney ANM Live." https://www.ssen.co.uk/our-services/active-network-management/, 2022. [Date Accessed: 2022-09-16].

[33] S. Dong, E. Kremers, M. Brucoli, R. Rothman, and S. Brown, "Techno-enviro-economic assessment of household and community energy storage in the UK," *Energy Conversion and Management*, vol. 205, p. 112330, 2020.

[34] S. van der Stelt, T. AlSkaif, and W. van Sark, "Techno-economic analysis of household and community energy storage for residential prosumers with smart appliances," *Applied Energy*, vol. 209, pp. 266–276, 2018.

[35] E. Barbour, D. Parra, Z. Awwad, and M. C. González, "Community energy storage: A smart choice for the smart grid?," *Applied Energy*, vol. 212, pp. 489–497, 2018.

[36] A. Walker and S. Kwon, "Analysis on impact of shared energy storage in residential community: Individual versus shared energy storage," *Applied Energy*, vol. 282, p. 116172, 2021.

[37] G. Chalkiadakis, *Computational aspects of cooperative game theory Georgios Chalkiadakis, Edith Elkind, Michael Wooldridge.* Synthesis digital library of engineering and computer science, Morgan & Claypool, 2012.

[38] S. Cremers, V. Robu, D. Hofman, T. Naber, K. Zheng, and S. Norbu, "Efficient methods for approximating the shapley value for asset sharing in energy communities," in *Proceedings of the Thirteenth ACM International Conference on Future Energy Systems*, e-Energy '22, (New York, NY, USA), p. 320–324, Association for Computing Machinery, 2022.

[39] W. Tushar, C. Yuen, H. Mohsenian-Rad, T. Saha, H. V. Poor, and K. L. Wood, "Transforming energy networks via peer-to-peer energy trading: The potential of game-theoretic approaches," *IEEE Signal Processing Magazine*, vol. 35, no. 4, pp. 90–111, 2018.

[40] M. Alam, S. D. Ramchurn, and A. Rogers, "Cooperative energy exchange for the efficient use of energy and resources in remote communities," in *12th International Conference on Autonomous Agents and Multiagent Systems 2013, AAMAS 2013*, vol. 2, pp. 731–738, 2013.

[41] CATAPULT Energy Systems, "Smart Local Energy Systems." https://es.catapult.org.uk/what-we-do/future-energy-system/decarbonising-local-places/smart-local-energy-systems/, 2022. [Date Accessed: 2022-08-31].

[42] D. Kirli, B. Couraud, V. Robu, M. Salgado-Bravo, S. Norbu, M. Andoni, I. Antonopoulos, M. Negrete-Pincetic, D. Flynn, and A. Kiprakis, "Smart contracts in energy systems: A systematic review of fundamental approaches and implementations," *Renewable and Sustainable Energy Reviews*, vol. 158, p. 112013, 2022.

[43] CATAPULT Energy Systems, "Policy Challenges and Future Changes for Smart Local Energy Systems." https://www.cenex.co.uk/app/uploads/2022/05/GreenSCIES-Policy-Paper-Public-V1.0-1.pdf, 2022. [Date Accessed: 2022-09-05].

[44] Elsevier, "Scopus." https://www.elsevier.com/en-gb/solutions/scopus, NOTE = [Date Accessed: 2023-02-27], 2023.

[45] UK Research and Innovation, "Accelerating net zero delivery." https://www.ukri.org/publications/accelerating-net-zero-delivery/, 2022. [Date Accessed: 2022-09-07].

[46] ofgem, "ofgem launches review into local energy system operation." https://www.ofgem.gov.uk/publications/ofgem-launches-review-local-energy-system-operation, 2022. [Date Accessed: 2022-09-06].

[47] CATAPULT Energy Systems, "Smart Systems and Flexibility Plan (2021): What it means for Smart Local Energy Systems." https://es.catapult.org.uk/report/smart-systems-and-flexibility-plan-2021-what-it-means-for-smart-local-energy-systems/, 2021. [Date Accessed: 2022-09-06].

[48] C. Walker, P. Devine-Wright, M. Rohse, L. Gooding, H. Devine-Wright, and R. Gupta, "What is 'local' about smart local energy systems? emerging stakeholder geographies of decentralised energy in the united kingdom," *Energy Research and Social Science*, vol. 80, p. 102182, 2021.

[49] C. Rae, S. Kerr, and M. M. Maroto-Valer, "Upscaling smart local energy systems: A review of technical barriers," *Renewable and Sustainable Energy Reviews*, vol. 131, p. 110020, 2020.

[50] S. Knox, M. Hannon, F. Stewart, and R. Ford, "The (in)justices of smart local energy systems: A systematic review, integrated framework, and future research agenda," *Energy Research and Social Science*, vol. 83, p. 102333, 2022.

[51] L. S. Vedantham, Y. Zhou, and J. Wu, "Information and communications technology (ict) infrastructure supporting smart local energy systems: A review," *IET Energy Systems Integration*, vol. n/a, no. n/a, 2022.

[52] C. Vigurs, C. Maidment, M. Fell, and D. Shipworth, "Customer privacy concerns as a barrier to sharing data about energy use in smart local energy systems: A rapid realist review," *Energies*, vol. 14, no. 5, 2021.

[53] T. Morstyn, K. A. Collett, A. Vijay, M. Deakin, S. Wheeler, S. M. Bhagavathy, F. Fele, and M. D. McCulloch, "Open: An open-source platform for developing smart local energy system applications," *Applied Energy*, vol. 275, p. 115397, 2020.

[54] B. Couraud, M. Andoni, V. Robu, S. Norbu, S. Chen, and D. Flynn, "Responsive flexibility: A smart local energy system," *Renewable and Sustainable Energy Reviews*, vol. 182, p. 113343, 2023.

[55] I. Antonopoulos, V. Robu, B. Couraud, D. Kirli, S. Norbu, A. Kiprakis, D. Flynn, S. Elizondo-Gonzalez, and S. Wattam, "Artificial intelligence and machine learning approaches to energy demand-side response: A systematic review," *Renewable and Sustainable Energy Reviews*, vol. 130, p. 109899, 2020.

[56] A. Zairi and M. Chaabene, "A review on home energy management systems," in *2018 9th International Renewable Energy Congress (IREC)*, pp. 1–6, 2018.

[57] N. Qayyum, A. Amin, U. Jamil, and A. Mahmood, "Optimization techniques for home energy management: A review," in *2019 2nd International Conference on Computing, Mathematics and Engineering Technologies (iCoMET)*, pp. 1–7, 2019.

[58] H. Shareef, M. S. Ahmed, A. Mohamed, and E. Al Hassan, "Review on home energy management system considering demand responses, smart technologies, and intelligent controllers," *IEEE Access*, vol. 6, pp. 24498–24509, 2018.

[59] H. Golmohamadi, R. Keypour, B. Bak-Jensen, and J. Radhakrishna Pillai, "Optimization of household energy consumption towards day-ahead retail electricity price in home energy management systems," *Sustainable Cities and Society*, vol. 47, p. 101468, 2019.

[60] H. Mehrjerdi, M. Bornapour, R. Hemmati, and S. M. S. Ghiasi, "Unified energy management and load control in building equipped with wind-solar-battery incorporating electric and hydrogen vehicles under both connected to the grid and islanding modes," *Energy*, vol. 168, pp. 919–930, 2019.

[61] R. Hemmati and H. Saboori, "Stochastic optimal battery storage sizing and scheduling in home energy management systems equipped with solar photovoltaic panels," *Energy and Buildings*, vol. 152, pp. 290–300, 2017.

[62] M. Castillo-Cagigal, E. Caamaño-Martín, E. Matallanas, D. Masa-Bote, A. Gutiérrez, F. Monasterio-Huelin, and J. Jiménez-Leube, "Pv self-consumption optimization with storage and active dsm for the residential sector," *Solar Energy*, vol. 85, no. 9, pp. 2338–2348, 2011.

[63] M. Beaudin and H. Zareipour, "Home energy management systems: A review of modelling and complexity," *Renewable and Sustainable Energy Reviews*, vol. 45, pp. 318–335, 2015.

[64] P. Siano, "Demand response and smart grids—a survey," *Renewable and Sustainable Energy Reviews*, vol. 30, pp. 461–478, 2014.

[65] P. Palensky and D. Dietrich, "Demand side management: Demand response, intelligent energy systems, and smart loads," *IEEE Transactions on Industrial Informatics*, vol. 7, no. 3, pp. 381–388, 2011.

[66] B. Lokeshgupta and S. Sivasubramani, "Multi-objective home energy management with battery energy storage systems," *Sustainable Cities and Society*, vol. 47, p. 101458, 2019.

[67] L. Zhou, Y. Zhang, X. Lin, C. Li, Z. Cai, and P. Yang, "Optimal sizing of pv and bess for a smart household considering different price mechanisms," *IEEE Access*, vol. 6, pp. 41050–41059, 2018.

[68] R. Hemmati, "Technical and economic analysis of home energy management system incorporating small-scale wind turbine and battery energy storage system," *Journal of Cleaner Production*, vol. 159, pp. 106–118, 2017.

[69] G. Liu, T. Jiang, T. B. Ollis, X. Zhang, and K. Tomsovic, "Distributed energy management for community microgrids considering network operational constraints and building thermal dynamics," *Applied Energy*, vol. 239, pp. 83–95, 2019.

[70] O. Erdinc, N. G. Paterakis, T. D. P. Mendes, A. G. Bakirtzis, and J. P. S. Catalão, "Smart household operation considering bi-directional ev and ess utilization by real-time pricing-based dr," *IEEE Transactions on Smart Grid*, vol. 6, no. 3, pp. 1281–1291, 2015.

[71] C. O. Adika and L. Wang, "Autonomous appliance scheduling for household energy management," *IEEE Transactions on Smart Grid*, vol. 5, no. 2, pp. 673–682, 2014.

[72] P. Samadi, H. Mohsenian-Rad, V. W. S. Wong, and R. Schober, "Tackling the load uncertainty challenges for energy consumption scheduling in smart grid," *IEEE Transactions on Smart Grid*, vol. 4, no. 2, pp. 1007–1016, 2013.

[73] Z. Zhao, W. C. Lee, Y. Shin, and K.-B. Song, "An optimal power scheduling method for demand response in home energy management system," *IEEE Transactions on Smart Grid*, vol. 4, no. 3, pp. 1391–1400, 2013.

[74] A.-H. Mohsenian-Rad and A. Leon-Garcia, "Optimal residential load control with price prediction in real-time electricity pricing environments," *IEEE Transactions on Smart Grid*, vol. 1, no. 2, pp. 120–133, 2010.

[75] N. Javaid, A. Ahmed, S. Iqbal, and M. Ashraf, "Day ahead real time pricing and critical peak pricing based power scheduling for smart homes with different duty cycles," *Energies*, vol. 11, no. 6, 2018.

[76] P. Cappers, C. A. Spurlock, A. Todd, and L. Jin, "Are vulnerable customers any different than their peers when exposed to critical peak pricing: Evidence from the u.s.," *Energy Policy*, vol. 123, pp. 421–432, 2018.

[77] S. Aslam, Z. Iqbal, N. Javaid, Z. A. Khan, K. Aurangzeb, and S. I. Haider, "Towards efficient energy management of smart buildings exploiting heuristic optimization with real time and critical peak pricing schemes," *Energies*, vol. 10, no. 12, 2017.

[78] S. Aslam, S. Javaid, N. Javaid, S. M. Mohsin, S. Sulman Khan, and M. Akbar, "An efficient home energy management and power trading in smart grid," in *Innovative Mobile and Internet Services in Ubiquitous Computing* (L. Barolli, F. Xhafa, N. Javaid, and T. Enokido, eds.), (Cham), pp. 231–241, Springer International Publishing, 2019.

[79] X. Wu, X. Hu, X. Yin, C. Zhang, and S. Qian, "Optimal battery sizing of smart home via convex programming," *Energy*, vol. 140, pp. 444–453, 2017.

[80] H. Rahimi-Eichi, U. Ojha, F. Baronti, and M.-Y. Chow, "Battery management system: An overview of its application in the smart grid and electric vehicles," *IEEE Industrial Electronics Magazine*, vol. 7, no. 2, pp. 4–16, 2013.

[81] G. Yan, D. Liu, J. Li, and G. Mu, "A cost accounting method of the li-ion battery energy storage system for frequency regulation considering the effect of life degradation," *Protection and control of modern power systems*, vol. 3, no. 1, pp. 1–9, 2018.

[82] G. He, Q. Chen, C. Kang, P. Pinson, and Q. Xia, "Optimal bidding strategy of battery storage in power markets considering performance-based regulation and battery cycle life," *IEEE Transactions on Smart Grid*, vol. 7, no. 5, pp. 2359–2367, 2016.

[83] M. A. Ortega-Vazquez, "Optimal scheduling of electric vehicle charging and vehicle-to-grid services at household level including battery degradation and price uncertainty," *IET Generation, Transmission & Distribution*, vol. 8, no. 6, pp. 1007–1016, 2014.

[84] C. Ju, P. Wang, L. Goel, and Y. Xu, "A two-layer energy management system for microgrids with hybrid energy storage considering degradation costs," *IEEE Transactions on Smart Grid*, vol. 9, no. 6, pp. 6047–6057, 2018.

[85] Y. WANG, Z. ZHOU, A. BOTTERUD, K. ZHANG, and Q. DING, "Stochastic coordinated operation of wind and battery energy storage system considering battery degradation," *Journal of modern power systems and clean energy*, vol. 4, no. 4, pp. 581–592, 2016.

[86] B. Xu, A. Oudalov, A. Ulbig, G. Andersson, and D. S. Kirschen, "Modeling of lithium-ion battery degradation for cell life assessment," *IEEE Transactions on Smart Grid*, vol. 9, no. 2, pp. 1131–1140, 2018.

[87] X. Ke, N. Lu, and C. Jin, "Control and size energy storage systems for managing energy imbalance of variable generation resources," *IEEE Transactions on Sustainable Energy*, vol. 6, no. 1, pp. 70–78, 2015.

[88] M. U. Hashmi and A. Busic, "Limiting energy storage cycles of operation," in *2018 IEEE Green Technologies Conference (GreenTech)*, pp. 71–74, 2018.

[89] E. Schaltz, A. Khaligh, and P. O. Rasmussen, "Influence of battery/ultracapacitor energy-storage sizing on battery lifetime in a fuel cell hybrid electric vehicle," *IEEE Transactions on Vehicular Technology*, vol. 58, no. 8, pp. 3882–3891, 2009.

[90] M. Koller, T. Borsche, A. Ulbig, and G. Andersson, "Defining a degradation cost function for optimal control of a battery energy storage system," in *2013 IEEE Grenoble Conference*, pp. 1–6, 2013.

[91] L. H. Thaller, "Expected cycle life versus depth of discharge relationships of well behaved single cells and cell strings," in *ENERGY PRODUCTION AND CONVERSION*, (Legacy CDMS), 1982.

[92] T. Dragičević, H. Pandžić, D. Škrlec, I. Kuzle, J. M. Guerrero, and D. S. Kirschen, "Capacity optimization of renewable energy sources and battery storage in an autonomous telecommunication facility," *IEEE Transactions on Sustainable Energy*, vol. 5, no. 4, pp. 1367–1378, 2014.

[93] N. Omar, M. A. Monem, Y. Firouz, J. Salminen, J. Smekens, O. Hegazy, H. Gaulous, G. Mulder, P. Van den Bossche, T. Coosemans, and J. Van Mierlo, "Lithium iron phosphate based battery – assessment of the aging parameters and development of cycle life model," *Applied Energy*, vol. 113, pp. 1575–1585, 2014.

[94] S. You and C. Rasmussen, "Generic modelling framework for economic analysis of battery systems," in *IET Conference Proceedings*, vol. 2011, (Stevenage), p. 122, IET, 2011.

[95] I. Duggal and B. Venkatesh, "Short-term scheduling of thermal generators and battery storage with depth of discharge-based cost model," *IEEE Transactions on Power Systems*, vol. 30, no. 4, pp. 2110–2118, 2015.

[96] D. Tran and A. M. Khambadkone, "Energy management for lifetime extension of energy storage system in micro-grid applications," *IEEE Transactions on Smart Grid*, vol. 4, no. 3, pp. 1289–1296, 2013.

[97] A. M. Gee, F. V. P. Robinson, and R. W. Dunn, "Analysis of battery lifetime extension in a small-scale wind-energy system using supercapacitors," *IEEE Transactions on Energy Conversion*, vol. 28, no. 1, pp. 24–33, 2013.

[98] S. Downing and D. Socie, "Simple rainflow counting algorithms," *International Journal of Fatigue*, vol. 4, no. 1, pp. 31–40, 1982.

[99] A. Nieslony, "Rain flow counting algorithm. file exchange-matlab central," 2010.

[100] T. Terlouw, T. AlSkaif, C. Bauer, and W. van Sark, "Multi-objective optimization of energy arbitrage in community energy storage systems using different battery technologies," *Applied Energy*, vol. 239, pp. 356–372, 2019.

[101] V. Z. Gjorgievski, S. Cundeva, and G. E. Georghiou, "Social arrangements, technical designs and impacts of energy communities: A review," *Renewable Energy*, vol. 169, pp. 1138–1156, 2021.

[102] G. Seyfang, J. J. Park, and A. Smith, "A thousand flowers blooming? an examination of community energy in the uk," *Energy Policy*, vol. 61, pp. 977–989, 2013.

[103] P. Hansen, "Optimising shared renewable energy systems: An institutional approach," *Energy Research and Social Science*, vol. 73, p. 101953, 2021.

[104] R. J. Hewitt, N. Bradley, A. Baggio Compagnucci, C. Barlagne, A. Ceglarz, R. Cremades, M. McKeen, I. M. Otto, and B. Slee, "Social innovation in community energy in europe: A review of the evidence," *Frontiers in Energy Research*, vol. 7, 2019.

[105] D. N. yin Mah, "Community solar energy initiatives in urban energy transitions: A comparative study of foshan, china and seoul, south korea," *Energy Research and Social Science*, vol. 50, pp. 129–142, 2019.

[106] S. Becker, C. Kunze, and M. Vancea, "Community energy and social entrepreneurship: Addressing purpose, organisation and embeddedness of renewable energy projects," *Journal of Cleaner Production*, vol. 147, pp. 25–36, 2017.

[107] T. Hargreaves, S. Hielscher, G. Seyfang, and A. Smith, "Grassroots innovations in community energy: The role of intermediaries in niche development," *Global Environmental Change*, vol. 23, no. 5, pp. 868–880, 2013.

[108] P. McCallum, D. P. Jenkins, A. D. Peacock, S. Patidar, M. Andoni, D. Flynn, and V. Robu, "A multi-sectoral approach to modelling community energy demand of the built environment," *Energy Policy*, vol. 132, pp. 865–875, 2019.

[109] T. Bauwens and P. Devine-Wright, "Positive energies? an empirical study of community energy participation and attitudes to renewable energy," *Energy Policy*, vol. 118, pp. 612–625, 2018.

[110] T. Bauwens, "Analyzing the determinants of the size of investments by community renewable energy members: Findings and policy implications from flanders," *Energy Policy*, vol. 129, pp. 841–852, 2019.

[111] V. Robu, D. Flynn, M. Andoni, and M. Mokhtar, "Consider ethical and social challenges in smart grid research," *Nature machine intelligence*, vol. 1, no. 12, pp. 548–550, 2019.

[112] Z. Huang, H. Yu, Z. Peng, and M. Zhao, "Methods and tools for community energy planning: A review," *Renewable and Sustainable Energy Reviews*, vol. 42, pp. 1335–1348, 2015.

[113] G. Mendes, C. Ioakimidis, and P. Ferrão, "On the planning and analysis of integrated community energy systems: A review and survey of available tools," *Renewable and Sustainable Energy Reviews*, vol. 15, no. 9, pp. 4836–4854, 2011.

[114] V. Robu, G. Chalkiadakis, R. Kota, A. Rogers, and N. R. Jennings, "Rewarding cooperative virtual power plant formation using scoring rules," *Energy*, vol. 117, pp. 19–28, 2016.

[115] A. Hany Elgamal, G. Kocher-Oberlehner, V. Robu, and M. Andoni, "Optimization of a multiple-scale renewable energy-based virtual power plant in the uk," *Applied Energy*, vol. 256, p. 113973, 2019.

[116] G. Chalkiadakis, V. Robu, R. Kota, A. Rogers, and N. Jennings, "Cooperatives of distributed energy resources for efficient virtual power plants," in *The Tenth International Conference on Autonomous Agents and Multiagent Systems (AAMAS 2011) (06/05/11)*, pp. 787–794, May 2011.

[117] R. Kota, G. Chalkiadakis, V. Robu, A. Rogers, and N. R. Jennings, "Cooperatives for demand side management," in *The Seventh Conference on Prestigious Applications of Intelligent Systems (PAIS @ ECAI) (30/08/12)*, pp. 969–974, August 2012.

[118] I. Antonopoulos, V. Robu, B. Couraud, and D. Flynn, "Data-driven modelling of energy demand response behaviour based on a large-scale residential trial," *Energy and AI*, vol. 4, p. 100071, 2021.

[119] H. Ma, V. Robu, N. Li, and D. C. Parkes, "Incentivizing Reliability in Demand-Side Response," in *IJCAI 2016: 25th International Joint Conference on Artificial Intelligence*, pp. 352–358, apr 2016.

[120] H. Ma, D. C. Parkes, and V. Robu, "Generalizing demand response through reward bidding," in *Proceedings of the 16th Conference on Autonomous Agents and Multi-Agent Systems*, AAMAS '17, p. 60–68, International Foundation for Autonomous Agents and Multiagent Systems, 2017.

[121] R. Meir, H. Ma, and V. Robu, "Contract design for energy demand response," in *Proceedings of the Twenty-Sixth International Joint Conference on Artificial Intelligence, IJCAI-17*, pp. 1202–1208, 2017.

[122] V. Robu, M. Vinyals, A. Rogers, and N. R. Jennings, "Efficient buyer groups with prediction-of-use electricity tariffs," *IEEE Transactions on Smart Grid*, vol. 9, no. 5, pp. 4468–4479, 2018.

[123] M. Andoni, V. Robu, W.-G. Früh, and D. Flynn, "Game-theoretic modeling of curtailment rules and network investments with distributed generation," *Applied Energy*, vol. 201, pp. 174–187, 2017.

[124] M. Andoni, V. Robu, B. Couraud, W.-G. Früh, S. Norbu, and D. Flynn, "Analysis of strategic renewable energy, grid and storage capacity investments via stackelberg-cournot modelling," *IEEE Access*, vol. 9, pp. 37752–37771, 2021.

[125] B. Couraud, S. Norbu, M. Andoni, V. Robu, H. Gharavi, and D. Flynn, "Optimal residential battery scheduling with asset lifespan consideration," in *2020 IEEE PES Innovative Smart Grid Technologies Europe (ISGT-Europe)*, pp. 630–634, 2020.

[126] M. Andoni, W. Tang, V. Robu, and D. Flynn, "Data analysis of battery storage systems," *Proceedings of CIRED*, 2017.

[127] D. Roman, S. Saxena, V. Robu, M. Pecht, and D. Flynn, "Machine learning pipeline for battery state-of-health estimation," *Nature Machine Intelligence*, vol. 3, no. 5, pp. 447–456, 2021.

[128] V. Robu, E. Gerding, S. Stein, D. Parkes, A. Rogers, and N. Jennings, "An online mechanism for multi-unit demand and its application to plug-in hybrid electric vehicle charging," *The Journal of Artificial Intelligence Research*, vol. 48, pp. 175–230, Oct. 2013.

[129] C. Etukudor, B. Couraud, V. Robu, W.-G. Früh, D. Flynn, and C. Okereke, "Automated negotiation for peer-to-peer electricity trading in local energy markets," *Energies*, vol. 13, no. 4, 2020.

[130] M. Andoni, V. Robu, and D. Flynn, "Blockchains: Crypto-control your own energy supply," *Nature*, vol. 548, p. 158, Aug. 2017.

[131] M. Andoni, V. Robu, D. Flynn, S. Abram, D. Geach, D. Jenkins, P. McCallum, and A. Peacock, "Blockchain technology in the energy sector: A systematic review of challenges and opportunities," *Renewable and Sustainable Energy Reviews*, vol. 100, pp. 143–174, 2019.

[132] K. Pumphrey, S. L. Walker, M. Andoni, and V. Robu, "Green hope or red herring? examining consumer perceptions of peer-to-peer energy trading in the united kingdom," *Energy Research and Social Science*, vol. 68, p. 101603, 2020.

[133] B. P. Koirala, E. van Oost, and H. van der Windt, "Community energy storage: A responsible innovation towards a sustainable energy system?," *Applied Energy*, vol. 231, pp. 570–585, 2018.

[134] J. Sardi and N. Mithulananthan, "Community energy storage, a critical element in smart grid: A review of technology, prospect, challenges and opportunity," in *2014 4th International Conference on Engineering Technology and Technopreneuship (ICE2T)*, pp. 125–130, 2014.

[135] D. Strickland, M. A. Varnosfederani, J. Scott, P. Quintela, A. Duran, R. Bravery, A. Corliss, K. Ashworth, and S. Blois-Brooke, "A review of community electrical energy systems," in *2016 IEEE International Conference on Renewable Energy Research and Applications (ICRERA)*, pp. 49–54, 2016.

[136] D. Parra, S. A. Norman, G. S. Walker, and M. Gillott, "Optimum community energy storage for renewable energy and demand load management," *Applied Energy*, vol. 200, pp. 358–369, 2017.

[137] M. Elkazaz, M. Sumner, E. Naghiyev, Z. Hua, and D. W. P. Thomas, "Techno-Economic Sizing of a community battery to provide community energy billing and additional ancillary services," *Sustainable Energy, Grids and Networks*, vol. 26, p. 100439, 2021.

[138] D. Parra, S. A. Norman, G. S. Walker, and M. Gillott, "Optimum community energy storage for renewable energy and demand load management," *Applied Energy*, vol. 200, pp. 358–369, 2017.

[139] D. Parra, M. Gillott, S. A. Norman, and G. S. Walker, "Optimum community energy storage system for PV energy time-shift," *Applied Energy*, vol. 137, pp. 576–587, 2015.

[140] M. A. Hossain, R. K. Chakrabortty, M. J. Ryan, and H. R. Pota, "Energy management of community energy storage in grid-connected microgrid under uncertain real-time prices," *Sustainable Cities and Society*, vol. 66, p. 102658, 2021.

[141] J. Sardi, N. Mithulananthan, M. M. Islam, and C. K. Gan, "Framework of virtual microgrids formation using community energy storage in residential networks with rooftop photovoltaic units," *Journal of Energy Storage*, vol. 35, p. 102250, 2021.

[142] D. Gebbran, S. Mhanna, Y. Ma, A. C. Chapman, and G. Verbič, "Fair coordination of distributed energy resources with Volt-Var control and PV curtailment," *Applied Energy*, vol. 286, p. 116546, 2021.

[143] J. Guerrero, B. Sok, A. C. Chapman, and G. Verbič, "Electrical-distance driven peer-to-peer energy trading in a low-voltage network," *Applied Energy*, vol. 287, p. 116598, 2021.

[144] B. Wang, G. Verbič, and W. Xiao, "Power Sharing in an Islanded LV Distribution Network Fully Installed with PV-Battery Systems Based on Grid-Forming Control," in *2020 International Conference on Smart Grids and Energy Systems (SGES)*, pp. 459–464, 2020.

[145] M. I. Azim, W. Tushar, and T. K. Saha, "Investigating the impact of P2P trading on power losses in grid-connected networks with prosumers," *Applied Energy*, vol. 263, p. 114687, 2020.

[146] M. Mokhtar, V. Robu, D. Flynn, C. Higgins, J. Whyte, C. Loughran, and F. Fulton, "Automating the verification of the low voltage network cables and topologies," *IEEE Transactions on Smart Grid*, vol. 11, no. 2, pp. 1657–1666, 2020.

[147] B. Couraud, P. Kumar, V. Robu, D. Jenkins, S. Norbu, D. Flynn, and A. R. Abhyankar, "Assessment of Decentralized Reactive Power Control Strategies for Low Voltage PV Inverters," in *2019 8th International Conference on Power Systems (ICPS)*, pp. 1–6, 2019.

[148] G. Tévar-Bartolomé, A. Gómez-Expósito, A. Arcos-Vargas, and M. Rodríguez-Montañés, "Network impact of increasing distributed PV hosting: A utility-scale case study," *Solar Energy*, vol. 217, pp. 173–186, 2021.

[149] M. Grzanić, J. M. Morales, S. Pineda, and T. Capuder, "Electricity Cost-Sharing in Energy Communities Under Dynamic Pricing and Uncertainty," *IEEE Access*, vol. 9, pp. 30225–30241, 2021.

[150] C. B. Heendeniya, "Agent-based modeling of a rule-based community energy sharing concept," *E3S Web Conf.*, vol. 239, 2021.

[151] S. Norbu, B. Couraud, V. Robu, M. Andoni, and D. Flynn, "Modelling the redistribution of benefits from joint investments in community energy projects," *Applied Energy*, vol. 287, p. 116575, 2021.

[152] S. Norbu, B. Couraud, V. Robu, M. Andoni, and D. Flynn, "Modeling economic sharing of joint assets in community energy projects under lv network constraints," *IEEE Access*, vol. 9, pp. 112019–112042, 2021.

[153] M. Moncecchi, S. Meneghello, and M. Merlo, "A game theoretic approach for energy sharing in the italian renewable energy communities," *Applied Sciences*, vol. 10, no. 22, 2020.

[154] L. Li, "Optimal coordination strategies for load service entity and community energy systems based on centralized and decentralized approaches," *Energies*, vol. 13, no. 12, 2020.

[155] P. Chakraborty, E. Baeyens, K. Poolla, P. P. Khargonekar, and P. Varaiya, "Sharing Storage in a Smart Grid: A Coalitional Game Approach," *IEEE Transactions on Smart Grid*, vol. 10, no. 4, pp. 4379–4390, 2019.

[156] M. Marzband, R. R. Ardeshiri, M. Moafi, and H. Uppal, "Distributed generation for economic benefit maximization through coalition formation–based game theory concept," *International Transactions on Electrical Energy Systems*, vol. 27, p. e2313, jun 2017.

[157] V. Robu, M. Vinyals, A. Rogers, and N. R. Jennings, "Efficient Buyer Groups With Prediction-of-Use Electricity Tariffs," *IEEE Transactions on Smart Grid*, vol. 9, no. 5, pp. 4468–4479, 2018.

[158] S. Thakur and J. G. Breslin, "Peer to Peer Energy Trade Among Microgrids Using Blockchain Based Distributed Coalition Formation Method," *Technology and Economics of Smart Grids and Sustainable Energy*, vol. 3, no. 1, p. 5, 2018.

[159] E. Tveita, M. Löschenbrand, S. Bjarghov, and H. Farahmand, "Comparison of Cost Allocation Strategies among Prosumers and Consumers in a Cooperative Game," in *2018 International Conference on Smart Energy Systems and Technologies (SEST)*, pp. 1–6, 2018.

[160] A. Chiş and V. Koivunen, "Coalitional Game-Based Cost Optimization of Energy Portfolio in Smart Grid Communities," *IEEE Transactions on Smart Grid*, vol. 10, no. 2, pp. 1960–1970, 2019.

[161] A. Safdarian, P. H. Divshali, M. Baranauskas, A. Keski-Koukkari, and A. Kulmala, "Coalitional game theory based value sharing in energy communities," *IEEE Access*, vol. 9, pp. 78266–78275, 2021.

[162] N. Vespermann, T. Hamacher, and J. Kazempour, "Access economy for storage in energy communities," *IEEE Transactions on Power Systems*, vol. 36, no. 3, pp. 2234–2250, 2021.

[163] I. Abada, A. Ehrenmann, and X. Lambin, "On the Viability of Energy Communities.," *Energy Journal*, vol. 41, pp. 113–150, jan 2020.

[164] C. Feng, F. Wen, S. You, Z. Li, F. Shahnia, and M. Shahidehpour, "Coalitional Game-Based Transactive Energy Management in Local Energy Communities," *IEEE Transactions on Power Systems*, vol. 35, no. 3, pp. 1729–1740, 2020.

[165] X. Liu, S. Wang, and J. Sun, "Energy management for community energy network with chp based on cooperative game," *Energies*, vol. 11, no. 5, 2018.

[166] Y. Yang, G. Hu, and C. J. Spanos, "Optimal sharing and fair cost allocation of community energy storage," *IEEE Transactions on Smart Grid*, vol. 12, no. 5, pp. 4185–4194, 2021.

[167] G. Prettico, F. Gangale, A. Mengolini, A. Lucas, and G. Fulli, "Distribution system operators observatory - european electricity distribution systems to representative distribution networks," 06 2016.

[168] J. Hamari, M. Sjöklint, and A. Ukkonen, "The sharing economy: Why people participate in collaborative consumption," *Journal of the Association for Information Science and Technology*, vol. 67, no. 9, pp. 2047–2059, 2016.

[169] J. Abdella and K. Shuaib, "Peer to peer distributed energy trading in smart grids: A survey," *Energies*, vol. 11, no. 6, 2018.

[170] C. Long, J. Wu, C. Zhang, M. Cheng, and A. Al-Wakeel, "Feasibility of peer-to-peer energy trading in low voltage electrical distribution networks," *Energy Procedia*, vol. 105, pp. 2227–2232, 2017. 8th International Conference on Applied Energy, ICAE2016, 8-11 October 2016, Beijing, China.

[171] C. Zhang, J. Wu, C. Long, and M. Cheng, "Review of existing peer-to-peer energy trading projects," *Energy Procedia*, vol. 105, pp. 2563–2568, 2017. 8th International Conference on Applied Energy, ICAE2016, 8-11 October 2016, Beijing, China.

[172] O. Jogunola, A. Ikpehai, K. Anoh, B. Adebisi, M. Hammoudeh, S.-Y. Son, and G. Harris, "State-of-the-art and prospects for peer-to-peer transaction-based energy system," *Energies*, vol. 10, no. 12, 2017.

[173] J. M. Guerrero, P. C. Loh, T.-L. Lee, and M. Chandorkar, "Advanced control architectures for intelligent microgrids—part ii: Power quality, energy storage, and ac/dc microgrids," *IEEE Transactions on Industrial Electronics*, vol. 60, no. 4, pp. 1263–1270, 2013.

[174] A. Lüth, J. M. Zepter, P. Crespo del Granado, and R. Egging, "Local electricity market designs for peer-to-peer trading: The role of battery flexibility," *Applied energy*, vol. 229, pp. 1233–1243, 2018.

[175] W. Lee, L. Xiang, R. Schober, and V. W. S. Wong, "Direct electricity trading in smart grid: A coalitional game analysis," *IEEE Journal on Selected Areas in Communications*, vol. 32, no. 7, pp. 1398–1411, 2014.

[176] M. R. Alam, M. St-Hilaire, and T. Kunz, "An optimal p2p energy trading model for smart homes in the smart grid," *Energy efficiency*, vol. 10, no. 6, pp. 1475–1493, 2017.

[177] I. Atzeni, L. G. Ordóñez, G. Scutari, D. P. Palomar, and J. R. Fonollosa, "Noncooperative and cooperative optimization of distributed energy generation and storage in the demand-side of the smart grid," *IEEE Transactions on Signal Processing*, vol. 61, no. 10, pp. 2454–2472, 2013.

[178] C. Zhang, J. Wu, M. Cheng, Y. Zhou, and C. Long, "A bidding system for peer-to-peer energy trading in a grid-connected microgrid," *Energy Procedia*, vol. 103, pp. 147–152, 2016. Renewable Energy Integration with Mini/Microgrid – Proceedings of REM2016.

[179] C. Zhang, J. Wu, Y. Zhou, M. Cheng, and C. Long, "Peer-to-peer energy trading in a microgrid," *Applied Energy*, vol. 220, pp. 1–12, 2018.

[180] A. Paudel, K. Chaudhari, C. Long, and H. B. Gooi, "Peer-to-peer energy trading in a prosumer-based community microgrid: A game-theoretic model," *IEEE Transactions on Industrial Electronics*, vol. 66, no. 8, pp. 6087–6097, 2019.

[181] J. Guerrero, A. C. Chapman, and G. Verbič, "Decentralized p2p energy trading under network constraints in a low-voltage network," *IEEE Transactions on Smart Grid*, vol. 10, no. 5, pp. 5163–5173, 2019.

[182] B. Hayes, S. Thakur, and J. Breslin, "Co-simulation of electricity distribution networks and peer to peer energy trading platforms," *International Journal of Electrical Power and Energy Systems*, vol. 115, p. 105419, 2020.

[183] V. Piyush, O. Brian, H. Barry, T. Subhasis, and B. J. G, "Enerport: Irish blockchain project for peer- ta-peer energy trading," *Energy Informatics*, vol. 1, no. 1, pp. 1–9, 2018.

[184] L. Han, T. Morstyn, and M. McCulloch, "Incentivizing prosumer coalitions with energy management using cooperative game theory," *IEEE Transactions on Power Systems*, vol. 34, no. 1, pp. 303–313, 2019.

[185] J. Mei, C. Chen, J. Wang, and J. L. Kirtley, "Coalitional game theory based local power exchange algorithm for networked microgrids," *Applied Energy*, vol. 239, pp. 133–141, 2019.

[186] I. S. Bayram, M. Z. Shakir, M. Abdallah, and K. Qaraqe, "A survey on energy trading in smart grid," in *2014 IEEE Global Conference on Signal and Information Processing (GlobalSIP)*, pp. 258–262, 2014.

[187] W. Tushar, T. K. Saha, C. Yuen, T. Morstyn, M. D. McCulloch, H. V. Poor, and K. L. Wood, "A motivational game-theoretic approach for peer-to-peer energy trading in the smart grid," *Applied Energy*, vol. 243, pp. 10–20, 2019.

[188] E. Sortomme and M. A. El-Sharkawi, "Optimal combined bidding of vehicle-to-grid ancillary services," *IEEE Transactions on Smart Grid*, vol. 3, no. 1, pp. 70–79, 2012.

[189] J. Kim, J. Lee, S. Park, and J. K. Choi, "Battery-wear-model-based energy trading in electric vehicles: A naive auction model and a market analysis," *IEEE Transactions on Industrial Informatics*, vol. 15, no. 7, pp. 4140–4151, 2019.

[190] S. Bae and S. Park, "Comparison between seller and buyer pricing systems for energy trading in microgrids," *IEEE Access*, vol. 7, pp. 54084–54096, 2019.

[191] J. Lee, J. Guo, J. K. Choi, and M. Zukerman, "Distributed energy trading in microgrids: A game-theoretic model and its equilibrium analysis," *IEEE Transactions on Industrial Electronics*, vol. 62, no. 6, pp. 3524–3533, 2015.

[192] W. Tushar, W. Saad, H. V. Poor, and D. B. Smith, "Economics of electric vehicle charging: A game theoretic approach," *IEEE Transactions on Smart Grid*, vol. 3, no. 4, pp. 1767–1778, 2012.

[193] S. Wang, A. F. Taha, J. Wang, K. Kvaternik, and A. Hahn, "Energy crowdsourcing and peer-to-peer energy trading in blockchain-enabled smart grids," *IEEE Transactions on Systems, Man, and Cybernetics: Systems*, vol. 49, no. 8, pp. 1612–1623, 2019.

[194] D. Han, C. Zhang, J. Ping, and Z. Yan, "Smart contract architecture for decentralized energy trading and management based on blockchains," *Energy*, vol. 199, p. 117417, 2020.

[195] M. Khorasany, Y. Mishra, and G. Ledwich, "Hybrid trading scheme for peer-to-peer energy trading in transactive energy markets," *IET Generation, Transmission & Distribution*, vol. 14, no. 2, pp. 245–253, 2020.

[196] R. Khalid, N. Javaid, A. Almogren, M. U. Javed, S. Javaid, and M. Zuair, "A blockchain-based load balancing in decentralized hybrid p2p energy trading market in smart grid," *IEEE Access*, vol. 8, pp. 47047–47062, 2020.

[197] N. Lasla, M. Al-Ammari, M. Abdallah, and M. Younis, "Blockchain based trading platform for electric vehicle charging in smart cities," *IEEE Open Journal of Intelligent Transportation Systems*, vol. 1, pp. 80–92, 2020.

[198] J. Kang, R. Yu, X. Huang, S. Maharjan, Y. Zhang, and E. Hossain, "Enabling localized peer-to-peer electricity trading among plug-in hybrid electric vehicles using consortium blockchains," *IEEE Transactions on Industrial Informatics*, vol. 13, no. 6, pp. 3154–3164, 2017.

[199] G. van Leeuwen, T. AlSkaif, M. Gibescu, and W. van Sark, "An integrated blockchain-based energy management platform with bilateral trading for microgrid communities," *Applied Energy*, vol. 263, p. 114613, 2020.

[200] M. Khorasany, Y. Mishra, and G. Ledwich, "A decentralized bilateral energy trading system for peer-to-peer electricity markets," *IEEE Transactions on Industrial Electronics*, vol. 67, no. 6, pp. 4646–4657, 2020.

[201] W. Saad, Z. Han, H. V. Poor, and T. Basar, "Game-theoretic methods for the smart grid: An overview of microgrid systems, demand-side management, and smart grid communications," *IEEE Signal Processing Magazine*, vol. 29, no. 5, pp. 86–105, 2012.

[202] J. Castro, D. Gómez, and J. Tejada, "Polynomial calculation of the shapley value based on sampling," *Computers and Operations Research*, vol. 36, no. 5, pp. 1726–1730, 2009. Selected papers presented at the Tenth International Symposium on Locational Decisions (ISOLDE X).

[203] V. Misra, S. Ioannidis, A. Chaintreau, and L. Massoulié, "Incentivizing peer-assisted services: A fluid shapley value approach," *SIGMETRICS Perform. Eval. Rev.*, vol. 38, p. 215–226, jun 2010.

[204] S. Deckmann, A. Pizzolante, A. Monticelli, B. Stott, and O. Alsac, "Studies on power system load flow equivalencing," *IEEE Transactions on Power Apparatus and Systems*, vol. PAS-99, no. 6, pp. 2301–2310, 1980.

[205] M. Baran and F. F. Wu, "Optimal sizing of capacitors placed on a radial distribution system," *IEEE Transactions on Power Delivery*, vol. 4, no. 1, pp. 735–743, 1989.

[206] W. F. Tinney and C. E. Hart, "Power flow solution by newton's method," *IEEE Transactions on Power Apparatus and Systems*, vol. PAS-86, no. 11, pp. 1449–1460, 1967.

[207] M. Grzanic, M. G. Flammini, and G. Prettico, "Distribution network model platform: A first case study," *Energies*, vol. 12, no. 21, 2019.

[208] T. Lord and P. McNally, "Powering Ahead: The Need to Reform UK Energy Markets." https://institute.global/sites/default/files/articles/Powering-Ahead-The-Need-to-Reform-UK-Energy-Markets.pdf, 2022. [Date Accessed: 2022-09-20].

[209] P.-H. Li and N. Strachan, "Energy modelling in the uk: Strengths and weaknesses of uk energy models," *UK Energy Research Centre*, 2021.

[210] R. Bray and B. Woodman, "Unlocking Local Energy Markets." https://www.centrica.com/media/4377/bray-unlocking-local-energy-markets_-002.pdf, 2022. [Date Accessed: 2022-09-20].

[211] Bray, Rachel and Woodman, Bridget and Connor, Peter, "Policy and Regulatory Barriers to Local Energy Markets in Great Britain." https://ore.exeter.ac.uk/repository/bitstream/handle/10871/33607/09.05.18_Policy_and_Regulatory_Barriers_to_LEMs_in_GB__BRAY._.pdf?sequence=1&isAllowed=y, 2018. [Date Accessed: 2022-09-20].

[212] CATAPULT Energy Systems, "The policy and regulatory context for new Local Energy Markets." https://es.catapult.org.uk/report/the-policy-and-regulatory-context-for-new-local-energy-markets/, 2019. [Date Accessed: 2022-09-25].

[213] S. Norbu, B. Couraud, V. Robu, M. Andoni, and D. Flynn, "Modelling the redistribution of benefits from joint investments in community energy projects," *Applied Energy*, vol. 287, p. 116575, 2021.

[214] Ofgem, "Behind The Meter (BTM)." https://www.ofgem.gov.uk/publications/p375-settlement-secondary-bm-units-using-metering-behind-site-boundary-point-0, 2022. [Date Accessed: 2022-11-23].

[215] UKERC Energy Data Centre, "Thames Valley Vision End Point Monitor Data." https://ukerc.rl.ac.uk/DC/cgi-bin/edc_search.pl?GoButton=Related&WantComp=146, 2022. [Date Accessed: 2022-09-25].

[216] UKERC Energy Data Centre, "MIDAS: UK Mean Wind Data. NCAS British Atmospheric Data Centre." https://catalogue.ceda.ac.uk/uuid/a1f65a362c26c9fa667d98c431a1ad38http://catalogue.ceda.ac.uk/uuid/5dca9487dc614711a3a933e44a933ad3, 2022. [Date Accessed: 2022-09-25].

[217] W.-G. Früh, "From local wind energy resource to national wind power production," *AIMS Energy*, vol. 3, no. 1, pp. 101–120, 2015.

[218] W.-G. Früh, "Long-term wind resource and uncertainty estimation using wind records from scotland as example," *Renewable Energy*, vol. 50, pp. 1014–1026, 2013.

[219] M. Andoni, V. Robu, W.-G. Früh, and D. Flynn, "Game-theoretic modeling of curtailment rules and network investments with distributed generation," *Applied Energy*, vol. 201, pp. 174–187, 2017.

[220] Enercon, GmbH, "ENERCON Wind Turbine - Product Overview." https://www.enercon.de/en/products/, 2022. [Date Accessed: 2022-09-25].

[221] Met Office, "MIDAS Open:UK hourly solar radiation data, v201901. Centre for Environmental Data Analysis." https://data.ceda.ac.uk/badc, 2022. [Date Accessed: 2022-09-25].

[222] Money Supermarket, "Fixed-price electricity tariffs comparison." https://www.moneysupermarket.com/gas-and-electricity/compare-electricity-prices/, 2022. [Date Accessed: 2022-09-26].

[223] The Office of Gas and Electricity Markets (Ofgem), "Compare gas and electricity tariffs: Ofgem-accredited price comparison sites." https://www.ofgem.gov.uk/consumers/household-gas-and-electricity-guide/how-switch-energy-supplier-and-shop-better-deal/compare-gas-and-electricity-tariffs-ofgem-accredited-price-comparison-sites, 2022. [Date Accessed: 2022-09-26].

[224] Octopus Energy, "Agile Octopus Tariff." https://octopus.energy/agile/, 2022. [Date Accessed: 2022-09-26].

[225] Claire Curry, "Lithium-ion Battery Costs and Market." https://data.bloomberglp.com/bnef/sites/14/2017/07/BNEF-Lithium-ion-battery-costs-and-market.pdf, 2017. [Date Accessed: 2022-09-27].

[226] BloombergNEF, "Battery Pack Prices Fall As Market Ramps Up With Market Average At $156/kWh In 2019." https://about.bnef.com/blog/battery-pack-prices-fall-as-market-ramps-up-with-market-average-at-156-kwh-in-2019/, 2019. [Date Accessed: 2022-09-27].

[227] PV Europe, "Price of li-ion batteries for vehicles below 200 USD/kWh in 2019." https://www.pveurope.eu/solar-storage/price-li-ion-batteries-vehicles-below-200-usd-kwh-2019, 2019. [Date Accessed: 2022-09-27].

[228] Russell Hensley, John Newman, and Matt Rogers, "Battery technology charges ahead ." https://www.mckinsey.com/capabilities/sustainability/our-insights/battery-technology-charges-ahead, 2022. [Date Accessed: 2022-09-27].

[229] EIA, "Cost and Performance Characteristics of New Generating Technologies, Annual Energy Outlook 2020." https://www.eia.gov/outlooks/aeo/assumptions/pdf/table_8.2.pdf, 2020. [Date Accessed: 2022-09-27].

[230] B. Couraud, S. Norbu, M. Andoni, V. Robu, H. Gharavi, and D. Flynn, "Optimal residential battery scheduling with asset lifespan consideration," in *2020 IEEE PES Innovative Smart Grid Technologies Europe (ISGT-Europe)*, pp. 630–634, 2020.

[231] M. Chawla, R. Naik, R. Burra, and H. Wiegman, "Utility energy storage life degradation estimation method," in *2010 IEEE Conference on Innovative Technologies for an Efficient and Reliable Electricity Supply*, pp. 302–308, 2010.

[232] Tesla, "Powerwall." https://www.tesla.com/powerwallhttps://www.ofgem.gov.uk/publications/p375-settlement-secondary-bm-units-using-metering-behind-site-boundary-point-0, 2022. [Date Accessed: 2022-11-28].

[233] Department for Business Energy & Industrial Strategy, "Quarterly Energy Prices: September 2022." https://www.gov.uk/government/statistics/quarterly-energy-prices-september-2022, 2022. [Date Accessed: 2022-11-28].

[234] M. Wooldridge, "Computational aspects of cooperative game theory," in *Agent and Multi-Agent Systems: Technologies and Applications* (J. O'Shea, N. T. Nguyen, K. Crockett, R. J. Howlett, and L. C. Jain, eds.), (Berlin, Heidelberg), pp. 1–1, Springer Berlin Heidelberg, 2011.

[235] S. S. Fatima, M. Wooldridge, and N. R. Jennings, "A linear approximation method for the shapley value," *Artificial Intelligence*, vol. 172, no. 14, pp. 1673–1699, 2008.

[236] Scottish & Southern Electricity Networks (SSEN), Active Network Management (ANM), "Orkney ANM Live." https://www.ssen.co.uk/ANMGeneration/, 2023. [Date Accessed: 2023-01-05].

[237] IEEE 13-bus feeder, "Resources | PES Test Feeder." https://site.ieee.org/pes-testfeeders/resources/, 2022. [Date Accessed: 2022-11-28].

[238] K. Movassagh, A. Raihan, B. Balasingam, and K. Pattipati, "A critical look at coulomb counting approach for state of charge estimation in batteries," *Energies*, vol. 14, no. 14, 2021.

[239] ABB, "UPS and power conditioning | ABB." https://new.abb.com/ups, 2022. [Date Accessed: 2022-11-28].

[240] C. Long, J. Wu, C. Zhang, L. Thomas, M. Cheng, and N. Jenkins, "Peer-to-peer energy trading in a community microgrid," in *2017 IEEE Power & Energy Society General Meeting*, pp. 1–5, 2017.

[241] A. Kothari, D. C. Parkes, and S. Suri, "Approximately-strategyproof and tractable multiunit auctions," *Decision Support Systems*, vol. 39, no. 1, pp. 105–121, 2005.

[242] S. Cremers, V. Robu, P. Zhang, M. Andoni, S. Norbu, and D. Flynn, "Efficient methods for approximating the shapley value for asset sharing in energy communities," *Applied Energy*, vol. 331, p. 120328, 2023.

[243] B. Couraud, S. Norbu, M. Andoni, V. Robu, H. Gharavi, and D. Flynn, "Optimal residential battery scheduling with asset lifespan consideration," in *2020 IEEE PES Innovative Smart Grid Technologies Europe (ISGT-Europe)*, pp. 630–634, 2020.

[244] S. Norbu and S. Bandyopadhyay, "Power pinch analysis for optimal sizing of renewable-based isolated system with uncertainties," *Energy*, vol. 135, pp. 466–475, 2017.

Appendix A

The Appendix provides additional information and sample codes for the simulation analysis of the research work presented in this thesis.

A.1 Simulation analysis presented in Chapter 3 & 4

Listing A.1: Sample code for simulation analysis in Section 3.4.2: battery degrdation model

```
%Battery Parameters & Specifications
MBCRange = Optimal_Battery_Capacity;% Optimal battery capacity in kWh
BatteryLifeTime = 20; %battery life time in years
Ec = 0.85;% Battery charging efficiency (Ec)
Ed = 0.85;% Battery discharging eficiency (Ed)
MaxBcap = MBCRange;% Maximum battery capcity in WHr [Variable
    Parameter]
MinBcap = MaxBcap*0.2;% Minimum battery capacity at 80% DoD (20%SoC)
IBC = MaxBcap; % Initial Battery Capacity (IBC)100% SoC
MaxPower = MaxBcap/2;%Battery Power Limit i.e 50% of maximum capacity
% battery SoC determined after applying battery control algorithm
% Ensuring the Starting SoC of battery is initial battery capacity (
    IBC)
SoC = [IBC,SoC'];
% Computing battery Depth of Discharge (DOD) based on State of Charge
    (SoC)
% Computing Battery Remaining Useful Life(RUL)
% rainflow(SoC);%Rainflow function used to count the cycles of the
    battery
[c] = rainflow(SoC);
TT = array2table(c,'VariableNames',{'Count','Range','Mean','Start','
    End'});
A = table2array(TT(:,[1,4,5]));% Converting table to array
Cyclecount = A(:,1); % Number of cycles counted
AStartSoC = SoC(A(:,2));% Actual Starting SoC
```

```
AEndSoC = SoC(A(:,3));%Actual Ending SoC
MaxSoC = MaxBcap;
%Starting DoD of a Cycle
StartDoD = round((100.-((AStartSoC./MaxSoC).*100))+0.5);
I = StartDoD>100;
StartDoD(I) = 100;
% End DoD of a Cycle
EndDoD = round((100.-((AEndSoC./MaxSoC).*100))+0.5);
J = EndDoD>100;
EndDoD(J) = 100;
load Battery_DoD_Vs_NCycles;
% Actual charging & discharging cycle of a battery at specific DoD's
ncycles = zeros(length(StartDoD),1);
%DF-Depreciation Factor for each Regular & Irregular Cycles.
DF = zeros(length(StartDoD),1);
for j = 1:1:length(StartDoD)
    if StartDoD(j)== 1
        ncycles(j) = Cyclecount(j);
        DF(j) =  ncycles(j)/FinalBNcyles(EndDoD(j));
    else
        ncycles(j) = Cyclecount(j);
        DF(j) = (ncycles(j)* abs(1/FinalBNcyles(StartDoD(j))-1/
            FinalBNcyles(EndDoD(j))));
    end
end
% Computation of final battery depreciation factor
DepreciationFactor = max(sum(DF),1/BatteryLifeTime); % Final Battery
   DF
```

Listing A.2: Sample code for simulation analysis in Section 3.4.1 & 3.5 of Chapter 3, and Section 4.3 & 4.3.2 of Chapter 4: battery control algorithm and techno-economic analysis

```
close all
% Battery Parameters & Specifications
CostofBattery = 150;% cost of the battery per kWh
BatteryLifeTime = 20; %battery life time in years
Ec = 0.85;% Battery charging efficiency (Ec)
Ed = 0.85;% Battery discharging eficiency (Ed)
% Final Wind Power and Demand at Half Hourly Basis
T = 2; %Power and Demand data time. Currently in half hour basis
load D1_to_D200; % Demand Input in Wh of 200 households/agents
%Price Scheme of Energy Buying from Grid at Agile Octopus Grid Buying
    Price
```

```
load AgileOctopusBP; %Input of Daily Agile Octopus Buying Price (p/
    kWH)
BP = AgileOctopusBP/10000; % Agile Octopus Buying Price (p/Wh)
%Zero export tariff
SP = 0; % Selling Price (SP) No Export Tariff
load Kirkwall_3kWhSolarEnergy; % Input of Solar PV energy in Wh
load PowerRatio; % Individual Optimal PV power ratio
load OptimalBattery; % Individual Optimal Battery
variablesInCurrentWorkspace = who('-file','D1_to_D200');
numVariables = length(variablesInCurrentWorkspace);
D_data1 = [];
D_head = {};
for d =1:1:length(variablesInCurrentWorkspace)
    D_name = variablesInCurrentWorkspace{d};
    D_vals = eval(variablesInCurrentWorkspace{d});%individual demand
    D_head{d,1} = D_name;
    P = Kirkwall_3kWhSolarEnergy./PowerRatio(d);%Individual Optimal
        PV
    MBCRange = OptimalBattery(d);
    MaxBcap = MBCRange;% Maximum battery capcity in WHr
    MinBcap = MaxBcap*0.2;% Minimum battery capacity at 80% DoD (20%
        SoC)
    IBC = MaxBcap; % Initial Battery Capacity (IBC)of 100%MacBcap
    MaxPower = MaxBcap/2;%Battery Power Limit i.e 50% of maximum
        capacity
    SoC = zeros(length(P),1);
    Energysold = zeros(length(P),1);
    Energybought = zeros(length(P),1);
    EbatMax = zeros(length(P),1);
    EBat = zeros(length(P),1);
    SoC(1) = IBC;
    for i = 1:1:length(P)
        if P(i)>= D_vals(i)
            if i == 1
                EbatMax(i) = 1/T*min((P(i)-D_vals(i))*T, MaxPower);
                EBat(i) = min(EbatMax(i)*Ec, MaxBcap-SoC(1));
                SoC(i) = SoC(1) + EBat(i);
                Energysold(i,:) = (P(i)-D_vals(i)-EBat(i)/Ec)*SP;
            else
                EbatMax(i) = 1/T*min((P(i)-D_vals(i))*T, MaxPower);
                EBat(i) = min(EbatMax(i)*Ec, MaxBcap-SoC(i-1));
                SoC(i) = SoC(i-1) + EBat(i);
```

```
                Energysold(i,:) = (P(i)-D_vals(i)-EBat(i)/Ec)*SP;
            end
        else
            if i==1
                EbatMax(i) = 1/T*min(abs((P(i)-D_vals(i))*T),
                   MaxPower);
                EBat(i) = min(EbatMax(i)/Ed, SoC(1)-MinBcap);
                SoC(i) = SoC(1) - EBat(i);
                Energybought(i,:) = (D_vals(i)-P(i)-EBat(i)*Ed)*BP(i)
                   ;
            else
                EbatMax(i) = 1/T*min(abs((P(i)-D_vals(i))*T),
                   MaxPower);
                EBat(i) = min(EbatMax(i)/Ed, SoC(i-1)-MinBcap);
                SoC(i) = SoC(i-1) - EBat(i);
                Energybought(i,:) = (D_vals(i)-P(i)-EBat(i)*Ed)*BP(i)
                   ;
            end
        end
    end
%% Computation of Battery Depreciation Factor (DF)
SoC = [IBC,SoC']'; % Ensuring the Starting SoC of battery is IBC
% Computing battery Depth of Discharge (DOD) based on State of Charge
    (SoC)
% Computing Battery Remaining Life(BRLife)
% rainflow(SoC);%Rainflow function used to count the cycles of the
    battery
[c] = rainflow(SoC);
TT = array2table(c,'VariableNames',{'Count','Range','Mean','Start','
    End'});
A = table2array(TT(:,[1,4,5]));% Converting table to array
Cyclecount = A(:,1); % Number of cycles counted
AStartSoC = SoC(A(:,2));% Actual Starting SoC
AEndSoC = SoC(A(:,3));%Actual Ending SoC
MaxSoC = MaxBcap;
%Starting DoD of a Cycle
StartDoD = round((100.-((AStartSoC./MaxSoC).*100))+0.5);
I = StartDoD>100;
StartDoD(I) = 100;
% End DoD of a Cycle
EndDoD = round((100.-((AEndSoC./MaxSoC).*100))+0.5);
J = EndDoD>100;
```

```
EndDoD(J) = 100;
load Battery_DoD_Vs_NCycles;
% Actual charging & discharging cycle of a battery at specific DoD's
ncycles = zeros(length(StartDoD),1);
%DF—Depreciation Factor for each Regular & Irregular Cycles.
DF = zeros(length(StartDoD),1);
for j = 1:1:length(StartDoD)
    if StartDoD(j)== 1
        ncycles(j) = Cyclecount(j);
        DF(j) =  ncycles(j)/FinalBNcyles(EndDoD(j));
    else
        ncycles(j) = Cyclecount(j);
        DF(j) = (ncycles(j)* abs(1/FinalBNcyles(StartDoD(j))—1/
            FinalBNcyles(EndDoD(j))));
    end
end
% Final Battery Depreciation Factor
DepreciationFactor = max(sum(DF),1/BatteryLifeTime);
%% Economic Analysis
%Computation of the Bill
% YEARLY total sum in pounds: cost of energy imported from grid
TotalCost_EnergyBought = sum(Energybought);
% YEARLY total sum in pounds: revenue from exporting energy into grid
TotalRevenue_EnergySold = sum(Energysold);
%Cost of 1kWh Battery assumed to be 150pounds per kWh
CostofNewBattery = CostofBattery*(MaxBcap/1000);
% Yearly Bill without battery cost and DF
BillWihtoutBCostandDF = TotalCost_EnergyBought —
    TotalRevenue_EnergySold;
%Yearly cost of battery
Yearlybatterycost = CostofNewBattery*DepreciationFactor;
%Yearly Bill considering the battery cost and DF
BillWithBCostandDF = BillWihtoutBCostandDF+Yearlybatterycost;
%Incuding the cost of Solar PV
CostofPV = 1100;% Total Overnight Cost of Solar PV = 2500 pounds per
    kW
YearlyPVCost = (CostofPV*(max(P)/1000))*2/20;
%Final annaul bill icluding the cost of battery, cost of PV and
    battery DF
YearlyBill = BillWithBCostandDF + YearlyPVCost;
%Data Exporting to Excel
YearlyDemand = sum(D_vals);
```

```
data1 = [YearlyDemand YearlyBill];
D_data1 = [D_data1; data1];
col_header={'Yearly Demand','Yearly Bill'};
xlswrite('Output1',D_data1,'Sheet1','B2');
xlswrite('Output1', D_head,'Sheet1','A2');
xlswrite('Output1', col_header,'Sheet1','B1');

end
```

A.2 Simulation analysis presented in Chapter 5

Listing A.3: Sample code for simulation analysis in Section 5.3: battery control algorithm with voltage control mechanism

```
%% Net Power from battery control algorithm
%Community Battery Capacity
Ec = 0.85;% Battery charging efficiency (Ec)
Ed = 0.85;% Battery discharging eficiency (Ed)
T = 2; %Power and Demand data time. Currently in half hour basis
Nbus = 14; %Number of buses
NslackBus = 1;  %number of the slack bus
NVcontrolledBus = [1]; %Number of the busses that are voltage
    controlled
V = 1; %reference Bus Voltage
Sbase = 10000;%358716/3;
Vbase = 410/sqrt(3);
Zbase = Vbase^2/Sbase;
%Data Input: Demands, Solar PV
load Datetime2020; %Date and time reference
load Demands200; %Demands of 200 agents
% For setting the frequecy of simulation (weekly,monthly,yearly)
Yearlydate = Datetime2020;
Yearlydemands = Demands200; %200 Agents individual demands, Yearly
%Final Admittance Matrix
Y = Ybus;
%% Defining load and generator buses
% Setting the order of the Buses
BN = [650;%Bus1
671;%Bus2
634;%Bus3
645;%Bus4
646;%Bus5
```

```
692;%Bus6
675;%Bus7
611;%Bus8
652;%Bus9
670;%Bus10
633;%Bus11
632;%Bus12
680;%Bus13
684];%Bus14
Load_Buses = [634;%Bus3
645;%Bus4
646;%Bus5
692;%Bus6
675;%Bus7
611;%Bus8
652];%Bus9
Generation_Buses = [675;
692;652]; %Bus7,%Bus6,%Bus9
%Existing bus load
factor = 0; % factor used to scale the loads that are due to
   households not bargaining. the goal is to have a grid close enough
    to break.
P671 = [385;220]*factor; %Load kW ; kVAR %Bus2
P634 = [ 160 ; 110 ]*factor; %Load kW ; kVAR %Bus3
P645 = [ 170 ; 125 ]*factor; %Load kW ; kVAR %Bus4
P646 = [ 230 ; 132 ]*factor; %Load kW ; kVAR %Bus5
P692 = [ 170 ; 151 ]*factor; %Load kW ; kVAR %Bus6
P675 = [ 485 ; 190 ]*factor; %Load kW ; kVAR %Bus7
P611 = [ 170 ; 80 ]*factor; %Load kW ; kVAR %Bus8
P652 = [ 128 ; 86 ]*factor;%[ 128 ; 86 ]*factor; %Load kW ; kVAR %
   Bus9
%% Definition of the initialization Voltage Vector
X = [zeros(size(Yearlydemands,1),Nbus) V*ones(size(Yearlydemands,1),
   Nbus)];
%% Computation of Voltages using Newton Raphson Algorithm
load D1toD200_Total;% Community Aggregated Demand input
% Scaled community demand in Wh at half hourly basis
D = factor1*D1toD200Total;
load Kirkwall_3kWhSolarEnergy; % Input of Individual Solar PV Energy
   in Wh
% Optimal Community Solar PV (309kW)[0.0099=optimal power ratio]
P = Kirkwall_3kWhSolarEnergy./0.0099;
```

```
MBCRange = 642000;% Optimal Community Battery of 642kWh
MaxBcap = MBCRange;% Maximum battery capcity in WHr [Variable
    Parameter]
MinBcap = MaxBcap*0.2;% Minimum battery capacity at 80% DoD (20%SoC)
IBC = MaxBcap; % Initial Battery Capacity (IBC)100% SoC
%Battery Power Limit i.e 50% of maximum battery capacity
MaxPower = MaxBcap/2;
SoC = zeros(length(P),1);
Pbus = zeros(length(P),1);
EbatMax = zeros(length(P),1);
EBat = zeros(length(P),1);
SoC(1) = IBC;
    pf = 0.95; % Definition of a constant power factor for the loads

for i = 1:1:17520
    if P(i)>= D(i)
        if i == 1
            EbatMax(i) = 1/T*min((P(i)-D(i))*T, MaxPower);
            EBat(i) = min(EbatMax(i)*Ec, MaxBcap-SoC(1));
            SoC(i) = SoC(1) + EBat(i);
            Pbus(i,:) = P(i)-EBat(i)/Ec;
        else
            EbatMax(i) = 1/T*min((P(i)-D(i))*T, MaxPower);
            EBat(i) = min(EbatMax(i)*Ec, MaxBcap-SoC(i-1));
            SoC(i) = SoC(i-1) + EBat(i);
            Pbus(i,:) = P(i)-EBat(i)/Ec;
        end
        Pgenbus = Pbus(i); % Take this as Pgen for the identified bus
                  %% Power Flow with Community Battery
                % 13 Bus Parameters
                % Definition of loads
                %Active power consumption definition
                    Ploads = zeros(1,Nbus);
                    for idx_PF = 1:size(Yearlydemands,2)
                        switch mod(idx_PF,7)
                            case 0
                                Ploads(3)=P634(1)+ Yearlydemands(i,
                                   idx_PF);
                            case 1
                                Ploads(4)=P645(1)+ Yearlydemands(i,
                                   idx_PF);
                            case 2
```

```
104                         Ploads(5)=P646(1)+ Yearlydemands(i,
                                idx_PF);
105                     case 3
106                         Ploads(6)=P692(1)+ Yearlydemands(i,
                                idx_PF);
107                     case 4
108                         Ploads(7)=P675(1)+ Yearlydemands(i,
                                idx_PF);
109                     case 5
110                         Ploads(8)=P611(1)+ Yearlydemands(i,
                                idx_PF);
111                     case 6
112                         Ploads(9)=P652(1)+ Yearlydemands(i,
                                idx_PF);
113                 end
114             end
115
116              Ploads(3)= factor1*Ploads(3);
117              Ploads(4)= factor1*Ploads(4);
118              Ploads(5)= factor1*Ploads(5);
119              Ploads(6)= factor1*Ploads(6);
120              Ploads(7)= factor1*Ploads(7);
121              Ploads(8)= factor1*Ploads(8);
122              Ploads(9)= factor1*Ploads(9);
123             %converting to per unit
124             Ploads = Ploads/Sbase; %pu
125             %Reactive power consumption definition
126             Qloads = zeros(1,Nbus);
127             Qloads(3) = tan(acos(pf))*Ploads(3);
128             Qloads(4) = tan(acos(pf))*Ploads(4);
129             Qloads(5) = tan(acos(pf))*Ploads(5);
130             Qloads(6) = tan(acos(pf))*Ploads(6);
131             Qloads(7) = tan(acos(pf))*Ploads(7);
132             Qloads(8) = tan(acos(pf))*Ploads(8);
133             Qloads(9) = tan(acos(pf))*Ploads(9);
134             %converting to per unit
135             Qloads = Qloads/Sbase;%pu
136             %% Definition of Generators
137             Pgen = zeros(1,Nbus);
138             Pgen(2)= Pgenbus;%Net Power Generation after
                    Community Battery Control Algorithm at
                    Identified Bus
```

```
139                 %Generator Reactive Power Defination
140                     Qgen = zeros(1,Nbus);
141                     %converting to per unit
142                     Pgen = Pgen/Sbase;%pu
143                     Qgen =Qgen/Sbase;%pu
144                     %% Computation of the Voltages
145                     X1 = [zeros(1,Nbus) V*ones(1,Nbus)] ;
146                     X0 = zeros(size(X1));
147                     number_iteration = 0;
148                     while max(abs(X1-X0))>0.001 && number_iteration
                            <200
149                         X0 = X1;
150                         X1 = iteration(Nbus, Ploads, Qloads, Pgen,
                                Qgen, NslackBus, NVcontrolledBus, Y, X0, V
                                );
151                         number_iteration = number_iteration +1;
152                     end
153                     number_iteration;
154                     %% Compute the final Power from each elements
155                     X0 = X1;
156                     yp = zeros(Nbus,1);
157                     yq = zeros(Nbus,1);
158                     for idx_PF = 1:Nbus
159                         for k = 1:Nbus
160                             yp(idx_PF) = yp(idx_PF) - X0(Nbus+idx_PF)
                                    *X0(Nbus+k)*abs(Y(idx_PF,k))*cos(angle
                                    (Y(idx_PF,k))+X0(k)-X0(idx_PF));
161                             yq(idx_PF) = yq(idx_PF) + X0(Nbus+idx_PF)
                                    *X0(Nbus+k)*abs(Y(idx_PF,k))*sin(angle
                                    (Y(idx_PF,k))+X0(k)-X0(idx_PF));
162                             %yp(i) = yp(i) + X0(Nbus+i)*X0(Nbus+k)*(
                                    real(Y(i,k))*cos(X0(i)-X0(k))+imag(Y(i
                                    ,k))*sin(X0(i)-X0(k)));
163                             %yq(i) = yq(i) + X0(Nbus+i)*X0(Nbus+k)*(
                                    real(Y(i,k))*sin(X0(i)-X0(k))-imag(Y(i
                                    ,k))*cos(X0(i)-X0(k)));
164                         end
165                     end
166
167                     %F = [yp ; yq]*Sbase;%actual P and Q
168                     F = [yp ; yq]*Sbase;%actual P and Q
```

```
169                 %Power650632(j,:) = abs(1/z650632 *(complex(X1
                        (15)*cos(X1(1)),X1(15)*sin(X1(1))) -complex(X1
                        (24)*cos(X1(12)),X1(24)*sin(X1(12)))))/1000;
170                  X(i,:) = X1;%bus voltages in pu
171
172                 %% Regulation of Battery control so the voltage
                        is maintained at the contractual limits, here
                        voltage should be <1.1V
173                 while max(X(i,15:28)) >1.1  &&i==1%if there is
                        too much export, although the battery is
                        charging
174
175                     if EbatMax(i)>= MaxPower -0.1 || SoC(i) >=
                            MaxBcap -0.1   % if the battery is already
                             charged
176                          Pbus(i,:) = Pbus(i,:)-Step_Control;  %we
                                 limit the PV export
177                     else
178                         EbatMax(i) = min(EbatMax(i)+Step_Control,
                                MaxPower);
179                         EBat(i) = min(EbatMax(i)*Ec, MaxBcap-SoC
                                (1));
180                         SoC(i) = SoC(1) + EBat(i);
181                         Pbus(i,:) = P(i)-EBat(i)/Ec;
182                     end
183                      Pgenbus = Pbus(i); % Take this as Pgen for
                            the identified bus
184
185                               %% Definition of Generators
186                             Pgen = zeros(1,Nbus);
187                             Pgen(2)= Pgenbus;%Identified Bus
188                             Qgen = zeros(1,Nbus);
189                             %converting to per unit
190                             Pgen = Pgen/Sbase;%pu
191                             Qgen =Qgen/Sbase;%pu
192                             %% Computation of the Voltages
193                             X1 = [zeros(1,Nbus) V*ones(1,Nbus)] ;
194                             X0 = zeros(size(X1));
195                             number_iteration = 0;
196                             while max(abs(X1-X0))>0.001 &&
                                    number_iteration<200
197                                  X0 = X1;
```

```
198                             X1 = iteration(Nbus, Ploads,
                                    Qloads, Pgen, Qgen, NslackBus,
                                     NVcontrolledBus, Y, X0, V);
199                             number_iteration =
                                    number_iteration +1;
200                         end
201                         number_iteration;
202                         X(i,:) = X1;%bus voltages in pu
203                     end
204                     %% Regulation of Battery control so the voltage
                           is maintained at the contractual limits, here
                           voltage should be <1.1V
205                     while max(X(i,15:28)) >1.1  &&i>1%if there is too
                            much export, although the battery is charging
206
207                         if EbatMax(i)>= MaxPower -0.1 || SoC(i) >=
                               MaxBcap -0.1   % if the battery is already
                                charged
208                              Pbus(i,:) = Pbus(i,:)-Step_Control;  %we
                                    limit the PV export
209                         else
210                             EbatMax(i) = min(EbatMax(i)+Step_Control,
                                   MaxPower);
211                             EBat(i) = min(EbatMax(i)*Ec, MaxBcap-SoC(
                                   i-1));
212                             SoC(i) = SoC(i-1) + EBat(i);
213                             Pbus(i,:) = P(i)-EBat(i)/Ec;
214                         end
215                          Pgenbus = Pbus(i); % Take this as Pgen for
                               the identified bus
216
217                                %% Definition of Generators
218                             Pgen = zeros(1,Nbus);
219                             Pgen(2)= Pgenbus;%Identified Bus
220                             Qgen = zeros(1,Nbus);
221                             %converting to per unit
222                             Pgen = Pgen/Sbase;%pu
223                             Qgen =Qgen/Sbase;%pu
224                             %% Computation of the Voltages
225                             X1 = [zeros(1,Nbus) V*ones(1,Nbus)] ;
226                             X0 = zeros(size(X1));
227                             number_iteration = 0;
```

```
228                             while max(abs(X1-X0))>0.001 &&
                                    number_iteration<200
229                                 X0 = X1;
230                                 X1 = iteration(Nbus, Ploads,
                                        Qloads, Pgen, Qgen, NslackBus,
                                         NVcontrolledBus, Y, X0, V);
231                                 number_iteration =
                                        number_iteration +1;
232                             end
233                             number_iteration;
234                             X(i,:) = X1;%bus voltages in pu
235                 end
236
237
238     else
239         if i==1
240             EbatMax(i) = 1/T*min(abs((P(i)-D(i))*T), MaxPower);
241             EBat(i) = min(EbatMax(i)/Ed, SoC(1)-MinBcap);
242             SoC(i) = SoC(1) - EBat(i);
243             Pbus(i,:) = P(i)+EBat(i)*Ed;
244         else
245             EbatMax(i) = 1/T*min(abs((P(i)-D(i))*T), MaxPower);
246             EBat(i) = min(EbatMax(i)/Ed, SoC(i-1)-MinBcap);
247             SoC(i) = SoC(i-1) - EBat(i);
248             Pbus(i,:) = P(i)+EBat(i)*Ed;
249         end
250         Pgenbus = Pbus(i); % Take this as Pgen for the identified bus
251                   %% Power Flow with Community Battery
252                 % 13 Bus Parameters
253                 % Definition of loads
254                 %Active power consumption definition
255                     Ploads = zeros(1,Nbus);
256                     for idx_PF = 1:size(Yearlydemands,2)
257                         switch mod(idx_PF,7)
258                             case 0
259                                 Ploads(3)=P634(1)+ Yearlydemands(i,
                                        idx_PF);
260                             case 1
261                                 Ploads(4)=P645(1)+ Yearlydemands(i,
                                        idx_PF);
262                             case 2
```

```
                            Ploads(5)=P646(1)+ Yearlydemands(i,
                                idx_PF);
                        case 3
                            Ploads(6)=P692(1)+ Yearlydemands(i,
                                idx_PF);
                        case 4
                            Ploads(7)=P675(1)+ Yearlydemands(i,
                                idx_PF);
                        case 5
                            Ploads(8)=P611(1)+ Yearlydemands(i,
                                idx_PF);
                        case 6
                            Ploads(9)=P652(1)+ Yearlydemands(i,
                                idx_PF);
                    end
                end

                Ploads(3)= factor1*Ploads(3);%Scaled Individual
                    Agents' Demand
                Ploads(4)= factor1*Ploads(4);
                Ploads(5)= factor1*Ploads(5);
                Ploads(6)= factor1*Ploads(6);
                Ploads(7)= factor1*Ploads(7);
                Ploads(8)= factor1*Ploads(8);
                Ploads(9)= factor1*Ploads(9);
                %converting to per unit
                Ploads = Ploads/Sbase; %pu
                %Reactive power consumption definition
                Qloads = zeros(1,Nbus);
                Qloads(3) = tan(acos(pf))*Ploads(3);
                Qloads(4) = tan(acos(pf))*Ploads(4);
                Qloads(5) = tan(acos(pf))*Ploads(5);
                Qloads(6) = tan(acos(pf))*Ploads(6);
                Qloads(7) = tan(acos(pf))*Ploads(7);
                Qloads(8) = tan(acos(pf))*Ploads(8);
                Qloads(9) = tan(acos(pf))*Ploads(9);
                %converting to per unit
                Qloads = Qloads/Sbase;%pu
                %% Definition of Generators
                Pgen = zeros(1,Nbus);
                Pgen(2)= Pgenbus;%Identified Bus
            %Generator reactive power
```

```
299                     Qgen = zeros(1,Nbus);
300                     %converting to per unit
301                     Pgen = Pgen/Sbase;%pu
302                     Qgen =Qgen/Sbase;%pu
303                     %% Computation of the Voltages
304                     X1 = [zeros(1,Nbus) V*ones(1,Nbus)] ;
305                     X0 = zeros(size(X1));
306                     number_iteration = 0;
307                     while max(abs(X1-X0))>0.001 && number_iteration
                            <200
308                          X0 = X1;
309                          X1 = iteration(Nbus, Ploads, Qloads, Pgen,
                                Qgen, NslackBus, NVcontrolledBus, Y, X0, V
                                );
310                          number_iteration = number_iteration +1;
311                     end
312                     number_iteration;
313                     %% Compute the final Power from each elements
314                     X0 = X1;
315                     yp = zeros(Nbus,1);
316                     yq = zeros(Nbus,1);
317                     for idx_PF = 1:Nbus
318                         for k = 1:Nbus
319                             yp(idx_PF) = yp(idx_PF) - X0(Nbus+idx_PF)
                                    *X0(Nbus+k)*abs(Y(idx_PF,k))*cos(angle
                                    (Y(idx_PF,k))+X0(k)-X0(idx_PF));
320                             yq(idx_PF) = yq(idx_PF) + X0(Nbus+idx_PF)
                                    *X0(Nbus+k)*abs(Y(idx_PF,k))*sin(angle
                                    (Y(idx_PF,k))+X0(k)-X0(idx_PF));
321                             %yp(i) = yp(i) + X0(Nbus+i)*X0(Nbus+k)*(
                                    real(Y(i,k))*cos(X0(i)-X0(k))+imag(Y(i
                                    ,k))*sin(X0(i)-X0(k)));
322                             %yq(i) = yq(i) + X0(Nbus+i)*X0(Nbus+k)*(
                                    real(Y(i,k))*sin(X0(i)-X0(k))-imag(Y(i
                                    ,k))*cos(X0(i)-X0(k)));
323                         end
324                     end
325
326                     %F = [yp ; yq]*Sbase;%actual P and Q
327                     F = [yp ; yq]*Sbase;%actual P and Q
```

```
328                 %Power650632(j,:) = abs(1/z650632 *(complex(X1
                        (15)*cos(X1(1)),X1(15)*sin(X1(1))) -complex(X1
                        (24)*cos(X1(12)),X1(24)*sin(X1(12)))))/1000;
329                 X(i,:) = X1;%bus voltages in pu
330
331                 %% Regulation of Battery control so the voltage
                        is maintained at the contractual limits, here
                        voltage should be <1.1V
332                 while max(X(i,15:28)) >1.1 &&i==1 %if there is
                        too much export, although the battery is
                        charging
333                  if EbatMax(i)<= 0+0.1  || SoC(i) <= MinBcap
                         +0.1   % if the battery is already
                         discharged
334                       Pbus(i,:) = max(0,Pbus(i,:)-Step_Control
                              );  %we limit the PV export
335                  else
336                      EbatMax(i) = max(0,EbatMax(i)-
                             Step_Control);%reduce the discharge
                             from battery
337                      EBat(i) = min(EbatMax(i)/Ed, SoC(1)-
                             MinBcap);
338                      SoC(i) = SoC(1) - EBat(i);
339                      %Energybought(i,:) = (P(i)-D(i)+ EBat(i)*
                             Ed);
340                      %Edeficit(i,:) = (P(i)-EBat(i)/Ec);%PV
                             production-Ebat
341                      Pbus(i,:) = P(i)+EBat(i)*Ed;
342                  end
343                   Pgenbus = Pbus(i); % Take this as Pgen for
                          the identified bus
344
345                           %% Definition of Generators
346                          Pgen = zeros(1,Nbus);
347                          Pgen(2)= Pgenbus;%Identified Bus
348                          Qgen = zeros(1,Nbus);
349                          %converting to per unit
350                          Pgen = Pgen/Sbase;%pu
351                          Qgen =Qgen/Sbase;%pu
352                          %% Computation of the Voltages
353                          X1 = [zeros(1,Nbus) V*ones(1,Nbus)] ;
354                          X0 = zeros(size(X1));
```

```
355                         number_iteration = 0;
356                         while max(abs(X1-X0))>0.001 &&
                                number_iteration<200
357                          X0 = X1;
358                          X1 = iteration(Nbus, Ploads,
                                 Qloads, Pgen, Qgen, NslackBus,
                                  NVcontrolledBus, Y, X0, V);
359                          number_iteration =
                                 number_iteration +1;
360                         end
361                         number_iteration;
362                         X(i,:) = X1;%bus voltages in pu
363                 end
364
365                 %% Regulation of Battery control so the voltage
                    is maintained at the contractual limits, here
                    voltage should be <1.1V
366                 while max(X(i,15:28)) >1.1 &&i>1 %if there is too
                     much export, although the battery is charging
367                     if EbatMax(i)<= 0+0.1  || SoC(i) <= MinBcap
                            +0.1   % if the battery is already
                            discharged
368                           Pbus(i,:) = max(0,Pbus(i,:)-Step_Control
                                 );  %we limit the PV export
369                     else
370                          EbatMax(i) = max(0,EbatMax(i)-
                                 Step_Control);%reduce the dicharge
                                 from battery
371                          EBat(i) = min(EbatMax(i)/Ed, SoC(i-1)-
                                 MinBcap);
372                          SoC(i) = SoC(i-1) - EBat(i);
373                          %Energybought(i,:) = (P(i)-D(i)+ EBat(i)*
                                 Ed);
374                          %Edeficit(i,:) = (P(i)-EBat(i)/Ec);%PV
                                 production-Ebat
375                          Pbus(i,:) = P(i)+EBat(i)*Ed;
376                     end
377                      Pgenbus = Pbus(i); % Take this as Pgen for
                            the identified bus
378
379                           %% Definition of Generators
380                         Pgen = zeros(1,Nbus);
```

```
                                Pgen(2)= Pgenbus;%Identified Bus
                                Qgen = zeros(1,Nbus);
                                %converting to per unit
                                Pgen = Pgen/Sbase;%pu
                                Qgen =Qgen/Sbase;%pu
                                %% Computation of the Voltages
                                X1 = [zeros(1,Nbus) V*ones(1,Nbus)] ;
                                X0 = zeros(size(X1));
                                number_iteration = 0;
                                while max(abs(X1-X0))>0.001 &&
                                    number_iteration<200
                                    X0 = X1;
                                    X1 = iteration(Nbus, Ploads,
                                        Qloads, Pgen, Qgen, NslackBus,
                                         NVcontrolledBus, Y, X0, V);
                                    number_iteration =
                                        number_iteration +1;
                                end
                                number_iteration;
                                X(i,:) = X1;%bus voltages in pu
                    end

    end

 if mod(i,50) ==0
 i
 end
end
%% Bus voltages
figureV = figure('Name','Voltage Profiles','Color',[1 1 1]);
% Create axes
axes1 = axes('Parent',figureV);
hold(axes1,'on');
% Create multiple lines using matrix input to plot
plot1 = plot(Yearlydate,X(:,15),Yearlydate,X(:,16)*1.001,Yearlydate,X
    (:,17),Yearlydate,X(:,18),Yearlydate,X(:,19),Yearlydate,X(:,20),
    Yearlydate,X(:,21),Yearlydate,X(:,22),Yearlydate,X(:,23),
    Yearlydate,X(:,24),Yearlydate,X(:,25),Yearlydate,X(:,26),
    Yearlydate,X(:,27),Yearlydate,X(:,28),'Parent',axes1,'LineWidth'
    ,2);
set(plot1(1),'DisplayName','V_{Bus1}');
set(plot1(2),'DisplayName','V_{Bus2}');
```

```
set(plot1(3),'DisplayName','V_{Bus3}');
set(plot1(4),'DisplayName','V_{Bus4}');
set(plot1(5),'DisplayName','V_{Bus5}');
set(plot1(6),'DisplayName','V_{Bus6}');
set(plot1(7),'DisplayName','V_{Bus7}');
set(plot1(8),'DisplayName','V_{Bus8}');
set(plot1(9),'DisplayName','V_{Bus9}');
set(plot1(10),'DisplayName','V_{Bus10}');
set(plot1(11),'DisplayName','V_{Bus11}');
set(plot1(12),'DisplayName','V_{Bus12}');
set(plot1(13),'DisplayName','V_{Bus13}');
set(plot1(14),'DisplayName','V_{Bus14}');
% Create ylabel
ylabel('Bus voltage (p.u)','FontWeight','bold');
% Create xlabel
xlabel('Time','FontWeight','bold');
box(axes1,'on');
% Set the remaining axes properties
set(axes1,'FontSize',12,'FontWeight','bold','GridAlpha',0.1,'
   GridLineStyle',':','LineWidth',1.5,'XGrid','on','YGrid','on');
% Create legend
legend(axes1,'show');
```

A.3 Simulation analysis presented in Chapter 6

Listing A.4: Sample code for simulation analysis in Section 6.3 & 6.4: battery control algorithm with local peer-to-community (P2C) market mechanism, and techno-economic analysis

```
%% Dtermining Excess and Defecit energy after each individual agents'
    optimization
%% Total agents and time slots
Total_Agents = 200;%Total agents (households) of the community
Total_HalfHour = 17520;%Total half hour in one year
%% Net Energy after the battery control Algorithm
Edeficit = EnergyDificit;
Eexcess =  EnergyExcess;
data1 = [Edeficit];
D_data1 = [D_data1, data1];
data2 = [Eexcess];
D_data2 = [D_data2, data2];
%Total Yearly cost: Cost of PV, Cost of Battery—including the DF
```

```
data3 = [YearlyCost_Assets];
D_data3 = [D_data3, data3];
%% Individual Agents Parameters
AAA_TotalDemand(d) = sum(D_vals)/1000; %Agents Total Yearly Demand (kWh)
AAA_TotalPower(d) = sum(P)/1000; %Agents Total Yearly PV Generation (kWh)
AAA_Battery(d) =  MBCRange/1000; %Agents Total Installed Battery (kWh)
AAA_PV_Power_Installed(d) = (max(P)/1000)*2; % Agents PV installed Capacity (kW)
%% Individual agent's Excess Energy to SELL or Defecit Energy to BUY after the battery control algorithm
DeficitENERGYtoBUY = D_data1;%Excess Energy to sell (half-hourly)
ExcessENERGYtoSELL = D_data2;%Dificit Eenrgy to buy (half-hourly)
% Total number of prosumers with Deficit Energy
Total_Number_of_Prosumers_withDeficitEnergy = sum(DeficitENERGYtoBUY>0, 2);
% Total Yearly Cost: Cost of PV, Cost of Battery-including the DF
Yearly_Cost_Assets = D_data3;% Yearly assets cost(PV cost & Battery cost including the depreciation cost)
%% P2C Pricing Mechanism Design
% Pricing Scheme:Only Import Tarriff for buying energy from Grid considered (Export tarriff considered zero)
BuyingPrice_From_Grid = 16/100000; % 16Pence/kWh or 0.16Pounds/kWh or 0.00016Pounds/Wh (fixed tariff)
%% Price Setting-1: Low Selling Price Ranges (10% to 30% of Grid Import price)
rng('default')
a = 0.1; % Minimum prosumer Low Selling Price as percentage of Buying Price From Grid
b = 0.3; % Maximum prosumer Low Selling Price as percentage of Buying Price From Grid
r = a+(b-a).*rand(1, 67);%randomly generated Low selling price of prosumers as percentage of Buying Price From Grid
Low_Selling_Price_Ranges = r.*BuyingPrice_From_Grid;%Prosumer Low Selling Price of the Excess Energy generated as percentage of BuyingPrice_From_Grid
%% Price Setting-2: Medium Selling Price Ranges (31% to 70% of Grid Import price)
a = 0.31; % Minimum prosumer Medium Selling Price as percentage of Buying Price From Grid
```

```
38 b = 0.7; % Maximum prosumer Medium Selling Price as percentage of
       Buying Price From Grid
39 r = a+(b-a).*rand(1, 67);%randomly generated Medium selling price of
       prosumers as percentage of Buying Price From Grid
40 Medium_Selling_Price_Ranges = r.*BuyingPrice_From_Grid;%Prosumer
       Medium Selling Price of the Excess Energy generated as percentage
       of BuyingPrice_From_Grid
41 %% Price Setting-3: High Selling Price Ranges (71% to 100% of Grid
       Import price)
42 a = 0.71; % Minimum prosumer High Selling Price as percentage of
       Buying Price From Grid
43 b = 1; % Maximum prosumer High Selling Price as percentage of Buying
       Price From Grid
44 r = a+(b-a).*rand(1, 66);%randomly generated High selling price of
       prosumers as percentage of Buying Price From Grid
45 High_Selling_Price_Ranges = r.*BuyingPrice_From_Grid;%Prosumer High
       Selling Price of the Excess Energy generated as percentage of
       BuyingPrice_From_Grid
46 %% Final Prosumer Selling Prices as percentage of Grid Buying Price
47 Prosumer_Selling_Price = [Low_Selling_Price_Ranges
       Medium_Selling_Price_Ranges High_Selling_Price_Ranges ];
48 %% Sorting the Cheapest Seller
49 [h, sortedCheapestSellerIndices] = sort(Prosumer_Selling_Price,'
       ascend');%Seller sorted from cheapest price to expensive price
50 %% Peer-to-Community (P2C) Trading Scheme
51 EnergyExported_Through_P2Pmarket = zeros(Total_HalfHour,Total_Agents)
       ;
52 EnergyExported_to_Grid = zeros(Total_HalfHour,Total_Agents);
53 ReminingEnergyImported_From_Grid = zeros(Total_HalfHour,1);
54 Net_DificitENERGYtoBUY = zeros(Total_HalfHour,1);
55 EnergyImported_From_P2Pmarket = zeros(Total_HalfHour,Total_Agents);
56 EnergyImported_From_Grid = zeros(Total_HalfHour,Total_Agents);
57 TotalP2P = zeros(Total_HalfHour,1);
58
59 for i = 1:Total_HalfHour
60     %Total Deficit and Excess energy at every half hour of 200 agents
61     Total_DificitENERGYtoBUY = sum(DeficitENERGYtoBUY(i,:)); %Total
           Deficit Energy at every half hour of 200 agents
62     Total_ExcessENERGYtoSELL = sum(ExcessENERGYtoSELL(i,:)); %Total
           Excess Energy at every half hour for 200 agents
63     Net_DificitENERGYtoBUY(i,:) = sum(DeficitENERGYtoBUY(i,:));
64     TOTAL_DificitENERGYtoBUY = Total_DificitENERGYtoBUY;
```

```
65      % To determine the total Energy avaialble for P2P market(export&
            import)at every half hour of 200 agents
66      if(Total_DificitENERGYtoBUY > Total_ExcessENERGYtoSELL)
67          TotalEnergy_AvaialbleFor_P2P = Total_ExcessENERGYtoSELL;
68      elseif(Total_DificitENERGYtoBUY <= Total_ExcessENERGYtoSELL)
69          TotalEnergy_AvaialbleFor_P2P = Total_DificitENERGYtoBUY;
70      end
71      TotalP2P(i) = TotalEnergy_AvaialbleFor_P2P;
72
73      %% Exported Energy: Sold through P2C trading to Buyers(prosumers
            with deficit energy) or sold to Grid
74      %Sellers for P2C trading are selected based on the cheapest
            selling price offered
75      for j = sortedCheapestSellerIndices %sorted cheapest seller
76          EnergySold_Through_P2Pmarket = min(ExcessENERGYtoSELL(i,j),
                Total_DificitENERGYtoBUY);
77          Total_DificitENERGYtoBUY = Total_DificitENERGYtoBUY -
                EnergySold_Through_P2Pmarket;
78          EnergySold_To_Grid = ExcessENERGYtoSELL(i,j)-
                EnergySold_Through_P2Pmarket;
79      % Individul agents Exported Energy
80          EnergyExported_Through_P2Pmarket(i,j) =
                EnergySold_Through_P2Pmarket; %Excess Energy Sold Through
                P2P Market to Buyers (prosumer with deficit energy)
81          EnergyExported_to_Grid(i,j) =  EnergySold_To_Grid; %Excess
                Energy Exported to Grid
82          ReminingEnergyImported_From_Grid(i,:) =
                Total_DificitENERGYtoBUY;%Deficit Energy not met from P2P
                market is exported from Grid (Grid-Seller)
83      end
84      %% Imported Energy: Bought from P2C trading Sellers(prosumers
            with excess energy) or energy bought from Grid
85      %Buyers for P2C market: Energy available from P2P market is
            distributed equally among the buyers (prosumers with defecit
            energy)
86      %% Deficit Energy to Buy Sorted Smallest Amount to Largest Amount
87      [SortedDeficitENERGYtoBuy, SortedDeficitENERGYtoBuyIndices] =
            sort(DeficitENERGYtoBUY(i,:),'ascend');%Deficit Energy to Buy
            Sorted
88      %
            ********************************************************************************
```

```
89      remaining_buyers = size(SortedDeficitENERGYtoBuyIndices,2);
90      for j = SortedDeficitENERGYtoBuyIndices
91          EnergyImported_From_P2Pmarket(i,j) = min(DeficitENERGYtoBUY(i
                ,j), TotalEnergy_AvaialbleFor_P2P/remaining_buyers);
92          TotalEnergy_AvaialbleFor_P2P = TotalEnergy_AvaialbleFor_P2P -
                EnergyImported_From_P2Pmarket(i,j);
93          remaining_buyers = remaining_buyers - 1;
94          EnergyImported_From_Grid(i,j) = DeficitENERGYtoBUY(i,j) -
               EnergyImported_From_P2Pmarket(i,j) ;
95      end
96      if TotalEnergy_AvaialbleFor_P2P>0.1
97          temp=1;
98      end
99  end
100
101 %% Determining the P2C market CLEARING PRICE: Weighted average of
       selcted P2C seller bids and Grid bid
102 P2P_Seller_Cost = EnergyExported_Through_P2Pmarket.*
       Prosumer_Selling_Price;%Energy and selected Seller bid
103 Grid_Seller_Cost = ReminingEnergyImported_From_Grid.*
       BuyingPrice_From_Grid;% Energy and Grid bid
104 %
       **************************************************************************

105 P2P_Clearing_PricePerUnit = zeros(Total_HalfHour,1);
106 for i = 1:Total_HalfHour
107     TOTAL_DificitEnergytoBUY = sum(DeficitENERGYtoBUY(i,:)); %Total
           Deficit Energy at every half hour of 200 agents
108     Total_P2Pseller_GridSeller_Cost = sum(P2P_Seller_Cost(i,:))+
           Grid_Seller_Cost(i);
109     if TOTAL_DificitEnergytoBUY > 0
110         Clearing_PricePerUnit = Total_P2Pseller_GridSeller_Cost ./
               TOTAL_DificitEnergytoBUY;% P2P per unit clearing price:
               Seller and Buyer price per unit of energy
111     else
112          Clearing_PricePerUnit = 0;
113     end
114     P2P_Clearing_PricePerUnit(i,:) =  Clearing_PricePerUnit;
115 end
116 %% Revenue from selling the excess energy through P2P market
```

```
117 Revenue_From_SellingEnergy_To_P2Pmarket =
        EnergyExported_Through_P2Pmarket.*P2P_Clearing_PricePerUnit;%
        Revenue earned from selling excess energy in P2P market
118 Yearly_Revenue_From_SellingEnergy_To_P2Pmarket = sum(
        Revenue_From_SellingEnergy_To_P2Pmarket);%Yearly revenue earned
        from selling excess energy in P2P market
119 %% Cost of buying energy from P2P market and Grid
120 Cost_of_BuyingEnergy_From_P2Pmarket = EnergyImported_From_P2Pmarket.*
        P2P_Clearing_PricePerUnit;%Cost incurred for buying deficit energy
         from P2P market
121 Cost_of_BuyingEnergy_From_Grid = EnergyImported_From_Grid.*
        BuyingPrice_From_Grid;%Cost incurred for buying deficit energy
        from Grid
122 Yearly_Cost_of_BuyingEnergy_From_P2Pmarket = sum(
        Cost_of_BuyingEnergy_From_P2Pmarket);%Yearly cost incurred for
        buying deficit energy from P2P market
123 Yearly_Cost_of_BuyingEnergy_From_Grid = sum(
        Cost_of_BuyingEnergy_From_Grid);% Yearly cost incurred for buying
        deficit energy from Grid
124 %% Yearly Bills of 200 Agents including the cost of solar PV &
        battery assets
125 Yearly_Bill = Yearly_Cost_Assets +
        Yearly_Cost_of_BuyingEnergy_From_Grid +
        Yearly_Cost_of_BuyingEnergy_From_P2Pmarket -
        Yearly_Revenue_From_SellingEnergy_To_P2Pmarket;
126 Final_Yearly_Bill_P2P = Yearly_Bill';
127 %% Yearly Bills Without P2P
128 Cost_of_Buying_from_Grid_WithoutP2P = DeficitENERGYtoBUY.*
        BuyingPrice_From_Grid;%Cost incurred for buying deficit energy
        from Grid
129 Yearly_Cost_of_Buying_from_Grid_WithoutP2P = sum(
        Cost_of_Buying_from_Grid_WithoutP2P);% Yearly cost incurred for
        buying deficit energy from Grid
130 % Yearly Bills of 200 Agents including the cost of solar PV & battery
         assets
131 Yearly_Bill_WithoutP2C = Yearly_Cost_Assets +
        Yearly_Cost_of_Buying_from_Grid_WithoutP2P ;
132 Final_Yearly_Bill_WithoutP2C = Yearly_Bill_WithoutP2C';
133 %% Parmeters for checking there is no import while exporting and vice
        -versa
```

```
134 %% Parameters: Difference of Total Deficit & Excess, Difference of
        Total Import & Export from Grid, Difference of Total Import &
        Export from P2P
135 A_Difference_Total_DeficitExcess = sum(sum(DeficitENERGYtoBUY,2)) -
        sum(sum(ExcessENERGYtoSELL,2));
136 A_Difference_Total_GridImportExport  = sum(sum(
        EnergyImported_From_Grid,2)) - sum(sum(EnergyExported_to_Grid,2));
137 A_Difference_Total_P2PImportExport  = sum(sum(
        EnergyImported_From_P2Pmarket,2)) - sum(sum(
        EnergyExported_Through_P2Pmarket,2));
138
139 %% Comparison of Yearly Bills With and Without P2C
140 figure1= figure('Name','Timeseries','Color',[1 1 1]);
141 axes1 = axes('Parent',figure1);
142 hold(axes1,'on');
143 x = 1:200;
144 y1 = Final_Yearly_Bill_P2P;
145 plot(x,y1,'g','linewidth',2)
146 y2 = Final_Yearly_Bill_WithoutP2C;
147 plot(x,y2,'r','linewidth',2)
148 hold(axes1,'off');
149 xlabel('Time Period')
150 ylabel('Yearly Bills')
151 legend('Bills With P2P', 'Bills Without P2P');
152 box(axes1,'on');
153 box(axes1,'on');
```

A.4 IEEE 13 bus test feeder data

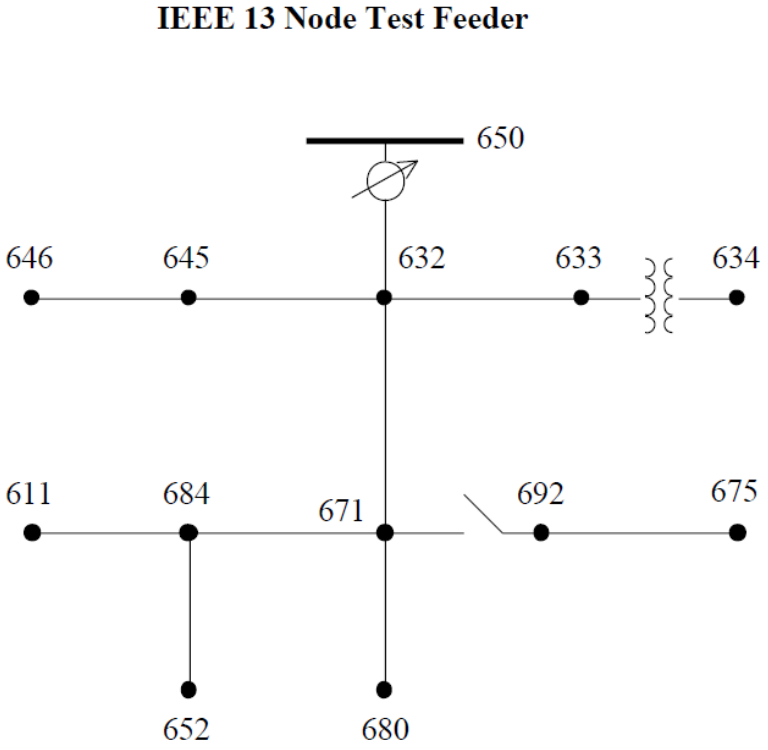

The following details of the IEEE 13 Bus Test Feeder is given below (as provided in [237]):

- Impedances
- Overhead line configuration data
- Underground line configuration data
- Line segment data
- Transformer data
- Capacitor data
- Regulator data
- Spot load data
- Distributed load data

Overhead Line Configuration Data:

Config.	Phasing	Phase	Neutral	Spacing
		ACSR	ACSR	ID
601	B A C N	556,500 26/7	4/0 6/1	500
602	C A B N	4/0 6/1	4/0 6/1	500
603	C B N	1/0	1/0	505
604	A C N	1/0	1/0	505
605	C N	1/0	1/0	510

Underground Line Configuration Data:

Config.	Phasing	Cable	Neutral	Space ID
606	A B C N	250,000 AA, CN	None	515
607	A N	1/0 AA, TS	1/0 Cu	520

Line Segment Data:

Node A	Node B	Length(ft.)	Config.
632	645	500	603
632	633	500	602
633	634	0	XFM-1
645	646	300	603
650	632	2000	601
684	652	800	607
632	671	2000	601
671	684	300	604
671	680	1000	601
671	692	0	Switch
684	611	300	605
692	675	500	606

Transformer Data:

	kVA	kV-high	kV-low	R - %	X - %
Substation:	5,000	115 - D	4.16 Gr. Y	1	8
XFM -1	500	4.16 – Gr.W	0.48 – Gr.W	1.1	2

Capacitor Data:

Node	Ph-A	Ph-B	Ph-C
	kVAr	kVAr	kVAr
675	200	200	200
611			100
Total	200	200	300

Regulator Data:

Regulator ID:	1		
Line Segment:	650 - 632		
Location:	50		
Phases:	A - B -C		
Connection:	3-Ph,LG		
Monitoring Phase:	A-B-C		
Bandwidth:	2.0 volts		
PT Ratio:	20		
Primary CT Rating:	700		
Compensator Settings:	Ph-A	Ph-B	Ph-C
R - Setting:	3	3	3
X - Setting:	9	9	9
Volltage Level:	122	122	122

Spot Load Data:

Node	Load	Ph-1	Ph-1	Ph-2	Ph-2	Ph-3	Ph-3
	Model	kW	kVAr	kW	kVAr	kW	kVAr
634	Y-PQ	160	110	120	90	120	90
645	Y-PQ	0	0	170	125	0	0
646	D-Z	0	0	230	132	0	0
652	Y-Z	128	86	0	0	0	0
671	D-PQ	385	220	385	220	385	220
675	Y-PQ	485	190	68	60	290	212
692	D-I	0	0	0	0	170	151
611	Y-I	0	0	0	0	170	80
	TOTAL	1158	606	973	627	1135	753

Distributed Load Data:

Node A	Node B	Load	Ph-1	Ph-1	Ph-2	Ph-2	Ph-3	Ph-3
		Model	kW	kVAr	kW	kVAr	kW	kVAr
632	671	Y-PQ	17	10	66	38	117	68

IEEE 13 NODE TEST FEEDER

Impedances

Configuration 601:

```
           Z (R +jX) in ohms per mile
 0.3465  1.0179   0.1560  0.5017   0.1580  0.4236
                  0.3375  1.0478   0.1535  0.3849
                                   0.3414  1.0348
          B in micro Siemens per mile
            6.2998   -1.9958   -1.2595
                      5.9597   -0.7417
                                5.6386
```

Configuration 602:

```
           Z (R +jX) in ohms per mile
0.7526  1.1814   0.1580  0.4236   0.1560  0.5017
                 0.7475  1.1983   0.1535  0.3849
                                  0.7436  1.2112
         B in micro Siemens per mile
           5.6990   -1.0817   -1.6905
                     5.1795   -0.6588
                               5.4246
```

Configuration 603:

```
           Z (R +jX) in ohms per mile
 0.0000  0.0000   0.0000  0.0000   0.0000  0.0000
                  1.3294  1.3471   0.2066  0.4591
                                   1.3238  1.3569
          B in micro Siemens per mile
            0.0000    0.0000    0.0000
                      4.7097   -0.8999
                                4.6658
```

Configuration 604:

```
           Z (R +jX) in ohms per mile
 1.3238  1.3569   0.0000  0.0000   0.2066  0.4591
                  0.0000  0.0000   0.0000  0.0000
                                   1.3294  1.3471
          B in micro Siemens per mile
            4.6658    0.0000   -0.8999
                      0.0000    0.0000
                                4.7097
```

Configuration 605:

```
           Z (R +jX) in ohms per mile
 0.0000  0.0000   0.0000  0.0000   0.0000  0.0000
                  0.0000  0.0000   0.0000  0.0000
                                   1.3292  1.3475
          B in micro Siemens per mile
            0.0000    0.0000    0.0000
                      0.0000    0.0000
                                4.5193
```

Configuration 606:

```
           Z (R +jX) in ohms per mile
0.7982  0.4463   0.3192  0.0328   0.2849 -0.0143
                 0.7891  0.4041   0.3192  0.0328
                                  0.7982  0.4463
          B in micro Siemens per mile
           96.8897    0.0000    0.0000
                     96.8897    0.0000
                               96.8897
```

Configuration 607:

```
           Z (R +jX) in ohms per mile
 1.3425  0.5124   0.0000  0.0000   0.0000  0.0000
                  0.0000  0.0000   0.0000  0.0000
                                   0.0000  0.0000
          B in micro Siemens per mile
           88.9912    0.0000    0.0000
                      0.0000    0.0000
                                0.0000
```